

ISSN 1983-4195



IBRACON Structures and Materials Journal
Revista IBRACON de Estruturas e Materiais

Special Edition: Concrete Sustainability

Editors: Edna Possan, Mark Alexander

Volume 15, Number 6
December 2022



Special Edition “Concrete sustainability”

It is a pleasure to edit the IBRACON Journal special issue on Concrete sustainability in the year the Brazilian Concrete Institute – IBRACON – celebrates its golden jubilee. This grand achievement represents 50 years of dedication to concrete, a durable material that is widely used globally.

Due to its abundant stock of natural raw materials, ease of production, adaptation to shapes, and low manufacturing cost, concrete has become an essential material for the development of humanity, establishing itself as one of the main construction materials today. However, to mitigate anthropogenic carbon emissions, new requirements are needed for the production and use of concrete. Reducing cement consumption and structural optimization are essential factors in reducing its environmental impact. These actions must be taken responsibly, considering the aspects of performance and project lifetime, requiring holistic studies for this scope.

In this context, new cement manufacturing solutions are needed since the largest share of concrete emissions comes from this material. Actions aimed at increasing clinker reactivity and energy efficiency and increase in use of low carbon emission fuels have been implemented by the cement industry to produce cement with lower CO₂ emission. The cement and concrete industries have also taken steps to reduce the clinker content in cement through substitution by supplementary cementitious materials (SCM) and fillers, leading to cements and concretes with lower CO₂ emission. At the same time, the development of new chemical admixtures has responded to the demands for carbon neutralization, allowing the production of concrete and mortars with lower cement consumption and good applicability.

Regarding the design of concrete structures, the use of concretes with higher strengths, as well as structural optimization, help reduce the consumption of materials in the structure, thereby improving the material's environmental performance. The use of reinforcements that are more resistant to corrosion, in addition to contributing to durability aspects, can allow the structure to capture carbon safely in its life cycle, partially offsetting the emissions associated with cement production. For non-structural concretes, CO₂ capture can be implemented in hydration matrices (carbon cure) or hydrated matrices (life cycle), with environmental and technical benefits (e.g. porosity reduction). However, primary data confirming the carbon capture potential of cement-based materials are still needed for this strategy to be considered a compensatory measure.

The production and manufacture of aggregates, formwork, admixtures, water, and concrete and mortar also represent an appreciable share of emissions. These must also be evaluated in the context of the environmental performance of the entire cement and concrete chain, with particular attention to the transport of materials and products, which depending on the region, have significant impacts. Reducing the generation and use of waste should also be prioritized, promoting the circular economy.



In Brazil in 2022, the Construction Environmental Performance Information System (SIDAC) was released, an online platform where information on the main construction materials is available, enabling the calculation of environmental indicators such as CO₂ emission, primary energy demand and water. It is a free accessible tool under development that needs the collaboration of the concrete chain for its dissemination, expansion, and continuous improvement. Notably, the growing global trend of pricing emissions - which has reached around US\$ 100 per ton of CO₂ - has motivated the productive sectors to develop product and process solutions aimed at carbon neutralization.

According to the Paris Agreement and the UN Sustainable Development Goals, moving to carbon neutrality is urgent and necessary, and the concrete chain is attentive to this demand. Industry, universities and research centers, and governments must work together to develop engineering solutions that reduce emissions while at the same time provide structures and facilities that serve the needs of populations in durable and sustainable ways. It is intended that this special edition of the IBRACON Journal will move these issues forward in tangible ways and contribute to a more sustainable planet.

PhD. Edna Possan and PhD. Mark Alexander
Special Edition Invited Editor-in-Chief,
IBRACON Structures and Materials Journal

IBRACON Statement on Concrete Sustainability

Sustainability is a fundamental value for today's society and also for IBRACON.

IBRACON has a holistic vision and focus on the need to develop information, documents, and tools to be used by the concrete production chain and society in general to achieve sustainability goals.

IBRACON is a non-profit association, of State and Federal Public Interest, whose mission is to create, disseminate and defend the correct knowledge of materials, design, construction, use and maintenance of concrete, developing its agents and acting for the benefit of consumers and society in harmony with the environment.

IBRACON was founded in 1972 as an independent society of professionals working in the field of plain and structural concrete, which includes building users, concessionaires and public companies, researchers from several areas, architects, engineers, academics, design companies, manufacturers, entrepreneurs, industries, builders, laboratories, and other entities.

IBRACON believes it should foster the defense and orientation of activities that promote the social, economic, and environmental performances of the concrete production chain, aiming at carbon neutralization, aligned with the Sustainable Development Goals (SDGs) in the United Nations 2030 Agenda and concerned about environmental, social and governance (ESG) responsibility and practices.

The knowledge developed and shared by IBRACON (books, congresses, exhibition, courses, competitions, seminars, best practices, scientific journal, and technical journal) is entirely the result of the work of volunteers dedicated to innovation and development of concrete structures.

Historically, IBRACON began addressing the sustainability theme in the late 1980s and introduced the concept of environmental performance in its technical books through the MPa/kg cement index. It has been strongly cooperating with ABNT (Associação Brasileira de Normas Técnicas), the Brazilian Association of Technical Standards, and, more recently, it has been fundamental in the change of the specifications of ABNT NBR 6122 standard, aiming at sustainability.

In 1997, IBRACON created a Technical Committee dedicated to the sustainability of structural concrete. This committee was named CT 206, later changed to CT MAB and currently it is called CT 101 Technical Committee for Concrete Sustainability.

This CT initially acted disseminating knowledge, technology and best practices for recycling and for the use of construction and demolition waste, in view of the implementation of CONAMA (National Environment Council) Resolution 307, which required waste generators to give an appropriate destination to the waste of their industrial processes. During this period, nine editions of the Seminar "Sustainable Development and Recycling in Civil Construction" were held, which brought to Brazil an important legacy of practices conducted in Europe and in the United States in the field of environmental research, standards, and policies.

Through this Technical Committee, IBRACON collaborated decisively in the preparation of the following technical standards:

- ABNT NBR 15113:2004 Solid Waste of Civil Construction and Inert Waste - Landfills: guidelines for design, implementation, and operation;
- ABNT NBR 15114:2004 Solid Waste of Civil Construction - Recycling Areas: guidelines for design, implementation, and operation;
- ABNT NBR 15115:2004 Recycled aggregates of solid waste from civil construction - Execution of paving layers: procedures;
- ABNT NBR 15116:2004 Recycled aggregates for use in Portland cement mortar and concrete: requirements and testing methods.

For years, sustainability has been incorporated among technical-scientific themes in editions of the Brazilian Concrete Congress (CBC). Sustainable constructions were the main issue in two of these Congresses, the 52nd CBC2010 and the 53rd CBC2011. In addition, three Sustainability Seminars were held in 2009, 2010 and 2011 CBCs. "CONCRETO & CONSTRUÇÕES" journal and "IBRACON Materials and Structures Journal" also published several technical and scientific articles on themes related to sustainability of concrete constructions.

Sustainability has always been part of IBRACON's activities, as well as all its related practices: to reuse and recycle materials and components, to reduce consumption of raw materials (dematerialization), and to promote the environmental product declarations and life cycle analysis.

This set of actions has promoted the development of scientific and technological research in an attempt to contribute to improve the environmental performance of the use of concrete in construction, generating publication of articles in national and international journals, boosting the dissemination of sustainable best practices in the construction sector. These publications have also contributed to provide subsidies for national technical standards to support eco-efficient constructive practices.

As a technical entity which gathers all segments of the concrete production chain, IBRACON is in a privileged position to promote a systemic and integrated sustainability vision of all stages of the construction process:

- **Conception:** to subsidize the sector with guiding criteria and parameters for the correct design of sustainable concrete structures;
- **Project:** to provide the sector with methodologies for evaluating energy, water, and raw materials consumption and for quantifying the emission of greenhouse gases, especially CO₂, and waste from choices of project typologies and construction systems; to build a project bank in collaboration with other Entities;
- **Materials:** to provide mix design and production methodologies to the sector focusing on sustainability; to build a concrete mix design reference and its main variables;
- **Construction:** to promote construction procedures of low energy consumption, low greenhouse gas emissions, low waste generation and high durability;
- **Durability:** to invest in methodologies that ensure the useful life of concrete structures with low or negligible maintenance;
- **Use:** to support and value entities that work on sustainability during operation and use throughout the service life of concrete structures;
- **Reuse:** to endorse methodologies and construction systems that enable reducing waste, reusing and recycling which goes with a circular economy vision.
- **Standards:** to collaborate with ABNT, proposing new standards and supporting the updating of standards related to concrete and its structures in view of sustainability as a driver of normative parameters.

IBRACON believes that the suppression of bottlenecks in the concrete chain with quality information that reaches its stakeholders is one of the necessary conditions to achieve sustainability in the sector.

Contributing to disseminate tools, methodologies, and information on sustainable best practices in the sector is the commitment of IBRACON, intensifying the collaboration with companies and entities aiming at reducing carbon emissions.

Among other initiatives, IBRACON supports *the Global Consensus on Sustainability in the Built Environment GLOBE* (RILEM, cib, ECCS, *fib* (CEB.FIP), IABSE, iaSS), Concrete Future (GCCA), SIDAC (CBCS) and CECarbon (SindusCon-SP).

IBRACON Structures and Materials Journal

Revista IBRACON de Estruturas e Materiais

Contents

The greenway for bridge column rehabilitation: a comparison between different techniques based on multi-criteria decision analysis 15601
B. BRISEGHIELLA, V. BORGHESE, C.P. CONTIGUGLIA, A. PELLE, D. LAVORATO, S. SANTINI and C. NUTIA

Circular economy in concrete production: Greenhouse Gas (GHG) emissions assessment of rice husk bio-concretes..... 15602
L.R. CALDAS, A.F. ARAUJO, N.P. HASPARYK, F. TIECHER, G. AMANTINO and R.D. TOLEDO FO.

Proposed durability parameters for reinforced concrete structures with design service life between 50 years and 100 years in Brazil..... 15603
F.B. MUMBERGER, B.F. TUTIKIAN and F.L. BOLINA

Optimized sizing of reinforced concrete structural elements considering the effect of carbonation..... 15604
J.J. ALIEVI, J.F. SANTORO and M. KRIPKA

On factors affecting probabilistic service life modeling of concrete structures under marine environments..... 15605
G.B. WALLY, F.C. MAGALHAES, M.V. REAL and L.C.P. SILVA FO.

Optimum design of precast and prestressed beams with focus on CO₂ emission reduction..... 15606
M.H.M. MORAES, W.M. PEREIRA JR., S.R.M. ALMEIDA, G.M. GONÇALVES FO. and R.F. VASCONCELOS

Feasibility analysis for implementing CO₂ curing in a concrete block industry in the São Paulo Region..... 15607
L.R. FORTUNATO, G.A. PARSEKIAN and A. NEVES JR.

Mechanical performance and chloride penetration resistance of concretes with low cement contents..... 15608
T.G. CÂNDIDO, G.R. MEIRA, M. QUATTRONE and V.M. JOHN

Transportation impact on CO₂ emissions of concrete: a case study in Rio Branco/Brazil..... 15609
A.A.L. PACHECO, L.S. OLIVEIRA, V.M. JOHN, S.C. ANGULO

Reduction of the environmental impacts of reinforced concrete columns by increasing the compressive strength: a life cycle approach..... 15610
B.A. BACELAR, T.C. DIAS and P. LUDVIG

Analysis of CO₂ emissions and waste elimination capacity of different recycling strategies applied in ready-mixed concrete plants..... 15611
L.B.P. VIEIRA, A.D. FIGUEIREDO, F. CIRILO, V.B. VERDIANI and L.M. LIMA

Assessment of properties of ultra-high performance cementitious composites with glass powder waste 15612
S.M. SOARES, T.O.G. FREITAS, A. OLIVEIRA JR., F.G.S. FERREIRA and J.A.A. SALVADOR FO.



Cover: Parametric Tower

Courtesy: Marcela Noronha P. de O. e Sousa



IBRACON

IBRACON Structures and Materials Journal is published bimonthly (February, April, June, August, October, and December) by IBRACON.

IBRACON

Instituto Brasileiro do Concreto Founded in 1972

Av. Queiroz Filho, nº 1700 — sala 407/408
Torre D — Villa Lobos Office Park
CEP 05319-000 — São Paulo, SP — Brazil
Phone: +55 11 3735-0202

Fax: +55 11 3733-2190

E-mail: riem@ibracon.org.br

Website: <http://www.ibracon.org.br>

Cover design & Layout: Editora Cubo
www.editoracubo.com.br

Support: Wallison Angelim Medeiros

Aims and Scope

Aims and Scope

The IBRACON Structures and Materials Journal (in Portuguese: Revista IBRACON de Estruturas e Materiais) is a technical and scientific divulgation vehicle of IBRACON (Brazilian Concrete Institute), published every two months. Each issue has 12 to 15 articles and, possibly, a technical note and/or a technical discussion regarding a previously published paper. All contributions are reviewed and approved by professionals with recognized scientific competence in the area. The IBRACON Structures and Materials Journal is an open access Journal, free of charges for authors and readers.

Objectives

The IBRACON Structures and Materials Journal's main objectives are:

- Present current developments and advances in concrete structures and materials.
- Make possible the better understanding of structural concrete behavior, supplying subsidies for a continuous interaction among researchers, producers, and users.
- Stimulate the development of scientific and technological research in the areas of concrete structures and materials, through papers peer-reviewed by a qualified Editorial Board.
- Promote the interaction among researchers, constructors and users of concrete structures and materials and the development of Civil Construction.
- Provide a vehicle of communication of high technical level for researchers and designers in the areas of concrete structures and materials.

Submission Procedure

The procedure to submit and revise the contributions, as well as the formats, are detailed in the Journal Website (ismj.org).

The papers and the technical notes are revised by at least two reviewers indicated by the editors. Discussions and replies are accepted for publication after a review by the editors and at least one member of the Editorial Board. In case of disagreement between the reviewer and the authors, the contribution will be sent to a specialist in the area, not necessarily linked to the Editorial Board. Conflict of interests is carefully handled by the Editors.

Contribution Types

The Journal will publish original papers, short technical notes, and paper discussions. Original papers will be accepted if they are in accordance with the objectives of the Journal and present quality of information and presentation. A technical note is a brief manuscript. It may present a new feature of research, development, or technological application in the areas of Concrete Structures and Materials, and Civil Construction. This is an opportunity to be used by industries, companies, universities, institutions of research, researchers, and professionals willing to promote their works and products under development.

A discussion is received no later than 3 months after the publication of the paper or technical note. The discussion must be limited to the topic addressed in the published paper and must not be offensive. The right of reply is granted to the Authors. The discussions and the replies are published in the subsequent issues of the Journal.

The submission file should be in accordance with the paper template available at the Journal Website. It is recommended that the length of the papers does not exceed 25 pages. Where available, URLs for the references should be provided.

The IBRACON Structures and Materials Journal will conduct the review process for manuscripts submitted in English. Titles, abstracts, and keywords are presented in English, and in Portuguese or Spanish. Articles and technical notes are peer-reviewed and only published after approval of the reviewers and the Editorial Board.

Once accepted, an article is typeset according to the journal layout. The author will be required to review and approve the galleys before publishing. At this stage only typesetting errors will be considered.

Internet Access

The IBRACON Structures and Materials Journal Webpage is available at <http://ismj.org>.

Sponsors

The funds for the maintenance of the Journal are currently obtained from the IBRACON. The Journal is not supposed to be maintained with funds from private sponsorship, which could diminish the credit of the publications.

Photocopying

Photocopying in Brazil. Brazilian Copyright Law is applicable to users in Brazil. IBRACON holds the copyright of contributions in the journal unless stated otherwise at the bottom of the first page of any contribution. Where IBRACON holds the copyright, authorization to photocopy items for internal or personal use, or the internal or personal use of specific clients, is granted for libraries and other users registered at IBRACON.

Copyright

All rights, including translation, reserved. Under the Brazilian Copyright Law N^o. 9610 of 19th February 1998, apart from any fair dealing for the purpose of research or private study, or criticism or review, no part of this publication may be reproduced, stored in a retrieval system, or transmitted in any form or by any means, electronic, mechanical, photocopying, recording or otherwise, without the prior written permission of IBRACON. Requests should be directed to IBRACON:

IBRACON

Av. Queiroz Filho, 1700 – sala 407/408 – Torre D
Villa Lobos Office Park
05319-000 – Vila Hamburguesa
São Paulo – SP
Phone: +55 (11) 3735-0202
E-mail: riem@ibracon.org.br

Disclaimer

Papers and other contributions and the statements made, or opinions expressed therein are published on the understanding that the authors of the contribution are the only responsible for the opinions expressed in them and that their publication does not necessarily reflect the views of IBRACON or of the Journal Editorial Board.

Editorial Board

Editor-in-chief emeritus (*in memoriam*)

José Luiz Antunes de Oliveira e Sousa, Universidade Estadual de Campinas - UNICAMP, Campinas, SP, Brazil.
<https://orcid.org/0000-0002-1108-4356>

Editor-in-chief

Guilherme Aris Parsekian, Universidade Federal de São Carlos - UFSCar, São Carlos, SP, Brazil, parsekian@ufscar.br
<https://orcid.org/0000-0002-5939-2032>

Associate Editors

Antônio Carlos dos Santos, Universidade Federal de Uberlândia - UFU, Uberlândia, MG, Brazil, acds@ufu.br
<https://orcid.org/0000-0001-9019-4571>

Bernardo Horowitz, Universidade Federal de Pernambuco - UFPE, Recife, PE, Brazil, bernardo.horowitz@ufpe.br
<https://orcid.org/0000-0001-7763-7112>

Bernardo Tutikian, Universidade do Vale do Rio dos Sinos - UNISINOS, São Leopoldo, RS, Brazil, bftutikian@unisinos.br
<https://orcid.org/0000-0003-1319-0547>

Bruno Briseghella, Fuzhou University, Fujian, China, bruno@fzu.edu.cn
<https://orcid.org/0000-0002-8002-2298>

Carmen Andrade, Universidad Politécnica de Catalunya, Spain, candrade@cimne.upc.edu
<https://orcid.org/0000-0003-2374-0928>

Diogo Rodrigo Ribeiro, Universidade do Porto - FEUP, Portugal, drr@isep.ipp.pt
<https://orcid.org/0000-0001-8624-9904>

Edna Possan, Universidade Federal da Integração Latino Americana - UNILA, Foz do Iguaçu, PR, Brazil, edna.possan@unila.edu.br
<https://orcid.org/0000-0002-3022-7420>

Fernando Pelisser, Universidade Federal de Santa Catarina - UFSC, Florianópolis, SC, Brazil, f.pelisser@ufsc.br
<https://orcid.org/0000-0002-6113-5473>

José Marcio Fonseca Calixto, Universidade Federal de Minas Gerais - UFMG, Belo Horizonte, MG, Brazil, calixto@dees.ufmg.br
<https://orcid.org/0000-0003-2828-0967>

José Tadeu Balbo Universidade de São Paulo - USP, São Paulo, SP, Brazil, jotbalbo@usp.br
<https://orcid.org/0000-0001-9235-1331>

Leandro Mouta Trautwein, Universidade Estadual de Campinas - UNICAMP, Campinas, SP, Brazil, leandromt@fec.unicamp.br
<https://orcid.org/0000-0002-4631-9290>

Lia Lorena Pimentel, Pontifícia Universidade Católica de Campinas - PUCCAMP, Campinas, SP, Brazil, lialp@puc-campinas.edu.br
<https://orcid.org/0000-0001-5146-0451>

Lúis Oliveira Santos, Laboratório Nacional de Engenharia Civil, Lisboa, Portugal, luis.osantos@lnec.pt
<https://orcid.org/0000-0003-2591-2842>

Mark G Alexander, University of Cape Town, Cape Town, South Africa, mark.alexander@uct.ac.za
<https://orcid.org/0000-0002-0986-3529>

María Josefina Positieri, Universidad Tecnológica Nacional, Argentina, mpositieri@gmail.com
<https://orcid.org/0000-0001-6897-9946>

Mário Jorge de Seixas Pimentel, Universidade do Porto - FEUP, Porto, Portugal, mjisp@fe.up.pt
<https://orcid.org/0000-0001-8626-6018>

Maurício de Pina Ferreira, Universidade Federal do Pará - UFPA, Belém, PA, Brazil, mpina@ufpa.br
<https://orcid.org/0000-0001-8905-9479>

Mauro de Vasconcellos Real, Universidade Federal do Rio Grande - FURG, Rio Grande, RS, Brazil, mauroreal@furg.br
<https://orcid.org/0000-0003-4916-9133>

Nigel G. Shrive, University of Calgary, Calgary, Canada, ngshrive@ucalgary.ca
<https://orcid.org/0000-0003-3263-5644>

Oswaldo Luís Manzoli, Universidade Estadual Paulista “Júlio de Mesquita Filho” - UNESP, Bauru, SP, Brazil, osvaldo.l.manzoli@unesp.br
<https://orcid.org/0000-0001-9004-7985>

Pedro Castro Borges, CINVESTAV, Mérida, Mexico, castro@cinvestav.mx
<https://orcid.org/0000-0001-6983-0545>

Rebecca Gravina, RMIT University, Melbourne, Australia, rebecca.gravina@rmit.edu.au
<https://orcid.org/0000-0002-8681-5045>

Editorial Board

Ricardo Carrazedo, Universidade de São Paulo - USP, São Carlos, SP, Brazil, carrazedo@sc.usp.br
<https://orcid.org/0000-0002-9830-7777>

Samir Maghous, Universidade Federal do Rio Grande do Sul - UFRGS, Porto Alegre, RS, Brazil, samir.maghous@ufrgs.br
<https://orcid.org/0000-0002-1123-3411>

Sérgio Hampshire de C. Santos, Universidade Federal do Rio de Janeiro - UFRJ, Rio de Janeiro, RJ, Brazil, sergiohampshire@gmail.com
<https://orcid.org/0000-0002-2930-9314>

Túlio Nogueira Bittencourt, Universidade de São Paulo - USP, São Paulo, SP, Brazil, tbitten@usp.br
<https://orcid.org/0000-0001-6523-2687>

Vladimir Guilherme Haach, Universidade de São Paulo - USP, São Carlos, SP, Brazil, vghaach@sc.usp.br
<https://orcid.org/0000-0002-9501-4450>

Yury Villagrán Zaccardi, Universidad Tecnológica Nacional Facultad Regional La Plata, Buenos Aires, Argentina, yuryvillagran@gmail.com
<https://orcid.org/0000-0002-0259-7213>

Former Editors

Américo Campos Filho, Universidade Federal do Rio Grande do Sul - UFRGS, Porto Alegre, RS, Brazil

Denise C. C. Dal Molin Universidade Federal do Rio Grande do Sul - UFRGS, Porto Alegre, RS, Brazil

Eduardo Nuno Brito Santos Júlio, Instituto Superior Técnico - IST, Lisboa, Portugal

Emil de Souza Sánchez Filho, Universidade Federal Fluminense - UFF, Rio de Janeiro, RJ, Brazil

Fernando Soares Fonseca, Brigham Young University – BYU, Provo, UT, USA

Geraldo Cechella Isaia, Universidade Federal de Santa Maria - UFSM, Santa Maria, RS, Brazil

Gonzalo Ruiz, Universidad de Castilla-La Mancha - UCLM, Ciudad Real, Spain

Guilherme Sales Melo, Universidade de Brasília - UnB, Brasília, DF, Brazil

Leandro Francisco Moretti Sanchez, University of Ottawa, Ottawa, ON, Canada

Luiz Carlos Pinto da Silva Filho, Universidade Federal do Rio Grande do Sul - UFRGS, Porto Alegre, RS, Brazil

Mounir Khalil El Debs, Universidade de São Paulo - USP, São Carlos, SP, Brazil

Nicole Pagan Hasparyk, Eletrobras Furnas, Aparecida de Goiânia, GO, Brazil

Paulo Helene, Universidade de São Paulo - USP, São Paulo, SP, Brazil

Paulo Monteiro, University of California Berkeley, Berkeley, CA, USA

Roberto Caldas de Andrade Pinto, Universidade Federal de Santa Catarina - UFSC, Florianópolis, SC, Brazil

Ronaldo Barros Gomes, Universidade Federal de Goiás - UFG, Goiânia, GO, Brazil

Romilde Almeida de Oliveira, Universidade Católica de Pernambuco - UNICAP, Recife, PE, Brazil

Romildo Dias Toledo Filho, Universidade Federal do Rio de Janeiro - UFRJ, Rio de Janeiro, RJ, Brazil

Rubens Machado Bittencourt, Eletrobras Furnas, Aparecida de Goiânia, GO, Brazil

Vladimir Antonio Paulon, Universidade Estadual de Campinas - UNICAMP, Campinas, SP, Brazil



Direction

Board of Direction 2021/2023

Biennium

President

Paulo Helene

1st Vice-President Director

Júlio Timerman

2nd Vice-President Director

Enio José Pazini Figueiredo

Presidency Advisors

Arnaldo Forti Battagin

Eduardo Antonio Serrano

Gilberto Antonio Giuzio

Iria Lícia Oliva Doniak

Jaques Pinto

João Luis Casagrande

Jorge Batlouni Neto

José Marques Filho

Mario William Esper

Ronaldo Tartuce

Rubens Machado Bittencourt

Selmo Chapira Kuperman

Simão Prizskulnik

Túlio Nogueira Bittencourt

Wagner Roberto Lopes

1st Director-Secretary

Cláudio Sbrighi Neto

2nd Director-Secretary

Carlos José Massucato

1st Treasurer Director

Júlio Timerman

2nd Treasurer Director

Hugo S. Armelin

Marketing Director

Alexandre Brites

Marketing Director Advisor

Guilherme Covas

Publications Director

Guilherme Parsekian

Publications Director Advisor

Túlio Nogueira Bittencourt

Event Director

Rafael Timerman

Event Director Advisor

Luis César De Luca

Technical Director

Carlos Brites

Technical Director Advisor

Emílio Takagi

Institutional Relations Director

César Henrique Daher

Institutional Relations Director Advisor

Adviser

José Vanderley de Abreu

Course Director

Jéssica Pacheco

Course Director Advisor

André Mendes

Student Activities Director

Jéssica Andrade Dantas

Student Activities Director Advisor

Patrícia Bauer

Personnel Certification Director

Adriano Damásio Soterio

Personnel Certification Director Advisor

Paula Baillot

Research and Development Director

Bernardo Tutikian

Research and Development Director Advisor

Roberto Christ

Council 2021/2023 Biennium

Individual Members

Alio Ernesto Kimura

Antônio Carlos dos Santos

Antônio Domingues de Figueiredo

Arnaldo Forti Battagin

Bernardo Fonseca Tutikian

Carlos José Massucato

César Henrique Sato Daher

Claudio Sbrighi Neto

Enio José Pazini Figueiredo

Geraldo Cechella Isaia

Iberê Martins da Silva

Inês Laranjeira da Silva Battagin

Iria Lícia Oliva Doniak

Jéssica Mariana Pacheco Misko

José Tadeu Balbo

Leandro Mouta Trautwein

Luiz Prado Vieira Júnior (*in memoriam*)

Mário William Esper

Rafael Timerman

Rubens Curti

Vladimir Antonio Paulon

Past President Members

Eduardo Antônio Serrano

José Marques Filho

Júlio Timerman

Paulo Roberto do Lago Helene

Ronaldo Tartuce

Rubens Machado Bittencourt

Selmo Chapira Kuperman

Simão Prizskulnik

Túlio Nogueira Bittencourt

Corporate Members

ABCIC - Associação Brasileira da Construção Industrializada de Concreto – Iria Lícia Oliva Doniak

ABCP - Associação Brasileira de Cimento Portland – Paulo Camilo Penna

ABECE - Associação Brasileira de Engenharia e Consultoria Estrutural – João Alberto de Abreu Vendramini

ABESC - Associação Brasileira das Empresas de Serviços de Concretagem – Wagner Roberto Lopes

EPUSP - Escola Politécnica da Universidade de São Paulo – Túlio Nogueira Bittencourt

IPT - Instituto de Pesquisas Tecnológicas do Estado de São Paulo – José Maria de Camargo Barros

MC-BAUCHEMIE BRASIL INDÚSTRIA E COMÉRCIO LTDA – Jaques Pinto

PhD Engenharia Ltda – Douglas de Andreza Couto

TQS Informática Ltda – Nelson Covas

VOTORANTIM Cimentos S/A – Mauricio Bianchi

Reviewers List 2021-2022

Abdalla Filho, João Elias
Adriano Rossignolo, João
Aguiar, Cássio
Aguilar, Maria Teresa
Albuquerque, Arthur
Almeida Filho, Fernando
Almeida, Luiz
Almeida, Saulo José de Castro
Alva, Gerson Moacyr Sisniegas
Alves, Antônio
Alves, Elcio
Andrade, Daniel
Andrade, Jairo José de Oliveira
Ângulo, Sérgio
Araújo, Daniel
Araújo, Francisco Celio de
Araújo, Tereza
Asche, Harry
Azevedo, Afonso
Azevedo, Crysthian Purcino
Balbo, José
Barboza, Aline
Barros, Rodrigo
Beck, André
Bernardin, Adriano
Bernardo, Luís
Bezerra, John
Bittencourt Junior, Luis
Bittencourt, Eduardo
Bolina, Fabrício
Botte, Wouter
Bounassar Filho, Jorge
Brito, José
Buttignol, Thomaz
Caldas, Rodrigo Barreto
Caldentey, Alejandro Perez
Calixto, José Marcio
Campelo, Henrique
Campos Filho, Américo
Campos, Heloisa
Capuzzo, Valdirene Maria Silva
Cardoso, Daniel Carlos Taissum
Carrazedo, Ricardo
Carrazedo, Rogério
Carvalho, Hermes
Carvalho, Roberto Chust
Castro, Alessandra Lorenzetti de
Cervenka, Jan
Cheung, Andrés
Christ, Roberto
Christoforo, André
Cincotto, Maria
Ciriades, Jean Pierre
Cordeiro, Luciana
Costa, Carla Neves
Costa, Fernanda Bianchi Pereira da
Couto, Douglas
Dalfré, Gláucia
De Nardim, Silvana
Delalibera, Rodrigo
Diniz, Sofia Carrato
Dominguez, Joel
Durand, Raúl
Fairbairn, Eduardo
Fakury, Ricardo
Feldmann, Markus
Ferreira, Fernanda
Ferreira, Gisleiva Cristina dos Santos
Ferreira, Luiz Eduardo Teixeira
Figueiredo, Antônio Domingues de
Flórez-López, Júlio
Folino, Paula
Fonseca, Ana
Formagini, Sidiclei
Frizon, Tiago
Futai, Marcos
Gachet, Luisa
Garcez, Mônica Regina
Garcia, Maria da Luz
Gaspar, Cássio
Gavilan, Sergio
Genikomsou, Aikaterini S.
Giuseppe, Guimarães
Golaszewski, Jacek
Gomes, Carlos Marmorato
Gomes, Francisco Augusto Aparecido
Gomes, Ronaldo
Gonçalves, Paulo J. P.
Greco, Marcelo
Gumieri, Adriana
Gusmão, Alexandre
Haach, Vladimir
Haselbach, Liv
Horowitz, Bernardo
Hosen, Akter
Hotza, Dachamir
Irassar, Edgardo F.
Iskander, Mina
Isoldi, Liércio André
Isufi, Brisid
Jacintho, Ana
Jacinto, Luciano
Joshaghani, Alireza
Justino Filho, Manoel Rodrigues
Kadhim, Majid M. A.
Karayannis, Chris G.
Kazmi, Syed
Kazmierczak, Cláudio
Kempka, Mariane
Kenai, S.
Khazanovich, Lev
Khoshnazar, Rahil
Kowalski, Robert
Krahl, Pablo Augusto
Kripka, Moacir
Kroetz, Henrique Machado
Lameiras, Rodrigo
Lantsoght, Eva O. L.
Lazzari, Bruna
Lazzari, Paula
Leite, Mônica Batista
Lemes, Igor
Li, Hui
Liang, Qing Quan
Liberati, Elyson
Lima, Flávio
Lima, Silvio Souza
Liu, Yi
Loredo-Souza, Acir
Lübeck, André
Ludvig, Péter
Luz, Caroline Angulski da
Machado, Roberto
Maciel, Geraldo
Maedo, Michael
Magalhães, Aldo de
Magalhães, Fábio
Mansur, Alexandra
Manzoli, Osvaldo
Mappa, Paulo César
Marques Filho, José
Marques, Marília
Marques, Severino
Mata, Rodrigo da
Matos, Ana Mafalda
Matos, Paulo de
Medeiros, Arthur
Medeiros, Marcelo
Medeiros, Ronaldo
Melges, José Luiz Pinheiro
Melo, Antônio
Mendes, Júlia Castro
Meneghetti, Leila Cristina
Menendez, E.
Menezes, Ruy
Mennucci, Marina Martins
Mesquita, Esequiel
Miguel, Leandro Fleck Fadel
Moahmed, Hoda
Modolo, Regina
Monte, Renata
Montes-Garcia, Pedro
Moraes, Poliana Dias de
Morsch, Inácio
Mota, Neusa
Munaiar Neto, Jorge
Muñoz-Rojas, Pablo
Neves Junior, Alex
Nóbrega, Petrus
Nogueira, Caio
Nogueira, Fernando
Nunes, David
Oliveira, Cristina
Oliveira, Dênio
Oliveira, Leonardo Henrique
Oliveira, Luciane Marcela Filizola de
Oliveira, Mateus Antônio Nogueira
Oliveira, Romilde
Paccola, Rodrigo
Pachêco, Alexandre
Pachêco, Fernanda
Paes, José Luiz
Palermo Junior, Leandro
Pantoja, João
Parente Junior, Evandro
Parsekian, Guilherme A.
Patil, Chetan
Pedroso, Cynthia
Peixoto, Ricardo André Fiorotti
Pelisser, Fernando
Pereira, Eduardo
Pereira, Sebastião Salvador Real

Reviewers List 2021-2022

Perlingeiro, Mayra
Pfeil, Michèle
Picelli, Renato
Pileggi, Rafael
Pimenta, Roberval
Pimentel, Lia Lorena
Pinto, Roberto Caldas de Andrade
Pinto, Silas
Pires, Tiago
Pituba, José Júlio de Cerqueira
Pontes, Helder
Possan, Edna
Pravia, Z. M. C
Punhagui, Katia
Quaranta, Giuseppe
Quinino, Uziel
Rashad, Alaa
Real, Mauro
Rêgo, João da Silva
Resende, Thomás Lima de
Ribeiro, Daniel
Ribeiro, Diogo
Rigobello, Ronaldo
Rizzatti, Eduardo
Rocha, Janaíde Cavalcante
Rocha, Marcelo
Roesler, Jeffery
Rojas, Rosangel
Romanel, Celso
Rossi, Alexandre
Sakata, Rafael Dors
Sanchez, Emil
Sandoval, Gersson Fernando Barreto
Santos, Ana Carolina Parapinski dos
Santos, Daniel
Santos, Sérgio Hampshire C.
Santos, White
Sarker, Prabir K.
Savija, Branko
Schulz, Mauro
Sciarretta, Francesca
Scott, Allan
Seara-Paz, Gumersinda
Setiawan, Andri
Shafigh, Payam
Shi, Jinjie
Shishegaran, Aydin
Silva Filho, José
Silva, Amilton Rodrigues da
Silva, Bruno do Vale
Silva, Fernando Marques da
Silva, José Guilherme da
Silva, Marcelo Araújo da
Silva, Maria Cecília Teixeira da
Silva, Renata Gomes Lanna da
Silva, Valdir
Silva, Wellington Andrade da
Silvestro, Laura
Simonetti, Camila
Siqueira, Gustavo
Snoeck, Didier
Soto, Orieta
Sousa, Adla
Stucchi, Fernando Rebouças
Tamayo, Jorge
Tarabia, Ahmed
Tavares, Maria Elizabeth
Tayeh, Bassam
Thamboo, Julian Ajith
Toralles, Berenice
Trautwein, Leandro
Trindade, Ana Carolina Constância
Tutikian, Bernardo
Valença, Jonatas
Veríssimo, Gustavo
Vianna, Sávio S. V.
Vieira, Geilma
Vieira, Manuel
Wahrhaftig, Alexandre de Macêdo
Wally, Gustavo
Wang, Wen-Wei
Wang, Xiao-Yong
Welter, Nathanaell Vinícius de Camargos
Wong, Patrick
Xie, Tianyu (Anson)
Yang, Shangtong
Yassin, Ahmed
Yu, Runqing



ORIGINAL ARTICLE

The greenway for bridge column rehabilitation: a comparison between different techniques based on multi-criteria decision analysis

O caminho verde para pilares de pontes: uma comparação entre as operações de retrofitting e substituição com análise de decisão multicritério

Bruno Briseghella^a Vittoria Borghese^b Carlotta Pia Contiguglia^b Angelo Pelle^b Davide Lavorato^b Silvia Santini^b Camillo Nuti^{a,b} ^aFuzhou University, College of Civil Engineering, Fuzhou, Fujian, China^bRoma Tre University, Department of Architecture, Roma, Italy

Received 08 September 2022

Accepted 19 September 2022

Abstract: One of the biggest issues in civil engineering is the poor performance of concrete repairs. In fact, in Europe only 50% of concrete structures restorations are estimated to be successful, even though rehabilitation costs account for about half of the yearly construction budgets. This research aims at investigating a potential green approach to the sustainability of rehabilitation solutions for infrastructures. Following a simplified analysis of CO₂ emissions, intervention costs, social aspects, structural performances and other variables considered relevant to the scope, possible rehabilitation techniques are compared and ranked. The following four different options have therefore been designed to be applied to an actual column of the Brabau Bridge in Sardinia (Italy): i. complete removal and replacement of the column, ii. replacement of the damaged longitudinal rebars by machined bars and ultra-high performance fibre-reinforced concrete (UHPFRC) strengthening, iii. longitudinal and transverse fiber reinforced polymers (FRP) wrapping, iv. concrete jacking. A methodological and procedural strategy is established through multi-criteria analysis that will allow future developments to assess the whole Life Cycle Assessment of the maintenance work.

Keywords: reinforced concrete, sustainability, bridge column rehabilitation, multi-criteria, AHP.

Resumo: Um dos maiores problemas da engenharia civil é o mau desempenho dos reparos em concreto. Estima-se que apenas 50% das restaurações de estruturas de concreto na Europa sejam bem-sucedidas, apesar de os custos de reabilitação e reparo serem estimados em cerca de metade dos orçamentos anuais de construção. Esta pesquisa visa investigar uma potencial abordagem verde para a sustentabilidade de soluções de reabilitação de infraestruturas. Após uma análise simplificada das emissões de CO₂, custos de intervenção, aspectos sociais, desempenhos estruturais e outros aspectos considerados relevantes para o escopo, as possíveis ações de manutenção são comparadas e classificadas. As seguintes quatro opções diferentes foram, portanto, projetadas para serem aplicadas a uma coluna da Ponte Brabau na Sardenha (Itália): i. remoção e substituição completas da coluna, ii. substituição das barras longitudinais danificadas por barras usinadas e reforço UHPFRC, iii. envolvimento longitudinal e transversal de CFRP, iv. revestimento de concreto. Uma estratégia metodológica e processual é estabelecida através de uma análise multicritério que permitirá em futuros desenvolvimentos avaliar todo o Ciclo de Vida da obra de manutenção

Palavras-chave: concreto reforçado, sustentabilidade, reabilitação de pilares de pontes, multicritério, AHP.

How to cite: B. Briseghella et al., "The greenway for bridge column rehabilitation: a comparison between different techniques based on multi-criteria decision analysis," *Rev. IBRACON Estrut. Mater.*, vol. 15, no. 6, e15601, 2022, <https://doi.org/10.1590/S1983-41952022000600001>

Corresponding author: Bruno Briseghella. E-mail: bruno@fzu.edu.cn

Financial support: This work is supported by the National Natural Science Foundation of China (Grant No. 51778148). The authors gratefully acknowledge the funding received by The Laboratories University Network of Seismic Engineering (ReLUIIS): research project ReLUIIS/DPC 2019–2021 Reinforced Concrete Existing Structures. The authors also gratefully acknowledge the funding received by PRIN-Progetto di Ricerca di Interesse Nazionale 2020. FIRMITAS: Multi-hazard assessment, control and retrofit of bridges to enhance Robustness using sMart IndusTriAlized Solutions.

Conflict of interest: Nothing to declare.

Data Availability: The data that support the findings of this study are available from the corresponding author, [BB], upon reasonable request.



This is an Open Access article distributed under the terms of the Creative Commons Attribution License, which permits unrestricted use, distribution, and reproduction in any medium, provided the original work is properly cited.

1 INTRODUCTION

1.1 Sustainability issue and life cycle assessment of concrete

Sustainability is a growing concern in the infrastructure sector, playing a central role in the assessment of construction works. Nevertheless, to the authors' knowledge, there is a lack in the current state-of-the-art of methodologies for the green design or repairing of existing infrastructures [1].

It is important to note that the term "Green Concrete" originated around the end of the 90's, when the concept of sustainability was first connected to infrastructure. It was coined (also on materials in general) in 1998 in Denmark at the Danish Technological Institute Concrete Centre (TELESCOP project 1997-2000) suggesting a renewed need for sustainability in the construction sector. At that time, the name did not have any special connotations, as the technologies that make innovative research possible today were not available yet [2].

In recent years, this definition has been implemented, identifying as *green concrete* a specific conglomerate that uses waste materials as aggregates, whose production does not involve high carbon dioxide emissions and whose structural performance is high throughout the life cycle [3].

The new terminology and research developments raised awareness in the academic community of the importance of energy containment, responsible raw material usage, and optimal construction technology practices. In terms of the sustainability of structures, the term "green" should be used to refer to the full life cycle assessment (LCA) rather than just the manufacture of a single element. Therefore, improved construction methodologies are studied to strongly decrease greenhouse gasses emissions even for infrastructures.

In Europe, the cost of interventions on the damaged or deteriorated portions of viaducts and bridges is estimated to be high, representing about half of the annual budget for constructions. Even so, no more than 50% of rehabilitation actions on reinforced concrete structures are considered to be effective. Often, the inefficacy is caused by wrong materials choices, sometimes by technological choices or inconsistency between the intervention and the original substrate. Renovation and rehabilitation projects must be carried out to restore or even improve initial performance. Only by taking a proactive approach that cost savings can be obtained [4].

A new discipline is emerging that includes the study of bridges through the entire life cycle, from the production of the material to the disposal of the work. The term life cycle means an integrated analysis that represents a multi-parametric investigation. This takes into account various aspects of sustainability commonly identified for the three macro categories: environmental, social and economic [5]. The triple dimension of sustainability (LCSA) is thus integrated through the cost of life (LCC), its environmental assessment (LCA) and social analysis (SLCA), namely (Equation 1):

$$LCSA = LCC + LCA + SLCA \quad (1)$$

This scenario may include circular economy approach identified as follow: from cradle to gate (the least detailed, from cradle to the construction site); from cradle to grave (the most frequent, understood in Italian from cradle to grave); from cradle to cradle (recognising the importance of recycling and reuse, from cradle to cradle) [6], [7].

Life-cycle sustainable assessment (life-cycle analysis) is regulated nationally and internationally by ISO 14040-14044. For this reason, there is a wide range of possible life cycle diagnostic alternatives, depending on the analysed structure and the chosen material [8], [9].

1.2 Ranking and classification method for sustainable retrofit of bridges

The infrastructure sector is still lagging in terms of the concept of sustainability of structures or materials and the theme of green concrete is only beginning to gain interest. For this reason, a general review of the current state-of-the-art has been conducted with the bibliographic research software VOS Viewer [10]. The software allows to carry out bibliometric and scientometric research through the analysis and identification of the main authors, the keywords, the number of publications, citations and their dispersion over time. This aims at identifying the most discussed themes, their correlation and their development over time.

An analysis through mapping and hierarchical clustering is used to produce useful graphical information that permits a first overview of the subject, recognizing in a short time which approaches may be most suitable for the study of the sustainability of concrete for bridges and infrastructures.

Two different types of searches are here presented: firstly the general state of the sustainability of interventions for concrete bridges is reviewed through the Scopus and Web Science databases; secondly, the same search is applied more in detail to multi-criteria decision analysis.

The first search revealed five clusters, and the dispersed results of a total of 67 articles highlighted the need for further study (Figure 1a). The second, filtered for multi-criteria analysis, included only 19 documents, showing three more defined clusters, in which themes are mainly the same: interventions for seismic actions and safety (Figure 1b).

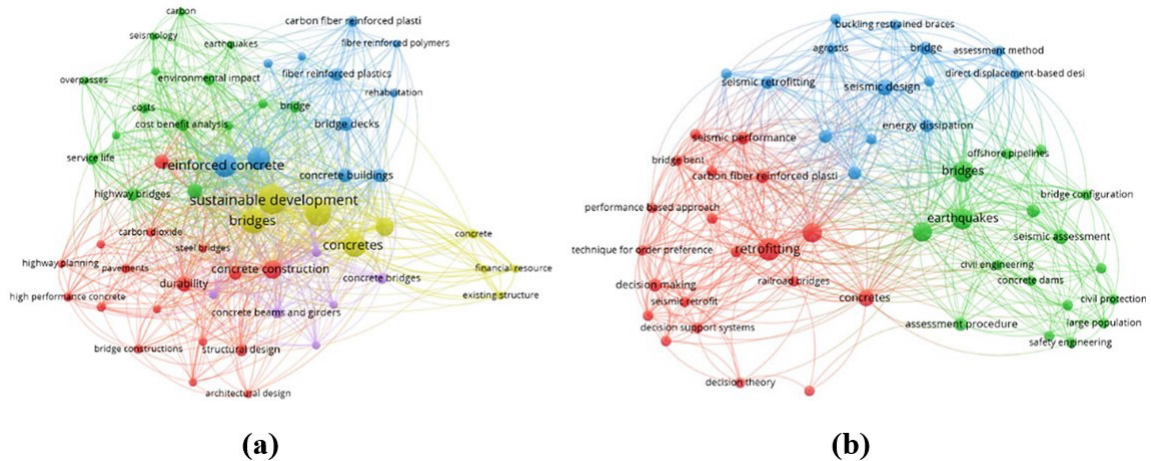


Figure 1. Sustainable retrofitting assessment scientometric: **(a)** data for bridges: in blue the mix design, in yellow the costs and composition, in red the structural analysis and in green the seismic assessment; **(b)** data for bridges with multi-criteria decision analysis. In blue, there is the mix design, in red and green the seismic analysis.

Only a few studies in the two groups extracted thanks to the second search are specifically relevant to sustainability. One uses decision-making to integrate seismic loss, sustainability and resilience. The approach is defined as innovative because it has not yet been extensively developed for the selection of the best intervention alternative from a long-term perspective [11].

To varying degrees, Multiple Attribute Decision Making (MADM) techniques have been applied throughout each stage of the bridge's life cycle as support for engineers and contractors. In the event of intervention on existing structures, each repairing strategy may present different benefits but also significant drawbacks that must be considered. Therefore, the multitude of solutions in the state-of-the-art may lead to an ineffective or even incorrect design decision.

A general overview of MADM analysis applied to bridges' sustainability is provided in [12], where the authors examine about 77 manuscripts classifying them into 4 main categories (planning and design, construction, operation and maintenance, demolition and recycling). According to this study, the maintenance phase emerges as the most investigated while Fuzzy logic and Analytical Hierarchy Process (AHP) techniques have emerged as the most employed approaches. Regarding the use of multi-criteria analysis techniques to compare alternative retrofitting options, they have been used to face many problems: to select material for the repair of structural concrete [4], to compare repair projects [13], to assess corrosion damage [14] and risk [15], etc. Only a small number of researches are available on the ranking and classification method used to assess the priority of the bridge to be repaired [16].

2 METHODOLOGY

The evaluation of four different alternatives for the sustainable repair of a bridge's column is carried out via an innovative procedure in the world of infrastructure. The following approach aims to compare alternatives from a sustainability point of view considering environmental, social, economic and structural aspects.

The research methodology is then summarized as follows:

1. The repair interventions are designed;
2. The alternatives are modelled through the BIM technology to extract the schedule of the quantities and all the data necessary for the successive evaluations;

3. The most sustainable alternative is established via multi-criterial analyses, in particular, the AHP approach with the implementation of MIVES (Modelo Integrado de Valor para Evaluación Sostenible);
4. Python code is developed to carry out the analysis.

These steps are necessary to quantify the sustainability of the selected alternatives and to obtain an index that allows comparison and a recommended and most suitable solution.

The non-exhaustive legislation (which does not specify a single methodology, even when it mentions it) and the challenge of selecting multi-criteria analysis that should be developed by the individual user with a team of decision experts are likely the reasons why multi-criteria analysis is still rarely used today (as evidenced in the literature) in this particular field.

2.1 Case study

An actual RC bridge located in Sardinia (Italy), in particular one column, as shown in Figure 2, serves as the case study for this research. The deck is made of simple multi-span precast concrete girders, which are supported by rigid frame columns. The analysed column has a circular cross-section with a 1200 mm diameter and its height is equal to 3850 mm (up to the cap). The bridge column is built of normal strength concrete (NSC), whose nominal compressive strength and associated strain are equivalent to 30 MPa and 0.2 percent, respectively, while the softening branch reaches zero stress at a strain value of 0.4 percent. The axial force on a single column is estimated to be 4500 kN, and the concrete cover has a depth of 40 mm. Twenty rebars with a diameter of 24 mm are arranged in a single concentric circular layer while transverse reinforcement is provided by a spiral with dimensions of 12 mm in diameter and 250 mm in pitch, respectively. The uncorroded reinforcing steel bars' yielding stress, ultimate stress, and corresponding strain are 536 MPa, 649 MPa, and 11.6%. The repairing interventions herein presented are designed by analysing the pier only in the transverse direction, therefore it is effectively modelled as a cantilever element (by neglecting the effect due to the frame).

2.2 Repair methods

- (1) *Column replacement*: the first option involves the removal of the severely damaged pier and its replacement with a new one designed as the original without providing for a code adaptation (Figure 3a).
- (2) *Rebar replacement*: the second intervention approach has been proposed to repair earthquake and corrosion-damaged piers in recent years [17]–[23].

The procedure is implemented as follows:

- The external layer of concrete is removed to allow for the replacement of damaged longitudinal rebars as well as to stop the corrosion of new steel rebars. The repaired zone extends along the column height and deeper than the original reinforcement's rear face. The height of the intervention area is assumed to equal to $2L_p$ (length of the plastic hinge), while the depth of the removed concrete area is equal to 110 mm. To adequately distribute the tensions at the pier footing, the repaired zone must also be expanded into the foundation.
- To improve the bond between old and new concrete sections, the surface of the concrete core is prepared.
- The damaged longitudinal rebars are cut and replaced with new machined steel rebars. $\alpha = A_m/A_s$ stands for the turning factor (here assumed to be equal to 0.6) where A_m and A_s are machined and the original rebar cross-section area, respectively. Bar replacement occurs mainly in two steps: firstly, the couplers (i.e., steel equal angles) are placed on the backside of the old rebars while the new machined steel rebar segments are first aligned with the existing rebars, then the coupler and the ends of the rebars are welded together.
- Part of the original longitudinal reinforcement within the intervention area can be eventually replaced with new unmachined steel rebars.
- Lastly, covering is accomplished using Ultra-high Performance Fibre-Reinforced Concrete (UHPFRC) [24] by arranging the formwork and casting the UHPFRC. Once enough time has passed, the formwork is removed. UHPFRC gains strength quite quickly, which cuts down on the total amount of time needed to complete the repair intervention.

It should be noted that the application of UHPFRC greatly improves the shear capacity, allowing the removal of the corroded transverse reinforcement in the repaired zone without replacement. Lastly, the UHPFRC's extremely low diffusion coefficient practically blocks chloride from penetrating concrete, which prevents the corrosion of steel reinforcement close to the repaired zone (Figure 3b).

- (3) *FRP jacketing*: in the third scenario, the repairing intervention is designed according to He et al. [25]. In the cited paper, the authors propose a rapid intervention technique for seriously damaged columns, with fractured or buckled

reinforcing bars. The repairing solution aim at restoring the column strength associated with the peak load of the original un-corroded pier (Figure 3c) and the original concrete confinement. The intervention is designed on the assumption that identical works, timing and “comparable” materials are utilised. The repair mortar is a normal strength concrete with a compressive strength of 37 MPa. The CFRP strengthening system is made up of carbon fibre tow sheets consisting of unidirectional fibres with the following properties: ultimate tensile strength of 3800 MPa; tensile modulus of 227 GPa; ultimate rupture strain of 0.0167; and nominal thickness of 0.165 mm per ply. The stress-strain relationship of the fibres is linear-elastic until rupture.

In the case of U-shape or wrapping, the contribution of the FRP reinforcement system can be estimated according to CNR-DT 200 [26], [27], and so, based on the Mörsch model, $V_{Rd,f}$ can be calculated by the following Equation 2:

$$V_{Rd,f} = \frac{1}{\gamma_{Rd}} \cdot 0.9 \cdot d \cdot f_{fed} \cdot 2 \cdot t_f \cdot (\cot\theta + \cot) \cdot \frac{b_f}{p_f} \quad (2)$$

where d = the height of the section, f_{fed} = the effective strength of the reinforcement system, t_f = the thickness of the FRP reinforcement system, b_f = the width of the strips, p_f = the pitch of the strips (in the case of strips placed adjacent to each other, $b_f/p_f = 1.0$ is assumed), γ_{Rd} = the partial coefficient given in Table 1-3 of the CNR-DT 200 (for shear/torsion is equal to 1,20). The f_{fed} has been evaluated choosing an effective strain in the CFP equal to 0.004. Hence, by assuming $V_{Rd,f}$ equal to the difference between the target resistance and the resistance of the damaged column, by inverting Equation 1 it was possible to calculate t_f , i.e. the thickness of FRP needed. The application of the FRP intends to re-establish also the confinement given by the transverse reinforcement in the damaged section (evaluated according to Mander et al. [28]), so the confinement pressure given by the wrapping system has been evaluated according to the following Equation 3 given by DCR-DT 200 [26], [27]:

$$f_1 = \frac{1}{2} \cdot \rho_f \cdot E_t \cdot \varepsilon_{fr,rid} \quad (3)$$

Where ρ_f = ratio of reinforcement, dependent on the shape of the section and the type of application, E_t = modulus of elasticity of the material in the direction of the fibres, $\varepsilon_{fr,rid}$ = reduced strain of the fibre-reinforced composite.

CFRP has been applied also with longitudinal fibres to compensate the loss of strength related to the fracture or buckling of longitudinal rebars. Because of uncertainty regarding the capacity of the existing longitudinal reinforcement, all the bars are severed and the required layers of CFRP are calculated by assuming that they will provide all of the resistant moment. As a result of the design outcomes, 10 vertical and 3 horizontal layers were used. A crucial aspect is to guarantee enough bond length to the CFRP wrap, avoiding premature failure mechanism in the strengthening system. For this reason, a metal anchorage system is designed to secure the longitudinal reinforcement at the crucial section at the base of the cantilever column. Details of the system are shown in Figure 3c.

(4) *Concrete jacketing*: this methodology has been proposed by Lehman et al. [29] to repair extensively damaged bridge columns. It entails installing a strong jacket to the damaged part of the pier, forcing new flexural hinging of the jacket. The jacket is designed to have comparable flexural strength to the original cross section. Damaged concrete to a depth of 110 mm of the column is removed while the remaining area of the intervention height of the existing column is roughened to encourage shear transfer. Given the uncertainties of the capacity of the damaged reinforcement, all the original longitudinal bars are severed and the fractured spiral is removed. Due to jacketing the base section thickens to a diameter of 1600 mm and it is reinforced by 15 ϕ 20 longitudinal rebars and a new column spiral with diameter and pitch equal to 12 mm and 100 mm, respectively. The jacket length L_j of 1800 mm is chosen to make it unlike that the column would yield above the jacket. The original column diameter is 400 mm smaller than the jacket diameter. The repair design strategy is depicted in Figure 3d.

The alternatives were thus modelled with BIM technology to extract the schedules of quantities (Figure 2-3). The modelling involved the creation of individual parametric elements, built according to the seven dimensions by UNI 11337 [30]. The level of details (LOD) geometry is equal to F and G depending on the elements since the degradation state has been only partially replicated. Only the deck turns out to be a LOD D (Figure 2).



Figure 2. Modelling of the current condition of the pier.

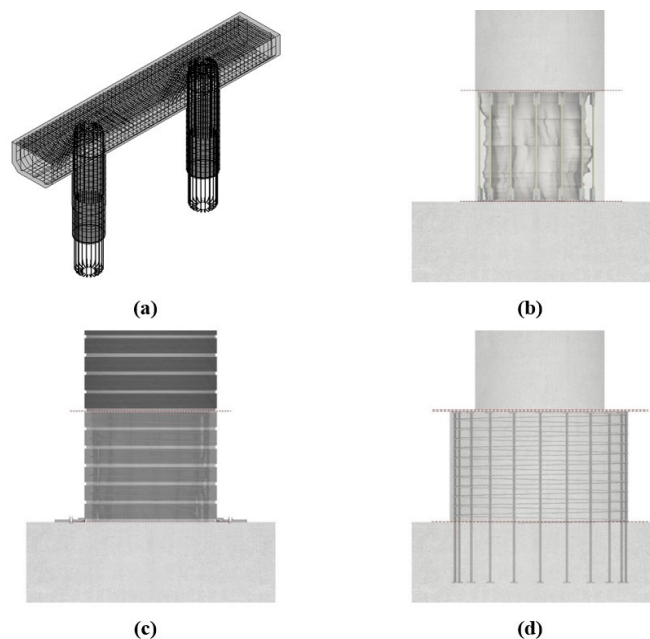


Figure 3. Modelling of the four alternatives: (a) complete replacement of the pier, (b) rebars replacement with UHPFRC cover, (c) CFRP wrapping, (d) concrete base jacketing

2.2 Multi-Criteria Decision Making

The decision-making analysis is a technique applied in many fields to determine the goals to be achieved and the optimal methodology to be used [31].

This systematic process is described by several steps that are respectively: the identification of the problem; the selection of criteria; the evaluation of alternatives; the final choice of the best alternative for that specific problem [32].

The multi-criteria analysis is applied to the most disparate subjects, from economy to teaching, with specific types of analysis considered more suitable for different fields [33].

The literature on this procedure is represented by a very wide range of publications resulting in detailed and specific papers for each hypothetical application. In particular, in the architectural field, there are countless applications that such an interesting methodology can have [34].

Often the multi-criteria analysis is employed in Economics to select investment for instance, but it has currently a little application in the infrastructures field. Despite these premises, the uses it has and could have are innumerable and

can lead, for example, to: optimization of structural decisions; greater understanding of alternatives; higher efficiency of buildings; greater sustainability of the entire life cycle of the bridge retrofiting projects.

The multi-criteria decision-making process, also known as MCDM (or MCDA multi-criteria decision analysis), is based on mathematical and analytical analyses that the decision-maker does to rank and select the best alternatives for solving a problem.

There are different types of analysis, but the main difference is between single-criteria and multi-criteria. Usually, the second one is used as it examines more options, finding the best one. A standard model used for these analyses is that of a systematic approach to evaluation, choosing priorities and selecting the best one [35].

2.3 Analytical Hierarchy Process

Decision-making through the use of analytical hierarchy is a technique for decision support in complex environments where many variables or criteria are considered in the prioritization and selection of alternatives [36].

The AHP was developed in the 1970s by Thomas L. Saaty and its application starts with a problem that is divided into a hierarchy of criteria so it can be more easily analysed and compared independently. Secondly, it must be constructed according to a logical hierarchy so that decision-makers can systematically evaluate and weight alternatives by making pair comparisons for each of the chosen criteria. The AHP approach, also compared to other MADM methodologies, allows giving a mathematical value to a judgment, to conduct coherent and valid comparisons. A decision tree is defined, with the criteria to be taken into account in assessing the chosen alternatives. Each criterion and tree branch will be assigned a weight [37],[38]. The tree is consequently divided into three parts: the macro categories called Requirements, the sub-criteria (or Criteria) and the so-called Indicators (more specific groupings). Each of the latter will then be assigned a value associated with each alternative (Figure 4).

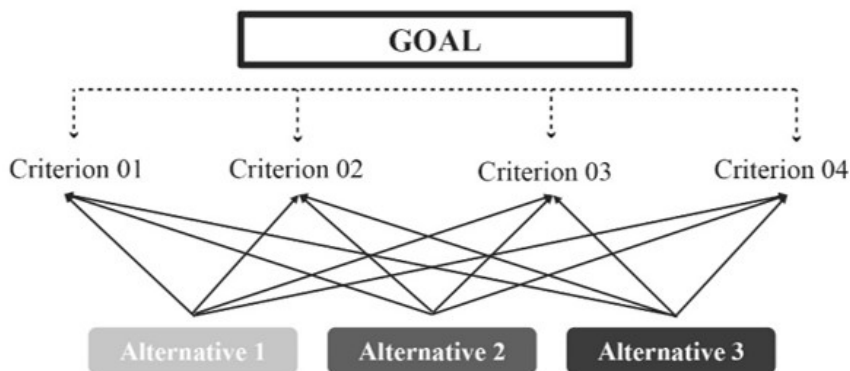


Figure 4. Flowchart showing how the AHP method works as pairwise comparison. Once the goal and the decision tree have been established, the alternatives are evaluated according to each criterion, weighted according to the importance of the goal.

The goal is to obtain a Sustainability Index (SI) that is given by the following Equation 4:

$$SI = \sum_{i=1}^n \alpha \cdot \beta \cdot \gamma \cdot (V_i) \tag{4}$$

Where n = total number of indicators; α = requirement weight (%); β = criterion weight (%); γ = indicator weight (%); V_i = is the so-called value index, taken by value function (%).

The weights are obtained from the AHP approach and the value index from the MIVES value function as the following chart explains (Figure 5).

In the state-of-the-art, there are various types of decision trees to assess the sustainability of concrete structures and infrastructures, mainly elaborated by Spanish Universities through teams of experts who have evaluated the weights of each criterion according to data collected and personal experience.

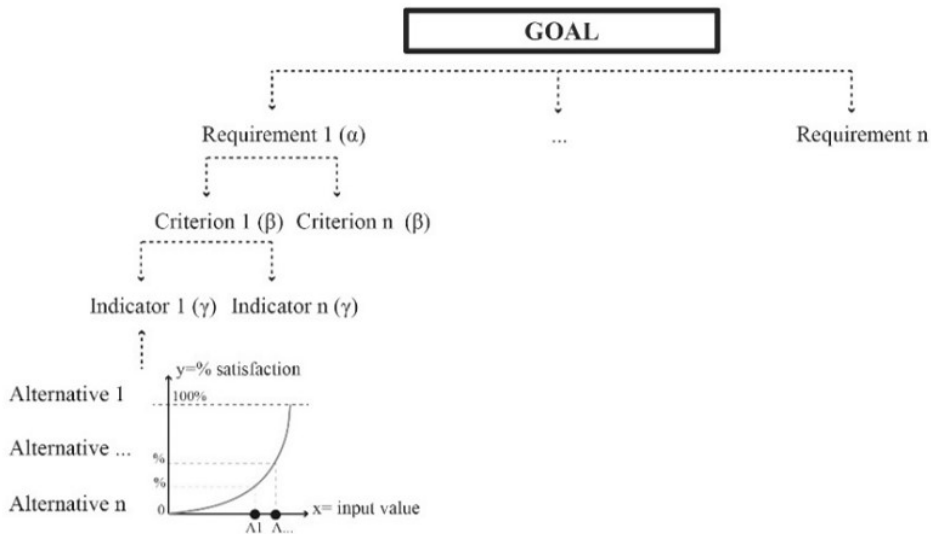


Figure 5. Decision tree taken as example with weights assigned and the value function correlated. It shows the association between value functions and indicators.

In the following image the selected criteria used to evaluate the different alternatives of intervention are specified (Figure 6):

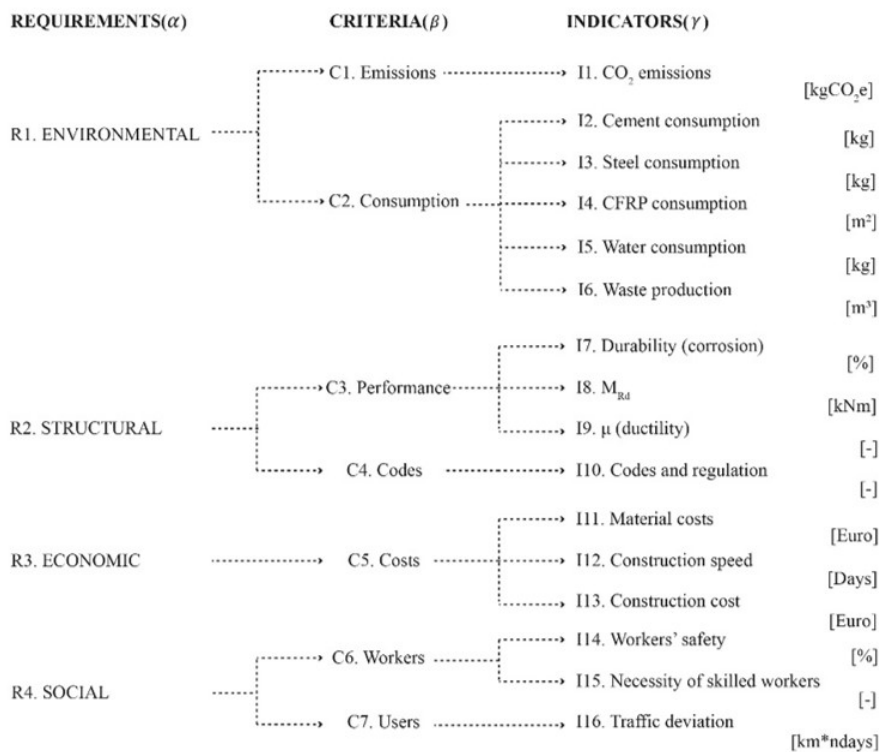


Figure 6. Decision tree for the considered study case, subdivided into Requirements (four clusters), Criteria (seven clusters) and Indicators (eighteen clusters).

The criteria selection methods refer to the assessment of the life cycle assessment of concrete infrastructures, evaluating macro-categories of economic, social and environmental indices, plus the structural component that is rarely considered. At this point the weights for each selected criterion must be established, making a comparison between the criteria themselves and defining the hierarchy. The weights expressed in percentages are verified and constructed through the matrix method (as explained later). Each of the steps, from the sub-criteria to the requirements of the macro-categories, is weighed through a specific function.

The values are taken as follows.

For each step, the decision maker derives a weight to evaluate each alternative. Once these steps have been carried out, it is necessary to get the summation of all obtained values to estimate the choice considered better through the parameters taken into consideration for every different alternative.

The most common comparison currently used to make judgments is still the one proposed by Saaty [37]. By assigning values ranging from 1 to 9 (possibly using odd numbers to increase the difference in judgments), the scale determines the relative importance of an alternative over another alternative [38].

The goal is to create a criteria comparison matrix according to the next model in Table 1.

Table 1. Criteria comparison following the AHP method.

	Criterion 1	Criterion 2
Criterion 1	1	rating
Criterion 2	1/rating (reciprocal)	1

Given an ordered pair of objects (n_i, n_j) of a level, the decision-maker expresses a judgment of comparison (n_{ij}) as follows (Equation 5):

$$n_{ij} = \frac{1}{n_{ji}} \text{ with } n_{ii} = 1 \forall i \tag{5}$$

At the end of the process, a weight is assigned to each level and the sum of the weights must be equal to 100% (Equation 6).

$$w = [w_1, \dots, w_i, \dots, w_j, \dots, w_n], \sum_{i=1}^n w_i = 1 \tag{6}$$

When the valuation method proposed by Saaty et al. is used, it is necessary to verify the so-called Consistency Ratio (CR), if it is less than 0.10, it is considered valid.

CR is a ratio between CI (Consistency index) and RI (Ratio Index).

In general, RI is a fixed number linked to the number of criteria (Table 2).

Table 2. RI reference values considering N as number of criteria.

N	1	2	3	4	5	6	7	8	9	10
RI	0	0	0.58	0.9	1.12	1.24	1.32	1.41	1.45	1.49

The matrix is considered always valid if the number of criteria is equal to one or two because the CR factor is usually used for complex matrices that need to be verified.

Once the decision tree and the weight have been elaborated, it is necessary to find the value function for each indicator, to assign an analytical validity and a precise preference. The V-value to be multiplied at the incidence calculated with the AHP methodology should therefore be obtained.

2.4 MIVES approach

The last step of this research involves the MIVES technique (Modelo Integrado de cuantificación de Valor para Edificación Sostenibles), developed by Spanish universities and institutions (UPC, UPV and Labein Tecnalia). While

the AHP method finds weight through matrix calculation, the MIVES approach finds the satisfaction value of each alternative through the study of an algorithm [39]. It is therefore necessary to calculate a value function for each indicator considered. Typical value functions can be: increasing or decreasing (monotony); S-shaped, linear, concave or convex (form). Other types of curves (such as the Gauss bell or parabola) can also be considered for particular cases. Monotony and form of functions are discretionary, according to the literature and the experience of decision makers.

The first step for creating functions is to consider the following parameters (Table 3).

Table 3. Possible monotonies and shapes of the functions.

Monotony	Shape
Increasing	Linear
Decreasing	Convex
	Concave
	S-shaped

The x-values for the reference indicator shall be set in the abscissa axis. The values of the extremes, x_{min} and x_{max} , are fixed and then the range that contains the trend of the function is established.

In the axis of the ordinates are inserted the maximum and minimum values of approval, which are always equal to 1 and 0, corresponding to 100% and 0% of satisfaction linked to the choice of the given alternative.

For instance, knowing the limit values of the function, the shape can be decided based on whether the decision maker wants the most collected data near the extremes (S-shape, as a combination between concave and convex) or constants (linear), etc.

Monotony is decided according to the liking of extreme values. For example, economic values curve is usually decreasing while carbon dioxide consumption may be increasing

The goal is to find the algorithm that finds the following two functions (Equation 7):

$$V_{ind} = A + B \cdot \left(1 - e^{-k \cdot \left(\frac{|x-x_{min}|}{c} \right)^P} \right) \tag{7}$$

where B is obtained by Equation 8:

$$B = \frac{1}{\left(1 - e^{-k \cdot \left(\frac{|x_{max}-x_{min}|}{c} \right)^P} \right)} \tag{8}$$

where unknown values have discretionary ranges depending on the curve the operator wants to obtain, x_{min} = the minimum x-axis of the space within which the interventions take place for the indicator under evaluation; x = the quantification of the indicator under evaluation (different or otherwise, for each intervention), P = the form factor that defines whether the curve is concave, convex, linear or an “S” shape: concave curves are obtained for values of $P < 1$, convex and “S” shaped forms for $P > 1$ and almost straight lines for values of $P = 1$. In addition, P gives an approximation of the slope of the curve at the inflection point. C approximates the x-axis of the inflection point. k approximates the ordinate of the inflection point. B is the factor that allows the function to be maintained within the value range of 0 to 1. A is usually equal to zero. If it is not equal to zero, the function is translated according to y, by a value equal to A [40], [41].

Parameters are chosen according to the monotony and the shape, as follows (Table 4 and 5).

Table 4. Parameters for increasing function.

Function	C	K	P
Linear	$C \approx x_{min}$	≈ 0	≈ 1
Convex	$x_{min} + ((x_{max} - x_{min})/2) < C < x_{min}$	< 0.5	> 1
Concave	$x_{min} < C < (x_{min} + (x_{max} - x_{min})/2)$	> 0.5	< 1
S-shaped	$x_{min} + ((x_{max} - x_{min})/5) < C < (x_{min} + 4(x_{max} - x_{min})/5)$	0.2/0.8	> 1

Table 5. Parameters for decreasing function.

Function	C	K	P
Linear	$C \approx X_{min}$	≈ 0	≈ 1
Convex	$X_{max} < C < (X_{max} + (X_{min} - X_{max})/2)$	< 0.5	> 1
Concave	$X_{min} - ((X_{min} - X_{max})/2) < C < X_{min}$	> 0.5	< 1
S-shaped	$(X_{max} - 4(X_{max} - X_{min})/5) < C < X_{max} - ((X_{max} - X_{min})/5)$	0.2/0.8	> 1

The first step is then the decision of the boundary ranges, x_{min} and x_{max} , to establish the domain of value functions. As alternatives deal with an existing column, maximum and minimum values cannot be derived from regulations or best practices. There are few case studies in the literature with alternatives for repair of the existing structures, so there are no predetermined procedures to understand how to select the extreme values. It emerged that among the four options considered, each time two of them should represent the extremes. This assumption is experimental and with this article, authors want to emphasize the possibility of intervening in the existing structures through the AHP multi-criteria analysis with the MIVES implementation. Chosen values are further described in the following section.

2.5 Indicators description

The values of the indicators for each alternative are evaluated as follows:

1. Emissions related to the production of cement include the first three steps declared in the Environmental Product Declaration (EPD) of the product (corresponding to the A1-A3 phases) of the Buzzi Unicem plant and published in “Report Cementi 2021” [42]. The reference factory is located in Sardinia, near the city of Nuoro. The emissions are taken equal to 862 [kgCO₂e] (Siniscola factory average), slightly above the company’s national average. The emissions parameter has also been included in the BIM environment modelling, to build the model following the seven dimensions. The emissions related to the A4 phase are then estimated and added to the total. The emissions related to the transport from the manufacturer to the batching plant, and from the latter to the construction site are estimated by evaluating the number of trucks (heavy vehicles) used for each alternative. The calculation refers to Commission Regulation EU 2017/2400 of 12 December 2017. The new VETCO software was used, an application developed by the European Commission and already became mandatory in 2019 for some categories of heavy vehicles. The vehicles hypothesized to be used in the case study can be classified in category 4 (truck carrying more than 16 tons), with an axle arrangement of four and a weight of about 40 tons. Regarding steel products emissions, they are taken from the environmental product declaration of an Italian steel company. The values include stages A1 to A4. Finally, emissions associated with the FRP production stages are deduced from the literature [43].
2. Data referring to the volume of the concrete are extracted from the BIM model (Figure 7). Knowing the data related to the mix design and the specific weight, it was possible to obtain the kg of cement needed.

A	B	C	D	E	F	G	H
Family	Volume	Pile diameter	Pile height	Reinforcement volume	Volume dep	Cost	Emission CO2
Pile	4.31 m³	1.200	3.850	111029.29 cm³	4.19 m³	€716.50	1084.72
Pile 2	4.31 m³	1.200	3.850	111029.29 cm³	4.19 m³	€716.50	1084.72
Total	2 8.61 m³			222058.59 cm³	8.39 m³	€1433.00	2169.44

Figure 7. Schedule example taken by BIM modelling of the elements. Each parameter has references and formulas inside to obtain the shown values.

3. Regarding the consumption of steel, all the rebars necessary for the realization of various interventions are modelled in a BIM environment and the kg of material used are obtained.
4. Modelling the CFRP components proved challenging. To get the intended result (the surface used), it is required to model a structural wall element and insert as many as the number of layers designed. CFRP modelling, like several other actions on the current structures, has several limitations in the BIM environment.
5. The water consumption is equal to a percentage of the selected mix design.
6. The production of waste is based on the simple calculation of the volumes involved in the disposal of the demolished portions.

7. Figure 8a shows the time-dependent evolution of the chloride-induced corrosion, expressed as the loss of reinforcement section or the ratio between corroded section A_{pt} and original bar section A'_s , predicted from multi-physics FE-based simulations for each intervention methodology [44]. As regards the first option, the replacement of the pier with a new one designed as the original without providing for a regulatory adaptation, there will be a loss of the reinforcement area after 50 years of about 11%. In Alternative 2, ultra-high performance concrete is used as repair materials, in this way, thanks to its great compactness, increasing the durability of RC members subjected to corrosive conditions. In this instance, the chloride penetration into the concrete is prevented since the diffusion coefficient is two to three orders of magnitude lower than that of ordinary strength concrete. Therefore, the results of Figure 8a, where rebar cross sections over time, are reasonable. It should be mentioned that the FRP jacketing used in Alternative 3, in addition to recovering the mechanical performance of the pier, can also serve to improve its durability as the external wrapping can significantly reduce the corrosion rate. Consequently, results do not show reduction of rebar cross sections also in Alternative 3. Finally, the intervention number four appears to have the worst behaviour when exposed to a corrosive environment. This is because the new bars placed in the repaired zone at the base have a smaller diameter (20 mm) than the original ones (24 mm). Subsequently, it has been estimated that the rebars will lose 15% of their cross section after 50 years.

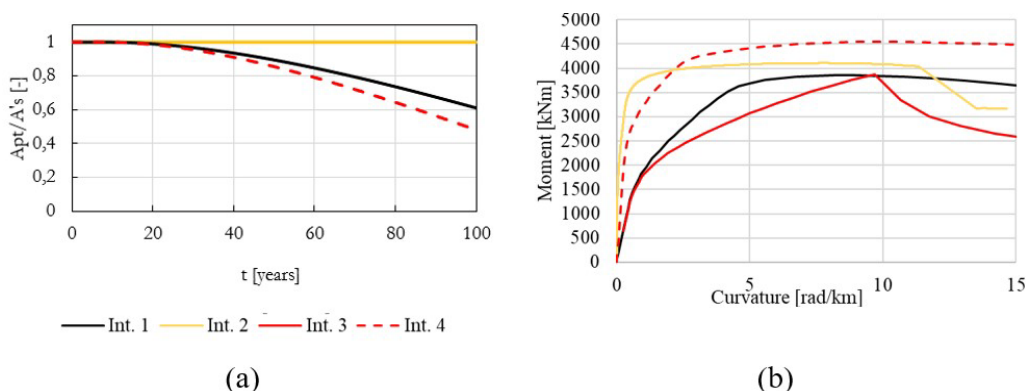


Figure 8. (a) Rebar section reduction over time (b) moment-curvature at the time of the repairment.

8. The model's structural criterion evaluates the structural capabilities of various interventional options. The variables taken into account are the retrofitting's capability to enhance durability, strength (load bearing capacity) and ductility. The repairs of the column are designed to restore the resistant moment of the original un-corroded pier. However, the engineering of the solutions meant that the final results are slightly different from the target values. There are slight differences in the resistant moment among the four solutions, with values ranging from 3868 to 4546 kNm (Figure 8b).
9. On the other hand, the differences when it comes to ductility are not minor. In particular, it should be noted that due to the material's brittle behaviour, the ductility was set to 0 in the case of the FRP intervention.
10. The presence of codes and regulations is considered a fundamental parameter and often overlooked. The importance of its inclusion refers to the difficulty of designing retrofitting interventions. It is indicated with zero the absence of current legislation and with one the presence. An intermediate parameter equal to 0.5 to consider the presence of non-prescriptive guidelines at the International level for CFRP (UNI EN 1015-12 2002; ASTM D 7234 2005) and Italian (CNR-DT 200 R1/2013 introduced in 2014 [26]).
11. Material costs are computed in the BIM environment by adding the cost parameter to each element created. The prices are taken from the Sardinia region's price list for construction. However, some costs that are not predicted in the latter are hypothesised by using instances from the literature or comparable items on the market. This is the case of the mechanical connectors that anchor the vertical FRP to the base of the pier. Similarly, as this product is not currently marketed in Italy, the cost of UHPFRC is estimated to be five times the price of an NSC [45].
12. As the duration of construction work is closely related to construction costs, it is considered a relevant parameter. The data are taken from literature [24], [25], [29] and only the actual days of work were considered, resulting in 10 days for the first alternative, and four for the remaining, respectively.

13. The regional construction price list for Sardinia is used to determine the construction costs, which also include safety costs. The construction site is designed and all the processes are planned, including safety equipment, site arrangements, the electrical panel, the scaffolding, etc. As the cost of machined reinforcing bars is not mentioned in the price list, reference is made to a similar procedure whose price is in the price list of a company in the steel industry.
14. The value of the safety risk for the workers is evaluated according to T. U. 81/08 and the modalities of the drafting of the document of Risk Assessment. This calculation refers to the Risk Matrix (Table 6), where it is possible to balance the probability of occurrence of a dangerous event and the damage it would cause.

Table 6. Values related to the risk matrix.

Risk	Improbable	Unlikely	Probable	Most likely
[R]	[P1]	[P2]	[P3]	[P4]
Slight damage	LOW	LOW	MEDIUM	MEDIUM
[E1]	[P1]X[E1]=1	[P2]X[E1]=2	[P3]X[E1]=3	[P4]X[E1]=4
Significant damage	LOW	MEDIUM	HIGH	HIGH
[E2]	[P1]X[E2]=2	[P2]X[E2]=4	[P3]X[E2]=6	[P4]X[E2]=8
Serious damage	MEDIUM	HIGH	HIGH	VERY HIGH
[E3]	[P1]X[E3]=3	[P2]X[E3]=6	[P3]X[E3]=9	[P4]X[E3]=12
Very serious damage	MEDIUM	HIGH	VERY HIGH	VERY HIGH
[E4]	[P1]X[E4]=4	[P2]X[E4]=8	[P3]X[E4]=12	[P4]X[E4]=16

The matrix allows obtaining values that, multiplied by reduction factors (Table 7) and summed among all the expected works, allows to calculate the percentage of risk. The risks considered are: falling and sliding; soar; falling of materials from above; failure of mechanical parts of machinery; contacts with machines or machines in motion; collapse or replenishment of deposited materials; disarmament; electrocution; electrocution due to the use of electrical equipment; jets, splashes; investment; manual handling of loads, powders, fibres; splinters, punctures, cuts, abrasions, wounds; overturning of the subsidence medium; noise; vibrations.

Table 7. Values related to risk reduction [46].

Preventive and protective measures implemented	k
General information training	0.95
Specific training	0.9
Category PPE training	1.0
Operating procedures and instructions	0.9
First aid and emergency	1.0
Health surveillance	0.9
Accidents missed accidents and near miss	0.9
PPE / DPC	0.8
Total attenuation coefficient (Ktot)	0.5

15. The ease of finding qualified and skilled workers is equal to zero to indicate situations in which it is considered particularly easy and there is no need for workers with special certifications, equal to one to underline greater difficulties. As for the regulations, an intermediate value has been inserted.
16. The traffic deviation is calculated considering the distance between Oristano (the closest city centre) and the bridge endpoint. To get to the latter there is only provincial road 56. The time of closure of the infrastructure (30 days for the first alternative, 10 for the second, 7 for the third and 10 also for the last one) is assessed and multiplied by the kilometres of the journey to account for the traffic deviation (1.8 km). This value is chosen because it is possible to derive as a result the CO₂ emissions, the journey time and the cost of fuel.

It is then elaborated the following table with the grouped values for all the Indicators of each alternative (Table 8).

Table 8. The values of each alternative to be associated with each indicator are given. Each time two values will be considered as X_{min} and X_{max} .

Indicators	Units	A1	A2	A3	A4
I1. CO ₂ emissions	[kgCO ₂ eq]	12110.81	589.36	521.70	1029.91
I2. Cement consumption	[kg]	10584.00	683.71	605.22	1194.79
I3. Steel consumption	[kg]	4066.30	244.83	296.94	238.13
I4. CFRP consumption	[m ²]	0.00	0.00	21.11	0.00
I5. Water consumption	[kg]	5292.00	108.70	89.10	468.00
I6. Waste production	[m ³]	26.57	0.66	0.66	0.39
I7. Durability (corrosion)	[%]	0.89	1.00	1.00	0.85
I8. M _{Rd}	[kNm]	3947.00	4087.00	3868.90	4546.00
I9. μ (ductility)	[%]	5.50	8.39	4.04	6.35
I10. Codes and regulation	-	1.00	0.00	0.50	0.00
I11. Material costs	[Euro]	9415.71	1045.30	35707.92	1163.16
I12. Construction speed	[days]	10.00	4.00	4.00	4.00
I13. Construction cost (including safety cost)	[Euro]	31348.71	17666.00	53732.40	17266.40
I14. Workers' safety	-	0.32	0.28	0.27	0.26
I15. Necessity of skilled workers	-	0.00	1.00	0.50	0.00
I16. Traffic deviation	[Km*n _{days}]	54.00	18.00	12.60	18.00

3 ANALYSIS AND RESULTS

Once the hierarchies, weights and extreme values are established, a code in Python language is setup to carry out the analysis and to find the most sustainable alternative based on the opinion expressed by the decision makers. In order to determine which of the proposed interventions is suitable for each of the four requirements α —environmental (R1), structural (R2), economic (R3), and social (R4)—each requirement is first investigated separately. Following this initial study, the authors combined the requirements by assigning them different weights to properly appreciate how they affect the ranking and the optimum solution. Conversely, the weights assigned to each criterion and indicator remained constant throughout the investigation. Specifically, the analysis starts with the structural requirement, which is discussed in detail, including the specifics of the code and the procedure followed to assign a value function curve and how the satisfaction values for each indicator is obtained. Each requirement is described separately below. All the first acronyms expressed in uppercase on Python have been indicated in lowercase to facilitate the algorithm and avoid mistakes.

3.1 Structural

The structural requirement (R2) is divided into 2 criteria, Performance (C3) and Codes (C4), respectively. These are further separated into 4 indicators: durability (I7), resistant moment MRd (I8), and ductility (I9) for criterion C3, and codes and regulations (I10) for criterion C4. The structural performances values are obtained from the sectional analysis carried out in Opensees for each intervention, as previous described in Section 2.5. The presence of codes and regulations is taken into account by indicating with zero the absence of current legislation and with 1 the presence. An intermediate parameter equal to 0.5 to consider the presence of non-prescriptive.

Values of approval are obtained to carry out the MIVES analysis by describing them as functions of each indication as shown in Figure 9 (the “suggested” curve is automatically processed by the algorithm, while the “chosen” is the curve selected by the decision maker).

On the x-axis are reported the values of each indicator, ranging between the minimum and maximum values obtained thought the analysis for each parameter. As the weight and the value of approval are established, the MIVES analysis is performed though the python code as shown in Figure 10.

The matrix with preferences is identified as 'pcm'. The weights, expressed through vectors, are indicated as 'weights' and follow the order of the decision tree. The consistency index is denoted by 'cr' as a number. Finally, the values associated with each final indicator are expressed as a vector with the alternatives in order (alternative 1 to the first place, alternative 2 to the second,...). The outcomes for the structural requirements are presented below (labelled as SI or sustainability index). The second alternative which includes the rebar replacement with UHPFRC cover resulted to be the more sustainable option when it comes to structural requirement.

$$SI\ 1 = 0.224 + 0.044 + 0.246 + 0.170 = 0.684$$

$$SI\ 2 = 0.373 + 0.052 + 0.373 + 0.000 = 0.798$$

$$SI\ 3 = 0.373 + 0.040 + 0.146 + 0.087 = 0.646$$

$$SI\ 4 = 0.179 + 0.083 + 0.298 + 0.000 = 0.560$$

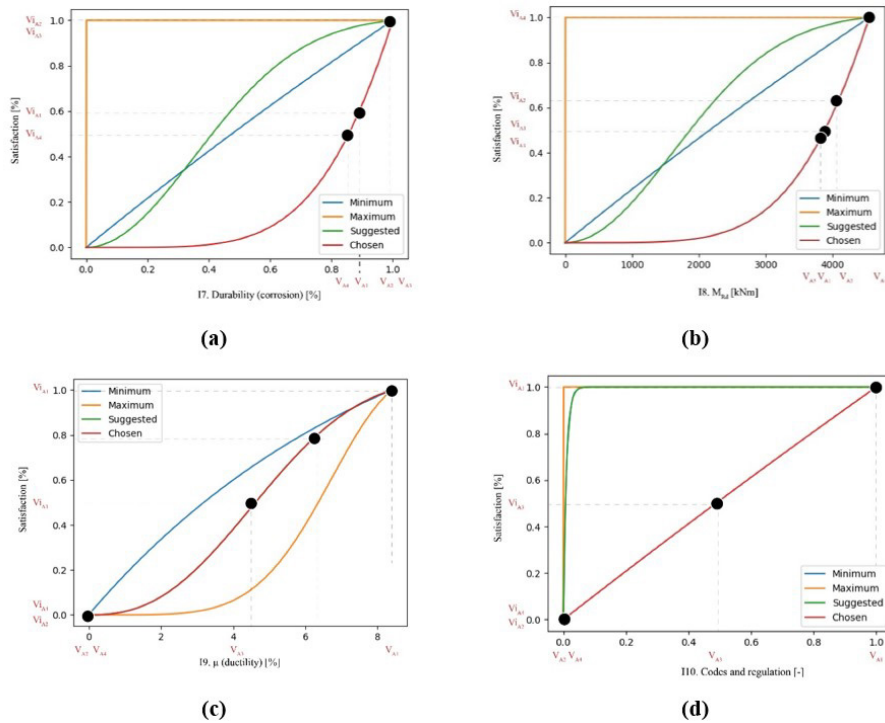


Figure 9. Value function curves for: **(a)** indicator I7, with a convex shape and increasing monotony (chosen parameters are: $p_c = 5.0$, $c_c = 0.5$ and $k_c = 0.01$), **(b)** indicator I8, with a convex shape and increasing monotony (chosen parameters are: $p_c = 5.0$, $c_c = 2200.0$ and $k_c = 0.01$), **(c)** indicator I9, with a s-shaped shape and increasing monotony (chosen parameters are: $p_c = 2.5$, $c_c = 4.19505$ and $k_c = 0.5$), **(d)** indicator I10, with a linear shape and increasing monotony (chosen parameters are: $p_c = 1.0$, $c_c = 0.001$ and $k_c = 0.0001$).

```
[{'parent_criterion': 'result', 'level': 0, 'level name': 'requirements',
'names': ['r2'], 'pcm': array([[1.]]), 'weights': [1.0], 'cr': 0}],

[{'parent_criterion': 'r2', 'level': 1, 'level name': 'criteria', 'names':
['c3', 'c4'], 'pcm': array([[1., 5. ],
[0.2, 1. ]]),
'weights': [0.833, 0.166], 'cr': 0}],

[{'parent_criterion': 'c3', 'level': 2, 'level name': 'indicators', 'names':
['i7', 'i8', 'i9'], 'pcm': array([[1., 4., 1. ],
[0.25, 1., 0.25],
[1., 4., 1. ]]),
'weights': [0.444, 0.111, 0.444], 'cr': 0.0,
'values': [[0.597, 1.0, 1.0, 0.483], [0.540, 0.632, 0.493, 1.0], [0.665, 1.0,
0.388, 0.803]]},

{'parent_criterion': 'c4', 'level': 2, 'level name': 'indicators', 'names':
['i10'], 'pcm': array([[1.]]),
'weights': [1.0],
'cr': 0,
'values': [[1.0, 0.0, 0.512, 0.0]]}]c
```

Figure 10. Algorithm results for structural requirement.

3.2 Environmental

The environmental requirement (R1) is divided into 2 criteria, Emissions (C1) and Consumption (C2), respectively, and in six indicators (I1. CO2 Emissions, I2. Cement Consumption, I3. Steel consumption, I4. CFRP consumption, I5. Water consumption, I6. Waste production) (Figure 11).

Regarding environmental requirement the most sustainable choice, according to the decisions taken, is again the second alternative. All alternatives, except the first, give however valid results. Values obtained for the alternative 1 are often used as extreme values of the functions, representing 0% of the satisfaction.

$$SI\ 1 = 0.000 + 0.000 + 0.000 + 0.036 + 0.000 + 0.000 = 0.036$$

$$SI\ 2 = 0.465 + 0.170 + 0.131 + 0.036 + 0.077 + 0.036 = 0.915$$

$$SI\ 3 = 0.470 + 0.172 + 0.125 + 0.000 + 0.078 + 0.036 = 0.881$$

$$SI\ 4 = 0.430 + 0.168 + 0.133 + 0.036 + 0.068 + 0.036 = 0.871$$

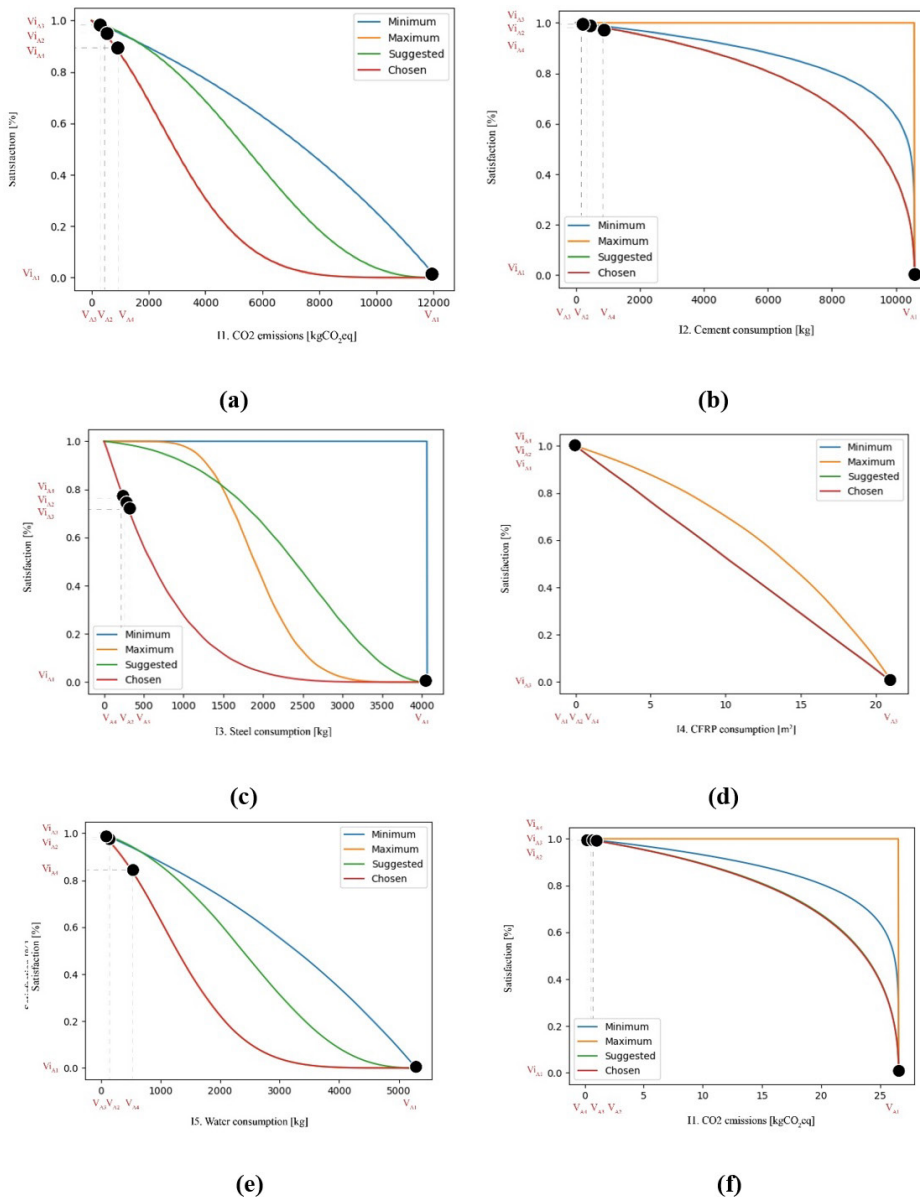


Figure 11. Value function curves for: (a) indicator I1, with a s-shaped shape and decreasing monotony ($p_c = 5.0$, $c_c = 9688.0$ and $k_c = 0.8$), (b) indicator I2, with a concave shape and decreasing monotony ($p_c = 0.5$, $c_c = 2646.0$ and $k_c = 0.75$), (c) indicator I3, with a convex shape and decreasing monotony ($p_c = 5.0$, $c_c = 2000.0$ and $k_c = 0.01$), (d) indicator I4, with a linear shape and decreasing monotony ($p_c = 1.0$, $c_c = 21.11$ and $k_c = 0.01$), (e) indicator I5, with a s-shaped shape and decreasing monotony ($p_c = 5.0$, $c_c = 4233.0$ and $k_c = 0.8$), (f) indicator I6, with a concave shape and decreasing monotony ($p_c = 0.5$, $c_c = 7.0$ and $k_c = 0.75$).

3.3 Economic

The economic requirement (R3) comprehends the criterion C5. Costs further organized in three indicators: I11. Material costs, I12. Construction speed, I13. Construction costs (Figure 12). SI values show two most suitable alternative: the second one and the fourth alternative, where the column is strengthened by a concrete base jacketing.

$$SI\ 1 = 0.372 + 0.000 + 0.348 = 0.720$$

$$SI\ 2 = 0.396 + 0.120 + 0.376 = 0.892$$

$$SI\ 3 = 0.000 + 0.120 + 0.000 = 0.120$$

$$SI\ 4 = 0.396 + 0.120 + 0.376 = 0.892$$

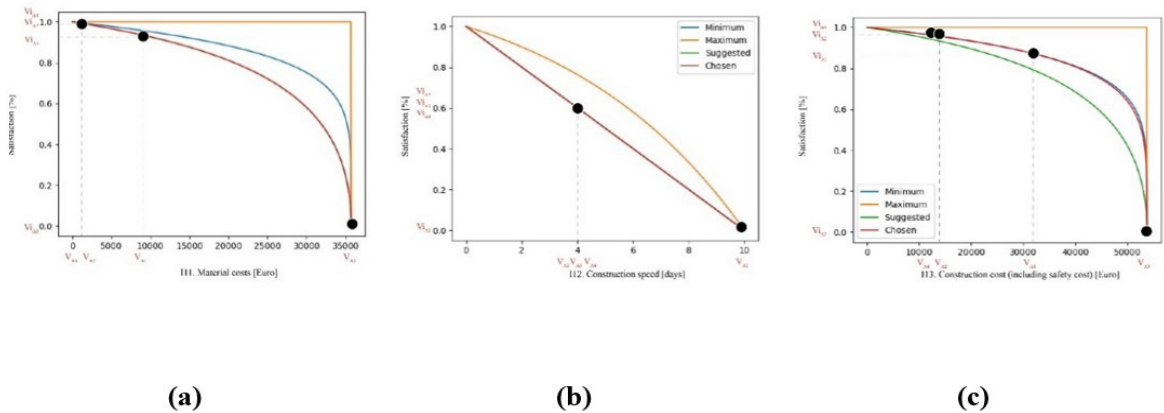


Figure 12. Value function curves for: (a) indicator I11, with a concave shape and decreasing monotony ($p_c=0.5$, $c_c = 8927.0$ and $k_c = 0.75$), (b) indicator I12, with a linear shape and decreasing monotony ($p_c=1.0$, $c_c = 10.0$ and $k_c = 0.01$), (c) indicator I13, with a concave shape and decreasing monotony ($p_c=0.25$, $c_c = 15000.0$ and $k_c = 0.75$).

3.4 Social

The social requirement (R4) is divided in two criteria, C6. Workers and C7. Users, respectively, and three indicators, I14. Workers' safety, I15. Necessity of skilled workers, I16. Traffic deviation (Figure 13). The most suitable alternative is the fourth.

$$SI\ 1 = 0.36 + 0.13 + 0.0000 = 0.49$$

$$SI\ 2 = 0.40 + 0.00 + 0.20 = 0.60$$

$$SI\ 3 = 0.41 + 0.06 + 0.25 = 0.72$$

$$SI\ 4 = 0.41 + 0.13 + 0.20 = 0.74$$

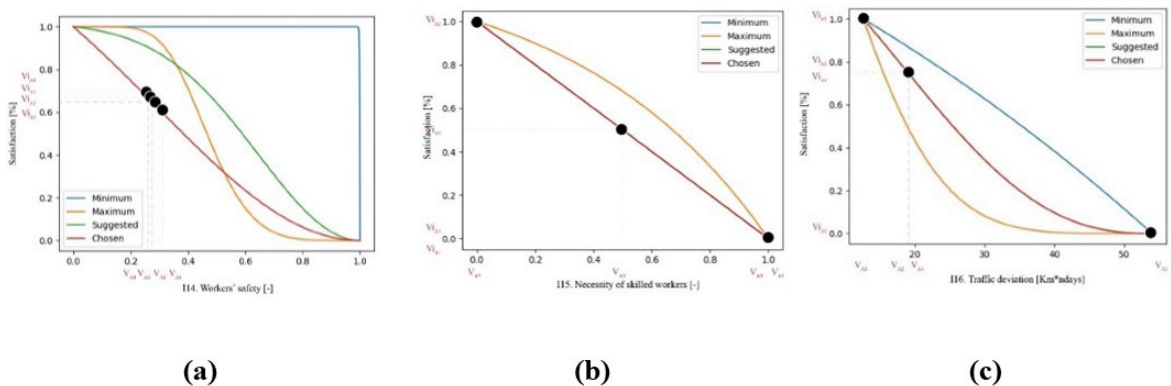


Figure 13. Value function curves for: (a) indicator I14, with a convex shape and decreasing monotony ($p_{sp}=2.00$, $c_{sp} = 0.10$ and $k_{sp} = 0.01$), (b) indicator I15, with a linear shape and decreasing monotony ($p_{sp} = 1.00$, $c_{sp} = 1.00$ and $k_{sp} = 0.01$), (c) indicator I16, with a convex shape and decreasing monotony ($p_{sp} = 2.50$, $c_{sp} = 33.30$ and $k_{sp} = 0.50$).

4 DISCUSSION

As previously stated, it is crucial to consider a variety of factors while carrying out structural rehabilitation, including both the problem of sustainability and the commonly encountered problem of cost reduction. Contrary to common belief, the themes are not necessarily in opposition to one another. As a result, it is possible to identify a solution that addresses both while utilizing limited resources, consuming less energy, and cutting costs. The application of this methodology is an innovative and relevant evaluation that, involving both widespread and theoretical solutions for the rehabilitation of R.C. bridge column, has rarely been made.

After comparing the alternatives individually, a first sensitivity attempt is made by assuming three potential weight combinations for the requirements. Through matrix study, more in-depth sensitivity analysis can be seen as a future development. As a result of having to conduct the analysis with a small group of decision-making professionals, the weights have been varied to give a general and impersonal point of view. The weights' variation has suggested in fact that further study is required to determine whether the results are reliable. Although the results themselves are not particularly remarkable, they do enable the reader to comprehend the analysis and research methodology.

Based on literature using MIVES and AHP for structures in RC, the authors decided to assess (Scenario1) the environmental requirement equal to 40%, economic equal to 40%, social equal to 14% and structural equal to 6% (Table 9). For the first evaluation the best intervention turns out to be the second, so the indices are verified to see if it changed the final judgment. About the second assessment (Scenario 2), changing the weights and using for the environmental requirement= 40%, economic= 32%, social= 10% and structural= 18%, the second one (alternative A2) results in in the best, with Alternative 4 following. Scenario 3 is evaluated using for the environmental requirement= 30%, economic= 42%, social= 10% and structural= 18%, where the most suitable one is, also in this case, the second one.

Table 9. Different scenarios with SI results.

	Scenario 1	Scenario 2	Scenario 3
SI 1	0.542	0.546	0.485
SI 2	0.855	0.844	0.853
SI 3	0.540	0.567	0.503
SI 4	0.842	0.809	0.780

By changing the weights, it is possible to appreciate the dynamics that cause one alternative to be characterized as more sustainable than the others. It is also possible to identify alternatives that are acceptable in multiple scenarios and those that result less sustainable in all or many scenarios. The sustainability indices (defined, as mentioned previously, with SI) are compared, which include the ratings obtained according to the values, for each index, and their multiplication by the weights of each branch of the decision tree. The three different scenarios have been chosen because they show possible preferences of the clients, designers, users, and other stakeholders, and plausible choices of the decision maker based on what it is requested to deepen in a given situation and what is meant in a specific one with sustainability. Consequently, SI are first analysed individually (considering the other requirements with a value equal to 0%) and then all the requirements are considered together. This could give a broader view. Taking the requirements individually (with each equal to 100%), it is clear how the second alternative (replacement of the bars), results to be the most sustainable in three requirements out of four (environmental and economic structural on a par), is the most suitable. For the social aspect, this solution results second only to the A4 intervention, which involves a concrete base jacketing; nonetheless, they are comparable from an economic perspective. These initial analyses suggest that there is already a clear preference for two alternatives (A2 and A4) over the others (A1 and A3). This is likely due to complete replacement A1 being the least efficient solution in most value functions (without considering the weights) because of the large consumption of material compared to the others. Intervention with the CFRP results unfavourable mainly because of costs, but also because of considerable emissions. Despite being the most common in practice, A1 and A3 should be discarded. This demonstrates how even more complex interventions may turn out to be the most cost-effective and environment friendly if properly investigated. Evidently, weight addition seems to support earlier analyses. Even after weights are added, the options that were ranked as optimal are still preferable. Despite this, there is a slight but significant preference for the A2 choice over the A4 alternative in the third scenario. On the contrary, two final values (SI2 and SI4) in the first scenario are closer because the social factor is given more weight than the structural one while the social and economic aspects are assumed equally. In fact, the two choices are very close for SI in the three analyses carried out. It is evident how modifying the importance of a requirement allows to vary the result. It must therefore be clear what the goal should be, in terms of sustainability, to avoid ambiguous and inconsistent results. In the second

scenario, the results remain unchanged. In fact, by increasing the preference for the structural requirement, the gap between alternative A2 and A4 increases. In the last analysis, however, the single criterion that determines whether the two options are equally acceptable differs. As consequence, the A2 alternative that involve replacing the bars is confirmed as the best choice. The second alternative, therefore, despite being the most challenging from a technological point of view, has proved to be the most sustainable overall and the most suitable from all points of view analysed.

The best alternative is an interesting example of how new retrofit solutions may be advantageous and sustainable, and how they can eventually replace rehabilitations options more conventional and ineffective from both an economic and environmental perspective. The replacement of the bars (alternative A2) is a valid option as it tends to consider long-term sustainability and increases awareness on the maintenance issue. In fact, the corroded bars, due not only to the strength but also to the ductility reduction, could cause serious long-term local and global damage if not replaced. Corrosion is still one of the most sensitive issues for infrastructure, as it leads to leakage of resistant section and ductility, causing a domino effect to the mechanical strength of the structure. Through matrix study, more in-depth sensitivity analysis can be seen as a future development.

5 CONCLUSIONS

In this paper a multi-criteria decision making approach is applied to assess the sustainability of bridge's column rehabilitation techniques. The analysis allows to rank the four rehabilitation solutions considered and select among them the intervention that most closely match the desired outcome. Therefore, this method enables all parties involved, including clients, designers, users, and other stakeholders, to select the intervention that is appropriate for the needs that must be addressed beforehand.

The primary subject of this article is sustainability, which is examined from a variety of perspectives, including those related to the environment, which is frequently investigated, the economy, which is always considered critical, society, and technology (usually not considered). This article has taken 16 indicators into account (referred to in paragraph 2.5). More of aspects were evaluated by the authors, who then ranked them. This serves to restrict the analysis to get less dispersed results and because raising the parameters decreases the experts' reliability.

The aesthetic component is undoubtedly an interesting aspect that was neglected. Replacement of the pier (A1) and replacement of the bars (A2) solutions have less impact than the other two options (A3 and A4). Future environmental considerations could also be integrated in the future, such as: noise pollution, chemical one and dust.

The repairing alternatives examined have been proposed by researchers to repair columns severely damaged. Each intervention has been properly designed, modelled, analysed and applied to a real case study in order to go forward with the bill of quantities, safety costs and appreciate the social impacts on workers. CO₂ emissions quantities for each material involved have been taken from product's environmental product declaration. Transport scenarios have been imagined evaluating CO₂ emissions due to transportation.

The MIVES analysis performed has a great deal of potential as it enables individuals or groups of individuals to evaluate new constructions or interventions on existing structures to preserve the environment and cut costs. To fully comprehend the changes in values and the impact that the weights have, the authors employed a novel approach by first looking at the requirements without the assigned weights and then with them. The sensitivity of the decision maker is a crucial component of the suggested technique. Obviously, the goal to be achieved must be clear from the outset and the choices, both in terms of weights and values, must always be consistent and coherent. Nevertheless, it is necessary to stress the importance of sensitivity analysis to assess the variation in the results (SI) and to understand if they reflect the initial decisions.

In this preliminary study, the number of decision makers being rather limited, a new tool was introduced that allowed to establish a range within defining the valuable functions. As results, the authors defined minimum, maximum and recommended curves by the algorithm. To comprehend the effectiveness of the method, however, more research and development are required. The results collected show how the studies conducted are sensitive to the desired outcome as well as the viewpoint of the experts. This strategy is consequently discretionary and delicate. Nevertheless, in the opinion of the authors it is interesting that replacement of the reinforcing bars was recommended in each of the hypothetical scenarios despite being the less known and seemingly more difficult alternative to implement. Future advances will involve the integration of additional costs and sustainability factors across the entire life cycle of the structure.

ACKNOWLEDGEMENT

The authors thank Gianlorenzo Sabatini for his support in reviewing the Python code, and Matheus Morais for reviewing the Portuguese abstract.

The authors also want to thank BuzziUnicem.

REFERENCES

- [1] C. Baglivo, P. M. Congedo, and F. Fazio, “Multi-criteria optimization analysis of external walls according to ITACA protocol for zero energy buildings in the Mediterranean climate,” *Elsevier Build. Environ.*, vol. 82, pp. 467–480, 2014.
- [2] B. Suhendro, “Toward green concrete for better sustainable environment,” *Procedia Eng.*, vol. 95, pp. 305–320, 2014, <http://dx.doi.org/10.1016/j.proeng.2014.12.190>.
- [3] American Concrete Institute, *Cement and concrete terminology*, ACI 116R-90, 1990.
- [4] B. Kiani, R. Y. Liang, and J. Gross, “Material selection for repair of structural concrete using VIKOR method,” *Case Stud. Constr. Mater.*, vol. 8, pp. 489–497, 2018.
- [5] W. Kloepffer, “Life cycle sustainability assessment of products,” *Int. J. Life Cycle Assess.*, vol. 13, no. 89, 2008, <http://dx.doi.org/10.1065/lca2008.02.376>.
- [6] J. Fava, A. Smerek, A. Heinrich, and L. Morrison, *The role of the Society of Environmental Toxicology and Chemistry (SETAC) in Life Cycle Assessment (LCA) development and application*. Dordrecht, Netherlands: Springer, 2014, https://doi.org/10.1007/978-94-017-8697-3_2.
- [7] D. Georgescu, R. Vacareanu, A. Aldea, A. Apostu, C. Arion, and A. Girboveneau, “Assessment of the sustainability of concrete by Ensuring performance during structure service life,” *Sustainability*, vol. 14, no. 2, pp. 617, 2022.
- [8] International Organization for Standardization, *Environmental management - Life cycle assessment - Principles and framework - Amendment 1*, ISO 14040:2006/AMD 1:2020, 2020.
- [9] International Organization for Standardization, *Environmental management - Life cycle assessment - Requirements and guidelines - Amendment 2*, ISO 14044:2006/AMD 2:2020, 2020.
- [10] VOS Viewer, *VOS Viewer version 1.6.18*, Jan. 2022.
- [11] E. Asadi, A. M. Salman, and Y. Li, “Multi-criteria decision-making for seismic resilience and sustainability assessment of diagrid buildings,” *Eng. Struct.*, vol. 191, pp. 229–246, 2019, <http://dx.doi.org/10.1016/j.engstruct.2019.04.049>.
- [12] V. Penadés-Plà, T. García-Segura, J. V. Martí, and V. Yepes, “A review of multi-criteria decision-making methods applied to the sustainable bridge design,” *Sustainability*, vol. 8, pp. 1295, 2016.
- [13] S. Abu Dabous, “A decision support methodology for rehabilitation management of concrete bridges,” Ph.D. dissertation, Concordia University, Montreal, Canada, 2008.
- [14] Z. Gao, R. Y. Liang, and T. Xuan, “VIKOR method for ranking concrete bridge repair projects with target-based criteria,” *Results Eng.*, vol. 3, pp. 100018, 2019.
- [15] B. Adey, R. Hajdin, and E. Brühwiler, “Risk-based approach to the determination of optimal interventions for bridges affected by multiple hazards,” *Eng. Struct.*, vol. 25, pp. 903–912, 2003.
- [16] C. Andrade and I. Martinez, “Use of indices to assess the performance of existing and repaired concrete structures,” *Constr. Build. Mater.*, vol. 23, pp. 3012–3019, 2009.
- [17] D. Lavorato et al., “Ultra-high-performance fibre-reinforced concrete jacket for the repair and the seismic retrofitting of Italian and Chinese RC bridges,” in *COMPADYN 2017*, Rhodes Island, Greece, June 2017, pp. 2149–2160.
- [18] D. Lavorato, C. Nuti, S. Santini, B. Briseghella, and J. Xue, “A repair and retrofitting intervention to improve plastic dissipation and shear strength of Chinese RC bridges,” in *IABSE 2015*, Geneva, Switzerland, Sept. 2015, pp. 1762–1767.
- [19] D. Lavorato, C. Nuti, B. Briseghella, S. Santini, and J. Xue, “Rapid repair technique to improve plastic dissipation of existing Chinese RC bridges,” *Appl. Mech. Mater.*, vol. 847, pp. 204–209, 2016.
- [20] J. Xue, D. Lavorato, G. Fiorentino, A. V. Bergami, B. Briseghella, and C. Nuti, “FRP reinforcement to retrofit bridge pier after repair: experimental test results,” in *CICE 2021*, Istanbul, Turkey, Dec. 2021, pp. 449–458.
- [21] J. Xue et al., “Severely damaged reinforced concrete circular columns repaired by turned steel rebar and high-performance concrete jacketing with steel or polymer fibers,” *Appl. Sci. (Basel)*, vol. 8, no. 9, pp. 1671, Sep 2018.
- [22] J. D. Xue et al., “New solutions for rapid repair and retrofit of rc bridge piers,” *Rev. Port. Eng. Estrut.*, vol. 3, no. 4, pp. 105–112, Jul 2017.
- [23] J. Xue, D. Lavorato, S. Nie, J. Chen, B. Briseghella, and C. Nuti, “Research on seismic behaviors of RC circular pier with longitudinal rebar of reduced diameter and CFRP wrap,” *China J. Of Hwy. And Transp.*, vol. 35, no. 2, pp. 124–135, 2022, <http://dx.doi.org/10.19721/j.cnki.1001-7372.2022.02.011>.
- [24] A. Pelle et al., “Repair of reinforced concrete bridge columns subjected to chloride-induced corrosion with UHPFRC,” *Struct. Concr.*, 2022, <http://dx.doi.org/10.1002/suco.202200555>.
- [25] R. He, S. Grelle, L. H. Sneed, and A. Belarbi, “Rapid repair of a severely damaged RC column having fractured bars using externally bonded CFRP,” *Compos. Struct.*, vol. 101, pp. 225–242, Jul 2013, <http://dx.doi.org/10.1016/j.compstruct.2013.02.012>.
- [26] Consiglio Nazionale delle Ricerche. *Istruzioni per la Progettazione, l'Esecuzione ed il Controllo di Interventi di Consolidamento Statico mediante l'utilizzo di Compositi Fibrorinforzati*. Roma, Italy: CNR, 2013.

- [27] Italy. Assemblea Generale Consiglio Superiore, “Linee guida per la Progettazione, l’Esecuzione ed il Collaudo di Interventi di Rinforzo di strutture di c.a., c.a.p. e murarie mediante FRP”, *LL.PP.*, June 24, 2009.
- [28] J. B. Mander, M. J. Priestley, and R. Park, “Theoretical stress-strain model for confined concrete,” *J. Struct. Eng.*, vol. 114, pp. 1804–1826, 1988.
- [29] D. E. Lehman, S. E. Gookin, A. M. Nacamuli, and J. P. Moehle, “Repair of earthquake-damaged bridge columns,” *ACI Struct. J.*, vol. 98, no. 2, pp. 233–242, Mar 2001. Accessed: September, 8, 2022. [Online]. Available: <https://www.concrete.org/publications/internationalconcreteabstractsportal/m/details/id/10192>
- [30] Italian National Unification, *Edilizia e Opere di Ingegneria Civile - Gestione Digitale dei Processi Informativi Delle Costruzioni*, UNI 11337-1:2017, 2017.
- [31] J. J. Thakkar, *Multi-Criteria Decision Making: Studies in Systems, Decision and Control*. Singapore, Republic of Singapore: Springer, 2021.
- [32] P. L. Yu, *Multiple-Criteria Decision Making: Concepts, Techniques, and Extensions*. New York: Springer Science & Business Media, 2013.
- [33] O. S. Vaidya and S. Kumar, “Analytic hierarchy process: an overview of applications,” *Eur. J. Oper. Res.*, vol. 169, no. 1, pp. 1–29, 2006, <http://dx.doi.org/10.1016/j.ejor.2004.04.028>.
- [34] R. Kurda, J. Brito, and J. D. Silvestre, “CONCRETOP: a multi-criteria decision method for concrete optimization,” *Elsevier Environ. Impact Assess. Rev.*, vol. 74, pp. 73–85, 2019.
- [35] Great Britain Department for Communities and Local Government, *Multi-Criteria Analysis: A Manual*. Wetherby, West Yorkshire: Communities and Local Government, 2009.
- [36] R. R. Nadkarni and B. Puthuvayi, “A comprehensive literature review of multi-criteria decision making methods in heritage buildings,” *J. Build. Eng.*, vol. 32, 2020., <http://dx.doi.org/10.1016/j.jobbe.2020.101814>.
- [37] T. L. Saaty, *The Analytic Hierarchy Process: Decision Making in Complex Environments*. Boston, MA, USA: Springer, 1984. https://doi.org/10.1007/978-1-4613-2805-6_12
- [38] J. Mirosla and L. Chao, “Evaluation of advanced construction technology with ahp method,” *J. Constr. Eng. Manage.*, vol. 118, no. 3, 1992.
- [39] B. Alarcon, A. Aguado, R. Manga, and A. A. Josa, “Value function for assessing sustainability: application to industrial buildings,” *Sustainability*, vol. 3, pp. 35–50, 2011.
- [40] I. Anejo, *Manual Mives Modelo Integrado de Valor para Evaluaciones Sostenibles*, Barcelona: CIMNE, 2009.
- [41] O. Pons, A. de la Fuente, and A. Aguado, “The use of MIVES as a sustainability assessment MCDM method for architecture and civil engineering applications,” *Sustainability*, vol. 8, no. 5, pp. 460, 2016.
- [42] Buzzi Unicem, “Bilancio di sostenibilità 2021: dichiarazione consolidata di carattere non finanziario ai sensi del d.lgs. 254/2016.” <https://www.buzziunicem.it/> (accessed Aug. 16, 2022).
- [43] N. Stoiber, M. Hammerl, and B. Kromoser, “Cradle-to-gate life cycle assessment of CFRP reinforcement for concrete structures: Calculation basis and exemplary application,” *J. Clean. Prod.*, vol. 280, pp. 124300, 2021.
- [44] A. Pelle et al., “Time-dependent cyclic behavior of reinforced concrete bridge columns under chlorides-induced corrosion and rebar buckling,” *Struct. Concr.*, vol. 23, no. 1, pp. 81–103, 2022, <http://dx.doi.org/10.1002/suco.202100257>.
- [45] O. A. Qasim, “Comparative study between the cost of normal concrete and reactive powder concrete,” *IOP Conf. Series Mater. Sci. Eng.*, vol. 518, no. 2, pp. 022082, May 2019.
- [46] Italia, “Testo Unico per la Sicurezza sul Lavoro, Decreto Legislativo 9 aprile 2008, n. 81 Attuazione dell’articolo 1 della legge 3 agosto 2007, n. 123, in materia di tutela della salute e della sicurezza nei luoghi di lavoro,” *Gazz. Uff.*, 30 Apr. 2008.

Author contributions: VB: conceptualization, methodology, formal analysis, data curation, original draft preparation, writing—review and editing; CC: formal analysis, data curation, original draft preparation, writing—review and editing; AP formal analysis, data curation; BB, SS, DL, and CN: conceptualization, methodology, supervision.

Editors: Edna Possan, Mark Alexander



ORIGINAL ARTICLE

Circular economy in concrete production: Greenhouse Gas (GHG) emissions assessment of rice husk bio-concretes

Economia circular na produção de concretos: avaliação das emissões de Gases de Efeito Estufa (GEE) de bioconcretos com casca de arroz

Lucas Rosse Caldas^{a,b}

Arthur Ferreira de Araujo^a

Nicole Pagan Hasparyk^c

Francieli Tiecher^d

Guilherme Amantino^d

Romildo Dias Toledo Filho^a



^aUniversidade Federal do Rio de Janeiro – UFRJ, Programa de Engenharia Civil – PEC, Instituto Alberto Luiz Coimbra de Pós-Graduação e Pesquisa de Engenharia – COPPE, Rio de Janeiro, RJ, Brasil

^bUniversidade Federal do Rio de Janeiro – UFRJ, Faculdade de Arquitetura e Urbanismo – FAU, Programa de Pós-Graduação em Arquitetura – PROARQ, Rio de Janeiro, RJ, Brasil

^cEletrobras-Furnas, Goiânia, GO, Brasil

^dFaculdade Meridional – IMED, Passo Fundo, RS, Brasil

Received 02 February 2022

Accepted 17 September 2022

Abstract: Circular Economy (CE) is progressively attracting interest from construction sector stakeholders to support the development of products with higher amounts of recovered materials in order to decrease greenhouse gas (GHG) emissions. Concrete is one of the most used materials in the world and can be produced using waste as raw materials, including, bio-based sources, from both agricultural and forest activities. This research aims to assess the GHG emissions in the life cycle of innovative rice husk bio-concretes (RBC) in which rice husk (RH) and rice husk ash (RHA) are used as circular solutions. Four RBC, considering ordinary Portland cement replacement by 8% of RHA and, different contents of sand substitution by RH (0; 5 and 10%), were assessed. The Life Cycle Assessment (LCA) methodology was used, with a cradle-to-gate scope, using the GWPbio method, that contemplate the influence of biogenic carbon on the emissions reduction. Different transportation scenarios were evaluated considering the RBC production in different Brazilian regions. The service life of RBC in terms of carbon stock was also evaluated. Two carbon-performance indicators are also evaluated in terms of RBC compressive strength and thermal conductivity values. As the main conclusion, cement replacement by RHA alongside with sand replacement by RH are promising strategies to produce bio-concretes for specific applications, such as panels, partitions and façade elements, and to reduce its GHG emissions. However, this benefit varies according to RH availability, transport efficiency and RBC service life. The RBC can be considered a potential alternative for concrete industry, for specific applications, to reduce GHG emissions and can be developed where rice waste is an available source. This study contributes by presenting a new material and a methodology for the evaluation of life cycle GHG emissions of bio-concretes, which can help to promote a circular construction sector.

Keywords: concrete, circular economy, life cycle assessment, LCA, CO₂, biogenic carbon, rice waste.

Resumo: A Economia Circular (EC) está progressivamente atraindo o interesse dos *stakeholders* do setor de construção para apoiar o desenvolvimento de produtos com maior quantidade de materiais recuperados, a fim de diminuir as emissões de Gases de Efeito Estufa (GEE). O concreto é um dos materiais mais utilizados no mundo e pode ser produzido utilizando resíduos como matéria-prima, incluindo fontes de base biológica, tanto de atividades agrícolas quanto florestais. Esta pesquisa tem como objetivo avaliar as emissões de GEE no

Corresponding author: Lucas Rosse Caldas. E-mail: lucas.caldas@fau.ufrj.br

Financial support: R&D Project from ANEEL - National Electric Energy Agency, "Use of bio-concretes and Bio-MMFs with low environmental impact aiming the increasing of energetic efficiency of public buildings" – PD.0394-1719/2017.

Conflict of interest: Nothing to declare.

Data Availability: None.



This is an Open Access article distributed under the terms of the Creative Commons Attribution License, which permits unrestricted use, distribution, and reproduction in any medium, provided the original work is properly cited.

ciclo de vida de Bioconcretos de Casca de Arroz (BCA) inovadores em que a Casca de Arroz (CA) e as Cinzas de Casca de Arroz (CCA) são empregadas como soluções circulares. Foram avaliados quatro BCA, considerando a substituição de cimento Portland comum por 8% de CCA e diferentes teores de substituição de areia por CA (0; 5 e 10%). Foi utilizada a metodologia da Avaliação do Ciclo de Vida (ACV), com escopo do berço ao portão, utilizando o método GWPbio, que contempla a influência do carbono biogênico na redução das emissões. Diferentes cenários de transporte foram avaliados considerando a produção do BCA em diferentes regiões brasileiras. Dois indicadores de desempenho de carbono dos BCA também são avaliados em termos de resistência à compressão e de valores de condutividade térmica. Como principal conclusão, a substituição do cimento por CCA e da areia por CA são estratégias promissoras para a produção de bioconcretos para aplicações específicas para reduzir suas emissões de GEE. No entanto, esse benefício varia de acordo com a disponibilidade de CA, eficiência de transporte e vida útil do BCA. O BCA pode ser considerado uma alternativa potencial para a indústria de concreto, para aplicações específicas, para reduzir as emissões de GEE e pode ser desenvolvido onde o resíduo de arroz é uma fonte disponível. Este estudo contribui ao apresentar um novo material e uma metodologia para a avaliação das emissões de GEE do ciclo de vida dos bioconcretos, que podem promover um setor de construção circular.

Palavras-chave: concreto, economia circular, avaliação do ciclo de vida, ACV, CO₂, carbono biogênico, resíduo de arroz.

How to cite: L. R. Caldas, A. F. Araujo, N. P. Hasparyk, F. Tiecher, G. Amantino, and R. D. Toledo Filho. "Circular Economy in Concrete Production: Greenhouse Gas (GHG) Emissions Assessment of Rice Husk Bio-Concretes," *Rev. IBRACON Estrut. Mater.*, vol. 15, no. 6, e15602, 2022, <https://doi.org/10.1590/S1983-41952022000600002>

1 INTRODUCTION

The construction and building sector is responsible for about 40% of global energy consumption, 40% of Greenhouse Gas (GHG) emissions, 25% of the water and 40% of the global resources consumptions [1], [2]. Cement and concrete are the most used industrial materials in the world. Cement industry alone is responsible for 5-8% of global CO₂ emissions [3]. Besides that, concrete is used in large quantities and considering its performance due to important properties (durability, fire safety, water resistance and others) and ease of usage, a great replacement of concrete by other materials does not seem to be feasible within the next years. Therefore, it is crucial to develop alternatives to reduce the environmental impacts of the concrete industry [3], [4]. To achieve this challenge, understanding and applying the concepts and principles of Circular Economy (CE) to construction materials are of vital importance.

CE can be understood as a new economic model that incentives the reduction of natural resources consumption, the minimization of waste generation by keeping them in a closed loop and the use of renewable and local resources. It is based on the 5R principles: Rethink, Reduce, Reuse, Repair and Recycle [5]–[8]. The concept of circularity involves essentially a decrease of the GHG emissions in the concrete industry and the whole construction sector [9], [10]. This could enable the sector to archive low carbon targets to meet the Paris Agreement goals of limiting global warming well below 2°C and even to reach a net-zero carbon pathway [11].

The Life Cycle Assessment (LCA) is one of the most used and scientifically accepted methodologies for evaluating the potential environmental impacts of products and processes, and it is especially important for the evaluation of the environmental performance of innovative materials. LCA is standardized by ISO series (ISO 14040 and ISO 14044) [12]–[14]. The Global Warming Potential (GWP), converted in life cycle GHG emissions, is one of the most evaluated impact category since climate change is perhaps the greatest contemporary challenge of humanity [15], [16].

The vast literature about LCA applied to concrete has demonstrated that the use of Supplementary Cementitious Materials (SCM), originated from other industrial processes (*e.g.*, waste and byproducts) for cement replacement is a very good strategy for reducing GHG emissions and, depending of the content, such replacements can also increase mechanical and durability performances [3], [17]–[21]. This has also been confirmed for bio-concretes [22]. However, the local availability of some SCM, such as fly ash or biomass ashes, can compromise its use due to the increase of GHG emissions related to other factors, like transportation, especially in continental countries, such as Brazil [15], [23]–[25]. Most of SCM used for concrete production are waste or byproducts from other industrial processes, such as fly ash, blast furnace slag, rice husk ash, municipal waste incineration ash, which can be considered examples of CE strategies [25].

Another strategy for the concrete industry aligned with the CE concept is the replacement of virgin mineral aggregates by recycled ones. Although most of the studies about LCA and GHG emissions evaluation in the literature are concerned about conventional concrete with only mineral aggregates, it is possible to produce bio-concretes that can reuse different kinds of bio-based materials as aggregates and/or even as SCM. The main advantages of using plant aggregates for the production of bio-concretes involve the reduction of material density, thermal conductivity and

carbon footprint. These aggregates can act as carbon stocks since the cementitious materials tend to store carbon by its mineralization in the matrix after hydration [26].

In the literature, the most studied bio-concrete is the hempcrete, that is a mixture between cement, lime and hemp shives. Hempcretes can have negative carbon footprint or, in other words, they can generate carbon credits [27]–[30]. However, the main issue of the hempcrete is attributed to its low mechanical strength (around 1-2 MPa) [23]. For this reason, it is regularly used as an insulation or filling material in buildings. On the other hand, different bio-concretes made with wood shavings and bamboo waste, have better mechanical performances, with compressive strengths values ranging from 5 MPa to 10 MPa [22], [26], [31] and can be used for other building applications, like walls (for internal partitions and façades), ceilings, shading elements, furniture, etc. In addition, there are other options and available sources of bio-based materials, such as rice husk, corn flakes, coconut, etc. However, there are few studies about the environmental performance of these bio-concretes, since most of the available research is concerned about its mechanical and thermal characterization [32].

Waste from rice production is substantial, especially in the south of Brazil. The global rice production reaches about 500 million tons/year and Brazil is responsible for around 11 million tons/year [33]. The waste husk generated by the rice processing is equivalent to 20% of the rice grains mass. In general, this rice husk (RH) is burned in an attempt to reduce its disposal problem. Furthermore, the potential benefits of the use of rice husk ash (RHA) in the concrete properties as well as in the durability are well known and depend on the burning conditions [34]–[37]. The RHA can be used in partial substitution to cement due to its chemical composition, with high contents of reactive silica. Nonetheless, not all the RH is burned and the remaining husk volume is available to be stocked, especially in cement matrices considering the use as bio-aggregates in substitution to mineral aggregates for producing bio-concretes.

Considering the above, this paper aims to assess GHG emissions in the life cycle of innovative RBC in which RH and RHA are used as circular solutions. Two carbon-performance indicators are also evaluated in terms of RBC compressive strength and thermal conductivity values. Finally, design guidelines for GHG emissions reduction during RBC production are proposed.

This study brings forward as its main contribution the presentation of a new bio-concrete, the RBC, with mixed types of aggregates (minerals and bio-based). In addition, the methodology used can be adapted for the evaluation of life cycle GHG emissions of other bio-concretes. Since the RBC makes use of two CE strategies, use of waste and renewable materials, it can promote a more sustainable and circular concrete production.

2 MATERIALS AND METHODS

Figure 1 presents the main stages followed in the Materials and Methods. The presented approach can be used for the evaluation of life cycle GHG emissions and choice of best mixture of other bio-concretes as well, even though a specific RBC is evaluated in this study.

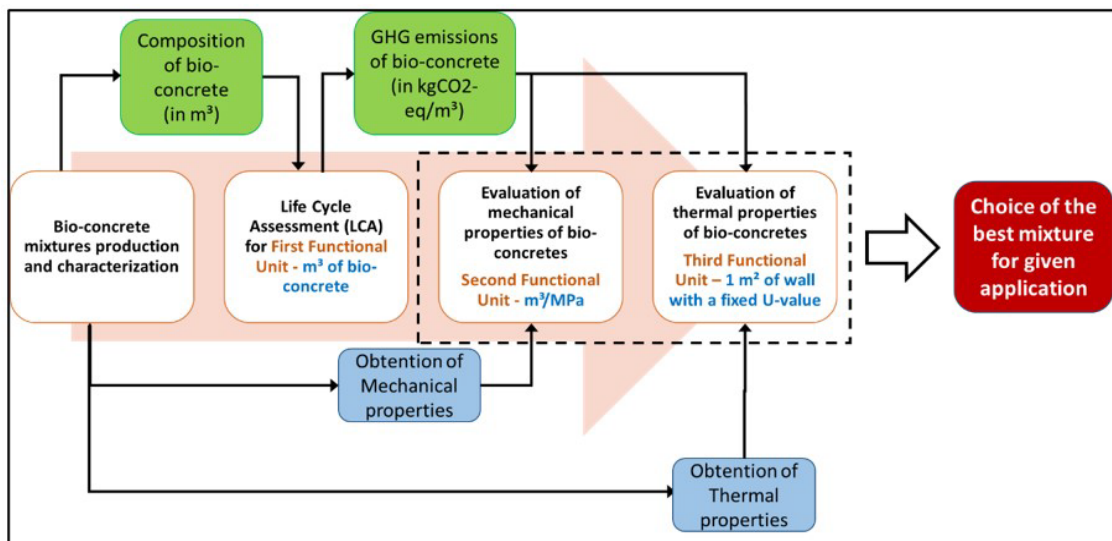


Figure 1. Stages followed in the Materials and Methods for the evaluation of different bio-concrete mixtures.

2.1 Bio-concrete Production and Characterization

RBC – Rice husk Bio-Concretes were cast with the following materials: Brazilian ordinary Portland cement (OPC): high early strength, CP V-ARI Type (equivalent to cement type III, ASTM-150); SCM: rice husk-ash (RHA) in partial substitution to cement at 8%, by weight; mineral aggregates: coarse and fine aggregates from granitic origin; bio-aggregate: rice husk used as a partial replacement of fine aggregate, by volume, in fractions of: 0%, 5%, 10%; chemical admixture: polyfunctional.

The concrete mix proportion was based on a conventional concrete to be applied in various construction elements. The mixture was obtained based on the fineness modulus method, considering the aggregates and a specific range of estimated strength. The four evaluated mixtures contained the same cementitious material content of 350 kg/m³ (of which 8% was RHA for the RH00, RH05 and RH10 mixtures), and a water: binder ratio equal to 0.58. The difference between them was the content of RH, as follows: 0% (RH00), 5% (RH05) and 10% (RH10) in substitution to the fine aggregate (by volume). The amount of chemical admixture was within the recommended range by the manufacturer. Throughout preliminary tests, the chemical admixture content of 0.30% by cement weight was established in order to produce proper workability, through the slump test [38]. The RBC mixtures composition is presented in Table 1. The main properties determined for the RBC (density, compressive strength and thermal conductivity) are presented in Table 2 [39]. The properties of materials used in the RBC production are detailed in the study of Amantino [39].

Table 1. Rice husk bio-concrete mixtures composition (kg/m³).

Mixtures	OPC	RHA	G	S	RH	CA	W
REF	350	0	1078	781	0	1.1	203
RH00	322	28	1078	781	0	1.0	203
RH05	322	28	1078	742	21	1.0	203
RH10	322	28	1078	704	42	1.0	203

REF – Reference mixture. OPC – Ordinary Portland Cement. RHA – Rice husk ash. G – Gravel. S – Sand. RH – Rice husk. CA – Chemical admixture. W – Water.

Table 2. Rice husk bio-concrete properties in 28 days.

BC-RH (in %)	REF	RH00	RH05	RH10
Density (kg/m ³)	2312,04	2218,9	2176,11	2009,13
Compressive Strength (MPa)	30.20	25.26	19.14	15.11
Thermal conductivity (W/m·K)	1.87	1.51	1.06	0.94

2.2 Life Cycle Assessment (LCA)

The LCA was performed according to ISO 14040 [40], ISO 14044 [41], EN 15978:2011 [42], and EN 15804:2019 [43]. The two first standards refer to the LCA of any product, while the last two are applied to the construction sector. According to them the LCA is divided in the following stages: (1) Goal and scope definition; (2) Life Cycle Inventory (LCI); (3) Life Cycle Impact Assessment (LCIA) and (4) Interpretation. They are presented below.

2.2.1 Goal and Scope definition

The goal of this LCA study is to evaluate the GHG emissions (in kgCO₂-eq) on the life cycle of different mixtures of RBC. The scope, from cradle-to-gate, considers raw materials supply (A1), transport (A2) and RBC manufacture (A3), following the recommendations of EN 15804 [43], as presented in Figure 2.

Three Functional Units (FUs) were adopted: first, “the volume (in m³) of the RBC”; second, a FU based on “the volume and compressive strength (in m³.MPa) of the RBC”, which is a common indicator used for the evaluation of new materials, including concretes and bio-concretes [22]; finally, a FU based on the thermal conductivity (presented in Table 2) and U-value (thermal transmittance), considering “1 m² of wall with a fixed U-value of 2.5 W/m².K”, according with the criteria of NBR 15575-4 [44] for façades in Brazil. With this value fixed, it was possible to calculate the wall thickness for each RBC mixture, according with the procedure of NBR 15220-2 [45], as presented in Table 3. This approach is common in the literature for the evaluation, by LCA, of materials, especially bio-based ones used in buildings’ façades [46].

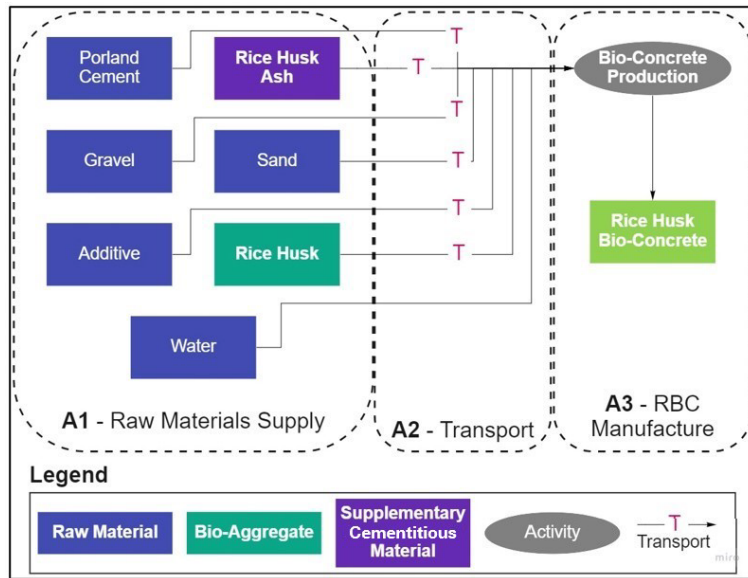


Figure 2. System boundaries for the production of Rice husk bio-concrete.

Table 3. Parameters for the calculation of wall thickness for the third FU.

BC-RH (in %)	REF	RH00	RH05	RH10
RBC thermal conductivity (W/m.K) [43]	1.87	1.51	1.06	0.94
Wall U-value (W/m ² .K)	2.5	2.5	2.5	2.5
Wall thickness (cm)	58	43	25	21

2.2.2 Life Cycle Inventory (LCI)

For the LCI primary data was collected in the laboratory during RBC production and development, while secondary data was collected from Ecoinvent v. 3.8 and literature. The electricity consumption of original Ecoinvent data was adapted to the Brazilian energy mix and market transports. The data used in the modeling is presented in Table 4, where it is possible to see that most of them are already developed for the Brazilian context. RH was considered with zero GHG burden since it is a recovered waste from rice production, while for RHA it was only considered the electricity for grinding, obtained from Silva [47].

Table 4. Raw materials, activities and datasets used in Rice husk bio-concrete (RBC) LCI.

Materials and Activities	Dataset
Portland cement	Cement, Portland {BR} cement production,
Sand	Sand {BR} sand quarry operation, extraction from riverbed
Gravel	Gravel, crushed {BR} gravel production, crushed
Rice husk ash	Modeled by the authors Based on Silva [47], Electricity, medium voltage {BR}
Chemical admixture	Plasticizer, for concrete, based on sulfonated melamine formaldehyde {GLO} production
Water	Tap water {BR}
Transportation	Transport, freight, lorry 16-32 metric ton, EURO3 {BR}
Electricity	Electricity, medium voltage {BR} market group for electricity
Bio-concrete production	Concrete, 25MPa {BR} concrete production

2.2.3 Life Cycle Impact Assessment (LCIA)

For the LCIA, the EN 15804 + A2 (v. 1.00) method [48] was used, considering the Climate Change impact (Climate Change – Fossil and; Land use and land use change). The Climate Change – Biogenic was modelled for the RH according with another method that is described below.

2.2.4 Biogenic Carbon

For the RH biogenic carbon quantification, the method developed by Guest et al. [49] that defines a GWP_{bio} index was employed. It was considered that the biologic CO₂ is stored indefinitely (for more than 100 years) since the cementitious materials of bio-concretes tend to mineralize the biomass [25], [30]. Furthermore, based on the rotation period of 1 year of the rice production and the storage period in the anthroposphere, the GWP_{bio} factor of -99% for rice husk based on Guest et al. [49] was adopted. As a sensitivity analysis, another service life was considered assuming that CO₂ would be stored for 50 years in the anthroposphere, resulting in a GWP_{bio} factor of -40%. The Equations 1 and 2 were used with the parameters presented in Table 5.

$$M_{CO_2} = m_{dry} \times GWP_{bio} \quad (1)$$

$$GWP_{bio} = C \times Factor_{bio} \times \frac{mm_{CO_2}}{mm_C} \quad (2)$$

Where M_{CO_2} = CO₂ uptake and storage (kg) – biogenic carbon; m_{dry} = dry mass of rice husk (kg); C = percentage of carbon in dry matter (%); GWP_{bio} Factor = considered according to Guest et al. [50]; mm_{CO_2} = molecular mass of CO₂ (44); and mm_C = molecular mass of C (12).

Table 5. Parameters and data for the biogenic carbon modeling of rice husk.

Scenario	C (%)	Time in Anthroposphere (years)	GWP _{bio} Factor (%)	MCO ₂ (kgCO ₂ /kg)
Best – 1	41	100	-99	-1,49
Intermediate – 1	38	100	-99	-1,38
Worst – 1	35	100	-99	-1,27
Best – 2	41	50	-40	-0,60
Intermediate – 2	38	50	-40	-0,56
Worst – 2	35	50	-40	-0,52

2.2.5 Sensitivity analysis

For the sensitivity analysis two items were evaluated in this research:

- RHA and RH transportation considering that these materials are locally available, using the approach presented by Caldas et al. [25] and Lima et al. [15] which assumes different transportation efficiency scenarios in terms of truck capacity and way of return (empty or loaded). The following scenarios were considered: (1) Round trip 100% loaded (more efficient); (2) Going 50% loaded and empty return (less efficient). For that, Ecoinvent datasets were used (Transport, truck 10-20t, EURO3, 100%LF, default/GLO Mass; Transport, truck 10-20t, EURO3, 50%LF, empty return/GLO Mass).
- Storage of biogenic carbon (described in the Biogenic carbon section). The sensitivity analysis was performed for the reference RBC (REF) and RBC with higher content of RH (RH10).

3 RESULTS AND DISCUSSION

This section is divided in: (3.1) GHG Emissions in the Three Functional Units (FU); (3.2) GHG Emissions Profile; (3.3) Sensitivity Analysis, and; (3.4) Design Guidelines for Producing Low-Carbon Bio-Concretes.

3.1 GHG Emissions in the Three Functional Units (FU)

The GHG emissions results considering the three FU are presented in Figures 3-5. Two scenarios of biogenic carbon storage in anthroposphere were considered, as follows: (A) for more than 100 years and (B) for 50 years.

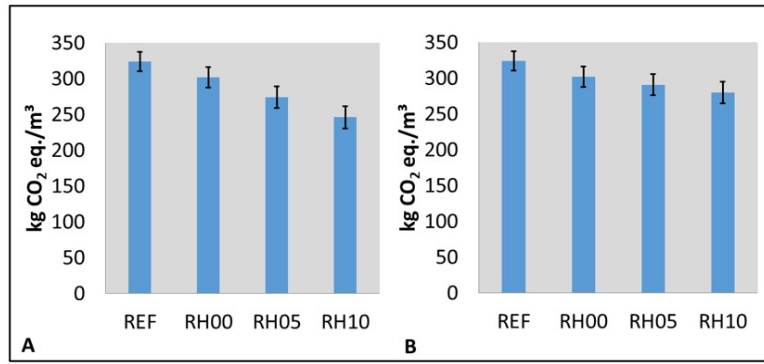


Figure 3. GHG emissions in the first Functional Unit (in m³ of bio-concrete). (A) Biogenic carbon scenario 1. (B) Biogenic carbon scenario 2.

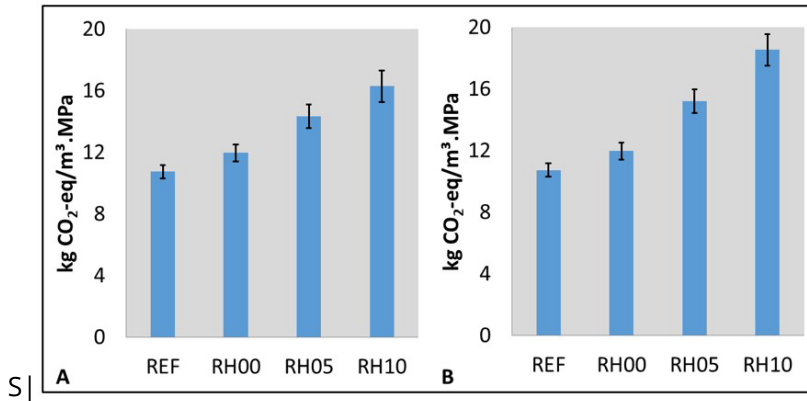


Figure 4. GHG emissions in the second Functional Unit (in m³ of bio-concrete and 1 MPa). (A) Biogenic carbon scenario 1. (B) Biogenic carbon scenario 2.

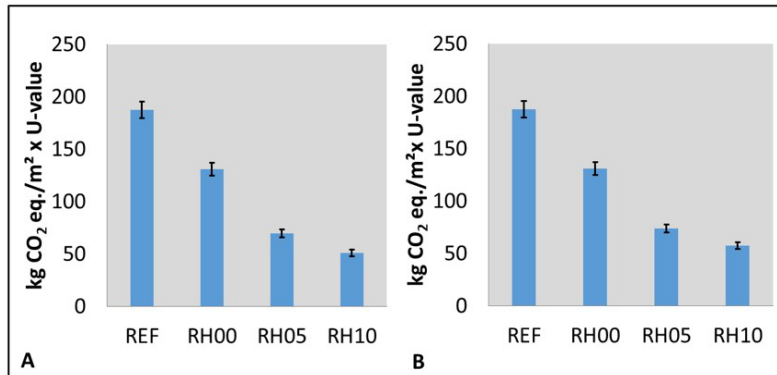


Figure 5. GHG emissions in the third Functional Unit (in m² of a bio-concrete wall with U-value of 2.5 W/m².K). (A) Biogenic carbon scenario 1. (B) Biogenic carbon scenario 2.

For the first FU, in “m³ of bio-concrete”, according to Figure 3, it can be noticed that the RBC with highest content of RH (RH10) presented the lowest GHG emission, while the RBC without any RH or RHA (REF) presented the highest value, for both scenarios of biogenic carbon, as expected. For the first scenario of biogenic carbon (considering biologic CO₂ is stored indefinitely, for more than 100 years), there is a difference of 24% between RH10 and REF. On the other hand, for the second scenario (assuming a storage period of 50 years) the difference between them was of 14%.

The evaluation of these two scenarios showed the influence that methodological choices for biogenic carbon storage accounting have in total GHG emissions estimation of the RBC, which meets with previous literature findings that have already highlighted the importance of the period of carbon storage in the building material to decrease the global

warming potential impact [25], [46], [50], [51]. Therefore, these results underline the importance of considering different carbon storage periods in LCA modeling of bio-based materials, even bio-concretes, due to the uncertainty of service life of building materials, especially innovative ones, like the RBC. Additionally, it highlights the importance of designing for durability, which results in lower GHG emissions.

When the second FU is analyzed, “m³ of bio-concrete for each 1 MPa”, in Figure 4, the results point to a different direction. The RBC RH10 presented the worst value, while the REF presented the best in terms of strength, reaching a difference of 42%. This is a direct consequence of the compressive strength that had suffered a pronounced decrease (around 50%) when more biomass was added, and sand was replaced. The biogenic carbon did not show an expressive influence in the results due to the low level of biomass used in the studied mixtures. In other words, this FU shows that 1 MPa of RH10 emits more GHG emissions than the REF RBC. However, the interpretation of this FU should be done with care since bio-concretes are not designed to be applied in buildings as structural elements, such as beams and columns. They are normally designed to be used as materials for the building envelope, especially façades and roofs, due to the better thermal performance [22], [52] of those materials. The bio-concretes should have a proper mechanical performance, that also influences durability aspects, allowing their use for this kind of application.

Based on this explanation, the third FU, “in m² of a bio-concrete wall with U-value of 2.5 W/m².K”, can be justified and understood in a better way. This FU allows a better realistic quantification of the material consumption that would be used in a building; advances in the scale analysis, from a material to a building element and is more related with one of the main bio-concretes’ advantages, the thermal performance. When this FU is used, according to Figure 5, differences of around 72% between RH10 and REF for the biogenic scenario 1 and of 69% for biogenic scenario 2 are observed.

The three presented FU, especially the last two, provide subsides for choosing the most appropriate RBC mixture in function of its application, and in this case, for a wall in a building façade. Pretot et al. [52], Pittau et al. [30] and Carcasi et al. [46] used the U-value as a reference for FU definition of buildings’ walls made of bio-based materials, mainly hempcretes. However, the studied properties (mechanical and thermal) are just two among a bigger universe of buildings performance (acoustic, waterproof, fire resistance, etc.).

If the target of the design is a concrete wall with a lower GHG emissions and a better thermal performance, thus, the RH10 tends to be the best option. Additional materials can be used as coverings of the bio-concrete wall such as paintings and plastering’s, and this choice can also be assisted by the LCA. For example, clay plasters reinforced with bio-based fibers tend to be a good low carbon option and compatible with bio-concretes [15], [53].

3.2 GHG Emissions Profile

The GHG emissions profile (considering the biogenic carbon scenario 1) is presented in Figure 6 in terms of the contribution for each material.

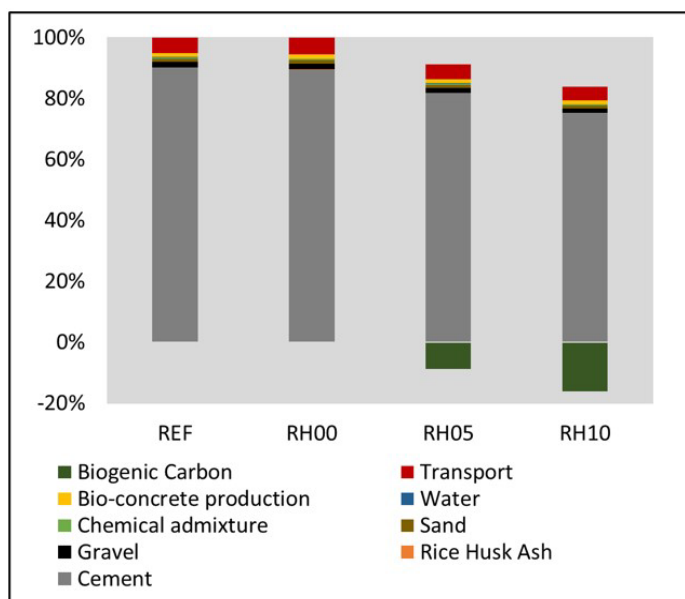


Figure 6. GHG emissions profile.

Cement production is the main GHG emitter, reaching average values of 80%. This occurs especially due to the calcination process of clinker that occurs during the production of cement and the use of fossil fuels, such as petrol coke, for the case of most Brazilian cement factories. This finding agrees with the literature that already showed that OPC is the main impactful material for concrete [19], [54], [55] and bio-concrete production [22], [25]. Transport contributed with around 10%, while sand and gravel presented a very small contribution in emissions, below 5% (both materials, together), since these materials are not energy intensive and, in this case, just the extraction process from nature is considered. The biogenic carbon present in the RH helps to the decrease of the final values, but since it is used in small fractions its influence is not so significant.

Based on these findings the use of different pozzolanic materials from other industrial waste or byproducts such as fly ash, should be evaluated as cement replacement, as an alternative for lowering life cycle GHG emissions. A greater amount of sand replacement by RH would also contribute for this reduction, however, resulting in a trade-off of deteriorating the mechanical properties.

About the allocation process of coproducts, such as fly ash and other commercial residues, it is important to mention that it is often a very controversial subject in LCA studies [25], [56]. In the present study, the allocation process was not considered, and, in the literature, it was verified that most studies that evaluate SCMs do not consider the allocation for concrete production. In the case of market practices, the tendency is to consider the economic allocation, which takes only a small amount of impact into the byproducts given its economic value in comparison to the primary product, in some cases, below 1% and, therefore, not influencing in the final results [22], [56]–[58].

3.3 Sensitivity Analysis

For the sensitivity analysis, the results considered the efficiency in transportation and the biogenic carbon scenarios, as presented in Figure 7.

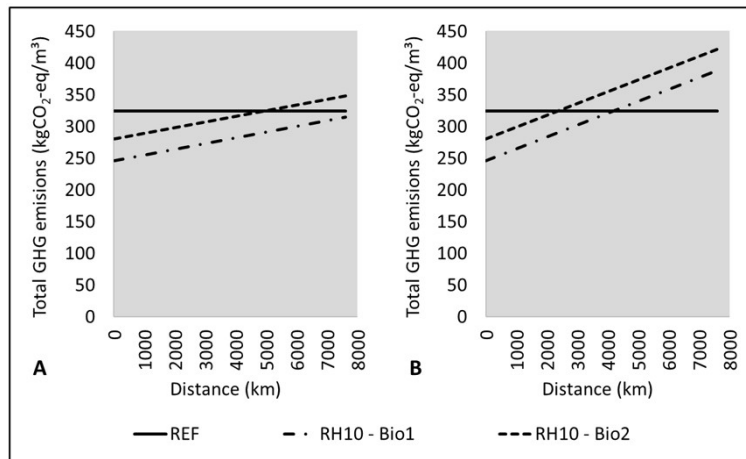


Figure 7. Analysis of RH and RHA transport distances influence in total GHG emissions. (A) More efficient transport (100% default). (B) Less efficient transport (50% empty). Bio 1 – Biogenic scenario 1. Bio 2 – Biogenic scenario 2.

It is clear that the transport distances of RHA and RH have a small influence in the total GHG emissions due to low biomass content in the mixtures. For a more efficient transport scenario these materials should be transported for more than 4.000 km, while for a less efficient scenario for more than 2.000 km (which is also an expressive value, considering the geographical conditions of the Brazilian territory), and RH10 would still have lower impact than REF RBC. Considering this comparison and the condition that RHA and RH mostly comes from the South region of Brazil, these materials could be transported to Southeast and West-Center regions for the worst scenario. For the more efficient scenario it could also reach Northeast and North regions. Based on these findings, the use of RBC could also be encouraged in terms of GHG emissions in regions where rice production is not available. However, this can completely change in terms of costs or other logistics aspects.

These results are different from the literature, e.g [25], where transport showed to have a big influence and the amount of bio-aggregate and residual SCM, namely fly ash, in bio-concrete composition was higher. On the other hand, in the present research RHA and RH in RBC composition reached 1% and 2% in dry mass, respectively. For RBC,

mineral coarse and fine aggregates are the materials that most influence in GHG emissions of transportation stage, since their participation in dry mass are around 50% and 30%, respectively, and normally, they are available materials in most of Brazilian regions.

3.4 Design Guidelines for Producing Low-Carbon Bio-Concretes

Based on the findings of this research and the analyzed literature, design guidelines are proposed for producing low-carbon bio-concretes. Table 6 summarizes these strategies, their priority level, and associated trade-offs that can influence technical/performance aspects of the bio-concretes.

Table 6. Design guidelines for producing low-carbon bio-concretes.

Strategy	Description	Priority	Technical trade-off	
			Positive	Negative
Decrease cement consumption	Use the least possible cement amount	High	Decrease density and increase thermal performance	Decrease mechanical performance and durability
Replace cement by waste based SCM	Replace cement by SCM (that have good pozzolanic reactivity) that are waste or by-products from industrial activities, such as fly ash and rice husk ash	High	It varies. The increase or decrease of mechanical performance and durability will depend on the content of replacement for each SCM	
Increase bio-aggregates amount	Use as much bio-aggregates as possible	High	Decrease density and increase thermal performance	Decrease mechanical performance and durability
Design for durability	Increase the service life of bio-concretes and the time that CO ₂ remains stocked (e.g., treat bio-aggregates for extractives removal).	High	Tend to increase building service life	Can increase costs
Prioritize bio-aggregates with higher carbon content	Biomaterials with higher carbon content stock more CO ₂ (e.g., timber and bamboo)	Medium	Can increase or decrease thermal, mechanical performance and durability depending on the compatibility with other materials in the mixture	
Prioritize bio-aggregates with shorter rotation periods	Biomaterials with shorter rotation periods have more climate benefits (e.g., rice, timber from planted forests, bamboo, etc.)	Medium	Can increase or decrease thermal, mechanical performance and durability depending on the compatibility with other materials in the mixture	
Use of chemical additives	Two kinds of chemical additives: (1) superplasticizer, that favor rheological properties and decrease water and cement consumption; (2) cement set accelerators, as extractives from bio-aggregates can affect setting process	Medium	Increase mechanical performance and rheological properties	Decrease thermal performance and can increase costs
Use of local materials	Use raw materials located near the factory where the bio-concrete will be produced	Medium	-	-

These strategies can be used as a first approach for the development of future bio-concrete mixtures that seek low carbon footprints and adequate performance. It can observe that the high priority should be given for the cement consumption reduction, cement replacement by SCM, and the bio-aggregate amount increase, since these materials are those with the greatest influence in the GHG emissions results. Besides, high priority should be also given for designing for durability strategy.

The trade-off between thermal and mechanical/durability performances must be evaluated with care for bio-concretes development. This is one of the most attractive characteristics of this type of material, an inorganic/mineral (concrete) and a bio (timber, bamboo, etc.) in-between material, making possible to take advantage of the positive properties of each one.

4 CONCLUSIONS

Based on the results obtained in the present study the main established findings were:

- The RH10 (rice husk - RH used as a partial replacement of fine aggregate, by volume, in a fraction of 10%) presented lower life cycle GHG emissions, with differences ranging from 14% to 72% when compared to the reference (REF) mixture, depending on the type of functional unit (FU) and biogenic carbon scenario.
- The biogenic carbon storage had an important influence in overall results. The results showed the importance of increasing the service life of building elements to improve the storage period of the biogenic carbon and, consequently, reduce the life cycle GHG emissions.
- The cement production was the main impactful source of GHG emissions in RBC production, reaching average values of 80%. Therefore, its use should be reduced, however, without compromising the mechanical performance and durability.
- The use of three types of FU helped in the understanding of which are the best applications of the evaluated bio-concretes (e.g., wall for façades) and provided a fairer comparison between the evaluated bio-concrete mixtures.
- The FU in "m² of a bio-concrete wall with U-value of 2.5 W/m².K" tends to provide the most appropriate analysis, considering the application of RBC for buildings' façades.
- Different transport distances of rice husk and rice husk ash were assessed. It was observed that the transportation distances of these materials have a small influence in total GHG emissions, even for a less efficient transportation scenario.
- Finally, the presented design guidelines for producing low-carbon bio-concretes can help bio-concrete researchers, developers and users.

Finally, this study verifies that RBC production has the potential to become a circular solution for the built environment. As RH gradually replaces sand content, mechanical performance tends to decrease, on the other hand, thermal performance is improved, and GHG emissions are lowered. Therefore, the material application must be carefully considered.

For future studies it is recommended the evaluation of RBC with higher contents of cement replacement by other pozzolanic materials and mineral aggregates replacement by rice husk and other types of biomasses. Other environmental impacts and life cycle stages of RBC should also be assessed.

ACKNOWLEDGEMENTS

This research was based upon a R&D Project from ANEEL - National Electric Energy Agency, "Use of bio-concretes and Bio-MMFs with low environmental impact aiming the increasing of energetic efficiency of public buildings" – PD.0394-1719/2017, supported by Eletrobras Furnas with NUMATS/POLI/COPPE/UFRJ and IMED cooperation.

REFERENCES

- [1] United Nations Environment Programme, *2020 Global Status Report for Buildings and Construction: towards a zero-emission, efficient and Resilient Buildings and Construction Sector*. Nairobi, Kenya: UNEP, 2020.
- [2] United Nations Environment Programme. *Sustainable buildings and climate initiative*. Paris, France: UNEP, 2009.
- [3] K. L. Scrivener, V. M. John, and E. M. Gartner, "Eco-efficient cements: potential economically viable solutions for a low-CO₂ cement-based materials industry," *Cement Concr. Res.*, vol. 114, pp. 2–26, 2018, <http://dx.doi.org/10.1016/j.cemconres.2018.03.015>.
- [4] G. Habert et al., "Environmental impacts and decarbonization strategies in the cement and concrete industries," *Nat. Rev. Earth Environ.*, vol. 1, no. 11, pp. 559–573, 2020, <http://dx.doi.org/10.1038/s43017-020-0093-3>.
- [5] Ellen MacArthur Foundation. "Towards the circular economy: economic and business rationale for an accelerated transition." www.ellenmacarthurfoundation.org/business/reports (accessed Feb. 2, 2012).
- [6] Ellen MacArthur Foundation. "Towards the circular economy - opportunities for the consumer goods sector." www.ellenmacarthurfoundation.org/business/reports (accessed Feb. 2, 2013).
- [7] G. Foster, "Circular economy strategies for adaptive reuse of cultural heritage buildings to reduce environmental impacts," *Resour. Conserv. Recycling*, vol. 152, pp. 104507, 2020, <http://dx.doi.org/10.1016/j.resconrec.2019.104507>.
- [8] H. Ping Tserng, C. M. Chou, and Y. T. Chang, "The key strategies to implement circular economy in building projects-a case study of Taiwan," *Sustain.*, vol. 13, no. 2, pp. 1–17, 2021, <http://dx.doi.org/10.3390/su13020754>.
- [9] J. Cantzler, F. Creutzig, E. Ayargarnchanakul, A. Javaid, L. Wong, and W. Haas, "Saving resources and the climate? A systematic review of the circular economy and its mitigation potential," *Environ. Res. Lett.*, vol. 15, no. 12, pp. 123001, Nov 2020, <http://dx.doi.org/10.1088/1748-9326/abeb7>.
- [10] A. Gallego-Schmid, H. M. Chen, M. Sharmina, and J. M. F. Mendoza, "Links between circular economy and climate change mitigation in the built environment," *J. Clean. Prod.*, vol. 260, pp. 121115, 2020, <http://dx.doi.org/10.1016/j.jclepro.2020.121115>.

- [11] World Business Council for Sustainable Development, *Decarbonizing construction: guidance for investors and developers to reduce embodied carbon*. Geneva, Switzerland: WBCSD, 2021.
- [12] M. R. M. Saade, G. Guest, and B. Amor, "Comparative whole building LCAs: how far are our expectations from the documented evidence," *Build. Environ.*, vol. 167, pp. 106449, 2020, <http://dx.doi.org/10.1016/j.buildenv.2019.106449>.
- [13] L. F. Cabeza, L. Rincón, V. Vilarinho, G. Pérez, and A. Castell, "Life cycle assessment (LCA) and life cycle energy analysis (LCEA) of buildings and the building sector: a review," *Renew. Sustain. Energy Rev.*, vol. 29, pp. 394–416, 2014, <http://dx.doi.org/10.1016/j.rser.2013.08.037>.
- [14] C. K. Anand and B. Amor, "Recent developments, future challenges and new research directions in LCA of buildings: a critical review," *Renew. Sustain. Energy Rev.*, vol. 67, pp. 408–416, 2017, <http://dx.doi.org/10.1016/j.rser.2016.09.058>.
- [15] R. Lima et al., "Potentiality of earth-based mortar containing bamboo particles for GHG emissions reduction," *Constr. Build. Mater.*, vol. 317, pp. 125971, 2022, <http://dx.doi.org/10.1016/j.conbuildmat.2021.125971>.
- [16] M. Röck et al., "Embodied GHG emissions of buildings: the hidden challenge for effective climate change mitigation," *Appl. Energy*, vol. 258, pp. 114107, 2020., <http://dx.doi.org/10.1016/j.apenergy.2019.114107>.
- [17] A. P. Gursel, H. Maryman, and C. Ostertag, "A life-cycle approach to environmental, mechanical, and durability properties of 'green' concrete mixes with rice husk ash," *J. Clean. Prod.*, vol. 112, pp. 823–836, 2016, <http://dx.doi.org/10.1016/j.jclepro.2015.06.029>.
- [18] K. Celik, C. Meral, A. P. Gursel, P. K. Mehta, A. Horvath, and P. J. M. Monteiro, "Cement & Concrete Composites Mechanical properties, durability, and life-cycle assessment of self-consolidating concrete mixtures made with blended portland cements containing fly ash and limestone powder," *Cement Concr. Compos.*, vol. 56, pp. 59–72, 2015, <http://dx.doi.org/10.1016/j.cemconcomp.2014.11.003>.
- [19] E. R. Teixeira, R. Mateus, A. F. Camõesa, L. Bragança, and F. G. Branco, "Comparative environmental life-cycle analysis of concretes using biomass and coal fly ashes as partial cement replacement material," *J. Clean. Prod.*, vol. 112, pp. 2221–2230, 2016., <http://dx.doi.org/10.1016/j.jclepro.2015.09.124>.
- [20] A. Petek Gursel, E. Masanet, A. Horvath, and A. Stadel, "Life-cycle inventory analysis of concrete production: a critical review," *Cement Concr. Compos.*, vol. 51, pp. 38–48, 2014, <http://dx.doi.org/10.1016/j.cemconcomp.2014.03.005>.
- [21] J. Li, W. Zhang, C. Li, and P. J. M. Monteiro, "Green concrete containing diatomaceous earth and limestone: workability, mechanical properties, and life-cycle assessment," *J. Clean. Prod.*, vol. 223, pp. 662–679, 2019, <http://dx.doi.org/10.1016/j.jclepro.2019.03.077>.
- [22] L. R. Caldas, M. Y. R. Gloria, F. Pittau, V. M. Andreola, G. Habert, and R. D. Toledo Fo., "Environmental impact assessment of wood bio-concretes: evaluation of the influence of different supplementary cementitious materials," *Constr. Build. Mater.*, vol. 268, pp. 121146, 2020, <http://dx.doi.org/10.1016/j.conbuildmat.2020.121146>.
- [23] Painel Brasileiro de Mudanças Climáticas, *Role of bio-based building materials in climate change mitigation: special report of the Brazilian panel on climate change*. Rio de Janeiro, Brasil: PBMC, 2018.
- [24] V. Göswein, A. B. Gonçalves, J. Dinis, F. Freire, G. Habert, and R. Kurda, "Transportation matters – Does it? GIS-based comparative environmental assessment of concrete mixes with cement, fly ash, natural and recycled aggregates," *Resour. Conserv. Recycling*, vol. 137, pp. 1–10, 2018, <http://dx.doi.org/10.1016/j.resconrec.2018.05.021>.
- [25] L. R. Caldas, A. B. Saraiva, A. F. P. Lucena, M. Y. Da Gloria, A. S. Santos, and R. D. Toledo Fo., "Building materials in a circular economy: The case of wood waste as CO₂-sink in bio concrete," *Resour. Conserv. Recycling*, vol. 166, pp. 2020, 2021., <http://dx.doi.org/10.1016/j.resconrec.2020.105346>.
- [26] L. R. Caldas, A. B. Saraiva, V. M. Andreola, and R. D. Toledo Fo., "Bamboo bio-concrete as an alternative for buildings' climate change mitigation and adaptation," *Constr. Build. Mater.*, vol. 263, pp. 120652, 2020.
- [27] M. Sinka, A. Korjajkins, D. Bajare, Z. Zimele, and G. Sahmenko, "Bio-based construction panels for low carbon development," *Energy Procedia*, vol. 147, pp. 220–226, 2018, <http://dx.doi.org/10.1016/j.egypro.2018.07.063>.
- [28] A. Arrigoni, R. Pelosato, P. Melià, G. Ruggieri, S. Sabbadini, and G. Dotelli, "Life cycle assessment of natural building materials: the role of carbonation, mixture components and transport in the environmental impacts of hempcrete blocks," *J. Clean. Prod.*, vol. 149, pp. 1051–1061, 2017, <http://dx.doi.org/10.1016/j.jclepro.2017.02.161>.
- [29] T. Lecompte, A. Lévasseur, and D. Maxime, "Lime and hemp concrete LCA: a dynamic approach of GHG emissions and capture," in *ICBBM Ecografi 2017*, Clermont-Ferrand, France, 2017.
- [30] F. Pittau, F. Krause, G. Lumia, and G. Habert, "Fast-growing bio-based materials as an opportunity for storing carbon in exterior walls," *Build. Environ.*, vol. 129, pp. 117–129, 2018, <http://dx.doi.org/10.1016/j.buildenv.2017.12.006>.
- [31] M. Y. R. da Gloria, V. M. Andreola, D. O. J. dos Santos, M. Pepe, and R. D. Toledo Filho, "A comprehensive approach for designing workable bio-based cementitious composites," *J. Build. Eng.*, vol. 34, pp. 101696, 2021, <http://dx.doi.org/10.1016/j.jobee.2020.101696>.
- [32] S. Amziane and M. Sonebi, "Overview on biobased building material made with plant aggregate", in *Fourth International Conference on Sustainable Construction Materials and Technologies*. Las Vegas, Nevada, USA, 2016, pp. 1-12. <http://dx.doi.org/10.18552/2016/SCMT4S257>.
- [33] EMBRAPA, "Estatística de produção." <https://www.embrapa.br/estatistica-de-producao> (accessed Feb. 2, 2021).

- [34] B. S. Thomas, "Green concrete partially comprised of rice husk ash as a supplementary cementitious material: a comprehensive review," *Renew. Sustain. Energy Rev.*, vol. 82, pp. 3913–3923, 2018, <http://dx.doi.org/10.1016/j.rser.2017.10.081>.
- [35] G. A. Akeke, M. E. Ephraim, and J. O. Ukpata, "Structural properties of rice husk ash concrete," *Int. J. Eng.*, vol. 3, no. 3, pp. 8269, 2013.
- [36] R. Kishore, V. Bhikshma, and P. J. Prakash, "Study on strength characteristics of high strength rice husk ash concrete," *Procedia Eng.*, vol. 14, pp. 2666–2672, 2011, <http://dx.doi.org/10.1016/j.proeng.2011.07.335>.
- [37] N. P. Hasparyk, "Investigação dos mecanismos da reação álcali – agregado: efeito da cinza de casca de arroz e sílica ativa," M.S. thesis, Universidade Federal de Goiás, Goiânia, Brasil, 1999.
- [38] Associação Brasileira de Normas Técnicas, *Concreto – Determinação da consistência pelo abatimento do tronco de cone* NBR NM 67, 1998.
- [39] G. M. Amantino, "Bioconcretos com resíduos a partir do arroz: análise de desempenho ao longo do tempo," M.S. thesis, IMED, Passo Fundo. 2021.
- [40] British Standards Institution, *Environmental management — Life cycle assessment — Principles and framework*, ISO 14040, 2006.
- [41] British Standards Institution, *Environmental management — Life cycle assessment — Requirements and guidelines*, ISO 14044, 2006.
- [42] British Standards Institution, *Sustainability of Construction Works - Assessment of Environmental Performance of Buildings - Calculation Method*, EN 15978, 2012.
- [43] British Standards Institution, *Sustainability of construction works — Environmental product declarations — Core rules for the product category of construction products*, EN 15804:2012 + A2:2019, 2012.
- [44] Associação Brasileira de Normas Técnicas, *Edificações Habitacionais – Desempenho*, NBR 15575, 2013.
- [45] Associação Brasileira de Normas Técnicas, *Thermal performance in buildings Part 2: Calculation methods of thermal transmittance, thermal capacity, thermal delay and solar heat factor of elements and components of buildings*, NBR 15220-2, 2005.
- [46] O. B. Carcassi, P. Minotti, G. Habert, I. Paoletti, S. Claude, and F. Pittau, "Carbon footprint assessment of a novel bio-based composite for building insulation," *Sustainability*, vol. 14, no. 3, pp. 1384, 2022, <http://dx.doi.org/10.3390/su14031384>.
- [47] L. Silva, "Avaliação de ciclo de vida de concretos com substituição parcial de cimento por cinzas do bagaço de cana-de-açúcar e da casca de arroz," M.S. thesis, UFRJ, Rio de Janeiro, Brasil, 2015.
- [48] V. Durão, J. D. Silvestre, R. Mateus, and J. de Brito, "Assessment and communication of the environmental performance of construction products in Europe: Comparison between PEF and EN 15804 compliant EPD schemes," *Resour. Conserv. Recycling*, vol. 156, pp. 104703, 2020, <http://dx.doi.org/10.1016/j.resconrec.2020.104703>.
- [49] G. Guest, F. Cherubini, and A. H. Strømman, "Global warming potential carbon dioxide emissions biomass stored anthroposphere used bioenergy end life," *J. Ind. Ecol.*, vol. 17, no. 1, pp. 20–30, 2012, <http://dx.doi.org/10.1111/j.1530-9290.2012.00507.x>.
- [50] G. Guest, F. Cherubini, and A. H. Strømman, "Global warming potential of carbon dioxide emissions from biomass stored in the anthroposphere and used for bioenergy at end of life," *J. Ind. Ecol.*, vol. 17, no. 1, pp. 20–30, 2013, <http://dx.doi.org/10.1111/j.1530-9290.2012.00507.x>.
- [51] E. Hoxha et al., "Biogenic carbon in buildings: a critical overview of LCA methods," *Build. Cities*, vol. 1, no. 1, pp. 504–524, 2020, <http://dx.doi.org/10.5334/bc.46>.
- [52] S. Pretot, F. Collet, and C. Garnier, "Life cycle assessment of a hemp concrete wall: impact of thickness and coating," *Build. Environ.*, vol. 72, pp. 223–231, 2014, <http://dx.doi.org/10.1016/j.buildenv.2013.11.010>.
- [53] R. L. M. Paiva, L. R. Caldas, A. P. S. Martins, P. B. Sousa, G. F. Oliveira, and R. D. Toledo Fo., "Thermal-energy analysis and life cycle ghg emissions assessments of innovative earth-based bamboo plastering mortars," *Sustainability*, vol. 13, no. 18, pp. 10429, 2021, <http://dx.doi.org/10.3390/su131810429>.
- [54] A. F. Araujo, C. F. Santos, G. L. Moraga, A. P. Kirchheim, and A. Passuelo, "Avaliação do ciclo de vida de concretos: impacto ambiental do uso de cimentos Portland," in: *59 Congresso Brasileiro do Concreto*, 2017.
- [55] A. P. Gursel, H. Maryman, and C. Ostertag, "A life-cycle approach to environmental, mechanical, and durability properties of 'green' concrete mixes with rice husk ash," *J. Clean. Prod.*, vol. 112, pp. 823–836, 2016, <http://dx.doi.org/10.1016/j.jclepro.2015.06.029>.
- [56] M. U. Hossain, C. S. Poon, Y. H. Dong, and D. Xuan, "Evaluation of environmental impact distribution methods for supplementary cementitious materials," *Renew. Sustain. Energy Rev.*, vol. 82, pp. 597–608, 2018, <http://dx.doi.org/10.1016/j.rser.2017.09.048>.
- [57] C. Chen, G. Habert, Y. Bouzidi, A. Jullien, and A. Ventura, "LCA allocation procedure used as an incitative method for waste recycling: an application to mineral additions in concrete," *Resour. Conserv. Recycling*, vol. 54, no. 12, pp. 1231–1240, 2010., <http://dx.doi.org/10.1016/j.resconrec.2010.04.001>.
- [58] E. R. Grist, K. A. Paine, A. Heath, J. Norman, and H. Pinder, "The environmental credentials of hydraulic lime-pozzolan concretes," *J. Clean. Prod.*, vol. 93, pp. 26–37, 2015, <http://dx.doi.org/10.1016/j.jclepro.2015.01.047>.

Author contributions: LRC: conceptualization, supervision, data curation, formal analysis, methodology, writing, reviewing; AFA: data curation, formal analysis, methodology, writing; NPH: data curation, formal analysis, writing, reviewing; FT: formal analysis, writing, reviewing; GA: data curation, formal analysis; RTF: formal analysis, reviewing.

Editors: Edna Possan, Mark Alexander



ORIGINAL ARTICLE

Proposed durability parameters for reinforced concrete structures with design service life between 50 years and 100 years in Brazil

Proposição de parâmetros para durabilidade de estruturas de concreto armado com vida útil de projeto entre 50 e 100 anos no Brasil

Francine Barcellos Mumberger^a Bernardo Fonseca Tutikian^a Fabrício Longhi Bolina^a 

^aUniversidade do Vale do Rio dos Sinos – UNISINOS, Programa de Pós-graduação em Engenharia Civil, São Leopoldo, RS, Brasil.

Received 02 March 2022

Accepted 20 September 2022

Abstract: The main system of a construction is the structure. Its replacement is most of the times unfeasible and its repair or demolition generates waste that is often difficult to recycle, reuse or dispose of. In this way, structures with longer design service life (DSL) will generate lower environmental impacts, in addition to being financially more interesting for their users. Reinforced concrete is one of the most used types of structure, and commonly suffers with attacks of chloride ions and carbon dioxide that can facilitate the corrosion of the reinforcement. Concrete structures also suffer effects from the passage of time, as probability of accidental load increase, creep and shrinkage. The objective of this study was to determine durability and time effect parameters for DSLs between 50 and 100 years. The durability study was conducted through a review of reference studies, a selection of DSL models based on characteristic forms of environmental aggressiveness and comparison with international standards, using DSLs between 50 and 100 years and the following parameters: w/c ratio, compression strength, minimum cement usage and minimum cover. The time effect study considered Brazilian standards and their probability for accidental loads, creep, shrinkage and variations of the compressive strength, using DSLs between 50 and 100 years. The durability results were compiled in a table with practical recommended dimensional parameters. Despite some proposed parameters being higher or lower than standard values, the differences in performance were accounted through other parameters in order to maintain safety levels and to obtain minimum cover thicknesses. Variable vertical loads presented increments of 4.29% for 75 years and 7.22% for 100 years and wind velocity demonstrated a variation of 5.08% increase at 75 years and 9.84% at 100 years. Compression strength of concrete, creep coefficient and specific shrinkage deformation did not present significant variations. FBM: conceptualization, formal analysis, methodology, writing; BFT e FLB: data curation, formal analysis.

Keywords: reinforced concrete, durability, design service life.

Resumo: O principal sistema de uma construção é a estrutura. A sua substituição é muitas vezes inviável e a sua reparação ou demolição gera resíduos muitas vezes de difícil reciclagem, reutilização ou descarte. Dessa forma, estruturas com maior vida útil do projeto (VUP) gerarão menores impactos ambientais, além de serem financeiramente mais interessantes para seus usuários. O concreto armado é um dos tipos de estrutura mais utilizados, e comumente sofre com ataques de íons cloreto e carbonatação que podem facilitar a corrosão da armadura. As estruturas de concreto também sofrem efeitos com a passagem do tempo, como aumento da probabilidade de carga accidental, fluência e retração. Este trabalho tem como objetivo propor parâmetros para vidas úteis de projeto superiores a 50 anos, relativos à durabilidade e ao efeito do tempo. O estudo da durabilidade foi conduzido a partir de uma revisão bibliográfica e escolha de modelos de previsão de vida útil baseados em formas características de agressividade ambiental e comparação com normas internacionais, com

Corresponding author: Francine Barcellos Mumberger. E-mail: barcellosfrancine@gmail.com

Financial support: None.

Conflict of interest: Nothing to declare.

Data Availability: The data that support the findings of this study are openly available in Unisinos Library Digital Repository at <http://www.repositorio.jesuita.org.br/handle/UNISINOS/9344>, reference number 9344.



This is an Open Access article distributed under the terms of the Creative Commons Attribution License, which permits unrestricted use, distribution, and reproduction in any medium, provided the original work is properly cited.

VUPs entre 50 e 100 anos e utilizando os seguintes parâmetros: relação *a/c*, resistência à compressão, consumo mínimo de cimento e cobrimento mínimo. O estudo do efeito do tempo considerou as normas brasileiras e sua probabilidade para cargas acidentais, fluência, retração e variações da resistência à compressão, utilizando VUPs entre 50 e 100 anos. Os resultados de durabilidade foram compilados em uma tabela com parâmetros dimensionais práticos recomendados. Apesar de alguns parâmetros propostos serem superiores ou inferiores aos valores de normas, as diferenças de desempenho foram contabilizadas através de outros parâmetros para manter os níveis de segurança e obter espessuras de cobertura mínimas. As cargas verticais variáveis apresentaram incrementos de 4,29% para 75 anos e 7,22% para 100 anos e a velocidade do vento demonstrou uma variação de 5,08% de aumento aos 75 anos e 9,84% aos 100 anos. A resistência à compressão do concreto, o coeficiente de fluência e a deformação específica de retração não apresentaram variações significativas. FBM: conceituação, análise formal, metodologia, redação; BFT e FLB: curadoria de dados, análise formal.

Palavras-chave: estruturas de concreto, durabilidade, vida útil de projeto.

How to cite: F. B. Mumberger, B. F. Tutikian, and F. L. Bolina, "Proposed durability parameters for reinforced concrete structures with design service life between 50 years and 100 years in Brazil," *Rev. IBRACON Estrut. Mater.*, vol. 15, no. 6, pp. e15603, 2022, <https://doi.org/10.1590/S1983-41952022000600003>

1 INTRODUCTION

The durability of a building relates both to its performance and variation over time, that is, how well it maintains its designed performance over its designed service life (DSL) [1]. In the case of structures, durability is a fundamental issue since being the main support system of a building, partial or total replacement is not viable due to high direct costs, risks in conducting repairs, indirect costs and inconvenience to users [2], [3].

From a financial point of view, a structure designed aiming durability and longer service life will incur less cost. Consequently, durability is a general worldwide concern for project managers, structural engineers and suppliers. There is a tendency among governments and builders, over the last decades, to design longer service lives for economical and practical reasons due to the possibility of unexpected durability issues [4].

In 2013, standard NBR 15575 [5], regarding structural performance, came into effect in Brazil. This standard defined structural safety parameters based on performance and durability of elements as well as deformations and fissuring. For residential constructions, required minimum, intermediate and superior performance levels must meet service lives of 50 years, 63 years and 75 years, respectively. For other constructions that contained reinforced concrete such as bridges, overpasses, walkways, dams and sculptures, durability and performance were of even higher importance and DSLs might become as long as 100 years [6].

Parameters for minimum concrete cover, water/cement ratio and minimum compressive strength are specified in standard NBR 6118 [7]. However, parameters to determine performance and durability of structures with DSL of more than 50 years are not listed. Consequently, a workaround combination of international standards and extensive reference works are currently used to perform calculations on reinforced and pre-stressed concretes with designed service lives longer than 50 years [8].

According to FIB Model Code [3], the performance of a reinforced concrete structure was related to its behavior due to applied or self-generated loads throughout its DSL. In order to achieve adequate performance, the structure must be able to fully resist expected combined loads throughout its DSL; have safe structural integrity to ensure global stability; allow adequate deformations and have adequate mechanical strength. From this definition, it was possible to identify design parameters that had significant influence on performance throughout the design service life of a structure: loads and combined loads applied to the structure and concrete strength, creep and shrinkage.

The general purpose of this study was to analyze design parameters regarding reinforced concrete to formulate further parameters for a DSL between 50 years and 100 years for structures to be built in Brazil. This was a necessity since, as noted previously, most Brazilian standards list durability and performance parameters only for a DSL of up to 50 years. The analysis was conducted through predictive models which considered structural corrosion mainly from carbonation and chloride ion aggression. Results from this study were compiled and compared to international standards that consider DSLs longer than 50 years in table format to be used as an aid for projects with similar DSLs.

This study also performed an analysis on the effect of time on variable vertical loads and wind actions, creep, shrinkage and variations in compressive strength. Standards and reference studies were used as a basis to determine the degree of influence of time on these factors. Thus, results would allow structural engineers to determine if more specific calculations should be needed in order to reach a DSL between 50 years to 100 years.

2 DURABILITY PARAMETERS FOR REINFORCED CONCRETE

2.1 Carbonation

The most common form of deterioration is corrosion of reinforcements caused by the destruction of the passivating layer. This may be a result of carbonation, chloride ion aggression or both, to the extent that Brazilian standards regarding environmental aggressiveness is based solely on these two agents [8], [9].

Carbonation of the concrete cover is the main cause of the destruction of the passivating layer on the outer surface of reinforcements and results in their corrosion. It is a slow, non-linear process that decelerates down over time: as cement becomes more hydrated and products from carbonation are formed, pores in the concrete clog up and carbon dioxide penetration becomes more difficult [1], [10].

Local carbon dioxide concentration affects carbonation depth and number of chemical reactions since the diffusion process is driven by concentration. Relative humidity (RH) also affects this process as low humidity limits the amount of soluble calcium hydroxide while too high humidity clogs the pores and prevents carbon dioxide transport. The ideal RH range for carbonation falls in the 50% to 70% range [1].

2.2 Chloride Ion Penetration

Chloride ions do not affect concrete directly but rather the reinforcement as it dissolves the iron oxide protective layer and allows corrosion, being one of the most common forms of deterioration [11]. Destruction of this passivating layer occurs once the chloride ion concentration reaches a high enough threshold [12], [13].

The main factor in corrosion is the water/cement (w/c) ratio, which affects the porosity and permeability of concrete and, consequently, the diffusion velocity and penetration of chloride ions. An increase in w/c ratio from 0.4 to 0.6 can increase the diffusion velocity by a factor of 4. High ambient temperatures also lead to higher molecular mobility, which increases ion penetration [13], [14].

2.3 Permeability and Water/Cement Ratio

Permeability is defined as the degree to which liquids or gases can permeate concrete through capillary pores, leading to chemical aggressions in the concrete and cover. Permeability depends on w/c ratio, hydration level of the cement paste and aggregate porosity. Higher w/c ratios result in higher permeability [15].

In theory, a w/c ratio of 0.25 should be enough to hydrate cement but the resulting mixture would lack workability and a substantial portion of water would be lost to the environment through evaporation. In practice, without the use of additives, the minimum w/c ratio is in the order of 0.40 [16], [17].

2.4 Cement Usage

The minimum amount of cement usage is a parameter defined in standards in accordance to expected environmental aggressiveness to ensure a certain durability level to the structure. It is considered to have a minimum effect by itself in some studies and relegated to a second tier of importance [18], [19].

The amount of carbon dioxide absorbed in the carbonation process is driven by the amount of calcium hydroxide present in the pores rather than its total amount. It is not affected by the amount of cement in the mixture either, despite cement being the source of calcium hydroxide [20]. With regards to chloride ion aggression, it is usual to recommend a higher amount of cement in the mix ratio since it is believed that tricalcium aluminate in the cement reacts with chloride ions to form calcium chloroaluminate and prevents corrosion. However, the current understanding is that this chemical reaction only occurs when chloride ions are present at the moment of mixing and becomes irrelevant after curing, thus negating any possible advantage [14], [21].

2.5 Design Service Life (DSL) Estimation Models

A DSL can be generally defined as the time period in which a structure maintains its performance without the need of corrective maintenance [20]. In the case of reinforced concrete, DSL estimates must account for environmental parameters, materials and types of chemical aggressions which may befall on the structures – which are difficult to determine in the initial phases of a project.

Table 1 presents the main estimation methods along with the input and output parameters. Carbonation and chloride ion penetration effects are considered in all methods.

Table 1. DSL estimation models

Model	Input parameter	Output parameter
Helene [20] and Tuutti [22]	Chloride penetration depth	- Chloride ion concentration within concrete; - Chloride ion concentration in the surroundings; - Time of exposure; - Maximum water absorption by the concrete; - Concrete specific mass; - Cement usage.
Clear and Hay [23]	Chloride penetration depth	- Time of exposure; - w/c ratio; - Chloride ion concentration in the surroundings.
Andrade [24]	Chloride penetration depth	- Average RH of the surroundings; - Average temperature of the surroundings; - Surface chloride concentration; - Correction factor for the type of cement; - Characteristic compression strength of concrete; - Correction factor for the mix ratio; - Level of additives in the concrete; - Exposure time.
Morinaga [25]	Carbonation depth	- Carbon dioxide concentration; - Carbonation coefficient of the protective layer; - Temperature of the surroundings; - RH of the surroundings; - w/c ratio; - Exposure time.
Possan [26]	Carbonation depth	- Characteristic axial compression strength of concrete; - Exposure time; - Level of pozzolans in the concrete; - Average RH of the surroundings; - Carbon dioxide levels in the surroundings; - Type of cement; - Rainfall exposure levels of the structure.

The Tuutti [22] model is the most used individually and as a basis for other models. The Possan [26] and Andrade [24] models are also used since their input values are easier to obtain. The estimation models of Table 1 are only a portion of available models in references and can be used individually or together. In addition to the models presented here, we can also mention the following models: Saetta and Vitaliani [27], Lorensini [28], Nilsson et al. [29], Bob [30], Liu [31], Cady and Weyers [32], Bažant [33], Güneyisi et al. [34].

3 REINFORCED CONCRETE PERFORMANCE AND DESIGN PARAMETERS

3.1 Variable actions under imposed loads

Brazilian standards NBR 6120 [35] and NBR 8681 [36] consider variable actions under imposed loads the live loads from furniture, vehicles and individuals. Minimum loads were defined in accordance with the use of the building while the final load was defined from statistical combinations of loads over a period of 50 years.

Bolina et al. [37] presented a methodology to determine variable vertical loads for a DSL longer than 50 years. This methodology consisted of a statistical model based on performance levels for DSLs of 50 years, 63 years and 75 years contained in standard NBR 15575 [5]. Data were taken from standard NBR 8681 [36] with a 35% probability of excess loads in a period of 50 years and assuming variable vertical loads as a random variable with standard distribution. A

general criterion was proposed in this study which resulted in a 2.7% increase in variable loads for a DSL of 63 years and a 4.4% increase for a DSL of 75 years. Based on these results, extrapolations were possible to cover DSLs between 50 years and 100 years.

3.2 Wind static actions

Wind static actions were determined from standard NBR 6123 [38] through dynamic pressure calculations based on characteristic wind velocity. The characteristic wind velocity was the multiplication of the base wind velocity with topographic features such as terrain roughness, construction dimensions and statistical factors.

The base wind velocity was represented by a 3-second wind gust, which had a statistical probability of being exceeded once in a period of 50 years. A statistical factor was defined that accounted for the safety of the building under the probability of the base wind velocity being exceeded within the DSL period. Standard NBR 6123 [38] presented a table of this statistical factor with a 63% probability of base wind velocity being exceeded in a DSL of 50 years. However, Annex B of NBR 6123 [38] also presented a mathematical equation which allowed the calculation of the statistical factor with different safety levels and DSL.

3.3 Increase in strength over time

Despite the increase in concrete strength over time related to the hydration level of the cement paste, long-term loads tend to have a cumulative detrimental effect on strength [11]. This decrease in strength is the same regardless of the value of compression strength but changes in accordance with the time at which initial loads are applied: the later the load, the less strength reduction [39]. This behavior is incorporated in national and international standards through coefficients applied to strength calculations. The *fib* Model Code [3] contains equations to calculate strength gains and losses more precisely so that a single coefficient may be determined.

Brazilian standards contained the same equations for gains of strength in concrete as *fib* Model Code [3]. These indicated that the coefficient for the decrease in strength under normal design conditions should be 1 since standards assumed that the increase in strength after 28 days should compensate for long-term load application. In the European standard EN 1992-1 [40], this same coefficient was recommended as 1 but variations between 0.8 and 1 were allowed depending on the country.

3.4 Concrete creep

Concrete creep is characterized by a non-linear increase in deformation under constant stress over time [3], [39]. The main factors affecting it are age of the concrete, length of time of load application, stress/strength relation, geometry of the structure, humidity, temperature, type of cement and additives, curing conditions and characteristics of aggregates [41], [42]. Factors that contribute negatively to creep are increase in centerline deflection, loss of prestress in concrete structures and increase in the curvature of columns. These factors introduce additional flexural moments which could increase second order effects, fissuring and corrosion of reinforcement [43]–[45].

Equations to determine creep are mostly obtained empirically and calibrated in laboratory tests. These make use of the difference in deflection between two equal elements, one loaded and another unloaded for the same length of time. Results are determined as specific creep, which represents creep deflection per unit of applied stress [3].

Comparing Brazilian and international standards, NBR 6118 [7] contained the same criteria to calculate the creep coefficient as *fib* Model Code [3], ACI 209 [24] and EN 1992-1 [40] standards despite the use of different equations.

3.5 Concrete Shrinkage

Shrinkage is a deformation of concrete over time caused by water loss which, in theory, does not depend on the applied stress. Shrinkage can generate internal stresses in the structure due to design restrictions and lead to fissuring [43]. The main consequences of concrete shrinkage are cracking, decrease in compression strength and decrease in durability.

Factors that affect shrinkage the most are: age of concrete, type of aggregate, water/cement (w/c) ratio used in the paste, relative air humidity (RH) and characteristic thickness of the slab. Aggregates have the most effect due to their sheer volume in concrete. Cement paste is affected by the w/c ratio, with increasing ratio also increasing shrinkage. The characteristic thickness of the slab is the ratio between volume and exposed surface of the structure, with smaller thicknesses associated with larger shrinkages [41], [43].

Comparison of Brazilian and international standards yielded similar results, despite not presenting the same formulation, the Brazilian standard used the same parameters as *fib* Model Code [3], ACI 209 [24] and EN 1992-1 [40] standards.

4 METHODOLOGY

The analysis of durability utilized the following suggested parameters: w/c ratio, compression strength, minimum cement usage and minimum cover as these were considered the most important for estimates for DSL. The time increment of the analyses was of 5 years.

The durability study was conducted through a review of reference studies and a selection of DSL models based on characteristic forms of environmental aggressiveness. These followed the four-tier environmental aggressiveness classification (EAC) of standard NBR 6118 [7]. Meteorological stations provided nation-wide temperature and humidity data which, coupled with the references, allowed the calibration of the DSL models and the calculation of CO₂ and Cl⁻ concentrations at each EAC. The calibrated models were applied to DSLs in 5 year increments and results were compared to international standards which contained DSLs longer than 50 years. Some of these standards were the Australian AS 3600 [46] with a DSL of 60 years and British BS 8500 [47] with a DSL of 100 years.

Temperature and RH data were obtained from 309 Brazilian meteorological stations measurements by the National Meteorological Institute (INMET) between 1981 and 2010. The average values were of 23.53 °C and 74.2%, respectively. Since higher temperatures promote chloride ion corrosion, a temperature of 25 °C was considered for all EAC as a form of rounding, simplifying of data and as margin of safety, as this temperature occurs in all Brazilian regions. Table 2 presents RH values used for each EAC and considerations based on the specific degradation of each classification. Note that RH values were selected to be as close as possible to the average INM value.

Table 2. Relative humidity values and considerations for each EAC

EAC	RH	Considerations
I	80%	Classification I represents an insignificant risk of deterioration. Consequently, the selected RH level optimizes carbonation, which is the main form of aggression.
II	70%	Classification II represents a small risk of deterioration. Consequently, the selected RH level was at the limit of optimum carbonation, which is the main form of aggression.
III	70%	Classification III represents an elevated risk of deterioration. Consequently, the selected RH level allows the transport of chloride ions.
IV	80%	Classification IV represents a high risk of deterioration. Consequently, the selected RH level was higher than for EAC III and approached chloride ion saturation.

The DSL estimation models were selected considering durability parameter analyses and carbonation or chloride ion corrosion as the main causes of deterioration of reinforced concrete structures [8], [12]. It should be noted that a combined carbonation and chloride ion aggression was not considered, nor were models that included sulfate corrosion or other possible chemical aggressions. Table 3 presents the selected models used at each EAC and output durability parameter.

Table 3. DSL estimation models, classification level and output durability parameters

Model	EAC	Output durability parameter
Possan [26]	I and II	Compression strength
Morinaga [25]	I and II	w/c ratio
Andrade [24]	III and IV	Compression strength
Helene [20] and Tuutti [22]	III and IV	Minimum cement usage
Clear and Hay [23]	III and IV	w/c ratio

Model calibration was conducted with parameters determined from standard NBR 6118 [7] for a DSL of 50 years. Control variables considered were concrete cover thickness, compression strength, w/c ratio, cement usage, temperature and RH. Environmental concentrations of CO₂ and chloride ions were given as output variables for each EAC and

structural element. This calibration defined environmental conditions for the EAC of each model and allowed their application in distinct designs with different designed DSLs. Results are shown in Table 4.

Table 4. Output environmental parameters

Model	EAC	Structural element	Temperature (°C)	RH (%)	Concentration of CO ₂ (for EAC I and II) or Cl ⁻ (for EAC III and IV)	Cover (mm)
Possan	I	Slab	-	80	0.0005%	12
		Beam / column	-	80	0.95%	15
	II	Slab	-	70	1.11%	15
		Beam / column	-	70	5.80%	20
Morinaga	I	Slab	25	80	0.0009%	9.8
		Beam / column	25	80	0.0021%	14.9
	II	Slab	25	70	0.0031%	14.9
		Beam / column	25	70	0.0056%	20
Andrade	III	Slab	25	70	0.38%	25
		Beam / column	25	70	0.43%	30
	IV	Slab	25	80	0.81%	35
		Beam / column	25	80	0.98%	40
Helene, Tuutti	III	Slab	-	-	0.39%	25
		Beam / column	-	-	0.47%	30
	IV	Slab	-	-	0.62%	35
		Beam / column	-	-	0.71%	40
Clear, Hay	III	Slab	-	-	80 mg/L	25
		Beam / column	-	-	150 mg/L	30
	IV	Slab	-	-	470 mg/L	35
		Beam / column	-	-	755 mg/L	40

Concrete structures analyzed were molded *in situ* with adequate quality control following current standards. The type of cement used was CP V with no chemical additives.

A maximum compression strength value of 50 MPa was proposed, which was common for most commercial applications. However, for each analysis, lower compression strength limits and minimum concrete cover thicknesses were used. The w/c ratios proposed were within the range between the maximum value for each EAC in standard NBR 6118 [7] and a minimum of 0.35. For each time interval of analysis, the higher w/c ratio mixtures were combined with the least cover thicknesses.

Cement usage was planned with a hard upper limit of 450 kg/m³. Cement substitutions such as fly ash or blast furnace slag were included within this limit. For EAC I and EAC II, the minimum cement usage at each stage of analysis was extrapolated between the usage recommended for 50 years in standard NBR 12655 [40] and 100 years in standard BS 8500 [47]. For the Helene [20] and Tuutti [22] models, a maximum water absorption of 17% was considered for a concrete with specific mass of 2,400 kg/m³.

The minimum concrete cover thickness for each EAC was determined based on all parameters of the DSL models with the intent to use the smaller thickness at each time interval of analysis. Changes in cover were rounded off to 5 mm increments in accordance with standard NBR 6118 [7]. Following the definition of durability parameters, the average, maximum and minimum cover values were analyzed in order to determine a minimum safety value. It should be noted that the minimum safety cover proposed in this study must be increased by a practical margin of safety as to become a nominal cover.

This part of the study focused on the effect of time on parameters of reinforced concrete projects, namely, variable vertical loads, creep deflections, shrinkages and compression strength. Variable loads were vertical or wind action, defined as a function of the probability of occurrence within a period of time. The mathematical formulas were defined to consider the same probabilities as listed in standards but with different periods of time. Time effects on compression strength, creep coefficient and shrinkage coefficient were conducted in accordance with equations presented in standards.

Variable vertical loading increments were determined using Bolina, Perrone and Tutikian [37] as a basis. It was assumed that the variable loads listed in standard NBR 6120 [35] were random variables with average normal distribution (μ) equal to 0 and standard deviation (σ) equal to 1. As shown in Bolina et al. [37], the variable vertical

loading increments are established by consensus and have a probability of 25% to 35% of being exceeded during a period of 50 years, in Brazil. Thus, a conservative estimate would result that the risk of these loads being matched or exceeded would be of 35%.

Wind action was accounted for in Annex B of standard NBR 6123 [38]. It was assumed that the probability of the base wind velocity be matched or exceeded at least once in the period of time analyzed would be 63%.

The variation in compression strength (f_{ck}) over time was analyzed following the methodology of *fib* Model Code [3], which prescribed that the increase in strength was due to delayed cement hydration and decrease in creep.

Creep deflection and shrinkage were calculated in accordance with standard NBR 6118 [7] with wet curing instead of steam curing. This standard was selected for being more thorough than the Australian and Indian standards and equivalent to *fib* Model Code [3].

Minimum age for initial loading was taken to be 28 days with CPV cement and slump between 100 mm and 150 mm. For a simulated age, air temperature and RH were considered to be the same as the durability parameters at each EAC. A cement factor (s) of 0.165 was used to determine the creep coefficient which accounted for the increase in strength over time.

The simulated thickness was calculated for a structural element 20 cm in width and 30 cm in height for a resulting surface area of 600 cm².

5 RESULTS AND DISCUSSION

5.1 Compression Strength

Table 5 shows proposed values for compression strength (f_{ck}) between DSLs of 50 years and 100 years with the Possan [26] model and EAC I and EAC II. Also shown are the minimum cover (C_{min}) needed for the specific strength at each age analyzed.

Table 5. Compression strength and minimum cover with the Possan [26] model

EAC	Structural element	f_{ck} (MPa)	C_{min} (mm)	f_{ck} (MPa)	C_{min} (mm)	f_{ck} (MPa)	C_{min} (mm)
		50 years		55 years		60 years	
I	Slab	20	10.0	20	12.7	20	13.3
	Beam / column	20	15.0	20	15.6	25	11.3
II	Slab	25	15.0	30	11.4	30	12.0
	Beam / column	25	20.0	30	15.0	30	15.7
		65 years		70 years		75 years	
I	Slab	25	9.6	25	10.0	25	10.4
	Beam / column	25	11.7	25	12.2	25	12.6
II	Slab	30	12.5	30	12.9	35	10.2
	Beam / column	30	16.3	30	16.6	35	13.2
		80 years		85 years		90 years	
I	Slab	25	10.7	25	11.0	25	11.4
	Beam / column	25	13.0	25	13.4	30	10.2
II	Slab	35	10.6	35	10.9	35	11.2
	Beam / column	35	13.7	35	14.1	35	14.5
		95 years		100 years			
I	Slab	25	11.7	25	12.0		
	Beam / column	30	10.5	30	10.8		
II	Slab	35	11.5	35	11.8		
	Beam / column	35	14.9	35	15.3		

For EAC I, the increases in compression strength between 50 years and 100 years were of 5 MPa for slabs (from 20 MPa to 25 MPa) and 10 MPa for beam/columns (from 25 MPa to 35 MPa). For EAC II, this increase was of 10 MPa for both slabs and beam/columns (from 25 MPa to 35 MPa). Minimum cover thicknesses varied slightly only for slabs in EAC I since the prediction model started with a slightly thicker cover as specified in standards. The remaining EACs presented no changes in cover over time since increases in compression strength supplied sufficient durability.

The insubstantial increase in compression strength between 50 years and 100 years and the maintenance of cover thickness with the selected DSL method were due to the low risk of deterioration attributed to EAC I and EAC II in standard NBR 6118 [7]. This was attributed to carbonation being the main form of aggression in these two classifications – a slow process that attenuated over time. Another consideration would be the effect on durability from the relation between compression strength and porosity. Since carbonation products could fill available pores and prevent the ingress of aggressive agents, the risk of deterioration also tended to be lower.

Table 6 compares the values of compression strength from EAC I and EAC II with international standards. Results from this study are similar to standard AS 3600 [46] at 60 years and more conservative than standard BS 8500 [47] at 100 years.

Table 6. Comparison of compression strength between Possan [26] model and international reference standards

EAC	Structural element	f _{ck} (MPa)			
		60 years		100 years	
		Possan [26]	AS 3600	Possan [26]	BS 8500
I	Slab	20	20	25	20
	Beam / column	25	25	30	20
II	Slab	30	32	35	25
	Beam / column	30	32	35	40

Table 7 presents compression strengths and minimum cover thickness of several DSL for the Andrade [24] model with EAC III and EAC IV. The time interval considered included the DSL range of Table 6.

Table 7. Compression strength and minimum cover thickness with the Andrade [24] model

EAC	Structural element	f _{ck} (MPa)	C _{min} (mm)	f _{ck} (MPa) C _{min} (mm)			
				50 years	55 years	60 years	75 years
III	Slab	30	25	35	22.4	35	23.4
	Beam / column	30	30	35	26.9	35	28.1
IV	Slab	40	35	45	32.6	45	34.1
	Beam / column	40	40	45	37.3	45	38.9
III	Slab	35	24.4	40	22.2	40	22.9
	Beam / column	35	29.2	40	26.5	40	27.5
IV	Slab	45	35.5	50	33.1	50	34.3
	Beam / column	45	40.5	50	37.8	50	39.2
III	Slab	40	23.7	40	24.4	45	22.3
	Beam / column	40	28.4	40	29.2	45	26.7
IV	Slab	50	35.4	50	36.5	50	37.6
	Beam / column	50	40.5	50	41.7	50	42.9
III	Slab	45	22.9	45	23.5		
	Beam / column	45	27.5	45	28.2		
IV	Slab	50	38.6	50	39.6		
	Beam / column	50	44.1	50	45.2		

The more substantial increases in compression strength were determined on slabs and beam/columns for EAC III: starting at 15 MPa, increasing to 30 MPa at 50 years and increasing further to 45 MPa at 100 years. Cover thickness did not change for EAC III within the period of this study due to the increase in compressive strength providing sufficient durability. For EAC IV, compression strength increases reached the upper limit of 50 MPa of this study at 70 years. For longer time periods, the prediction method compensated the locked compression strength with increases in minimum cover thickness.

Structures with EAC III and EAC IV had deterioration risks classified as elevated and high, respectively, in standard NBR 6118 [7] which explained the resulting predicted increase in compression strength. In these classifications, the main mechanism of aggression was chloride ion attack, which represented more significant corrosion than general

types. This aggression could be airborne or from contact with seawater or industrial runoff, which stressed the need of a less porous structure and, by extension, one with higher compression strength when compared to other EACs.

Compression strength results from the Andrade [24] model are also compared to international standards as shown in Table 8. In this case the values obtained in this study are very much of the same order of magnitude as the standards.

Table 8. Comparison of compression strength between Andrade [24] model and international reference standards

EAC	Structural element	f_{ck} (MPa)			
		60 years		100 years	
		Andrade [24]	AS 3600	Andrade [24]	BS 8500
III	Slab	35	32	45	45
	Beam / column	35	40	45	45
IV	Slab	45	50	50	45
	Beam / column	45	50	50	45

5.2 Water/cement Ratio

Table 9 shows the proposed values for w/c ratio for EAC I and EAC II and relevant DSL intervals for the Morinaga [25] model. Also shown are the corresponding minimum cover thickness.

Table 9. w/c ratio and minimum cover thickness with the Morinaga [25] model

EAC	Structural element	50 years		55 years		60 years	
		w/c	C_{min} (mm)	w/c	C_{min} (mm)	w/c	C_{min} (mm)
I	Slab	0.65	10	0.60	8.5	0.60	8.9
	Beam / column	0.65	15	0.60	12.7	0.60	13.3
II	Slab	0.60	15	0.55	13.7	0.55	14.3
	Beam / column	0.60	20	0.55	18.4	0.55	19.2
		65 years		70 years		75 years	
I	Slab	0.60	9.3	0.60	9.6	0.60	9.9
	Beam / column	0.60	13.8	0.60	14.3	0.60	14.9
II	Slab	0.55	14.9	0.50	13.2	0.50	13.7
	Beam / column	0.55	20.0	0.50	17.8	0.50	18.4
		80 years		85 years		90 years	
I	Slab	0.55	9.0	0.55	9.3	0.55	9.6
	Beam / column	0.55	13.5	0.55	13.9	0.55	14.3
II	Slab	0.50	14.2	0.50	14.6	0.45	12.4
	Beam / column	0.50	19.0	0.50	19.6	0.45	16.6
		95 years		100 years			
I	Slab	0.55	9.8	0.50	8.6		
	Beam / column	0.55	14.7	0.50	12.9		
II	Slab	0.45	12.7	0.45	13.0		
	Beam / column	0.45	17.1	0.45	17.5		

Starting from the listed w/c ratio of 0.65 for EAC I at 50 years in standard NBR 6118 [7], the predicted value decreased to 0.50 at 100 years with little effect on cover thickness as their values remained lower than the standard value at 50 years. As for EAC II, the starting w/c ratio was defined as 0.60 at 50 years in standard NBR 6118 [7] and decreased to 0.45 at 100 years, with the same effect in cover thickness as observed for EAC I. These results demonstrated that the need of further protection for EAC I and EAC II was lower and, consequently, the w/c ratio could be kept the same for longer DSLs when compared to other EACs. The same observation could be made for minimum cover thickness.

Comparison of w/c ratios and international reference standards are shown in Table 10. However, direct comparison at 60 years was not possible since standard AS 3600 [46] did not include w/c ratio amongst its recommended durability parameters. A comparison at 100 years with standard BS 8500 [47] showed that both EAC recommendations from this study were more conservative. This result was not entirely surprising since standard BS 8500 [47] maintained the same w/c ratio recommendations at 50 years through 100 years.

Table 10. Comparison of w/c ratio between Morinaga [25] model and international reference standards

EAC	Structural element	w/c ratio			
		60 years		100 years	
		Morinaga [25]	AS 3600	Morinaga [25]	BS 8500
I	Slab	0.60	-	0.50	0.70
	Beam / column	0.60	-	0.50	0.70
II	Slab	0.55	-	0.45	0.65
	Beam / column	0.55	-	0.45	0.45

Table 11 presents the proposed value of w/c ratio at EAC III and EAC IV for the Clear and Hay [23] model and corresponding minimum cover thickness for the time periods evaluated in this study.

Table 11. w/c ratio and minimum cover thickness for the Clear and Hay [23] model

EAC	Structural element	w/c	C _{min} (mm)	w/c	C _{min} (mm)	w/c	C _{min} (mm)
		50 years		55 years		60 years	
III	Slab	0.55	25	0.55	26.9	0.50	26.7
	Beam / column	0.55	30	0.55	32.2	0.50	32.0
IV	Slab	0.45	35	0.45	37.8	0.40	36.8
	Beam / column	0.45	40	0.45	43.2	0.40	42.2
		65 years		70 years		75 years	
III	Slab	0.50	28.5	0.45	27.8	0.45	29.4
	Beam / column	0.50	34.1	0.45	33.3	0.45	35.2
IV	Slab	0.40	39.3	0.35	37.5	0.35	39.6
	Beam / column	0.40	45.0	0.35	42.9	0.35	45.4
		80 years		85 years		90 years	
III	Slab	0.40	28.2	0.40	29.6	0.40	31.0
	Beam / column	0.40	33.7	0.40	35.4	0.40	37.1
IV	Slab	0.35	41.8	0.35	43.9	0.35	46.0
	Beam / column	0.35	47.8	0.35	50.3	0.35	52.7
		95 years		100 years			
III	Slab	0.40	32.4	0.40	33.8		
	Beam / column	0.40	38.8	0.40	40.5		
IV	Slab	0.35	48.1	0.35	50.2		
	Beam / column	0.35	55.1	0.35	57.4		

Table 11 shows that the starting w/c ratio of 0.55 for EAC III at 50 years, which was also the maximum value recommended in standard NBR 6118 [7], decreased to 0.40 at 80 years and remained at this level until 100 years. This variation was also observed in other EACs but, only for EAC III resulted in an increase in minimum cover thickness to maintain required durability since it occurred in a shorter time span. The w/c ratio for EAC IV started at 0.45 at 50 years, reached the minimum allowed value of this study of 0.35 at 70 years and remained at this level until 100 years. This result suggests how highly aggressive environments classified as EAC IV are, because in addition to a decrease in the w/c ratio, they need an increase in the cover thickness to ensure durability levels.

Permeability is fundamental to chloride ion attack since the aggressive agent must penetrate concrete through humidity in the air or in liquid form. Consequently, the less permeable the surface, the less ingress of chloride ions, and this effect could be achieved by controlling the w/c ratio. This explained the model predictions of lower w/c ratios for EAC III and EAC IV compared to the other EACs at lower DSLs. However, a lower hard limit of w/c ratio of 0.35 was needed to allow the most quantity of cement to be hydrated without compromising mechanical strength.

Table 12 compares the w/c ratio results of this study with standard BS 8500 [47] at 100 years. For EAC III, the w/c ratios of this study were slightly higher while for EAC IV the w/c ratios were the same as the standard. As in the case of Table 10, comparison at 60 years was not possible since standard AS 3600 [46] did not report w/c ratio.

Table 12. Comparison of w/c ratio between Clear and Hay [23] model and international reference standards

EAC	Structural element	w/c ratio			
		60 years		100 years	
		Clear and Hay [23]	AS 3600	Clear and Hay [23]	BS 8500
III	Slab	0.50	-	0.40	0.35
	Beam / column	0.50	-	0.40	0.35
IV	Slab	0.40	-	0.35	0.35
	Beam / column	0.40	-	0.35	0.35

5.3 Minimum Cement Usage

Minimum cement usage was included as a parameter in this study as it was also listed in NBR 6118 [7] despite some disagreement in this field regarding its use and effect on the durability of reinforced concrete structures.

Table 13 presents the proposed values of minimum cement usage for EAC I and EAC II as extrapolated from standards NBR 12665 [40] and BS 8500 [47]. As DSL increased, the minimum cement usage increased almost linearly. For EAC I, cement usage was 260 kg/m³ for the entirety of the period studied. For EAC II, cement usage started at 280 kg/m³ at 50 years and increased to 340 kg/m³ at 100 years.

Table 13. Minimum cement usage extrapolated from standards NBR 12665 [40] and BS 8500 [47]

EAC	Structural element	Cement usage (kg/m ³)					
		50 years	55 years	60 years	65 years	70 years	75 years
I	Slab	260	260	260	260	260	260
	Beam / column	260	260	260	260	260	260
II	Slab	280	285	290	295	300	305
	Beam / column	280	285	290	295	300	305
I		80 years	85 years	90 years	95 years	100 years	
	Slab	260	260	260	260	260	
	Beam / column	260	260	260	260	260	
II	Slab	310	315	325	335	340	
	Beam / column	310	315	325	335	340	

Table 14 presents proposed minimum values of cement usage and cover thickness over the DSL period of this study with the Helene [20] and Tuutti [22] models

Table 14. Minimum cement usage and cover thickness from the Helene [20] and Tuutti [22] models

EAC	Structural element	Cem. Use. (kg/m ³)	C _{min} (mm)	Cem. Use. (kg/m ³)	C _{min} (mm)	Cem. Use. (kg/m ³)	C _{min} (mm)
III	Slab	320	25	355	24.7	385	24,8
	Beam / column	320	30	355	29.7	385	29,9
IV	Slab	360	35	395	34.9	435	34,6
	Beam / column	360	40	395	39.8	435	39,4
III		65 years	70 years	75 years			
	Slab	415	24.9	450	24.8	450	26,5
	Beam / column	420	29.7	450	29.8	450	32,0
IV	Slab	450	36.2	450	39.0	450	41,8
	Beam / column	450	41.3	450	44.4	450	47,6
III		80 years	85 years	90 years			
	Slab	450	28.3	450	30.1	450	31,8
	Beam / column	450	34.1	450	36.2	450	38,4
IV	Slab	450	44.6	450	47.4	450	50,2
	Beam / column	450	50.8	450	53.9	450	57,1
III		95 years	100 years				
	Slab	450	33.6	450	35.4		
	Beam / column	450	40.5	450	42.6		
IV	Slab	450	53.0	450	55.8		
	Beam / column	450	60.3	450	63.5		

As classified in Brazilian standards, the minimum cement usages were 320 kg/m³ for EAC III and 360 kg/m³ for EAC IV. In this study, the maximum stipulated usage of 450 kg/m³ was reached for EAC III at 70 years and for EAC IV at 65 years. Since usage was not allowed to increase further, only increases in minimum cover were allowed to ensure durability for longer DSLs.

A comparison of cement usage between the Helene [20] and Tuutti [22] models and standard BS 8500 [47] are presented in Table 15. In this case, standard BS 8500 [47] maintained the same minimum cement usage for DSLs between 50 years and 100 years, which made the results of this study more conservative estimations.

Table 15. Comparison of minimum cement usage Helene [20] and Tuutti [22] and international reference standards

EAC	Structural element	Minimum cement usage (kg/m ³)			
		60 years		100 years	
		Helene [20] and Tuutti [22]	AS 3600	Helene [20] and Tuutti [22]	BS 8500
III	Slab	385	-	450	380
	Beam / column	385	-	450	380
IV	Slab	435	-	450	380
	Beam / column	435	-	450	380

For EAC III and EAC IV, the Helene [20] and Tuutti [22] models resulted in elevated minimum cement consumption, even reaching the maximum consumption considered for this study at 70 years and 65 years, respectively. These hard upper limits were set from safety concerns since the chemical effect of cement consumption on the passivating layer was still a topic of discussion in this field. Additionally, an elevated amount of cement could favor fissuring and shrinkage, which would promote chemical aggressions listed in the EACs. Consequently, the use of cement substitutes could be a technically and economically viable alternative.

5.4 Minimum cover

Table 16 presents the proposed average cover thickness over all the models of this study with respect to EACs and DSLs analyzed.

Table 16. Proposed average cover of all DSL models with respect to EAC and time period

EAC	Structural element	Average cover (mm)										
		50 years	55 years	60 years	65 years	70 years	75 years	80 years	85 years	90 years	95 years	100 years
I	Slab	10.0	10.0	10.0	10.0	10.0	10.0	10.0	10.0	10.0	10.0	10.0
	Beam / column	15.0	15.0	15.0	15.0	15.0	15.0	15.0	15.0	15.0	15.0	15.0
II	Slab	15.0	15.0	15.0	15.0	15.0	15.0	15.0	15.0	15.0	15.0	15.0
	Beam / column	20.0	20.0	20.0	20.0	20.0	20.0	20.0	20.0	20.0	20.0	20.0
III	Slab	25.0	25.0	25.0	25.0	25.0	30.0	30.0	30.0	30.0	35.0	35.0
	Beam / column	30.0	30.0	30.0	30.0	30.0	35.0	35.0	35.0	35.0	40.0	45.0
IV	Slab	35.0	35.0	35.0	40.0	40.0	45.0	45.0	50.0	50.0	55.0	55.0
	Beam / column	40.0	40.0	40.0	45.0	45.0	50.0	50.0	55.0	55.0	60.0	60.0

For EAC I and EAC II, average cover for slabs or beam/columns remained the same when considering only 5 mm increments in cover as prescribed by standard NBR 6118 [7] over all DSL periods. This was a direct result of the type of aggression associated with EAC I and EAC II, which acted slowly and decelerated over time. Thus, deterioration levels were considered insignificant or small and, while average cover varied little, changes to other parameters were sufficient to attain the desired durability.

For EAC III at 75 years, average cover had an increase of 5 mm which further repeated itself at 90 years. On the other hand, EAC IV had the most variation in cover: a 5 mm increase at 65 years which repeated every 10 years until a cover of 60 mm for beam/columns at 100 years. Since chloride ion aggression was predominant in EAC III and EAC IV, starting minimum cover values were already higher than other EACs.

Table 17 shows a comparison of the minimum covers proposed in this study and international reference standards. Minimum cover for a DSL of 60 years differed considerably with a Δc between 5 mm and 10 mm between the proposed

values and Australian standard AS 3600 [46]. In fact, the proposed values for EAC I and EAC II at 60 years were closer to the British standard BS 8500 [47] of 100 years. For the remaining EAC classifications, the minimum cover listed in standards were more conservative than the proposed values of this study. For example, for EAC III and EAC IV with a DSL of 100 years, the proposed minimum cover values were similar to standard BS 8500 [47] with differences between 5 mm and 10 mm.

Table 17. Comparison of proposed average covers and international reference standards

EAC	Structural element	Minimum cover (mm)			
		60 years		100 years	
		Proposed	AS 3600	Proposed	BS 8500
I	Slab	10	20	10	15
	Beam / column	15	30	15	15
II	Slab	15	40	15	25
	Beam / column	20	40	20	30
III	Slab	25	40	35	45
	Beam / column	30	45	45	45
IV	Slab	35	50	55	60
	Beam / column	40	65	60	60

5.5 Compilation of results

As the objective of this study was to propose parameters of consultation for structural reinforced concrete projects, all durability parameters for DSLs between 50 years and 100 years were compiled and are presented in Tables 18 and 19.

Table 18. Compilation of durability parameters for DSL between 50 years and 75 years

EAC	Structural element	f _{ck} (MPa) / Cement usage (kg/m ³)					
		w/c ratio / minimum cover thickness (mm)					
		50 years	55 years	60 years	65 years	70 years	75 years
I	Slab	20 / 260 0.65 / 10	20 / 260 0.6 / 10	20 / 260 0.6 / 10	25 / 260 0.6 / 10	25 / 260 0.6 / 10	25 / 260 0.6 / 10
	Beam / column	20 / 260 0.65 / 15	20 / 260 0.6 / 15	25 / 260 0.6 / 15	25 / 260 0.6 / 15	25 / 260 0.6 / 15	25 / 260 0.6 / 15
II	Slab	25 / 280 0.6 / 15	30 / 285 0.55 / 15	30 / 290 0.55 / 15	30 / 295 0.55 / 15	30 / 300 0.5 / 15	35 / 305 0.5 / 15
	Beam / column	25 / 280 0.6 / 20	30 / 285 0.55 / 20	30 / 290 0.55 / 20	30 / 295 0.55 / 20	30 / 300 0.5 / 20	35 / 305 0.5 / 20
III	Slab	30 / 320 0.55 / 25	35 / 355 0.55 / 25	35 / 385 0.5 / 0.25	35 / 415 0.5 / 25	40 / 450 0.45 / 25	40 / 450 0.45 / 30
	Beam / column	30 / 320 0.55 / 30	35 / 355 0.55 / 30	35 / 385 0.5 / 30	35 / 420 0.5 / 30	40 / 450 0.45 / 30	40 / 450 0.4 / 35
IV	Slab	40 / 360 0.45 / 35	45 / 395 0.45 / 35	45 / 435 0.4 / 35	45 / 450 0.4 / 40	50 / 450 0.35 / 40	50 / 450 0.3 / 45
	Beam / column	40 / 360 0.45 / 40	45 / 395 0.45 / 40	45 / 435 0.4 / 40	45 / 450 0.4 / 45	50 / 450 0.35 / 45	50 / 450 0.35 / 50

Table 19. Compilation of durability parameters for DSL between 80 years and 100 years

EAC	Structural element	f _{ck} (MPa) / Cement usage (kg/m ³)				
		w/c ratio / minimum cover (mm)				
		80 years	85 years	90 years	95 years	100 years
I	Slab	25 / 260 0.55 / 10	25 / 260 0.55 / 10	25 / 260 0.55 / 10	25 / 260 0.55 / 10	25 / 260 0.55 / 10
	Beam / column	25 / 260 0.55 / 15	25 / 260 0.55 / 15	30 / 260 0.55 / 15	30 / 260 0.55 / 15	30 / 260 0.5 / 15
II	Slab	35 / 310 0.5 / 15	35 / 315 0.5 / 15	35 / 325 0.45 / 15	35 / 335 0.45 / 15	35 / 340 0.45 / 15
	Beam / column	35 / 310 0.5 / 20	35 / 315 0.5 / 20	35 / 325 0.45 / 20	35 / 355 0.45 / 20	35 / 340 0.45 / 20
III	Slab	40 / 450 0.4 / 30	40 / 450 0.4 / 30	45 / 450 0.4 / 30	45 / 450 0.4 / 35	45 / 450 0.4 / 35
	Beam / column	40 / 450 0.4 / 35	40 / 450 0.4 / 35	45 / 450 0.4 / 35	45 / 450 0.4 / 40	45 / 450 0.4 / 45
IV	Slab	50 / 450 0.35 / 45	50 / 450 0.35 / 50	50 / 450 0.35 / 50	50 / 450 0.35 / 55	50 / 450 0.35 / 55
	Beam / column	50 / 450 0.35 / 50	50 / 450 0.35 / 55	50 / 450 0.35 / 55	50 / 450 0.35 / 60	50 / 450 0.35 / 60

In the proposed durability parameters of Table 18 and Table 19, rounded values were used in accordance with Brazilian standards, which were considered important for practical design applications. In the case of a desired intermediate DSL within the intervals presented, it was recommended to select the highest closer value.

5.6 Increases in variable vertical loads

Table 20 presents increases of variable vertical loads for the DSLs of this study. The load increased, starting with the load for a DSL of 50 years had a parabolic behavior over the years, reaching a 7.22% increase for a DSL of 100 years.

Table 20. Increase of variable vertical loads

n	R	p	T	Q	Fk	Load increase coefficient	% load increase with respect to 50 years
50	0.35	0.00858	116.57	2.38	3.38		
55	0.35	0.00780	128.18	2.42	3.42	1.010	1.03%
60	0.35	0.00715	139.78	2.45	3.45	1.020	1.95%
65	0.35	0.00661	151.39	2.48	3.48	1.028	2.80%
70	0.35	0.00614	163.00	2.50	3.50	1.036	3.58%
75	0.35	0.00573	174.60	2.53	3.53	1.043	4.29%
80	0.35	0.00537	186.21	2.55	3.55	1.050	4.96%
85	0.35	0.00506	197.82	2.57	3.57	1.056	5.58%
90	0.35	0.00478	209.42	2.59	3.59	1.062	6.16%
95	0.35	0.00452	221.03	2.61	3.61	1.067	6.71%
100	0.35	0.00430	232.64	2.63	3.63	1.072	7.22%

5.7 Increases of variable wind actions

The variation in the statistical factor (S3) used to determine wind velocity for variable actions between 50 years and 100 years is presented in Table 21. The increase of S3, from its value at 50 years, was of 9.84% at 100 years. This was necessary as higher base wind velocity would produce corresponding increases for DSLs longer than 50 years.

Table 21. Values for statistical wind factor S3 for DSL between 50 years and 100 years

Age (years)	S3	Relative S3 increase
50	1.0000	
55	1.0018	0.18%
60	1.0153	1.53%
65	1.0279	2.79%
70	1.0397	3.97%
75	1.0508	5.08%
80	1.0613	6.13%
85	1.0713	7.13%
90	1.0808	8.08%
95	1.0898	8.98%
100	1.0984	9.84%

5.8 Variations in compression strength over time

The variations in compression strength over time are represented by coefficient α_c , with values shown in Figure 1 for ages between 50 years and 100 years.

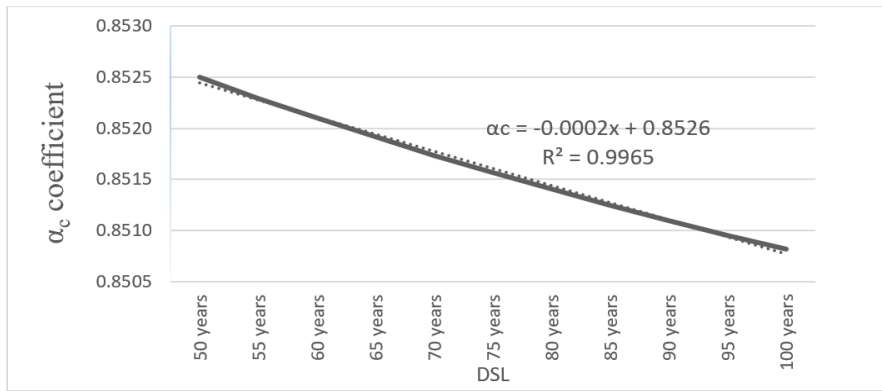


Figure 1 – Values of α_c coefficient between 50 years and 100 years

As noted from *fib* Model Code [3], the α_c coefficient had little variation after the first year and decreased progressively slower over time, to the point that variations past 50 years were almost negligible. Figure 1 attested that the relative variation between 50 years and 100 years was in the order of 0.17%. This behavior could be attributed to the hydration level reached by cement in the initial years, which consumed all available water inside the structure.

Since α_c did not present any significant variation, no analysis was necessary to evaluate its effect for the ages above 50 years under normal conditions. However, a factor not included in this study was the effect of different types of cement, which references showed could induce an increase on this coefficient. In this case, a positive effect would occur with an increase in compression resistance over time despite long-term loading.

5.9 Concrete deformations from creep and shrinkage

The variation of the coefficient of creep for DSLs between 50 years and 100 years is shown in Figure 2. Results are classified according to EAC and RH. It was determined that there was little variation in between ages and only some variation between EACs. The overall trend observed was that the smaller the RH, the larger the creep coefficient. This produced a higher deformation from creep in the structure and denoted that humidity was a more important factor than age for DSLs between 50 years and 100 years. The relationship between RH and shrinkage was related to creep from drying, which produced an exchange of humidity between the structure and the environment. Drying or loss of humidity to the environment under loading reduced water available to the hydration process of the paste and allowed increases in deformations. Thus, environments with low RH incurred higher creep coefficients and higher deformation in structures [42].

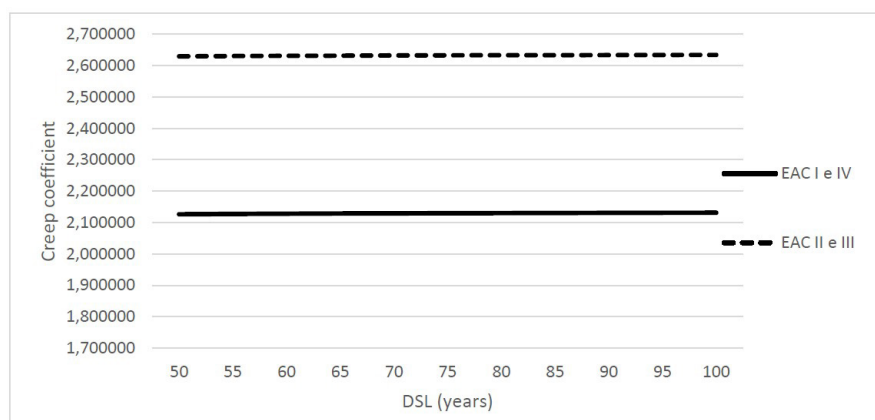


Figure 2 – Variation of creep coefficient for DSLs between 50 years and 100 years

Variations in specific shrinkage deformation for DSLs between 50 years and 100 years are shown in Figure 3. Similar to the coefficient of creep, some variations were observed but were not significant and the most changes were observed in between EAC classifications. The overall trend observed was that higher RH resulted in smaller shrinkages. Shrinkage from drying, also known as hydraulic shrinkage, was always a result of water loss from the inner portions of the concrete to an unsaturated environment.

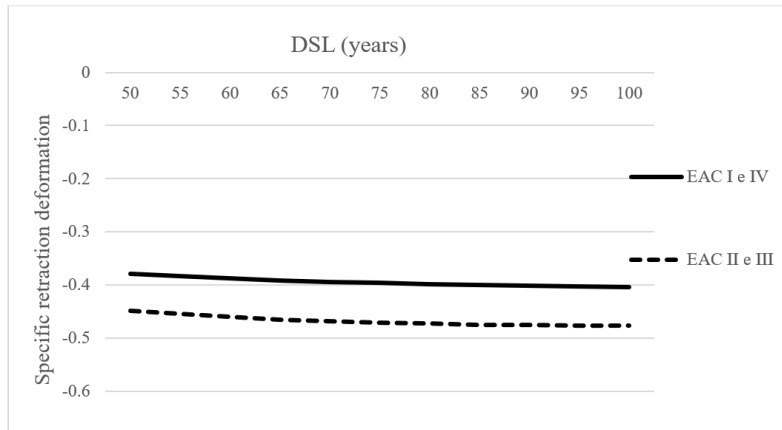


Figure 3 – Variation of specific shrinkage deformation for DSLs between 50 years and 100 years

It should be noted that creep and shrinkage results from this study were evaluated solely and relative to time. Ambient temperature, type of cement, specific thickness of the structure and loading age should also affect the creep coefficient $\phi(t, t_0)$ and specific shrinkage deformation $\epsilon_{cs}(t, t_0)$, but these factors vary according to the design of the project.

6 CONCLUSIONS

The objective of this study was to propose design parameters for reinforced concrete structures to ensure durability for DSLs between 50 years and 100 years. This was performed with DSL prediction models and reference standards. Despite some proposed parameters being higher or lower than standard values, the differences in performance were accounted through other parameters in order to maintain safety levels and to obtain minimum cover thicknesses. This was possible due to the superposition of effects that the parameters had with respect to each other and the preference to minimize cover thickness. Another cause of this effect was the flexibility of the British standard, which presented several combinations of parameters to ensure durability for each EAC. The possibility of achieving a desired performance through a flexible combination of parameters could be an interesting addition to Brazilian standards and would allow a designer to select the most parameters for a particular project.

Evaluation of the effect of time on design parameters did not produce relevant variations that could affect negatively structural performance for DSLs between 50 years and 100 years. Thus, no special consideration could be needed for these DSLs unless structural designers should deem them necessary.

Variable vertical loads presented small increments for the DSLs considered: 4.29% for 75 years and 7.22% for 100 years. In addition, these relatively small variations were based on a normalized vertical load for structural use and additional combinations of loads would further decrease their contribution to the total load.

The S3 factor used to determine the characteristic wind velocity demonstrated a slightly higher variation than variable vertical loads: 5.08% increase at 75 years and 9.84% at 100 years. This increase could be applied to base wind velocities between 30 m/s and 50 m/s. Thus, it was a factor as important as DSL period, especially for higher velocities above 40 m/s. However, it should be noted that wind action contribution to total load would also be diluted once additional combination of loads are incorporated.

Compression strength of concrete did not show considerable variation for DSLs between 50 years and 100 years, with the α_c coefficient remaining above 0.85. This value was recommended in standard NBR 6118 [7] for 50 years and further confirmed that no changes were needed to this coefficient for the DSLs of this study,

The creep coefficient and specific shrinkage deformation did not present significant variations for DSLs between 50 years and 100 years. For both parameters, variations were more evident in between EACs due to differences in RH.

Results indicated that deformations from these parameters were already stabilized at 50 years and further considerations were not necessary for ages of up to 100 years.

The main contribution of the durability study was in filling a niche gap in reference standards since the proposed durability parameters could be used as reference for designing reinforced concrete structures with DSLs longer than 50 years but less or equal than 100 years.

The evaluation of the effect of time on design parameters main contribution was to provide insight on which parameters should be analyzed more closely so that the workload engineers could be optimized.

REFERENCES

- [1] K. Li, *Durability Design of Concrete Structures*, 1st ed. Singapura: Wiley, 2016.
- [2] C. C. D. Dal Molin, A. B. Masuero, J. J. O. Andrade, E. Possan, J. R. Masuero, and M. M. Mennucci, *Contribuição à Previsão da Vida Útil de Estruturas de Concreto*, 1a ed. Porto Alegre: ANTAC, 2016.
- [3] Comité Euro-Internacional Du Béton, *Model Code 2010 – Textbook on Behaviour, Design and Performance*. Lausanne: CEB-FIB, 2010.
- [4] T. Dyer, *Concrete Durability*. Boca Raton: CRC Press, 2014.
- [5] Associação Brasileira de Normas Técnicas, *Desempenho de Edificações Habitacionais*, NBR 15575, 2013.
- [6] M. R. Penn and P. J. Parker, *Introdução a Infraestrutura*. Rio de Janeiro: LTC, 2017.
- [7] Associação Brasileira de Normas Técnicas, *Projeto de Estruturas de Concreto – Procedimento*, NBR 6118, 2014.
- [8] F. L. Bolina and B. F. Tutikian, "Especificação de parâmetros da estrutura de concreto armado segundo os preceitos de desempenho, durabilidade e segurança contra incêndio," *Rev. Concreto Construcoes*, vol. 76, pp. 133–147, 2014.
- [9] P. Helene, "A nova NBR 6118 e a vida útil das estruturas de concreto," in *An. II Semin. Patol. Constr.* 2004.
- [10] T. Dyer, *Concrete Durability*. Boca Raton: CRC Press, 2014.
- [11] A. Poursaee, *Corrosion of Steel in Concrete Structures*. Duxford: Elsevier, 2016.
- [12] C. L. Page and M. M. Page, *Durability of Concrete and Cement Composites*, 1st ed. Cambridge: Woodhead, 2007.
- [13] A. Scott and M. G. Alexander, "Effect of supplementary cementitious materials (binder type) on the pore solution chemistry and the corrosion of steel in alkaline environments," *Cement Concr. Res.*, vol. 89, pp. 45–55, 2016.
- [14] E. P. Figueiredo, "Ação dos cloretos no concreto," in *Concreto: Ciência e Tecnologia*, G. C. Isaia, Ed., São Paulo: Ibracon, 2011, pp. 887–902.
- [15] A. M. Neville and J. J. Brooks, *Concrete Technology*. Harlow: Pearson Education Limited, 2010.
- [16] S. M. Ashraf, *Practical Design of Reinforced Concrete Buildings*. Boca Raton: CRC Press, 2018.
- [17] M. Setareh and R. Darvas, *Concrete Structures*. Springer, 2017.
- [18] Y. Porras, C. Jones, and N. Schmiedeke, "Freezing and thawing durability of high early strength portland cement concrete," *J. Mater. Civ. Eng.*, vol. 32, no. 5, pp. 1–9, 2020.
- [19] D. Saje and J. Lopatič, "The effect of constituent materials on the time development of the compressive strength of high-strength concrete," *Mag. Concr. Res.*, vol. 62, no. 4, pp. 291–300, 2010.
- [20] P. Helene, "Contribuição ao estudo da corrosão em armaduras de concreto armado," Ph.D. dissertation, Dep. Eng. Constr. Civ., Univ. São Paulo, São Paulo, 1993.
- [21] A. M. Neville, "Chloride attack of reinforced concrete: an overview," *Mater. Struct.*, vol. 28, no. 2, pp. 63–70, 1995.
- [22] K. Tuutti, *Corrosion of Steel in Concrete*. Stockholm: Stockholm Royal Inst. Technol., 1982, 472 p.
- [23] K. C. Clear and R. E. Hay, *Time to Corrosion of Reinforcing Steel In Concrete Slabs (Report FHWA/RD-73132)*. Washington, D.C., 1983.
- [24] J. J. O. Andrade, "Contribuição à previsão da vida útil das estruturas de concreto armado atacadas pela corrosão de armaduras: iniciação por cloretos," Ph.D. dissertation, Univ. Fed. Rio Grande do Sul, Porto Alegre, 2001.
- [25] S. Morinaga, "Prediction of service lives of reinforced concrete buildings based on the corrosion rate of reinforcing steel," in *Proc. 5th Int. Conf. Durability Build. Mater. Componente*, 1990, 795 p.
- [26] E. Possan, "Modelagem da carbonatação e previsão de vida útil de estruturas de concreto em ambiente urbano," Ph.D. dissertation, Prog. Pós-grad. Eng. Civ., Univ. Fed. Rio Grande do Sul, Poto Alegre, 2010.
- [27] A. V. Saetta and R. V. Vitaliani, "Experimental investigation and numerical modeling of carbonation process in reinforced concrete structures. Part I: theoretical formulation," *Cement Concr. Res.*, vol. 34, pp. 571–579, 2004.
- [28] V. R. Lorensini, "Avaliação probabilística da deterioração de estruturas em concreto armado," M.S. thesis, Curso de Pós-grad. Eng. Estrut., Univ. Fed. Minas Gerais, Belo Horizonte, 2006.
- [29] L. Nilsson, A. Andersen, T. Luping, and P. Utgenannt, "Chloride ingress data from field exposure in a swedish road environment," in *Proc. 2nd Int. Rilem Workshop Test. Modell. Chloride Ingress Concr.*, 2000.

- [30] C. Bob, "Probabilistic assessment of reinforcement corrosion in existing structures," in *Proc. Int. Conf. Concr. Repair, Rehabil. Prot.*, 1996, pp. 17–28.
- [31] Y. Liu, "Modeling the time-to-corrosion cracking in chloride contaminated reinforced concrete structures," Ph.D. dissertation, Virginia Polytech. Inst. State Univ., Virginia, 1996.
- [32] P. D. Cady and R. E. Weyers, "Deterioration rates of concrete bridge decks," *J. Transp. Eng.*, vol. 100, no. 1, pp. 34–44, 1984.
- [33] Z. Bažant, "Physical model for steel corrosion in sea structures – applications," *J. Struct. Div.*, vol. 105, no. 6, pp. 1155–1166, 1979.
- [34] E. M. Güneçyisi, K. Mermerdas, E. Güneçyisi, and M. Gesoglu, "Numerical modeling of time to corrosion induced cover cracking in reinforced concrete using soft-computing based methods," *Mater. Struct.*, vol. 48, pp. 1739–1756, 2015.
- [35] Associação Brasileira de Normas Técnicas, *Ações para o Cálculo de Estruturas de Edificações*, NBR 6120, 2020.
- [36] Associação Brasileira de Normas Técnicas, *Ações e Segurança nas Estruturas – Procedimento*, NBR 8681, 2003.
- [37] F. Bolina, V. Perrone, and B. Tutikian, "Discussão sobre as ações variáveis de projeto segundo os requisitos mínimo, intermediário e superior de desempenho da ABNT NBR 15575," *Rev. Conc. Constr.*, vol. 79, pp. 65–78, 2015.
- [38] Associação Brasileira de Normas Técnicas, *Forças Devidas ao Vento em Edificações*, NBR 6123, 1988.
- [39] H. Rüşch, "Researches toward a general flexural theory for structural concrete," *ACI J. Proc.*, no. 57-1, pp. 1–28, 1960.
- [40] European Committee for Standardization, *Eurocode 2: Design of Concrete Structures*, EN 1992-1, 2004.
- [41] J. Z. F. Diniz, J. F. Fernandes, and S. C. Kuperman, "Retração e fluência," in *Concreto: Ciência e Tecnologia*, G. C. Isaia, Ed., São Paulo: Ibracon, 2011, pp. 673–703.
- [42] A. M. Neville, *Properties of Concrete*, 5th ed. Essex: Trans-Atlantic Publications, Inc., 2012.
- [43] J. M. Araújo, *Estruturas de Concreto – Modelos de Previsão da Fluência e da Retração do Concreto*, 4a ed. Rio Grande: Dunas, 2002.
- [44] Z. P. Bažant and O. Buyukozturk, "Creep analysis of structures," in *Mathematical Modeling of Creep and Shrinkage of Concrete*. New York: Wiley, pp. 217–273, 1988.
- [45] L. T. Katakao, "Estudo experimental e numérico da deformabilidade por fluência e sua utilização na monitoração de estruturas de concreto," Ph.D. dissertation, Progr. Pós-grad. Eng. Civ., Univ. São Paulo, São Paulo, 2010.
- [46] Australian Standard, *Concrete Structures*, AS 3600, 2009.
- [47] British Standard, *Concrete Complementary British Standard to BS EN 206-1 – Part 1 : Method of Specifying and Guidance for the Specifier*, BSI 8500-1, 2006.

Author contributions: FBM: conceptualization, formal analysis, methodology, writing; BFT e FLB: data curation, formal analysis.

Editors: Edna Possan, Mark Alexander



ORIGINAL ARTICLE

Optimized sizing of reinforced concrete structural elements considering the effect of carbonation

Dimensionamento otimizado de elementos estruturais em concreto armado considerando o efeito da carbonatação

Jeferson Junior Alievi^a Jair Frederico Santoro^b Moacir Kripka^a ^aUniversidade de Passo Fundo – UPF, Programa de Pós-graduação em Engenharia Civil e Ambiental, Passo Fundo, RS, Brasil^bInstituto Federal Sul-Riograndense – IFSul, Faculdade de Engenharia, Passo Fundo, RS, Brasil

Received 10 March 2022

Accepted 27 September 2022

Abstract: The environmental impact of reinforced concrete structures occurs during all phases of the building's life cycle, with emphasis on the stages of extraction and transport of raw materials and concrete production. An effective way to reduce the impact of these structures is to reduce the consumption of materials with the use of optimization techniques. The present study evaluates carbon dioxide emissions of concrete with two different compressive strengths for the region of Chapecó, SC. With these data, the optimization of structural elements was performed aiming to minimize their environmental impact. The carbonation of optimized elements was also evaluated. Among the results, it was observed that concretes with lower strength have better CO₂ absorption rates (for the elements analyzed 20MPa concrete absorbed about 90% and 112% more CO₂ than 35MPa concrete to columns and beams, respectively). In addition, it was observed that local factors can strongly influence the impacts, with the transport of materials reaching up to 6.4% of total emissions.

Keywords: reinforced concrete, optimization, carbonation, environmental impact, sustainability.

Resumo: O impacto ambiental das estruturas de concreto armado ocorre durante todas as fases do ciclo de vida da edificação, com destaque para as etapas de extração e transporte de matérias-primas e produção de concreto. Uma forma eficiente de reduzir o impacto dessas estruturas é reduzir o consumo de materiais com o uso de técnicas de otimização. O presente estudo avalia as emissões de dióxido de carbono de concreto com duas diferentes resistências à compressão para a região de Chapecó, SC. Com esses dados, foi efetuada a otimização de elementos estruturais visando a minimização de seu impacto ambiental. A carbonatação dos elementos otimizados também foi calculada. Dentre os resultados, observou-se que concretos com menor resistência apresentam melhores taxas de absorção de CO₂ (para os elementos analisados o concreto de 20 MPa absorveu aproximadamente 90% e 112% mais CO₂ que o concreto de 35 MPa para pilares e vigas, respectivamente). Além disso, observou-se que fatores locais podem influenciar significativamente os impactos, com o transporte atingindo até 6,4% das emissões totais.

Palavras-chave: concreto armado, otimização, carbonatação, impacto ambiental, sustentabilidade.

How to cite: J. J. Alievi, J. F. Santoro, and M. Kripka, "Optimized sizing of reinforced concrete structural elements considering the effect of carbonation", *Rev. IBRACON Estrut. Mater.*, vol. 15, no. 6, e15604, 2022, <https://doi.org/10.1590/S1983-41952022000600004>.

1 INTRODUCTION

The production, consumption, and lifestyle of the world's population is potentially impacted by economic development, population growth, urbanization, and the technological revolution. As a result, the need for housing and infrastructure work is increasing.

Corresponding author: Moacir Kripka. E-mail: mkripka@gmail.com

Financial support: Brazilian National Council for Scientific and Technological Development (Grant CNPq- 306578/2020-4).

Conflict of interest: Nothing to declare.

Data Availability: The data that support the findings of this study are available from the corresponding author, MK, upon reasonable request.



This is an Open Access article distributed under the terms of the Creative Commons Attribution License, which permits unrestricted use, distribution, and reproduction in any medium, provided the original work is properly cited.

The construction sector is the biggest contributor to CO₂ emissions, accounting for about 30% of all greenhouse gas emissions on the planet. In addition, it accounts for about 40% of global resource use, including 12% of all freshwater. Concrete is one of the most important building materials in the world and the second most used on the planet, after water. Thus, considering the volume of concrete produced and the associated environmental impacts, the optimized design of reinforced concrete structures is an alternative for sustainable development. CO₂ emissions from fuel combustion, cement production, and other industrial processes accounts for about 70% of total global greenhouse gas emissions [1]. Despite the fact that the built environment contributes a large part of global greenhouse gas emissions, it has a great capacity for improvement through the modernization of processes [2].

To assess the environmental impact of civil construction, Life Cycle Assessment (LCA) can be used. Various environmental impacts can be assessed by LCA: global warming, destruction of the ozone layer, eutrophication, depletion of natural resources, energy consumption, land, and water use, among others. The LCA methodology is divided into four main steps: definition of goals (objective and scope), inventory analysis, evaluation, and analysis [3].

In recent years, the themes of sustainability and environmental impact in civil construction have been studied with greater intensity, with the common objective of the studies being the reduction of pollutant emissions into the atmosphere. Due to its importance, reinforced concrete structures have been the subject of several research projects aimed especially at reducing CO₂ emissions and energy consumption [1], [3–11]. However, a small number of studies consider that concrete has the property of absorbing CO₂ from the environment through carbonation, making a kind of compensation through the capture of the gas. In these studies, the results obtained are quite different in the estimation of the amount of carbon dioxide reabsorbed by the concrete. For example, according to research conducted by Jacobsen and Jahren [12] in Norway, it was estimated that 11% of CO₂ emissions in the production of concrete are reabsorbed by the concrete, due to carbonation, during its life cycle. The research by Gajda and Miller [13] report a reabsorption percentage of 7.6%. In Denmark, a study developed by Pade and Guimarães [14] estimated, from a 100-year perspective, an absorption of 57% of CO₂ emissions generated in the production of concrete, considering the demolition of the structure (if the demolition of the structure is not considered, this value is reduced to 24%). In a similar study conducted in the United States, Haselbach and Thomas [15] estimated CO₂ capture of 28.2% during the useful life of the structure. According to Possan et al. [7], these differences recorded in the literature are due to the influence of several factors on the carbonation of concrete (such as strength, exposure environment, content and type of cement, etc.), in addition to differences in the methodology used for its determination.

The present work aimed to evaluate the environmental impact of reinforced concrete taking as a measurement factor the CO₂ emissions. This evaluation was conducted based on the emissions of 1m³ of concrete with different characteristic strengths, adjusting the data from the SimaPro Software for the region under study. The values obtained were used for the optimized design of beams and columns, also including the consideration of the carbonation effect of concrete. To achieve these objectives, this article is structured as follows. The introductory section describes the motivation and objectives of the study. Section 2 presents some concepts that support the study related to life cycle assessment, while the third section addresses concepts related to carbonation in concrete structures. The fourth section describes the methodology used to obtain the impacts of the materials and the formulations adopted to optimize the elements. Section 5 presents the results, and in section 6 the conclusions of the study are summarized.

2 LIFE CYCLE ASSESSMENT

Life Cycle Assessment (LCA) is a tool used to identify the environmental impacts of a product, service, or process throughout its life cycle. The ABNT NBR ISO 14040 standards [16] present a methodological framework for the analysis and assessment of environmental effects throughout the life cycle of a product. Several types of environmental impacts can be estimated by LCA: global warming, ozone layer depletion, eutrophication, acidification, toxicity to humans and ecosystems, depletion of natural resources, energy consumption, land use, and water, among others. ACVs performance depends on the information to be used and the quality of this information, as well as knowledge of the technology adopted.

LCA models the life cycle of an object through its product system performing one or more defined functions. The essential property of a product system is characterized by its function and does not necessarily need to be defined in terms of end products. The subdivision of a product system into the elementary processes that compose it facilitates the identification of inputs and outputs of the product system [16].

With the beginning of the concept of the LCA term, divergent approaches, terminologies, and results emerged, as there was no specific scientific platform. Therefore, the initial analyzes were conducted considering different techniques without a common reference. The results obtained were different, even when the objectives of the study were the same [17].

LCA includes the definition of the object and scope, inventory analysis, impact assessment, and interpretation of results. The definition of objectives and scope is the moment when, among others, the study boundary, the functional unit and the impact categories to be considered are determined. Life Cycle Inventory (LCI) analysis involves data

collection and calculation procedures to quantify the relevant inputs and outputs of a product system. The result of this step is the quantification of all the resources used and the emissions associated with the production of a certain quantity (functional unit) of the product under study. The impact assessment phase of the LCA aims to link inventory data with specific impact categories and category indicators. The calculation of the results of the indicators takes place by converting the results into common units and aggregating them into the same impact category. Its result is a numerical value of the indicator. The two main impact modeling approaches are midpoint and endpoint. While the midpoint approach uses indicators located along the environmental mechanism, the endpoint approach refers to a specific damage, related to a broader area of production that can be human health, the natural environment, or natural resources.

Increased attention has been paid to the environmental impacts attributed to the built environment in recent years, and this occurs both in the form of academic research and the initiative of the civil construction industry. In academic environments, 1068 papers on green buildings were published between 2010 and 2019 [18].

Navarro et al. [19] highlight the importance of environmental impacts being considered in the life cycle of buildings, and that this assessment needs to be conducted in the initial stages of the project.

In recent years, several studies have been developed with an emphasis on the Life Cycle Assessment of buildings, covering everything from the extraction of raw materials to the final disposal of the demolition of the building. The studies aim the search for alternative materials and a lower generation of pollutants for the construction of environmentally sustainable buildings. As an example of the search for viable economic, technical, and environmental solutions for the manufacture of concrete, there is the study developed by Rajan et al. [20], which investigates the addition of rubber waste from naturally treated tires for partial replacement of fine aggregate; the study by Verma et al. [21], which seeks efficient solutions in the use of silica fume and stone dust in partial replacement of cement and fine aggregate; the work of Joanna et al. [22], which uses fly ash to replace cement in the manufacture of concrete; and the study by Majhi and Nayak [23] that uses blast furnace slag of high aggregated volume and recycled with lime activator, in partial or total replacement of the natural aggregate.

Regarding the materials involved in the construction and maintenance of buildings and infrastructures, cement is one of the most important building materials. It is responsible for 5% to 7% of global CO₂ emissions and 12% to 15% of the total energy consumed in the industry worldwide. In addition, cement production is projected to increase annually by 0.8% to 1.2% [24]. In the cement life cycle, 95% of the total CO₂ emitted comes from the production stage, and almost all the emission in the cement industry is concentrated in the production of clinker. During the cement production process, half of the CO₂ emitted refers to the calcination of limestone rock, while the remaining part is due to the burning of fuels for energy generation, in the clinkerization process [25]. The cement industry generates for each ton of cement produced, between 0.7 and 1.0 tons of CO₂ [26]. Currently, the Brazilian cement industry has one of the lowest specific CO₂ emission rates in the world, thanks to mitigating actions that have been implemented by the sector in recent decades. For example, from 1990 to 2014, total emissions decreased from 0.7 tons of CO₂ to 0.564 tons of CO₂/t of cement [27].

The iron and steel sector are relevant to the global economy in terms of employment and economic growth. Worldwide more than six million jobs are directly or indirectly linked to the steel sector. On the other hand, this sector is responsible for about 17% of energy consumption in the industrial sector [28]. The carbon dioxide emission from the steel industry is 997 kg per ton of steel, accounting for 4 to 5% of global emissions [29].

Aggregates (fine and coarse) used in civil construction are the most consumed minerals in the world. Globally, it is estimated that annually eleven billion tons of concrete are consumed, and sand and gravel account for 60–80% of the volume of concrete [30,31]. The extraction, processing, and transport operations involving aggregates produce considerable amounts of unfavorable effects on the environment. Among the main environmental impacts caused by the mineral extraction of aggregates, landscape alterations, vegetation suppression, alteration in watercourses, instability of banks and slopes, and water turbidity stand out.

3 CARBONATION OF CONCRETE STRUCTURES

The carbonation of concrete occurs due to the ingress of CO₂ atmospheric in concrete. Several factors influence the carbonation process, highlighting the relative humidity of the air, the type of cement, the concrete mix, curing, and temperature [32]. According to Possan et al. [7] concrete has the property of absorbing CO₂ from the environment through carbonation. Almost all cement-based materials undergo a certain amount of carbonation reaction during their lifetime, and this is due to the presence of carbon dioxide in the earth's atmosphere. This process begins at construction, through the structure's life cycle, and continues through the demolition process.

Given the importance of the carbonation process of reinforced concrete structures, the number of works in the literature that describe in detail the methodology for calculating CO₂ absorptions can be considered small. A mathematical model for calculating the carbonation depth y over time is presented by Felix and Possan [25], according to Equation 1:

$$y = k_c \cdot \left(\frac{20}{f_c}\right)^{k_{fc}} \cdot \left(\frac{t}{20}\right)^{\frac{1}{2}} \cdot \exp \left[\left(\frac{k_{ad} \cdot a_d^{\frac{3}{2}}}{40 + f_c} \right) + \left(\frac{k_{co_2} \cdot co_2^{\frac{1}{2}}}{60 + f_c} \right) - \left(\frac{k_{ur} \cdot (UR - 0,58)^2}{100 + f_c} \right) \right] \cdot k_{ce} \quad (1)$$

Where:

y – Average depth of concrete carbonation (mm);

f_c – Characteristic strength of compression of concrete (MPa);

k_c – Variable factor referring to the type of cement used;

k_{fc} – Variable factor referring to the compressive strength of the concrete, depending on the type of cement used;

t – Concrete age (years);

a_d – Content of pozzolanic addition in the concrete (% in relation to the mass of cement);

k_{ad} – Variable factor referring to the pozzolanic additions of the concrete – silica fume, metakaolin, and rice husk ash, depending on the type of cement;

UR – Average relative humidity (%/100);

k_{ur} – Variable factor referring to relative humidity, depending on the type of cement used; co_2 – CO₂ content of the atmosphere (%);

k_{co_2} – Variable factor referring to the CO₂ content the environment, depending on the type of cement used;

k_{ce} – Variable factor referring to exposure to rain, depending on the exposure conditions of the structure.

The amount of CO₂ (in kg) captured during the service life (carbonation) of reinforced concrete structures (unpainted and exposed concrete) is determined from Equation 2:

$$CO_2 = y \cdot c \cdot CaO \cdot r \cdot A \cdot M \quad (2)$$

Where:

c – It is the amount of cement used to produce one m³ of concrete (kg/m³);

CaO – It is the amount of calcium oxide contained in the cement (%);

r – Proportion of CaO =fully carbonated (%);

A – Surface area of the concrete exposed to the action of CO₂ (m²);

M – Molar fraction of CO₂/CaO.

4 METHODOLOGY

4.1. Carbon dioxide emissions from component materials of reinforced concrete

In the present study, the environmental impact assessment of the component materials of reinforced concrete was conducted for the region of Chapecó, SC, based on the CO₂ emissions generated for the production and transport of concrete, steel, and wooden formworks. The concrete analyzed in this study was 20 MPa and 35 MPa, the dosages being supplied by a concrete batcher in the region and summarized in Table 1. The concrete batcher also provided a list of its suppliers of materials to produce concrete. The coarse aggregate and fine aggregate (industrial sand) used are produced in the same city, about 4 km from the concrete plant. The fine aggregate (natural sand) is produced in the city of São Cristóvão do Sul, SC, 294 km away. Cement is produced in the city of Rio Branco do Sul, PR, 505 km away, steel is produced in Sapucaia do Sul, RS, 446 km Away, and wood used for formworks production is extracted in the city of União do Oeste, SC (distance of 60 km).

The calculation of CO₂ emissions was done using the Simapro Software, version 9.2.0.1 Faculty UPF 003, considering the Ecoinvent 3.7.1 database of 2021, impact category ReciPe 2016 Midpoint method (H) version 1-05 Hierarchical (standard method with characterizing factors for the global scale). The Simapro Software database was adjusted to the reality of the region under study. Emissions from steel, formworks, and concrete were determined in Simapro according to the flowcharts in Figures 1 to 4. These Figures indicate which data were obtained directly from the software base, and which were adjusted from the distances and dosages used in the present study. The calculation of CO₂ emissions was made for a cubic meter of concrete, a kilo of steel, and a cubic meter of wood for formworks.

Table 1. Concrete dosage

Raw material	Amount (kg/m ³)	
	Concrete 20 MPa	Concrete 35 MPa
Coarse aggregate	625	730
Fine aggregate	315	290
Industrial sand	300	350
Natural sand	670	550
Cement (CPII-F-32)	270	340

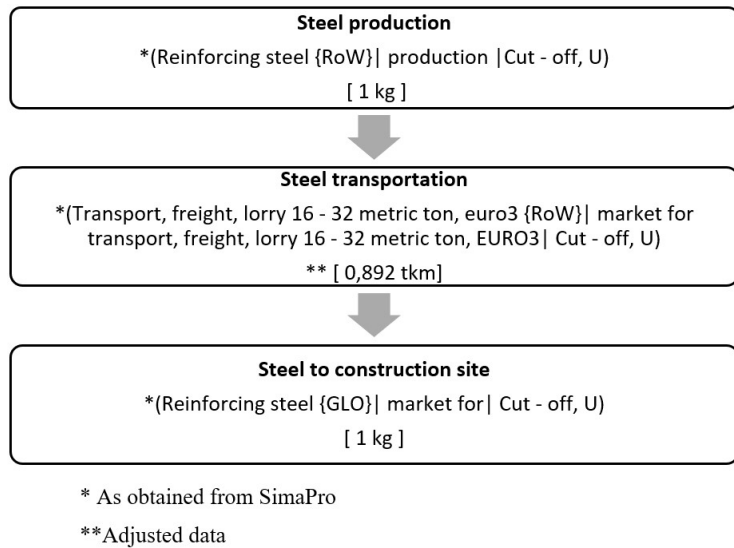


Figure 1. Flowchart with adjusted data for steel

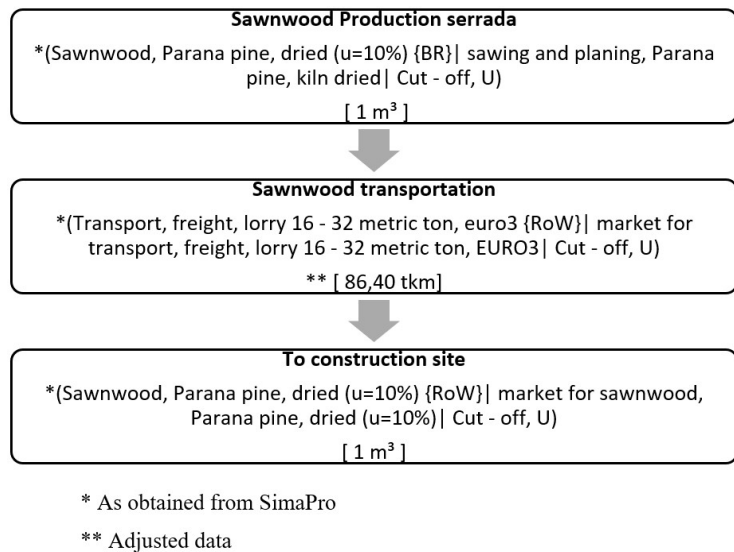
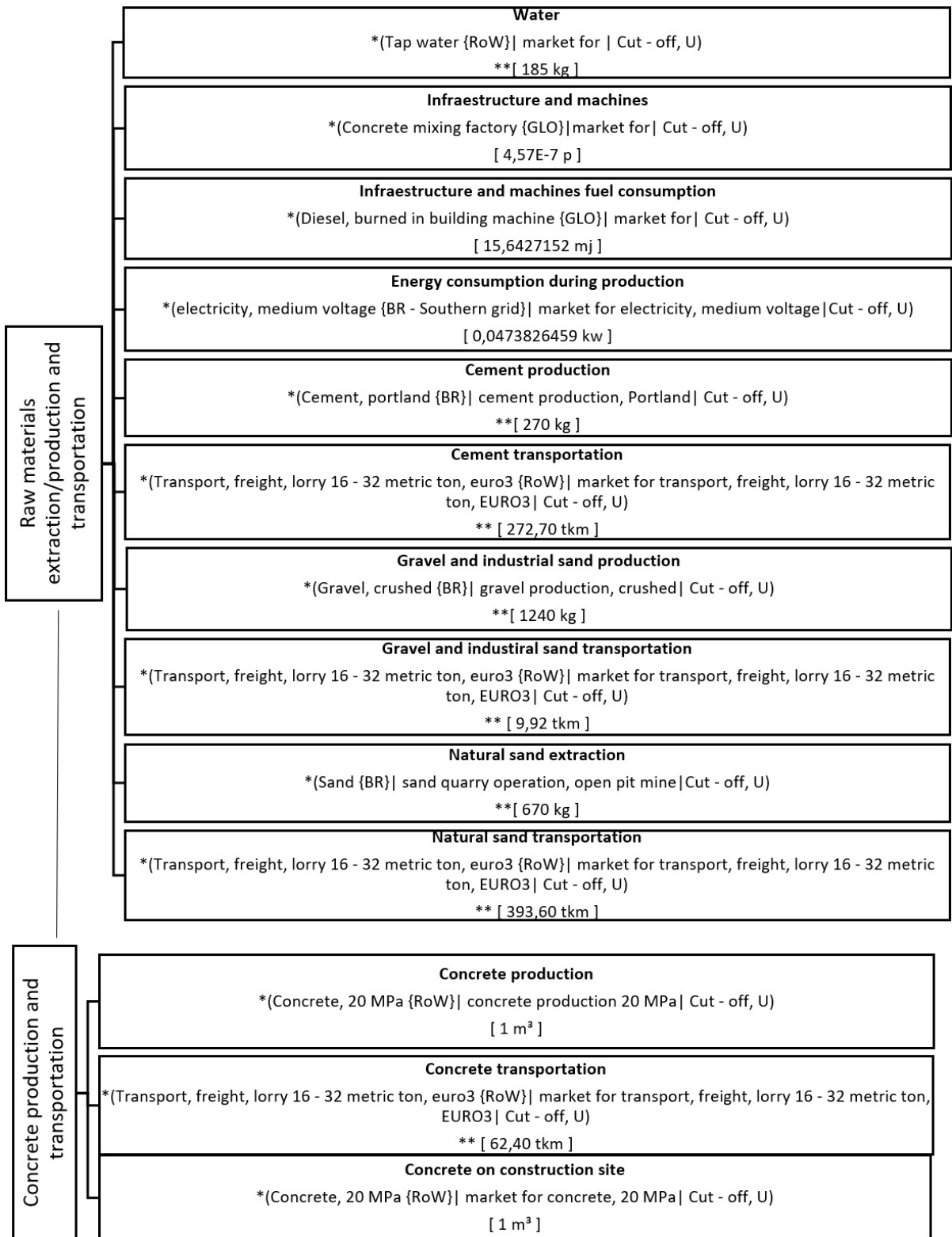


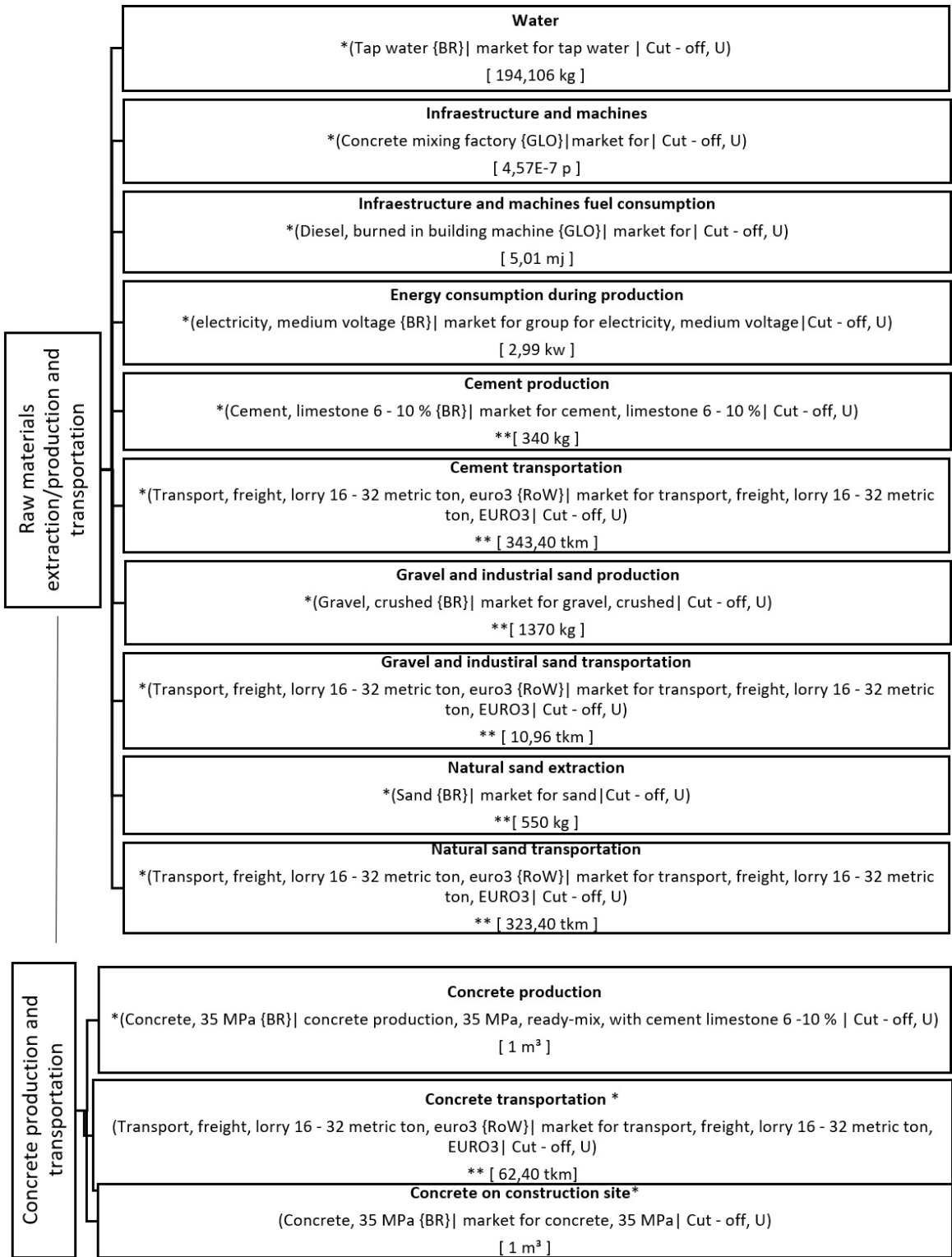
Figure 2. Flowchart with adjusted data for wooden shapes.



* As obtained from SimaPro

** Adjusted data

Figure 3. Flowchart with adjusted data for 20 MPa concrete.



* As obtained from SimaPro

** Adjusted data

Figure 4. Flowchart with adjusted data for 35 MPa concrete.

4.2 Columns optimization

The optimized design of reinforced concrete column sections subjected to uniaxial bending-compression was conducted using a software developed by Bordignon and Kripka [33] and updated in 2019, where the Simulated Annealing method was used for the optimization associated with a routine for checking the strength of columns.

Considering a rectangular cross-section, the objective of optimal design is to obtain a configuration that is capable of producing resistant bending and axial forces (M_{rd} and N_{rd}), equal to or greater than the acting forces (M_{sd} and N_{sd}), with minimal environmental impact. The design variables were considered as discrete, with the values related to the dimensioning of the concrete cross-section (x_1 and x_2) varying every centimeter, and the areas, quantities, and disposition of the reinforcements (x_3 to x_7 , respectively) limited to commercial values, as shown in Figure 5.

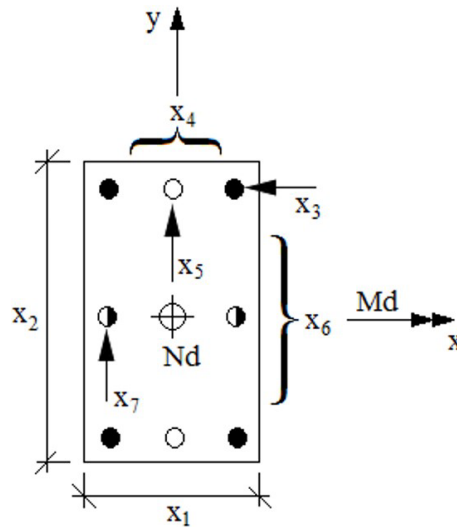


Figure 5. Column optimization design variables Source: Bordignon and Kripka [33]

The original objective function was adapted to minimize the environmental impact produced by the component materials of the section, per linear meter of column. From the variables described in Figure 6, the objective function can be written as in Equation 3:

$$f(x)=(x_1 \cdot x_2) \cdot C_c + (4 \cdot x_3 + 2 \cdot x_4 \cdot x_5 + 2 \cdot x_6 \cdot x_7) \cdot C_s + 2 \cdot (x_1 + x_2) \cdot C_f \tag{3}$$

The first part of the function represents the CO₂ emissions from the concrete, where C_c is the CO₂ emission per unit volume. The second part represents the emissions from the longitudinal reinforcement, being C_s the respective impact per unit of mass. The last part represents the CO₂ emission relative to wood forms, where C_f is the CO₂ emission per unit area.

The constraints imposed on the optimization problem refer to the strength criteria and aspects related to minimum and maximum dimensions of the concrete section, the reinforcement ratio, and spacing between bars. More details on the formulation and implementation aspects can be found in Bordignon and Kripka [33].

Based on the formulation described, four sections of columns were optimized with acting forces taken from [33] and listed in Table 2.

Table 2. Values of forces acting on the columns

	N (kN)	M (kN.cm)
P1	500	6,250
P2	2,250	28,125
P3	5,000	62,500
P4	7,250	90,625

4.3 Beams optimization

To perform the optimized design of the reinforced concrete beams, the software developed by Tres Junior and Kripka [34] was used, which adopts a modified version of Harmony Search as the optimization method [35]. As with the optimization of the columns, the objective was to minimize the total impact produced by the concrete, steel, and formworks, measured in kgCO₂. Aiming to reduce the cost of reinforced concrete beams, the following design variables were defined, also represented in Figure 6: b is the beam width; h is the beam height; Nb_{int} is the number of internal rebars; $\varnothing e$ is the diameter of the outer rebars, and $\varnothing i$ is the diameter of the inner rebars. All design variables of the problem are discrete and can assume pre-established values. The constraints of the problem involve the verification of the ultimate and service limit states, according to the guidelines of the Brazilian standard ABNT NBR 6118 [36], related to bending moments, rebar spacing, crack opening, and displacements [34].

In this study, double-supported beams with span L from 3 to 10m were designed for live loads and dead loads of 9.5 kN/m and 2 kN/m, respectively (plus self-weight).

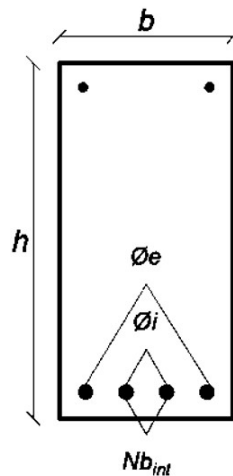


Figure 6. Optimization problem design variables

4.4. Effect of carbonation

To evaluate the effect of carbonation in reducing the total CO₂ emission of the structures, the optimized columns and beams of the previous examples were considered. To calculate the carbonation depth, the structures were considered to be built in an urban environment protected from rain, with an average annual humidity of 70% and a CO₂ content of 0.04%, in exposed and unpainted concrete. Initially, the useful life of 50 years was adopted, and again, concrete with a compressive strength of 20 MPa and 35 MPa with CP II-F-32 cement was used (Portland cement with filler). Based on the methodology previously described, CO₂ emissions from component materials of reinforced concrete were obtained. Carbonation depth over time and the amount of CO₂ captured during the service life of the structures were obtained from Equations 1 and 2 previously presented. It was considered that the surface area of the concrete section is fully exposed to the action of CO₂. This last consideration is not verified to inner beams and columns of buildings, for example, and in this case, can be seen as an “upper limit” of carbonation.

5 OPTIMIZED SIZING OF REINFORCED CONCRETE ELEMENTS

The corresponding values are presented in Table 3, considering the phase from cradle to gate of the raw materials.

Table 3. CO₂ emissions from component materials of reinforced concrete structures.

	Extraction/Production	Transport	Total Emissions
Steel (kgCO ₂ /kg)	1.85	0.12	1.97
Formworks (kgCO ₂ /m ²)	20.44	0.48	20.92
Concrete 20 MPa (kgCO ₂ /m ³)	330.17	8.79	338.96
Concrete 35 MPa (kgCO ₂ /m ³)	401.49	4.61	406.10

From the table, the emissions from the extraction and production phases of the materials correspond to most of the impacts produced. However, the impact of transport cannot be neglected either, as it can reach up to 6.4% of total emissions, as in the case of steel. It can also be seen that, in unitary terms, the impact of concrete is significantly greater than that of other materials. Comparing the results obtained for concrete emissions from the city of Passo Fundo, RS [10], less than 200 km distant, the impacts of the present study are higher (6.4% for 35MPa concrete and 10.2% for 20MPa). The 35MPa concrete, as it uses a greater amount of cement, also has a greater impact compared to the 20MPa concrete (about 20% greater). On the other hand, it is interesting to notice that in terms of efficiency, concrete 35MPa produces an impact of 11.60 kgCO₂/m³/MPa, 31.5% lesser than 20MPa concrete (16.94 kgCO₂/m³/MPa). It is clear that a fair comparison between these materials must be made considering their application to a structural element.

The result of the optimized dimensioning of the sections of the columns proposed for the concretes with characteristic strengths of 20 MPa and 35 MPa, for the unit impacts listed in Table 3, are presented in Figure 7, where the value of emissions is given in kgCO₂/m of the column.

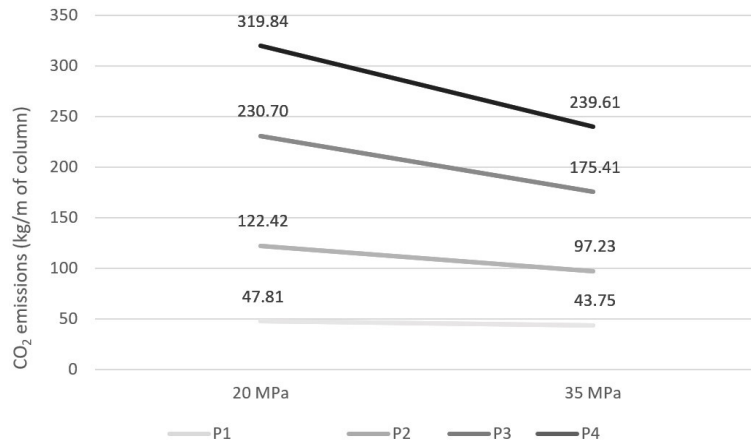


Figure 7. CO₂ emissions of the optimized design of reinforced concrete columns.

From Figure 7 it can be noticed that CO₂ emissions progressively decrease with increasing concrete strength for all considered stresses. When considering the efficiency in terms of kgCO₂/m³/MPa, the advantage regarding the usage of higher strengths is even greater.

Figure 8 presents the percentage contributions of CO₂ emissions from materials to the optimized columns. The percentage contributions are given in %/m of column, for the four optimized columns, considering the strengths and materials used (concrete, steel, and formworks). It was observed that for smaller acting moments (P1) a significant reduction of concrete section due to the increase in concrete strength (about 25%) does not imply in a percentual reduction of the total contribution of concrete regarding global emissions. To the other acting forces considered, the reduction of the concrete section was more significant, leading to an effective reduction in its relative contribution to total impact.

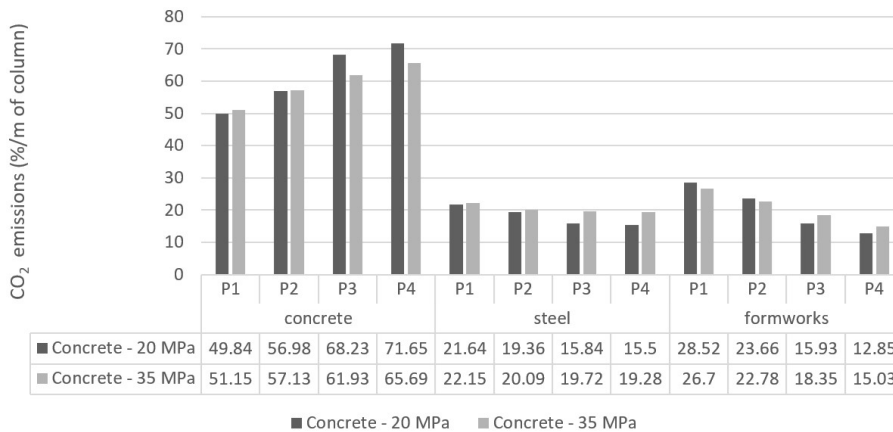


Figure 8. Percentage contributions of CO₂ emissions of materials for the optimized abutments.

Regarding the results presented in Figure 8, the analysis shows that the percentage contributions of concrete tend to increase as the stress increase, whereas for steel and wooden formworks the percentage contributions tend to decrease as the stress increases.

Figure 9 shows the result of the optimized dimensioning of the beams in relation to the impact measured in terms of kgCO₂/m for the two analyzed strengths.

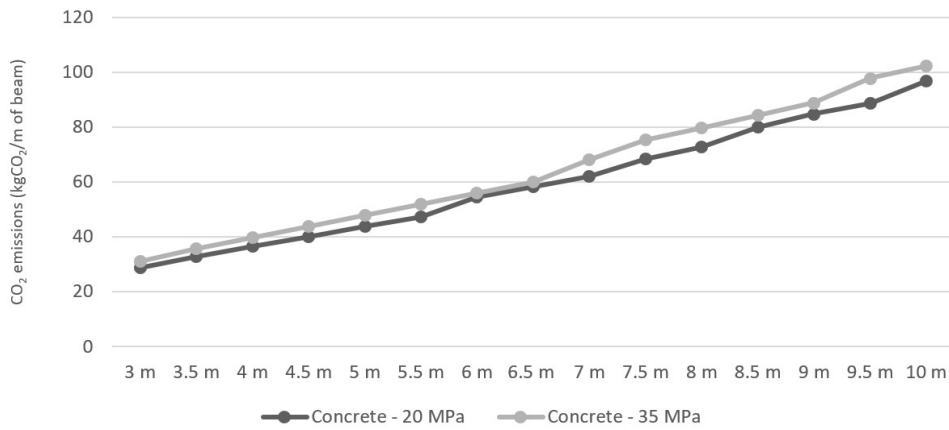


Figure 9. CO₂ emissions of reinforced concrete beams.

In the analysis of the results, it is observed that CO₂ emissions/m of beam increase progressively as the span of the beam increases. Contrary to what was observed for the columns, the lower-strength concrete produced less impact for all the spans analyzed. The beams dimensioned with 35MPa concrete presented an impact between 3 and 10% greater, with an average value of 7.5%. A similar trend had been obtained by Medeiros and Kripka [37] considering the cost of the beams.

Figure 10 shows the percentage of CO₂ absorbed during the life of the columns in relation to CO₂ emissions during their production.

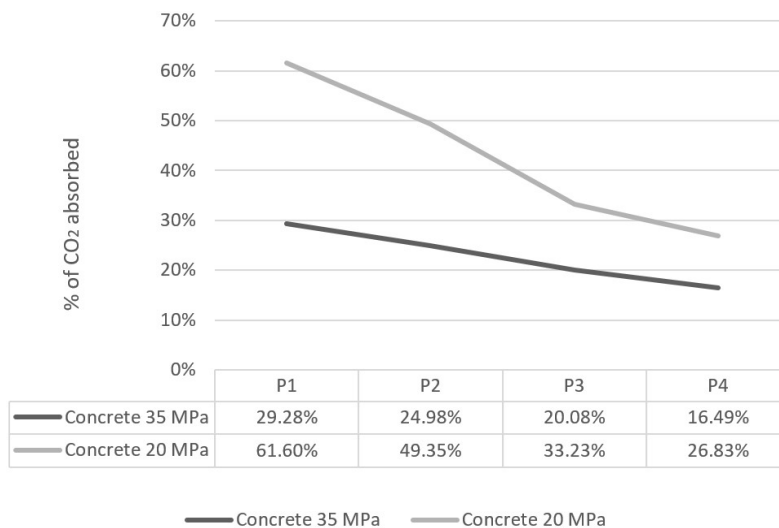


Figure 10. CO₂ capture during the useful life of columns designed with 20 and 35 MPa concrete.

The average carbonation for the columns with 20 MPa concrete was on average around 42%, which means that the columns absorbed approximately 42% of the CO₂ emitted during the entire process of material extraction, transport, and production. For the columns optimized with 35 MPa concrete, the average absorption was about 22% of the CO₂ produced. It was observed that, with the increase of the compressive strength of the concrete, the depth of carbonation of the concrete decreases, and consequently, the amount of CO₂ absorbed by the structural element also decreases.

Figure 11 presents the results of the carbonation calculation for the reinforced concrete beams. It was observed that the beams dimensioned with concrete of 35 MPa absorbed an average of 31% of the emitted CO₂ and that the beams dimensioned with concrete of 20 MPa absorbed an average of 66%.

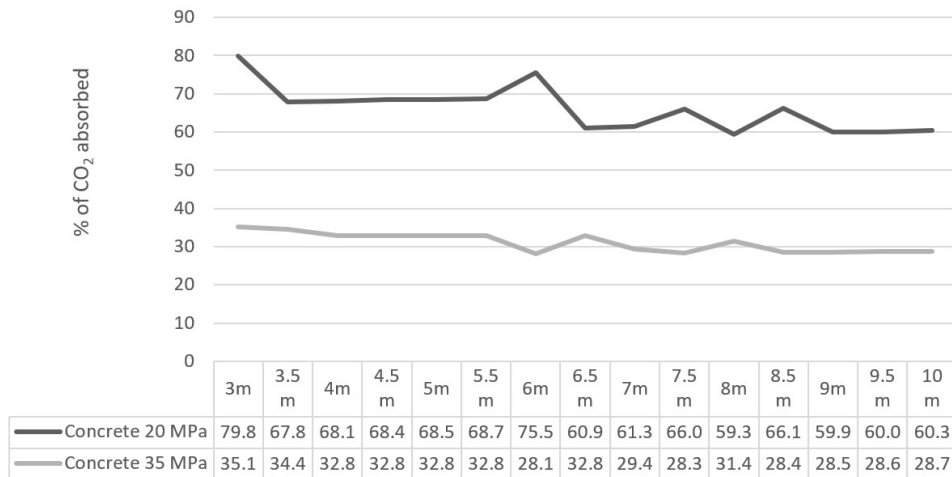


Figure 11. CO₂ capture during the service life of beams dimensioned with 20 and 35 MPa concrete.

Figure 12 shows the carbonation of the beam with an intermediate span (beam V8, with a span of 6.5m), with a useful life ranging from 10 to 100 years.

Through the analysis of Figure 12, it is possible to see that the capture of CO₂ increases in percentage when considering the longer useful life of the reinforced concrete structure. For example, for a lifetime of 50 years, the beam absorbs approximately 31.97% of the CO₂ emitted during its entire manufacturing process. For the 100-year lifespan, the absorption rises to about 45.34% of the CO₂ emitted (an increase of 41.8%). Furthermore, the 20 MPa concrete beam would absorb almost twice as much CO₂ as the 35 MPa beam in the same period.

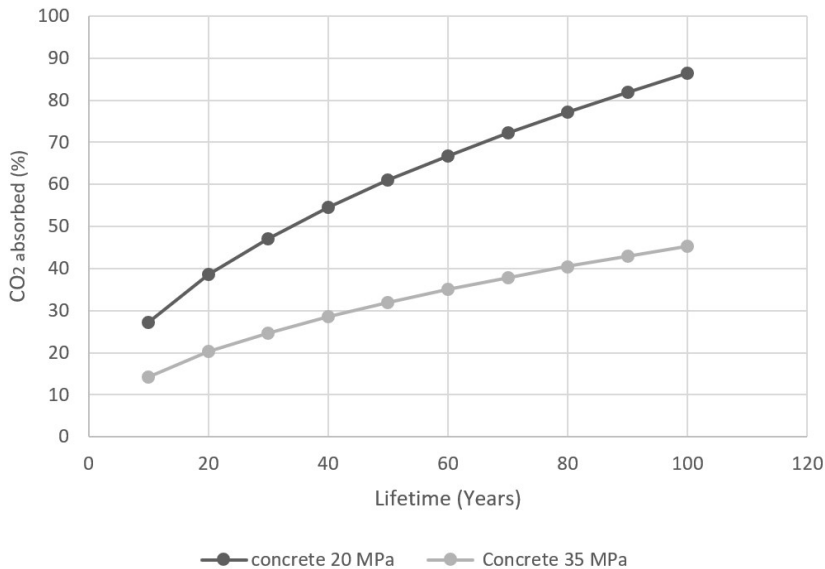


Figure 12. Comparison of the carbonation of the beam with a span of 6.50 m for a useful life ranging from 10 to 100 years.

6 CONCLUSIONS

The present work aimed to evaluate the environmental impact of reinforced concrete structures from the determination of CO₂ emissions in optimized structures. This assessment was conducted based on the emissions determined for the City of Chapecó, SC, Brazil. Based on data provided by a concrete batcher in the region, the emissions of concrete with two different characteristic strengths were determined, in addition to steel and wood formworks. In general, it was observed that these values are significantly different from those obtained in a study conducted in another city in the southern region, evidencing the influence of factors such as distances and dosage of concrete. Mainly due to the greater amount of cement used, the 35MPa concrete presented emissions about 20% higher than the 20MPa concrete.

The emission values obtained were used in the optimization of beams and columns, considering the emissions of concrete, steel, and formworks. In general, it was observed that in columns it is interesting to use higher-strength concrete. To the beams, on the contrary, the lowest total emissions were obtained with concrete of lower strength.

Finally, the influence of the concrete carbonation process on total CO₂ emissions was evaluated. It was observed that, invariably, the percentage absorbed compared to that emitted is quite significant, and must be considered in the global assessment of impacts. It is interesting to observe that the lower strength concrete, even producing the lowest emission per unit volume, is also the one that absorbs the most CO₂, which increases its positive impact compared to the higher strength concrete.

In general, the present study aimed to identify the main factors that influence the impacts produced by reinforced concrete structures, as a subsidy for the designers and decision-makers. In addition to the results presented, it is suggested as a guideline for the mitigation of impacts the study of substitutes for portland cement, as well as the use of raw materials that require a shorter transport distance.

As a continuation of the study, concretes with other characteristic strengths will be evaluated, as well as the influence of the selected impact category on the results. In addition, although the behavior regarding carbonation agrees with the observed in the literature, it is important to deepen the studies related to factors that allow a better estimate that total percentage of reduction.

Although the present study was developed with data obtained for a specific region of the country, it is understood that the proposed methodology can be easily adapted to other locations.

7. ACKNOWLEDGEMENTS

The first and the second author are grateful to Universidade de Passo Fundo for the financial support for their studies. The third author is grateful for the financial support received from the Brazilian government in the form of grant (National Council for Scientific and Technological Development – CNPq, Grant CNPq- 306578/2020-4).

REFERENCES

- [1] A. B. Rohden and M. R. Garcez, "Increasing the sustainability potential of reinforced concrete building through design strategies: case study," *Case Stud. Constr. Mater.*, vol. 9, pp. e00174, 2018, <http://dx.doi.org/10.1016/j.cscm.2018.e00174>.
- [2] M. Roberts, S. Allen, and D. Coley, "Life cycle assessment in the building design process – A systematic literature review," *Build. Environ.*, vol. 185, pp. 107274, 2020, <http://dx.doi.org/10.1016/j.buildenv.2020.107274>.
- [3] J. Ferreira-Cabello, E. Fraile-Garcia, E. Martinez-Camara, and M. Perez-de-la-Parte, "Sensitivity analysis of life cycle assessment to select reinforced concrete structures with one-way slabs," *Eng. Struct.*, vol. 132, pp. 586–596, 2017, <http://dx.doi.org/10.1016/j.engstruct.2016.11.059>.
- [4] D. Yeo and R. D. Gabbai, "Sustainable design of reinforced concrete structures through embodied energy optimization," *Energy Build.*, vol. 43, pp. 2028–2033, 2011, <http://dx.doi.org/10.1016/j.enbuild.2011.04.014>.
- [5] G. F. Medeiros and M. Kripka, "Optimization of reinforced concrete columns according to different environmental impact assessment parameters," *Eng. Struct.*, vol. 59, pp. 185–194, 2014, <http://dx.doi.org/10.1016/j.engstruct.2013.10.045>.
- [6] A. K. Al-Tamimi, A. Ibrahim, and N. Al-Sughaiyer, "Evaluation of sustainability of multistory reinforced concrete structure," *Phys. Procedia*, vol. 55, pp. 445–450, 2014, <http://dx.doi.org/10.1016/j.phpro.2014.07.064>.
- [7] E. Possan, W. A. Thomaz, G. A. Aleandri, E. F. Felix, and A. C. P. Santos, "CO₂ uptake potential due to concrete carbonation: a case study," *Case Stud. Constr. Mater.*, vol. 6, pp. 147–161, 2017, <http://dx.doi.org/10.1016/j.cscm.2017.01.007>.
- [8] H. Li, Q. Deng, J. Zhang, B. Xia, and M. Skitmore, "Assessing the life cycle CO₂ emissions of reinforced concrete structures: four cases from China," *J. Clean. Prod.*, vol. 210, pp. 1496–1506, 2019., <http://dx.doi.org/10.1016/j.jclepro.2018.11.102>.
- [9] N. Stoiber, M. Hamerl, and B. Kromoser, "Cradle-to-gate life cycle assessment of CFRP reinforcement for concrete structures: calculation basis and exemplary application," *J. Clean. Prod.*, vol. 280, pp. 124300, 2021, <http://dx.doi.org/10.1016/j.jclepro.2020.124300>.
- [10] J. F. Santoro, "*Subsídios para a minimização do impacto ambiental de estruturas em concreto armado*", Ph.D. dissertation, Prog. Pós-grad. Eng. Civ. Amb., Univ. Passo Fundo, Passo Fundo, RS, 2021.
- [11] L. Yepes-Bellver, A. Brun-Izquierdo, J. Alcalá, and V. Yepes, "CO₂-optimization of post-tensioned concrete slab-bridge decks using surrogate modeling," *Materials (Basel)*, vol. 15, no. 14, pp. 4776, 2022, <https://doi.org/10.3390/ma15144776>.
- [12] S. Jacobsen and P. Jahren, "Binding of CO₂ by carbonation of Norwegian OPC concrete", in *CANMET/ACI International Conference on Sustainability and Concrete Technology*, Lyon, 2002.
- [13] J. Gajda and F. M. Miller, *Concrete as a Sink for Atmospheric Carbon Dioxide: a Literature Review and Estimation of CO₂ Absorption by Portland Cement Concrete*, Skokie, IL, USA: Portland Cement Association, 2000, Accessed: Mar. 10, 2022. [Online]. Available: http://www.portcement.org/pdf_files/SN2255.pdf

- [14] C. Pade and M. Guimarães, "The CO₂ uptake of concrete in a 100-year perspective," *Cement Concr. Res.*, vol. 37, no. 9, pp. 1348–1356, 2007, <http://dx.doi.org/10.1016/j.cemconres.2007.06.009>.
- [15] L. Haselbach and A. Thomas, "Carbon sequestration in concrete sidewalk," *Constr. Build. Mater.*, vol. 54, pp. 47–52, 2014, <http://dx.doi.org/10.1016/j.conbuildmat.2013.12.055>.
- [16] Associação Brasileira de Normas Técnicas, *Environmental Management - Life Cycle Assessment - Principles and Structure*, NBR ISO 14040, 2014.
- [17] J. B. Guinée et al., "Life cycle assessment: past, present and future," *Environ. Sci. Technol.*, vol. 45, no. 1, pp. 90–96, 2011, <http://dx.doi.org/10.1021/es101316v>.
- [18] X. Zhang, L. Song, and M. Huang, "The state-of-the-art of green building research (2010-2019): a bibliometric review", *IOP Conf. Ser.: Earth Environ. Sci.*, vol. 376, pp. 012025, 2019, <http://dx.doi.org/10.1088/1755-1315/376/1/012025>.
- [19] I. Navarro, V. Yepes, and J. V. A. Martí, "A review of multicriteria assessment techniques applied to sustainable infrastructure design," *Adv. Civ. Eng.*, vol. 2019, pp. 6134803, 2019, <http://dx.doi.org/10.1155/2019/6134803>.
- [20] R. G. Rajan, N. Sakthieswaran, and O. G. Babu, "Experimental investigation of sustainable concrete by partial replacement of fine aggregate with treated waste tyre rubber by acidic nature," *Mater. Today Proc.*, vol. 37, pp. 1019–1022, 2020, <http://dx.doi.org/10.1016/j.matpr.2020.06.279>.
- [21] S. K. Verma, C. S. Singla, G. Nadda, and R. Kumar, "Development of sustainable concrete using silica fume and stone dust," *Mater. Today Proc.*, vol. 32, pp. 882–887, 2020, <http://dx.doi.org/10.1016/j.matpr.2020.04.364>.
- [22] P. S. Joanna, T. S. Parvati, J. Rooby, and R. Preetha, "A study on the flexural behavior of sustainable concrete beams with high volume fly ash," *Mater. Today Proc.*, vol. 33, pp. 1149–1157, 2020, <http://dx.doi.org/10.1016/j.matpr.2020.07.343>.
- [23] R. K. Majhi and A. N. Nayak, "Production of sustainable concrete utilizing high-volume blast furnace slag and recycled aggregate with lime activator," *J. Clean. Prod.*, vol. 255, pp. 120188, 2020, <http://dx.doi.org/10.1016/j.jclepro.2020.120188>.
- [24] A. S. Gutiérrez, J. J. Cabello Eras, C. A. Gaviria, J. Van Caneghem, and C. Vandecasteele, "Improved selection of the functional unit in environmental impact assessment of cement," *J. Clean. Prod.*, vol. 168, pp. 463–473, 2017, <http://dx.doi.org/10.1016/j.jclepro.2017.09.007>.
- [25] E. F. Felix and E. Possan, "Modeling the carbonation front of concrete structures in the marine environment through ANN," *IEEE Lat. Am. Trans.*, vol. 16, no. 6, pp. 1772–1779, Jun 2018, <http://dx.doi.org/10.1109/TLA.2018.8444398>.
- [26] S. Z. Carvalho, F. Vermilli, B. Almeida, M. D. Oliveira, and S. N. Silva, "Reducing environmental impacts: the use of basic oxygen furnace slag in Portland cement," *J. Clean. Prod.*, vol. 172, pp. 385–390, 2018., <http://dx.doi.org/10.1016/j.jclepro.2017.10.130>.
- [27] Sindicato Nacional da Indústria do Cimento. *ROADMAP tecnológico do cimento: potencial de redução das emissões de carbono da indústria do cimento brasileira até 2050*. Rio de Janeiro, RJ, Brasil: SNIC, 2019, 64 p.
- [28] S. Vogeles, M. Grajewski, K. Govorukha, and D. Rubbelke, "Challenges for the European steel industry: analysis, possible consequences and impacts on sustainable development," *Appl. Energy*, vol. 264, pp. 114633, 2020, <http://dx.doi.org/10.1016/j.apenergy.2020.114633>.
- [29] P. V. Nidheesh and M. S. Kumar, "An overview of environmental sustainability in cement and steel production," *J. Clean. Prod.*, vol. 231, pp. 856–887, 2019, <http://dx.doi.org/10.1016/j.jclepro.2019.05.251>.
- [30] N. B. R. Monteiro, J. M. Moita Neto, and E. A. da Silva, "Environmental assessment in concrete industries," *J. Clean. Prod.*, vol. 327, pp. 129516, 2021, <http://dx.doi.org/10.1016/j.jclepro.2021.129516>.
- [31] S. Roh, R. Kim, W. J. Park, and H. Ban, "Environmental evaluation of concrete containing recycled and by-product aggregates based on life cycle assessment," *Appl. Sci. (Basel)*, vol. 10, pp. 7503, 2020, <http://dx.doi.org/10.3390/app10217503>.
- [32] S. O. Ekolu, "Implications of global CO₂ emissions on natural carbonation and service lifespan of concrete infrastructures – Reliability analysis," *Cement Concr. Compos.*, vol. 114, pp. 103744, 2020, <http://dx.doi.org/10.1016/j.cemconcomp.2020.103744>.
- [33] R. Bordignon and M. Kripka, "Optimum design of reinforced concrete columns subjected to uniaxial flexural compression," *Comput. Concr.*, vol. 9, no. 5, pp. 327–340, 2012, <http://dx.doi.org/10.12989/cac.2012.9.5.327>.
- [34] F.L. Tres Junior, and M. Kripka, "Modified improved harmony search applied to reinforced concrete beams", in *CILAMCE-PANACM*, Rio de Janeiro, RJ, Brasil, 2021.
- [35] G. F. Medeiros and M. Kripka, "Modified harmony search and its application to cost minimization of RC columns," *Adv. Comp. Des.*, vol. 2, pp. 1–13, 2017, <http://dx.doi.org/10.12989/acd.2017.2.1.001>.
- [36] Associação Brasileira de Normas Técnicas, *Design of Concrete Structures – Procedure*, NBR 6118, 2014.
- [37] G. F. Medeiros and M. Kripka, "Structural optimization and proposition of pre-sizing parameters for beams in reinforced concrete buildings," *Comput. Concr.*, vol. 11, no. 3, pp. 253–270, 2013, <http://dx.doi.org/10.12989/cac.2013.11.3.253>.

Author contributions: JJA and MK: conceptualization, methodology, formal analysis, writing; JFS: methodology, formal analysis

Editors: Edna Possan, Mark Alexander



REVIEW

On factors affecting probabilistic service life modeling of concrete structures under marine environments

Fatores que afetam a modelagem probabilística da vida útil de estruturas de concreto armado expostas a ambientes marinhos

Gustavo Bosel Wally^{a,b} Fábio Costa Magalhães^{b,c} Mauro de Vasconcellos Real^c Luiz Carlos Pinto da Silva Filho^a 

^aUniversidade Federal do Rio Grande do Sul – UFRGS, Laboratório de Ensaios e Modelos Estruturais – LEME, Porto Alegre, RS, Brasil

^bInstituto Federal de Educação, Ciência e Tecnologia do Rio Grande do Sul – IFRS, Laboratório de Estruturas e Materiais de Construção Civil – LEMCC, Rio Grande, RS, Brasil

^cUniversidade Federal do Rio Grande – FURG, Programa de Pós-graduação em Engenharia Oceânica – PP GEO, Rio Grande, RS, Brasil

Received 23 March 2022
Accepted 19 September 2022

Abstract: Concrete durability design has received increasing importance recently, with specifications moving from prescriptive to performance based. In performance-based approaches, it is essential to evaluate and calibrate service life models capable of reliably representing the phenomenon that triggers the degradation process. This paper aims to discuss the main concepts related to the probabilistic service life modeling of reinforced concrete structures under chloride environments, considering the application of different prediction models. Through numerical analysis, parametric differences among chloride penetration models are evidenced, and the results, their variability, and the admitted failure conditions are analyzed. An overview of the current scenario of the durability design of concrete structures is presented. Aspects associated with characteristic service life, the definitions of durability limit states, and their respective target failure probabilities are discussed.

Keywords: service life modeling, performance-based approach, durability limit states, probability-based design.

Resumo: O projeto de durabilidade de estruturas de concreto tem ganhado crescente importância nos últimos anos, havendo a transição das especificações prescritivas às baseadas em desempenho. No contexto das abordagens de desempenho, é essencial avaliar e calibrar modelos de previsão de vida útil capazes de representar o fenômeno que desencadeia o processo de degradação. Este artigo visa discutir os principais conceitos relacionados à modelagem da vida útil de estruturas de concreto armado expostas a ambientes ricos em cloretos, considerando a aplicação de diferentes modelos de estimativa da penetração de cloretos no concreto. Através de uma análise numérica, diferenças paramétricas entre os modelos são evidenciadas, bem como são analisados os resultados, suas variabilidades e as condições de falha admitidas. Uma visão geral do atual cenário dos projetos de durabilidade de estruturas de concreto é apresentada. Aspectos associados ao conceito de vida útil característica, às definições de estados limites de durabilidade e suas respectivas probabilidades de falha admissíveis são discutidos.

Palavras-chave: modelagem de vida útil, abordagem baseada em desempenho, estados limite de durabilidade, análise probabilística.

How to cite: G. B. Wally, F. C. Magalhães, M. V. Real, and L. C. P. Silva Filho, "On factors affecting probabilistic service life modeling of concrete structures under marine environments," *IBRACON Struct. Mater. J.*, vol. 15, no. 6, e15605, 2022, <https://doi.org/10.1590/S1983-41952022000600005>

Corresponding author: Gustavo Bosel Wally. E-mail: gustavo.wally@gmail.com

Financial support: The authors thank FAPERGS (Research Support Foundation of Rio Grande do Sul) for the financial support (PqG 07/2021). M. V. Real thanks CNPq (Brazilian National Council for Scientific and Technological Development) for the research grant (Process 302548/2021-1).

Conflict of interest: Nothing to declare.

Data Availability: The data that support the findings of this study are available from the corresponding author, GBW, upon reasonable request.



This is an Open Access article distributed under the terms of the Creative Commons Attribution License, which permits unrestricted use, distribution, and reproduction in any medium, provided the original work is properly cited.

1 INTRODUCTION

The sustainability of cement-based materials is a hot topic nowadays, primarily due to the carbon footprint of cement industries [1]–[3]. However, in the case of reinforced concrete structures, sustainability does not only comprise the production of concrete and its constituent materials but also involves strength, durability, performance, service life, and the life cycle of the structural elements [4]. Ensuring durability, therefore, is a crucial point for concrete sustainability [5].

Regarding reinforced concrete structures exposed to marine environments, many structural elements have had a service life shorter than the designed service life due to the various attacks from seawater, mainly due to chloride-induced reinforcement corrosion [6]. In several cases, in addition to the environmental aggressiveness, the concrete quality does not meet minimum parameters, reducing the service life of the structures. For these reasons, concrete durability specifications are moving from prescriptive to performance-based approaches [7].

In a performance-based approach, at least one parameter directly related to the concrete durability must be assessed – for example, the chloride diffusivity in the case of structures in marine environments. Additionally, the service life of the structure must be modeled considering the characteristics of the placed concrete, the environmental aggressiveness, and the durability limit states (DLS) [8], [9]. The definition of the service life model to be adopted, as well as the considered failure criterion, however, are quite complex. Incorrect selection of these factors can lead to significantly different service life predictions. Added to these facts is the difficulty of establishing long-term verification processes for the estimates made by each model, contributing to the increase in uncertainties related to the estimated service life of reinforced concrete structures.

This paper presents an overview of the current scenario of the durability design of concrete structures. The main parameters related to concrete service life prediction are analyzed through a probabilistic assessment. Three well-known chloride penetration models are addressed – namely, the Duracon model [10], the *fib* model [11], and the *Life-365* model [12]. Emphasis is placed on the influence of uncertainties in concrete durability design, especially related to concrete properties, cover depth, and environmental characteristics.

1.1 Factors affecting chloride penetration in concrete – a brief review

Chloride penetration in concrete is a complex process, affected by several factors. The durability of reinforced concrete structures against chloride penetration depends fundamentally on the characteristics of the reinforcement cover, both on the concrete properties and the cover depth. Additionally, the proper construction procedure of the structure and the adequate consideration of environmental aggressiveness are fundamental to guarantee concrete durability.

For example, the solution of Fick's 2nd Law of Diffusion [13], widely adopted in estimating chloride penetration in concrete, synthesizes the environmental aggressiveness in a parameter called surface chloride content (C_s) and summarizes the structural characteristics in chloride diffusion coefficient (D) and cover depth (x_c).

In general terms, the durability potential of a reinforced concrete structure is, therefore, a relationship between the environmental aggressiveness and the resistance presented by the structure, as illustrated in Figure 1. It is necessary to realize, however, that these parameters can be influenced by several other factors, such as, for example, characteristics of the constituent materials of concrete, temperature, relative humidity, and the structure construction process. Several chloride penetration models seek to introduce the influence of these parameters in estimating service life. However, there is great difficulty in accurately measuring how each factor affects the process of chloride penetration. Such effects are discussed below.

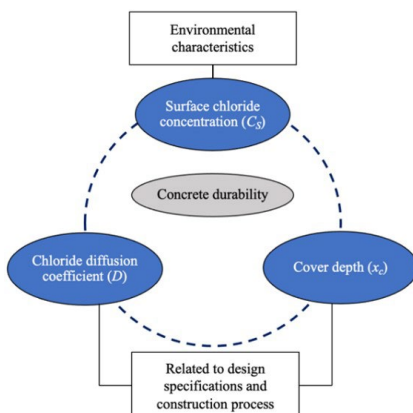


Figure 1. Leading factors affecting chloride penetration in concrete.

1.1.1 Chloride diffusion coefficient

In the case of durability analyses, the main concrete characteristic to be addressed is its penetrability. Concrete penetrability is how the concrete allows ions or fluids to move through its pore structure. Therefore, penetrability comprises transport mechanisms such as diffusion, permeability, capillary absorption, and migration. Despite this, most models that aim to describe chloride penetration in concrete adopt the diffusion process as the main responsible for the ingress of these ions through the pore structure of concrete. Thus, the chloride diffusion coefficient of concrete is considered the primary indicator of concrete performance against the action of these ions.

It is known that several factors affect concrete diffusivity, and these can be related to the concrete mix design, such as the water/binder ratio [14], [15], cement type and content [16], [17], and the use of mineral admixtures [18]–[20]. Other factors are related to concrete curing [21]–[24]. Some are related to characteristics of the environment in which the structure is inserted, such as temperature [25], [26], relative humidity [27], [28], and concrete saturation degree [29], [30]. These influences, however, seem to be clear and well established in the concrete production chain.

Special attention is given to test methods to determine the chloride penetrability in concrete. When chloride penetration into concrete is evaluated using diffusion-based test methods, long periods are required. From a technical perspective, however, test methods linked to durability-related properties must be easy and quick to perform, facilitating quality control of the placed material and decision-making in cases of non-compliance. Therefore, several migration-based test methods have been proposed and used in concrete specification and quality control, as discussed by Bjegović et al. [31], Nanukuttan et al. [32], and Milla et al. [33].

Using different test methods to determine the chloride penetrability in the concrete, however, lead to different results for the same concrete. This variation in the results was observed, for example, by Castellote and Andrade [34] and Sell Junior et al. [35]. Thus, it is essential that when specifying a specific target value for the chloride penetrability in a durability design, there is a clear indication of which test method should be adopted and the definition of which coefficient should be considered - whether effective or apparent, for example. It should also be noted that, regardless of the test method adopted, it is necessary to understand how the results obtained relate to the concrete performance *in situ*.

In addition to determining the diffusion coefficient, it is essential to consider the time dependence of the diffusion coefficient when estimating chloride penetration in reinforced concrete structures. This reduction in diffusivity is mainly due to the refinement of the concrete pore structure during the cement hydration process and possible pozzolanic reactions. It depends, among other factors, on the w/b ratio, the cement type and content, and the mineral admixtures type and content [36], [37]. This topic has been the subject of several discussions [38]–[40] and has contributed to the increase in uncertainties about estimating the service life of reinforced concrete elements. The calibration of the concrete diffusivity reduction level requires long-term analyses, which are more complex to perform. However, it should be noted that using the diffusion coefficient measured in the first ages as an input parameter in service life prediction models is a factor that favors safety. Many phenomena that occur in the first years after the structure's construction tend to reduce the chloride diffusivity.

Although the decisions made during the structure design are of great importance for ensuring concrete durability, the processes of concrete production and construction also strongly influence the durability potential of a reinforced concrete structure. For example, according to Helene and Terzian [41], the influence of labor on concrete properties, including variability in time and mixing procedure, is on the order of 30%. Depending on several factors related to concrete production and placing, the quality achieved by the placed concrete can present an even more significant variability.

Magalhães et al. [42], in turn, highlight that gross errors that affect the properties of concrete in a generalized way, such as overdoses of additives, excess water, or failures in cement weighing, are more easily detected. However, systematic variations in the production process tend to be more difficult to identify and correct. Also, the effects of slump corrections carried out without criteria, which strongly influence the porosity and, consequently, the diffusivity of the concrete, cannot be neglected. In the Brazilian context, NBR 7212 [43] indicates that a strict system must be established to control and record the amount of water added to the concrete at the plant and the complementation to be carried out at the construction site to avoid excess water. In some Brazilian constructions, however, the requirement of additional water to facilitate the concrete placing persists by those responsible for the placing process.

1.1.2 Cover depth

Reinforcement cover depth constitutes, together with the characteristics of concrete expressed by the chloride diffusion coefficient, the resistant capacity of the concrete against the chloride penetration. The stipulation of minimum

x_C values ($x_{C,min}$) is a common practice in prescriptive durability specifications of many current codes. The Brazilian NBR 6118 [44], for example, indicates $x_{C,min}$ between 35 and 50 mm for structures exposed to marine environments, depending on exposure class and structural element type.

Naturally, the increase in the cover depth makes it difficult to start the chloride-induced corrosion since the path to be followed by the aggressive ions increases. In this sense, the Eurocode 2 [45] suggests that an increase of 10 mm can increase the structural service life from 50 to 100 years. However, it should be noted that excessive increases in the cover depth may not be the most appropriate measure since there is a greater risk of concrete cracking. Within the acceptable limits of cover depth, the best alternative is to ensure that the concrete has low penetrability.

It is also necessary to pay attention to the fact that the cover depths, although measured and considered adequate before the concrete placing, can undergo alterations during this process, resulting, in some instances, in inadequate reinforcement covers in the placed structure. The guarantee that the structure will present adequate cover depth to reach the required service life is, therefore, a function of the specification of the appropriate nominal cover depth for a certain exposure class and of rigorous quality control at the construction time.

1.1.3 Environmental characteristics

Surface chloride content is a critical parameter in concrete durability design, being a quantitative measure of the environmental aggressiveness against the structure [46]. Previous studies show that C_S is strongly affected by various factors, especially exposure duration and environmental conditions, such as wind directions and speed, chloride concentration of seawater, distance from seawater, and rain fallout [47]–[49].

Due to many environmental parameters that affect the surface chloride content and its high variability, it is not easy to make an accurate estimate of C_S values. Additionally, several of these factors have characteristics or influences that vary over time, making C_S also time-dependent ($C_{S(t)}$). Despite this, many service life prediction models adopt constant C_S values – as is the case in the models addressed in this paper. It should be noted that the constant value adopted is usually higher than the effective value of C_S during the first ages of the structure; on the other hand, although C_S can become elevated at advanced ages, it tends to stabilize. Thus, an average value of C_S is usually adopted in service life prediction models and tends not to generate significant distortions in the analyzes performed.

In reporting the Norwegian experience on concrete durability specifications, GjØrv [10] also highlights the high variability of C_S , pointing to the need for C_S values to be appropriately estimated and selected and be as representative as possible, especially regarding the most exposed elements of the structure. In some instances, it is appropriate to consider different surface chloride contents for different parts of the same structure, as highlighted by Saassouh and Lounis [50] and proposed by Beushausen et al. [51] for the upcoming *fib* Model Code 2020.

Therefore, correctly estimating environmental aggressiveness tends not to be an easy task for designing a new structure. Although data obtained from structures exposed to similar environments can be taken as a basis for designing new structures, these also tend to present great variations. For example, Helene [52] guides de adoption of $C_S = 0,9\%$. Nunes et al. [53] evaluated the chloride content in the outer layers of structures located in the city of Rio Grande, southern Brazil, and obtained surface chloride contents equal to 3.1%, 1.1% and 0.6% at distances of 0 m, 160 m, and 630 m from the coastline. In turn, Balestra et al. [54] evaluated the C_S at three different points of the same structure, with values of 3.14% in the tidal zone, 2.32% in the splash zone, and 0.65% in the airborne zone.

1.2 Concrete service life modeling

Estimating the time during which a specific reinforced concrete structure can perform its functions without significant deterioration is of great technical and economic importance. Service life modeling, in turn, is of fundamental importance in ensuring the performance of reinforced concrete structures under chloride environments. However, concrete service life modeling requires some parameters to be known during the structural design, e.g., surface chloride content. In many cases, however, estimating these parameters can pose difficulties.

At the conceptual level, the model presented by Tuutti [55] (Figure 2) is commonly adopted to describe the degradation process of reinforced concrete structures due to reinforcement corrosion. The initiation period comprises the penetration of harmful agents through the cover layer until they reach the rebar. This process is directly influenced by the concrete characteristics, environmental exposure conditions, reinforcement cover depth, and the nature of the ingress agent. The corrosion process is established during the propagation phase, causing the progressive degradation of the concrete and the structure. Due to the significant damage caused to the structure during the propagation period and the fact that it is considerably shorter than the initiation period, many models focus their analysis on the initiation period.

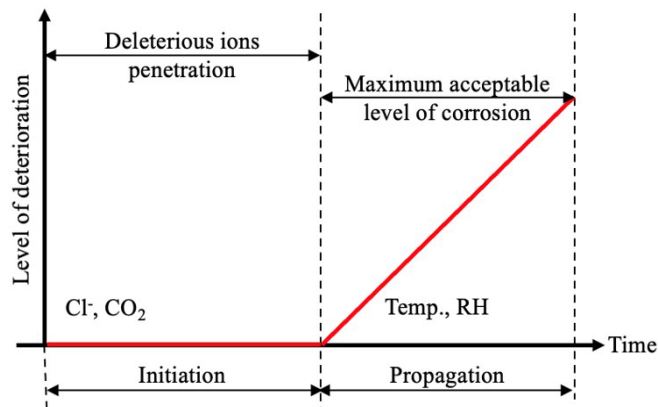


Figure 2. Tuutti [55] two-phase model for concrete service life.

In the case of chloride penetration, the corrosion begins when the chloride content at the reinforcement depth ($C_{(x,t)}$) reaches levels above the chloride threshold (C_{CR}), causing the rebar depassivation. The chloride threshold, however, is a parameter that depends on several factors, such as, among others, characteristics of the constituent materials, water/binder ratio, and concrete saturation degree. Even so, in many cases, the value of 0.4% by mass of cement is adopted as C_{CR} [56]–[59].

Adopting depassivation as the durability limit state aims to prevent reinforcement corrosion. According to Andrade [60], however, depassivation does not comprise the classic definition of the serviceability limit state presented in ISO 16204 [61] and ISO 2394 [62] codes. This is because, at the time of depassivation, there is only the triggering of the corrosive process, without any negative effect on the structural behavior. According to the author [60], an adequate definition is that depassivation indicates a limit state of initiation of deterioration, as presented in ISO 13823 [63]. Additionally, *in situ* identification of the exact moment of depassivation is only possible using electrochemical measurements. For these reasons, the adoption of the moment of the appearance of rusts or spots or the beginning of concrete cracking as DLS is discussed. However, it is necessary to pay attention to the fact that, from a technical perspective, reversing the corrosion process after depassivation can be quite difficult. Thus, although adopting a post-depassivation limit state has an important role in evaluating existing structures, taking depassivation as a DLS is a conservative measure, which may be interesting in the design phase and the definition of the maintenance plan of the structure.

Andrade [64] proposed considering four different levels to estimate the service life of reinforced concrete structural elements: deemed to satisfy, hybrid approach, deterministic performance-based, and probabilistic performance-based. This methodology is like that presented by ISO 13823 [63] and has been discussed in some studies (e.g., [7], [65]–[69]).

The deemed to satisfy, also called the prescriptive approach, is adopted by important current codes ([44], [70], [71]). It is limited to stipulating limit values for parameters such as maximum water/binder ratio, minimum concrete compressive strength, minimum cement content, and minimum cover depth. In a hybrid approach, the evaluation of concrete properties directly linked to its durability is included, especially using accelerated test methods - called durability indicators. However, it should be noted that in a hybrid approach, prescriptive specifications are still heavily demanded, with durability indicators usually adopted as a complementary test method. Additionally, in this approach, service life numerical modeling is not required.

Service life prediction models are used when deterministic or probabilistic performance-based approaches are adopted. Among the deterministic service life models against chloride penetration, the most used expression is the solution of Fick's 2nd Law of Diffusion, which allows estimating the $C_{(x,t)}$ value. When a purely deterministic model is used, only the average values of each variable involved in the process are considered.

In practice, however, the concrete resistance to chloride penetration and the environmental aggressiveness are variable parameters of a random nature. Because of such randomness of the parameters involved in the chloride penetration in concrete, strictly deterministic models tend to present flaws in the representation of the phenomenon and, consequently, in the estimate performed. Thus, the use of probabilistic models constitutes a possibility for a more realistic assessment of the mechanisms, variables, and processes that cause the deterioration of reinforced concrete structures [72], [73].

1.2.1 Probabilistic modeling

Most probabilistic analyses of concrete durability adopt deterministic models and introduce probabilistic parameters of the variables involved in the process. In these cases, simulations are carried out based on a model considered adequate for representing the chloride penetration in concrete (e.g., Fick's 2nd Law of Diffusion), considering the average values and the variability allowed for each parameter involved.

In a general and simplified way, the achievement of a specific limit state can be evaluated based on the limit state function presented in Equation 1.

$$g = R - S \tag{1}$$

In Equation 1, g indicates the limit state function, R refers to the resistant capacity of the structure under the evaluated situation, and S concerns the demand or loading that can lead the structure to reach the limit state in question.

In cases of service life analysis of concrete structures under chloride penetration, taking depassivation as the durability limit state, Equation 1 can be rewritten as a function of $C_{(x,t)}$ and C_{CR} (Equation 2).

$$g_{(x,t)} = C_{CR} - C_{(x,t)} \tag{2}$$

By adopting a probability-based approach, analyzes are performed by evaluating the probability of failure (P_f). Therefore, the aim is to determine the probability of reaching the limit state in question. From the limit state function established in Equation 2, it is possible to calculate P_f based on Equation 3.

$$P_f = P(C_{(x,t)} \geq C_{CR}) \tag{3}$$

Since the performance of a structure against chloride penetration is a function of several random variables, its service life will also be a random variable. Thus, probability-based service life estimates must also be analyzed from the perspective of probability.

The consideration of characteristic service life (SL_k) is analogous to the already familiar concept of concrete characteristic compressive strength (f_{ck}). Such characteristic resistance refers to a value with a predefined probability of not being reached. Thus, the characteristic service life of a structure can be defined as the age from which a probability of failure is greater than the admitted probability of failure ($P_{f,lim}$), as shown in Figure 3.

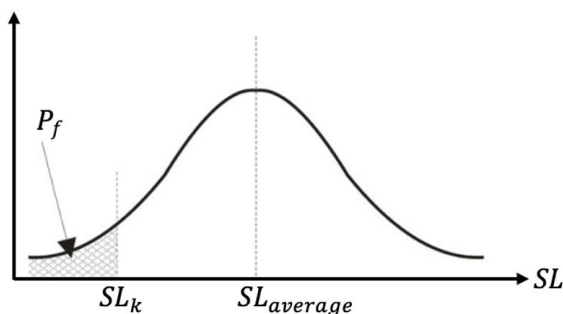


Figure 3. Characteristic service life concept illustration (adapted from [74]).

It should be noted, however, that $P_{f,lim}$ value is another non-consensual aspect. Helland [75] reports that Norway has adopted $P_{f,lim} = 10\%$ for the calibration of standardized prescriptive parameters. Additionally, the author reports $P_{f,lim}$ values of 2%, 30%, and 50% in other European countries. In terms of service life, this $P_{f,lim}$ variations imply estimates between 50 and 109 years if considering the same structure exposed to the same environment.

2 PROBABILISTIC SERVICE LIFE ASSESSMENT

Three chloride penetration models were used to evaluate the service life of concrete structures – namely, the Duracon model [10], the *fib* Model [11], and the *Life-365* model [12]. These models were chosen because they result from well-structured research programs, are presented in normative or pre-normative texts, and have already been applied in the durability design of reinforced concrete structures exposed to marine environments. The three models are based on Fick's 2nd Law of Diffusion.

2.1 Duracon model

The Duracon model [10] was developed from improvements to the model proposed by the European project DuraCrete [76]. Since then, several organizations have adopted this model in normative codes that deal with reinforced concrete structures and probability-based service life design, especially in Nordic countries. The model is presented in Equations 4, 5, and 6.

$$C_{(x,t)} = C_S \left[1 - \operatorname{erf} \left(\frac{x_C}{2\sqrt{D(t)t}} \right) \right] \quad (4)$$

where $C_{(x,t)}$ is the chloride content at depth x_C after time t (%), C_S is the surface chloride content (%), erf is the Gauss error function, and $D(t)$ is the time-dependent chloride diffusion coefficient (Equation 5), adopted by the Duracon model based on the study presented by Tang and Gulikers [77].

$$D(t) = \frac{D_0}{1-\alpha} \left[\left(1 + \frac{t'}{t} \right)^{1-\alpha} - \left(\frac{t'}{t} \right)^{1-\alpha} \right] \left(\frac{t_0}{t} \right)^\alpha k_e \quad (5)$$

where D_0 is the diffusion coefficient at the reference time t_0 (m^2/s), t' is the age of concrete at the time of first chloride exposure (years), α represents the concrete aging factor, and k_e is a parameter that considers temperature's effect (Equation 6).

$$k_e = \exp \left[\frac{E_A}{R} \left(\frac{1}{293} - \frac{1}{273+T} \right) \right] \quad (6)$$

where \exp is the exponential function, E_A is the activation energy for chloride diffusion (kJ/mol), R is the gas constant ($\text{J}/(\text{mol} \times \text{K})$), and T is the temperature ($^\circ\text{C}$).

2.2 *fib* model

The *fib* model for chloride penetration was initially presented in the *fib* Model Code for Service Life Design [11]. Later, it was also included in the text of the *fib* Model Code 2010 [78] and ISO 16204 [61]. Like the Duracon model, the *fib* model also adopts the solution of Fick's 2nd Law of Diffusion and includes the consideration of a time-dependent diffusion coefficient. This model is presented in Equations 7 and 8.

$$C_{(x,t)} = C_S - (C_S - C_0) \left[\operatorname{erf} \left(\frac{x_C}{2\sqrt{D_{app}(t)t}} \right) \right] \quad (7)$$

where $C_{(x,t)}$ is the chloride content at depth x_C after time t (%), C_S is the surface chloride content (%), C_0 is the initial chloride content of concrete, erf is the Gauss error function, and $D_{app}(t)$ is the time-dependent chloride diffusion coefficient (Equation 8).

$$D_{app}(t) = D_{app}(t_0) \left(\frac{t_0}{t} \right)^\alpha \quad (8)$$

where $D_{app}(t)$ is the time-dependent chloride diffusion coefficient, $D_{app}(t_0)$ is the apparent diffusion coefficient measured at a reference time t_0 , and α is the concrete aging factor.

2.3 Life-365 model

The *Life-365* software [12] enables the analysis of corrosion initiation and propagation periods, the determination of the structure's maintenance plan, and the estimation of the structure's life cycle costs. In this paper, however, only the initiation period is considered. Like *Duracon* and *fib* models, *Life-365* estimates the initiation period based on Fick's 2nd Law of Diffusion. However, the diffusion coefficient is considered time- and temperature-dependent, as shown in Equation 9.

$$D(t, T) = D_{ref} \left(\frac{t_{ref}}{t} \right)^\alpha \exp \left[\frac{U}{R} \left(\frac{1}{T_{ref}} - \frac{1}{T} \right) \right] \quad (9)$$

where $D(t, T)$ is the diffusion coefficient at time t and temperature T , D_{ref} is the diffusion coefficient at a referent time (in *Life-365* = 28 days), α is the concrete aging factor, exp is the exponential function, U is the activation energy for chloride diffusion (kJ/mol), R is the gas constant (J/(mol \times K)), and T_{ref} is the reference temperature (K).

It should be noted that the *Life-365* model, unlike the *Duracon* and *fib* models, considers that the reduction in the diffusion coefficient of concrete over time, expressed by the aging factor, occurs until the age of 25 years. After this age, the diffusion coefficient becomes only temperature dependent. Furthermore, in *Life-365*, the values of α can be determined experimentally or calculated considering the type and content of mineral admixture used in the concrete.

3 NUMERICAL ANALYSIS

The depassivation probabilities were calculated using the expression previously presented in Equation 3, using the $C_{(x,t)}$ values estimated based on the three models analyzed. The Monte Carlo Simulation was used to determine the P_f , being performed 10^6 simulations in each analysis.

The influence of surface chloride content was evaluated considering mean C_S values (μ_{C_S}) = 2.0 and 3.5%. While $C_S = 2.0\%$ refers to one of the values obtained by Guimarães [79]; 3.5% is recommended by GjØrv [10] for marine environments with an average environmental load. The influences of C_S variabilities were also evaluated. For this, were considered coefficients of variation (CV) of C_S (CV_{C_S}) equals to 0.10, 0.20, and 0.30. In all cases, C_S was admitted following lognormal probability distribution.

The chloride diffusion coefficient was assumed with a normal probability distribution, being adopted in the analysis mean values equal to 3.0×10^{-12} and 5.0×10^{-12} m^2/s , and coefficients of variation (CV_D) of 0.10, 0.20, and 0.30. Regarding the cover depth, a normal probability distribution was assumed, with mean value = 50 mm and coefficients of variation (CV_{x_c}) = 0.05, 0.10, and 0.20.

In all the analyzes carried out, service life was considered equal to 100 years. When required by the models used, the aging factor was taken with a normal probability distribution, with mean = 0.4 and standard deviation (σ) = 0.04 (N(0.4; 0.04)). As for temperature, $\mu = 18$ °C, $\sigma = 3.6$ °C, and normal probability distribution (N(18; 3.6)). C_{CR} was assumed with a normal probability distribution, $\mu = 0.4\%$, and $\sigma = 0.04\%$ (N(0.4; 0.04)).

The results about the influence of surface chloride concentration on $C_{(x,t)}$ are shown in Figure 4 and Figure 5. A greater environmental aggressiveness, represented by a greater C_S value, increases $C_{(x,t)}$. However, what is most evident in all models analyzed is the strong influence of CV_{C_S} in the prediction of chloride concentration. This variation is a fact that generates many uncertainties in the use of service life prediction models since, as discussed in Section 1.1.3, the definition of C_S is extremely complex and presents great variability because it depends on a series of environmental variables not controllable.

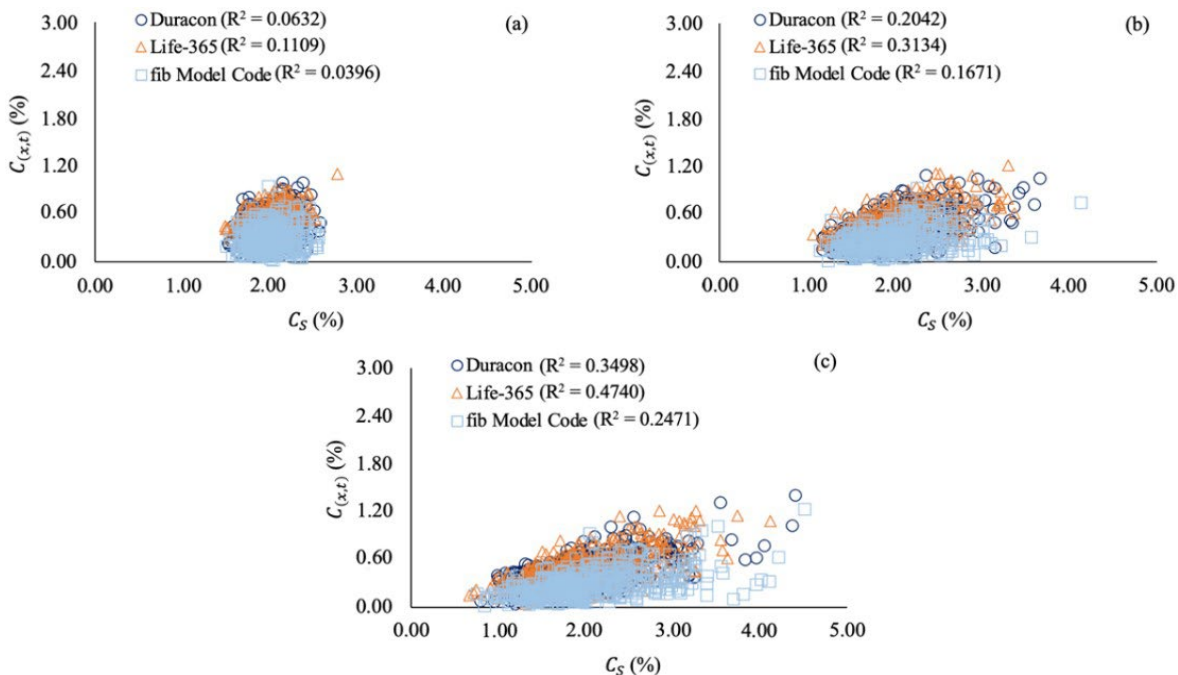


Figure 4. Influences of C_S on chloride penetration. $\mu_{C_S} = 2.00$; CV_{C_S} : (a) = 0.10, (b) = 0.20, and (c) = 0.30. Note: $D = N(3.00; 0.30)$, $x_C = N(50.00; 5.00)$, $\alpha = N(0.40; 0.04)$, $T = N(18.00; 3.60)$, and $t = 100$ years.

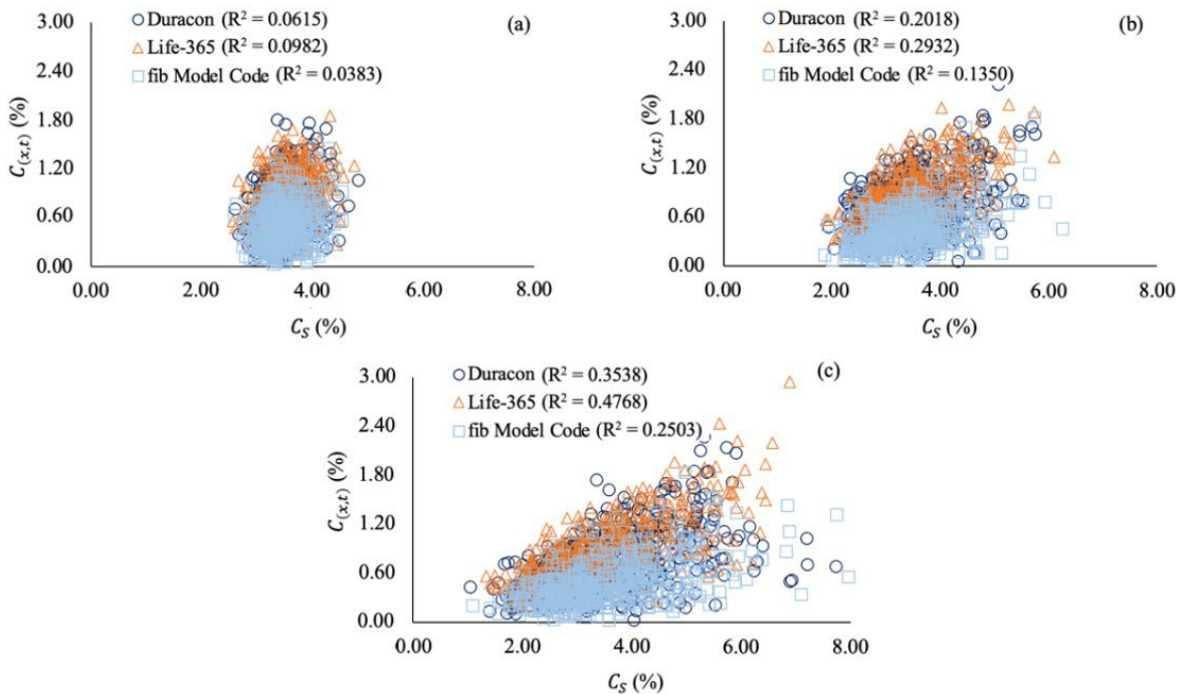


Figure 5. Influences of C_S on chloride penetration. $\mu_{C_S} = 3.50$; CV_{C_S} : (a) = 0.10, (b) = 0.20, and (c) = 0.30. Note: $D = N(3.00; 0.30)$, $x_C = N(50.00; 5.00)$, $\alpha = N(0.40; 0.04)$, $T = N(18.00; 3.60)$, and $t = 100$ years.

Figure 6 and Figure 7 present the influences of the chloride diffusion coefficient in $C_{(x,t)}$. It is important to remember that D is the main indicator of concrete resistance to chloride penetration; therefore, lower D values provide less chloride penetration and tend to give a longer service life to the structure. The variability of D , in turn, is mainly affected by the characteristics of the test method used and by the concrete production and placing processes. However, variability

related to the test method can be easily quantified and considered. As can be seen, increasing CV_D leads to significant increases in the scatter of the estimated $C_{(x,t)}$ values.

Thus, the importance of a technical framework for evaluating the concrete characteristics and its durability potential based on durability indicators test methods is reaffirmed. Additionally, it is essential to establish control methodologies of the concrete at the construction site to quantify the mean values of D and its variability, allowing the *in-situ* conformity control of durability specifications.

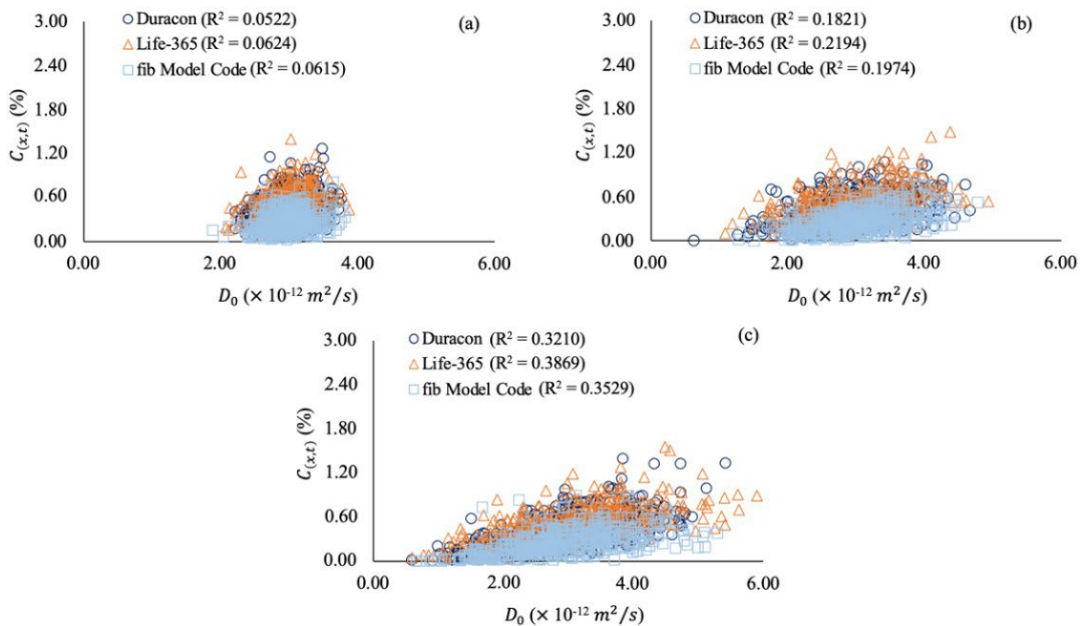


Figure 6. Effects of D_{28d} on chloride penetration. $\mu_D = 3.00$; CV_{CS} : (a) = 0.10, (b) = 0.20, and (c) = 0.30. Note: $C_S = \text{LN}(2.00; 0.40)$, $x_C = \text{N}(50.00; 5.00)$, $\alpha = \text{N}(0.40; 0.04)$, $T = \text{N}(18.00; 3.60)$, and $t = 100$ years.

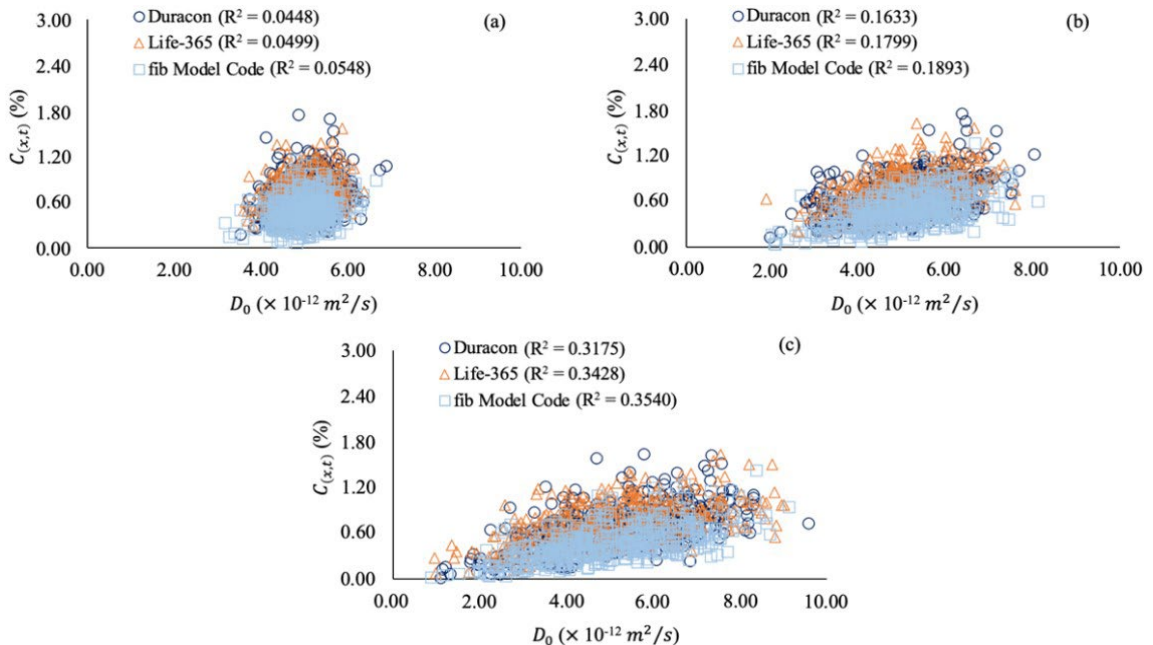


Figure 7. Effects of D_{28d} on chloride penetration. $\mu_D = 5.00$; CV_{CS} : (a) = 0.10, (b) = 0.20, and (c) = 0.30. Note: $C_S = \text{LN}(2.00; 0.40)$, $x_C = \text{N}(50.00; 5.00)$, $\alpha = \text{N}(0.40; 0.04)$, $T = \text{N}(18.00; 3.60)$, and $t = 100$ years.

The influence of cover depth variabilities in $C_{(x,t)}$ is shown in Figure 8. Among the parameters analyzed in this paper, x_c is the one that is easier to stipulate since it is recommended in prescriptive durability specifications and can also be calculated through numerical modeling. The variabilities of x_c , however, have a strong influence in $C_{(x,t)}$, significantly increasing the scatter of the results obtained, as also observed by Magalhães [74]. It should be noted that CV_{x_c} is directly related to the structure construction process, which confirms the importance of strict quality control in producing concrete structural elements, especially under aggressive environments.

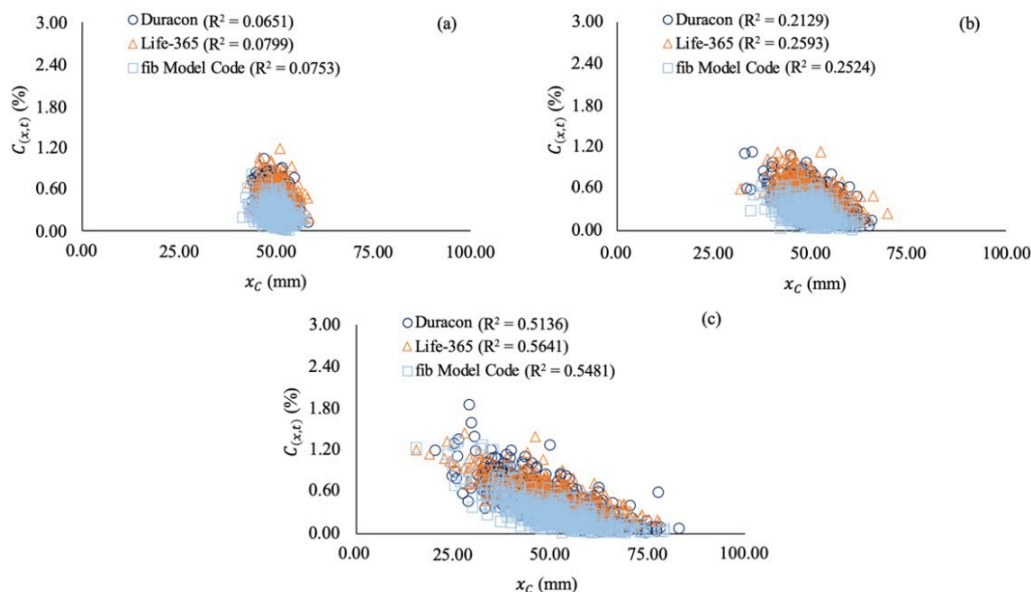


Figure 8. Influences of cover depth variability on chloride penetration. $\mu_{x_c} = 50.00$; CV_{x_c} : (a) = 0.05, (b) = 0.10, and (c) = 0.20. Note: $C_S = LN(2.00; 0.40)$, $D = N(3.00; 0.30)$, $\alpha = N(0.40; 0.04)$, $T = N(18.00; 3.60)$, and $t = 100$ years.

Lastly, the influence of C_{CR} on P_f of reinforced concrete structural elements under chloride penetration was evaluated. Since C_{CR} is widely discussed in the literature, and there is no consensus on its average value, a range of C_{CR} between 0.0 e 1.2% (Figure 9) and coefficients of variation between 0.0 e 0.5 (Figure 10) were considered. It is known that $C_{CR} = 1.2\%$ is a high value and naturally leads to a very low corrosion probability. This value was adopted to visualize the influences of the chloride threshold on the service life prediction of concrete structures. It should also be noted that, although the value of 0.4% is the most adopted for C_{CR} , the North American code ACI 318 [71] suggests a chloride threshold equal to 1.00% for concrete exposed to dry environments; on the other hand, standards such as Brazilian NBR 12655 [80] indicate values between 0.15 and 0.40%, depending on the concrete exposure conditions.

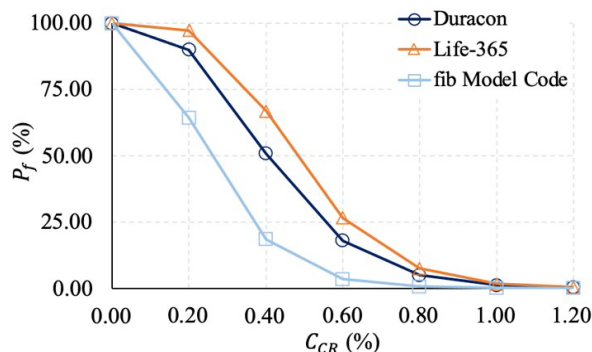


Figure 9. Influence of C_{CR} in P_f ($CV_{C_{CR}} = 0.1$). Note: $C_S = LN(2.00; 0.40)$, $D = N(3.00; 0.30)$, $x_c = N(50.00; 5.00)$, $\alpha = N(0.40; 0.04)$, $T = N(18.00; 3.60)$, and $t = 100$ years.

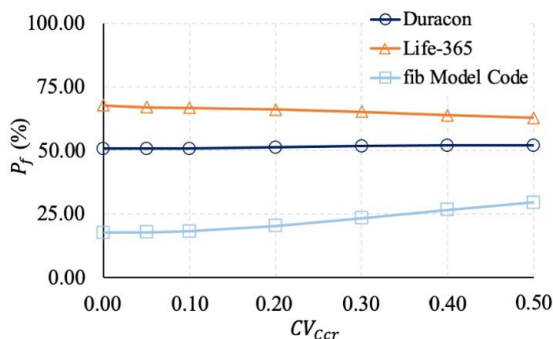


Figure 10. Effects of CV_{Ccr} in the probability of chloride-induced corrosion ($\mu_{Ccr} = 0.4\%$). Note: $C_S = LN(2.00; 0.40)$, $D = N(3.00; 0.30)$, $x_c = N(50.00; 5.00)$, $\alpha = N(0.40; 0.04)$, $T = N(18.00; 3.60)$, and $t = 100$ years.

It is observed that the P_f presented in Figures 9 and 10 are quite high. However, it should be noted that this occurs due to the set of the evaluated scenario. A diffusion coefficient lower than the one considered ($= 3.0 \times 10^{-12} \text{ m}^2/\text{s}$) would lower corrosion probabilities.

Lastly, the evolution of P_f over time was evaluated. The results are shown in Figure 11. At all ages, the probability of failure calculated based on the *fib* Model [11] was significantly lower than that obtained from the other models. Another fact to note is that if $P_{f,lim} = 10\%$ is taken, the characteristic service life obtained through the Duracon model is less than 50 years, while the *Life-365* model leads to SL_k of approximately 52 years, and the *fib* Model indicates SL_k next to 80 years.

Although probabilistic approaches are an important tool in the service life design of reinforced concrete structures, it is necessary to remember that different models can lead to very different scenarios. Thus, it is essential that studies on concrete durability also seek to understand the relationship between the estimates made considering accelerated test methods and chloride penetration prediction models and the actual behavior of concrete structures in marine environments. It should be noted that many intervening factors and uncertainties are associated with the degradation process of reinforced concrete structures due to chloride penetration. So, the results obtained through numerical modeling should not be taken as absolute numbers of the concrete service life but as a basis for analyzing its behavior over time and making decisions related to maintenance and other interventions.

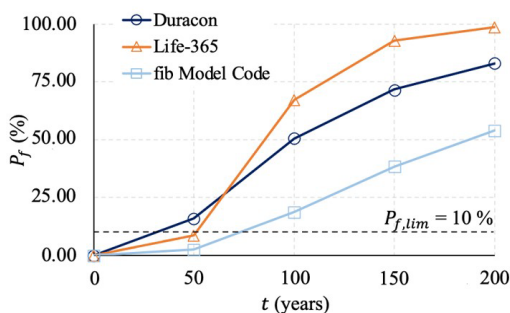


Figure 11. Evolution of P_f over time. Note: $C_S = LN(2.00; 0.40)$, $D = N(3.00; 0.30)$, $x_c = N(50.00; 5.00)$, $\alpha = N(0.40; 0.04)$, $T = N(18.00; 3.60)$, $C_{CR} = N(0.40; 0.04)$, and $t = 100$ years.

4 CLOSURE

This paper discussed the main factors affecting the service life of reinforced concrete structures in marine environments. Emphasis was given to the surface chloride content, which indicates the aggressiveness of the environment, and the cover depth and chloride diffusion coefficient, which refer to the resistance of the structural element to the penetration of ions. Important concepts related to probability-based durability design were reviewed and discussed.

The importance of adequate control of specification and construction of the concrete structure was observed concerning the cover depth and the chloride diffusion coefficient. The variability of these parameters, directly related

to the conditions of the construction process, significantly affects the estimated $C_{(x,t)}$. In many of the cases analyzed, there was a low correlation between the analyzed variables and $C_{(x,t)}$, corroborating the data presented by Yu et al. [73].

The significance of considering adequate C_{CR} values was discussed. Although the variability of C_{CR} and the effect of several parameters on the chloride threshold is widely discussed in the literature; in many cases C_{CR} is considered a value applicable to structures regardless of their properties, as discussed by Käthler et al. [81]. Due to their significant influence on service life estimates, test methods for determining C_{CR} of structural elements are important tools for designing and evaluating reinforced concrete structures.

Regarding the service life prediction models adopted in this paper, it should be noted that considering $P_{f,lim} = 10\%$, the SL_k range obtained was greater than 30 years. This fact shows the strong influence that the model used has on the estimates made. While certain models can lead to overestimated service life analyses, generating the need for unforeseen interventions, others can present underestimated results, increasing the cost of the project in order to achieve the desired service life. Thus, although probability-based approaches represent the analyzed phenomenon better, service life prediction models must be used judiciously. As possible, calibration processes with long-term exposure data should be carried out.

Concrete durability approaches move towards performance specifications. Thus, the introduction of durability indicators, service life prediction models, and the concept of characteristic service life are fundamental in evaluating reinforced concrete structures' durability under aggressive environments. Therefore, it is necessary that experimental programs linked to the numerical application be established. In this way, clear procedures can be set to determine the characteristic service life and admitted probabilities of failure for each environment and structure through new normative references. These procedures would contribute to decision-making in the design phase and the design of structural elements capable of fulfilling a minimum service life, guaranteeing the desired performance, and avoiding premature costs with conservation activities.

REFERENCES

- [1] J. de Brito and R. Kurda, "The past and future of sustainable concrete: a critical review and new strategies on cement-based materials," *J. Clean. Prod.*, vol. 281, pp. 123558, Jan. 2021, <http://dx.doi.org/10.1016/j.jclepro.2020.123558>.
- [2] L. Poudyal and K. Adhikari, "Environmental sustainability in cement industry: an integrated approach for green and economical cement production," *Resour. Environ. Sustainab.*, vol. 4, pp. 100024, Jun. 2021, <http://dx.doi.org/10.1016/j.resenv.2021.100024>.
- [3] E. Benhelal, E. Shamsaei, and M. I. Rashid, "Challenges against CO₂ abatement strategies in cement industry: a review," *J. Environ. Sci.*, vol. 104, pp. 84–101, Jun 2021, <http://dx.doi.org/10.1016/j.jes.2020.11.020>.
- [4] E. Possan, D. C. C. dal Molin, and J. J. O. Andrade, "A conceptual framework for service life prediction of reinforced concrete structures," *J. Build. Path. Rehab.*, vol. 3, no. 2, pp. 1–11, Jan 2018, <http://dx.doi.org/10.1007/s41024-018-0031-7>.
- [5] G. de Schutter, "No concrete is sustainable without being durable!" in *XIII DBMC*, São Paulo, 2014, pp. 38–44.
- [6] Y. Yi et al., "A review on the deterioration and approaches to enhance the durability of concrete in the marine environment," *Cement Concr. Compos.*, vol. 113, pp. 103695, Oct. 2020, <http://dx.doi.org/10.1016/j.cemconcomp.2020.103695>.
- [7] G. B. Wally, F. C. Magalhães, and L. C. P. Silva Filho, "From prescriptive to performance-based: an overview of international trends in specifying durable concretes," *J. Build. Eng.*, vol. 52, pp. 104359, Jul. 2022, <http://dx.doi.org/10.1016/j.job.2022.104359>.
- [8] M. Alexander and H. Beushausen, "Durability, service life prediction, and modelling for reinforced concrete structures – review and critique," *Cement Concr. Res.*, vol. 122, pp. 17–29, Aug 2019, <http://dx.doi.org/10.1016/j.cemconres.2019.04.018>.
- [9] M. Alexander, H. Beushausen, and M. Otieno, "Service life and durability design of RC structures: general considerations and selected Southern African perspectives and experiences," *Sustainab. Resilient Infrastruct.*, Online first, May 2021, <http://dx.doi.org/10.1080/23789689.2021.1916854>.
- [10] O. E. Gjorv, *Durability Design of Concrete Structures in Severe Environments*, 2nd ed. Boca Raton, United States of America: CRC Press, 2014.
- [11] International Federation for Structural Concrete, *fib Model Code for Service Life Design*, Bulletin n° 34, Lausanne, Int. Fed. Struct. Concr., 2006.
- [12] E. C. Bentz and M. D. A. Thomas, *Life-365 Service Life Prediction Model and Computer Program for Predicting the Service Life and Life-Cycle Cost of Reinforced Concrete Exposed to Chlorides, Version 2.2.3*. Life-365TM Consortium III, 2020.
- [13] M. Collepardi, A. Marcialis, and R. Turriziani, "Penetration of Chloride Ions into Cement Pastes and Concretes," *J. Am. Ceram. Soc.*, vol. 55, pp. 534–535, Oct. 1972, <http://dx.doi.org/10.1111/j.1151-2916.1972.tb13424.x>.
- [14] W. Chalee and C. Jaturapitakkul, "Effects of w/b ratios and fly ash finenesses on chloride diffusion coefficient of concrete in marine environment," *Mater. Struct.*, vol. 42, pp. 505–514, Jul 2009, <http://dx.doi.org/10.1617/s11527-008-9398-2>.

- [15] S. L. Poulsen, H. E. Sørensen, and U. Jönsson, "Chloride ingress in concrete blocks at the Rødbyhavn Marine Exposure Site – Status after 5 years," in *Proc. 4th Int. Conf. Serv. Life Des. Infrastruct.*, Delft, 2018, pp. 192-203.
- [16] R. K. Dhir et al., "Role of cement content in specifications for concrete durability: cement type influences," *Struct. Build.*, vol. 157, pp. 113–127, Apr. 2004, <http://dx.doi.org/10.1680/stbu.2004.157.2.113>.
- [17] D. V. Ribeiro et al., "Effects of binders characteristics and concrete dosing parameters on the chloride diffusion coefficient," *Cement Concr. Compos.*, vol. 122, pp. 104114, Sep. 2021, <http://dx.doi.org/10.1016/j.cemconcomp.2021.104114>.
- [18] M. C. G. Juenger, R. Snellings, and S. A. Bernal, "Supplementary cementitious materials: new sources, characterization, and performance insights," *Cement Concr. Res.*, vol. 122, pp. 257–273, Aug 2019, <http://dx.doi.org/10.1016/j.cemconres.2019.05.008>.
- [19] M. Kasaniya, M. D. A. Thomas, and E. G. Moffatt, "Pozzolanic reactivity of natural pozzolans, ground glasses and coal bottom ashes and implication of their incorporation on the chloride permeability of concrete," *Cement Concr. Res.*, vol. 139, pp. 106259, Jan 2021, <http://dx.doi.org/10.1016/j.cemconres.2020.106259>.
- [20] G. B. Wally et al., "Estimating service life of reinforced concrete structures with binders containing silica fume and metakaolin under chloride environment: durability indicators and probabilistic assessment," *Mater. Struct.*, vol. 54, pp. 98, Apr 2021, <http://dx.doi.org/10.1617/s11527-021-01698-7>.
- [21] K. Tan and O. E. Gjörv, "Performance of concrete under different curing conditions," *Cement Concr. Res.*, vol. 26, pp. 355–361, Mar 1996, [http://dx.doi.org/10.1016/S0008-8846\(96\)85023-X](http://dx.doi.org/10.1016/S0008-8846(96)85023-X).
- [22] P. S. Mangat and M. C. Limbachiya, "Effect of initial curing on chloride diffusion in concrete repair materials," *Cement Concr. Res.*, vol. 29, pp. 1475–1485, Sep. 1999, [http://dx.doi.org/10.1016/S0008-8846\(99\)00130-1](http://dx.doi.org/10.1016/S0008-8846(99)00130-1).
- [23] C.-M. Aldea et al., "Effects of curing conditions on properties of concrete using slag replacement," *Cement Concr. Res.*, vol. 30, pp. 465–472, Mar. 2000, [http://dx.doi.org/10.1016/S0008-8846\(00\)00200-3](http://dx.doi.org/10.1016/S0008-8846(00)00200-3).
- [24] J. M. Khatib and P. S. Mangat, "Influence of high-temperature and low-humidity curing on chloride penetration in blended cement concrete," *Cement Concr. Res.*, vol. 32, pp. 1743–1753, Nov. 2002, [http://dx.doi.org/10.1016/S0008-8846\(02\)00857-8](http://dx.doi.org/10.1016/S0008-8846(02)00857-8).
- [25] B. H. Oh and S. Y. Jang, "Effects of material and environmental parameters on chloride penetration profiles in concrete structures," *Cement Concr. Res.*, vol. 37, pp. 47–53, Jan. 2007., <http://dx.doi.org/10.1016/j.cemconres.2006.09.005>.
- [26] M. Isteita and Y. Xi, "The effect of temperature variation on chloride penetration in concrete," *Constr. Build. Mater.*, vol. 156, pp. 73–82, Dec 2017, <http://dx.doi.org/10.1016/j.conbuildmat.2017.08.139>.
- [27] R. A. Medeiros-Junior, M. G. Lima, and M. H. F. Medeiros, "Service life of concrete structures considering the effects of temperature and relative humidity on chloride transport," *Environm., Developm., and Sustainab.*, vol. 17, pp. 1103–1119, Oct. 2015, <http://dx.doi.org/10.1007/s10668-014-9592-z>.
- [28] X.-J. Niu et al., "Effects of ambient temperature, relative humidity and wind speed on interlayer properties of dam concrete," *Constr. Build. Mater.*, vol. 260, pp. 119791, Nov 2020, <http://dx.doi.org/10.1016/j.conbuildmat.2020.119791>.
- [29] E. P. Nielsen and M. R. Geiker, "Chloride diffusion in partially saturated cementitious material," *Cement Concr. Res.*, vol. 33, pp. 133–138, Jan 2003, [http://dx.doi.org/10.1016/S0008-8846\(02\)00939-0](http://dx.doi.org/10.1016/S0008-8846(02)00939-0).
- [30] H. Mercado-Mendoza, S. Lorente, and X. Bourbon, "Ionic aqueous diffusion through unsaturated cementitious materials – A comparative study," *Constr. Build. Mater.*, vol. 51, pp. 1–8, Jan 2014, <http://dx.doi.org/10.1016/j.conbuildmat.2013.10.026>.
- [31] D. Bjegović et al. "Test methods for concrete durability indicators," in *Performance-based Specifications and Control of Concrete Durability – State-of-the-art Report RILEM TC 230-PSC*, H. Beushausen and L. F. Luco, Eds., London: Springer, 2016, ch. 4, pp. 51–105.
- [32] S. Nanukuttan et al., "Methods for assessing the durability and service life of concrete structures," in *Annual Technical Symposium – The Institute of Concrete Technology*, Belfast, 6th April 2017, pp. 1–16.
- [33] J. Milla et al., "Methods of test for concrete permeability: a critical review," *Adv. Civ. Eng. Mater.*, vol. 10, pp. 172–209, Apr 2021, <http://dx.doi.org/10.1520/ACEM20200067>.
- [34] M. Castellote and C. Andrade, "Round-Robin test on methods for determining chloride transport parameters in concrete," *Mater. Struct.*, vol. 39, pp. 955, Oct. 2006, <http://dx.doi.org/10.1617/s11527-006-9193-x>.
- [35] F. K. Sell Junior et al., "Experimental assessment of accelerated test methods for determining chloride diffusion coefficient in concrete," *IBRACON Struct. Mater. J.*, vol. 14, pp. e14407, Aug. 2021, <http://dx.doi.org/10.1590/s1983-41952021000400007>.
- [36] L. Tang and L.-O. Nilsson, *Chloride Diffusivity in High Strength Concrete at Different Ages* (Publication n. 11), The Nordic Concr. Fed., 1992. pp. 162–171.
- [37] C. Andrade, M. Castellote, and R. d'Andrea, "Measurement of aging effect on chloride diffusion coefficients in cementitious matrices," *J. Nucl. Mater.*, vol. 412, pp. 209–216, May 2011, <http://dx.doi.org/10.1016/j.jnucmat.2010.12.236>.
- [38] K. Audenaert, Q. Yuan, and G. De Schutter, "On the time dependency of the chloride migration coefficient in concrete," *Constr. Build. Mater.*, vol. 24, pp. 396–402, Mar. 2010, <http://dx.doi.org/10.1016/j.conbuildmat.2009.07.003>.
- [39] H. S. Al-alaily and A. A. A. Hassan, "Time-dependence of chloride diffusion for concrete containing metakaolin," *J. Build. Eng.*, vol. 7, pp. 159–169, Sep. 2016, <http://dx.doi.org/10.1016/j.jobe.2016.06.003>.

- [40] P. Lehner, P. Ghosh, and P. Konečný, "Statistical analysis of time dependent variation of diffusion coefficient for various binary and ternary based concrete mixtures," *Constr. Build. Mater.*, vol. 183, pp. 75–87, Sep 2018., <http://dx.doi.org/10.1016/j.conbuildmat.2018.06.048>.
- [41] P. Helene and P. Terzian, *Manual de Dosagem e Controle do Concreto*, São Paulo, SP, Brasil: PINI, 1991. (in Portuguese).
- [42] F. C. Magalhães, M. V. Real, and L. C. P. Silva Filho, "The problem of non-compliant concrete and its influence on the reliability of reinforced concrete columns," *Mater. Struct.*, vol. 49, pp. 1485–1497, Mar. 2016, <http://dx.doi.org/10.1617/s11527-015-0590-x>.
- [43] Associação Brasileira de Normas Técnicas, *Ready-mixed concrete - Preparation, supply and control*, NBR 7212, 2021. (in Portuguese).
- [44] Associação Brasileira de Normas Técnicas, *Design of Structural Concrete – Procedure*, NBR 6118, 2014. (in Portuguese).
- [45] European Committee for Standardization, *Eurocode 2: Design of Concrete Structures – Part 1-1: General Rules and Rules for Buildings, EN 1991-1-1*, 2004.
- [46] L. Yang, L. Wang, and B. Yu, "Time-varying behavior and its coupling effects with environmental conditions and cementitious material types on surface chloride concentration of marine concrete," *Constr. Build. Mater.*, vol. 303, pp. 124578, Oct 2021, <http://dx.doi.org/10.1016/j.conbuildmat.2021.124578>.
- [47] S. N. Muthulingam and B. N. Rao, "Consistent models for estimating chloride ingress parameters in fly ash concrete," *J. Build. Eng.*, vol. 3, pp. 24–38, Sep 2015, <http://dx.doi.org/10.1016/j.jobe.2015.04.009>.
- [48] M. Shakouri and D. Trejo, "A time-variant model of surface chloride build-up for improved service life predictions," *Cement Concr. Compos.*, vol. 84, pp. 99–110, Nov 2017, <http://dx.doi.org/10.1016/j.cemconcomp.2017.08.008>.
- [49] L. Yang, R. Cai, and B. Yu, "Investigation of computational model for surface chloride concentration of concrete in marine atmosphere zone," *Ocean Eng.*, vol. 138, pp. 105–111, July, 2017, <https://dx.doi.org/10.1016/j.oceaneng.2017.04.024>.
- [50] B. Saassouh and Z. Lounis, "Probabilistic modeling of chloride-induced corrosion in concrete structures using first- and second-order reliability methods," *Cement Concr. Compos.*, vol. 34, pp. 1082–1092, Oct. 2012, <http://dx.doi.org/10.1016/j.cemconcomp.2012.05.001>.
- [51] H. Beushausen et al., "Developments in defining exposure classes for durability design and specification," *Struct. Concr.*, vol. 22, pp. 2539–2555, Oct. 2021, <http://dx.doi.org/10.1002/suco.202000792>.
- [52] P. R. L. Helene, "Contribution to the study of steel corrosion in reinforced concrete," (in Portuguese), Tese de Livre Docência, Univ. São Paulo, São Paulo, SP, 1993.
- [53] J. L. O. Nunes et al., "Chloride attack intensity: considerations on concrete distance from seawater," in *Seminário e Workshop em Engenharia Oceânica*, Rio Grande, 2004, pp. 1–11. (in Portuguese).
- [54] C. E. T. Balestra et al., "Environmental and material parameters that affect chloride ingress in reinforced concrete structures – Case study of Arvoredos Island," *Rev. Eletr. Eng. Civ.*, vol. 12, pp. 270–282, Jan. 2017., <http://dx.doi.org/10.5216/reec.v13i1.43054>.
- [55] K. Tuutti, *Corrosion of Steel in Concrete*. Stockholm: Swedish Cem. Concr. Res. Inst. , 1982.
- [56] U. Angst et al., "Critical chloride content in reinforced concrete — A review," *Cement Concr. Res.*, vol. 39, pp. 1122–1138, Dec 2009, <http://dx.doi.org/10.1016/j.cemconres.2009.08.006>.
- [57] Y. Cao et al., "Critical chloride content in reinforced concrete — An updated review considering Chinese experience," *Cement Concr. Res.*, vol. 117, pp. 58–68, Mar. 2019, <http://dx.doi.org/10.1016/j.cemconres.2018.11.020>.
- [58] Y. A. Villagrán-Zaccardi and C. Andrade, "Chloride ingress rate and threshold content, as determined by the ‘Integral’ test method, in concrete with several w/c ratios in saturated and unsaturated conditions," *Developm. Built Environ.*, vol. 8, pp. 100062, Sep. 2021, <http://dx.doi.org/10.1016/j.dibe.2021.100062>.
- [59] Y. Zhu et al., "corrosion of rebar in concrete. Part II: Literature survey and statistical analysis of existing data on chloride threshold," *Corros. Sci.*, vol. 185, pp. 109439, Jun. 2021, <http://dx.doi.org/10.1016/j.corsci.2021.109439>.
- [60] C. Andrade, "Reliability analysis of corrosion onset: initiation limit state," *J. Struct. Integr. Maint.*, vol. 2, pp. 200–208, Nov. 2017, <http://dx.doi.org/10.1080/24705314.2017.1388693>.
- [61] International Organization for Standardization, *Durability – Service Life Design of Concrete Structures*, ISO 16204, 2012.
- [62] International Organization for Standardization, *General Principles on Reliability for Structures*, ISO 2394, 2015.
- [63] International Organization for Standardization, *General Principles on the Design of Structures for Durability*, ISO 13823, 2008.
- [64] C. Andrade, "Multilevel (four) methodology for durability design," in *Int. RILEM Workshop on Performance Based Evaluation and Indicators for Concrete Durability*, Madrid, 2006, pp. 101-108.
- [65] M. Alexander and M. Thomas, "Service life prediction and performance testing — Current developments and practical applications," *Cement Concr. Res.*, vol. 78, pp. 155–164, Dec 2015., <http://dx.doi.org/10.1016/j.cemconres.2015.05.013>.
- [66] D. V. Ribeiro and O. Cascardo "Durability and service life of concrete structures," in *Corrosão e Degradação em Estruturas de Concreto – Teoria, controle e técnicas de análise e intervenção*, D. V. Ribeiro, Ed., Rio de Janeiro: Elsevier, 2018, ch. 3, pp. 33–50.

- [67] H. Beushausen and M. Alexander "Performance-based service life design of reinforced concrete structures using durability indicators," in *2nd Int RILEM Workshop on Concrete Durability and Service Life Planning*, Haifa, 2009, pp. 15-22.
- [68] B. Sangoju, R. Gopal and B. Bhajantri, H., "A review on performance-based specifications toward concrete durability," *Struct. Concr.*, vol. 22, pp. 2526–2538, Oct. 2021, <http://dx.doi.org/10.1002/suco.201900542>.
- [69] H. Beushausen, R. Torrent, and M. G. Alexander, "Performance-based approaches for concrete durability: State of the art and future research needs," *Cement Concr. Res.*, vol. 119, pp. 11–20, May., 2019, <https://dx.doi.org/10.1016/j.cemconres.2019.01.003>.
- [70] European Committee for Standardization, *Concrete: Specification, Performance, Production and Conformity*, EN 206, 2013.
- [71] American Concrete Institute, *Building Code Requirements for Structural Concrete*, ACI 318-19, 2019.
- [72] G. Vera et al., "Depassivation time estimation in reinforced concrete structures exposed to chloride ingress: a probabilistic approach," *Cement Concr. Compos.*, vol. 79, pp. 21–33, May 2017, <http://dx.doi.org/10.1016/j.cemconcomp.2016.12.012>.
- [73] B. Yu, C. Ning, and B. Li, "Probabilistic durability assessment of concrete structures in marine environments: Reliability and sensitivity analysis," *China Ocean Eng.*, vol. 31, pp. 63–73, Jan. 2017, <http://dx.doi.org/10.1007/s13344-017-0008-3>.
- [74] F. C. Magalhães, "Proposition of a model for penetration of chloride ions in concrete: studies of intervening parameters and probabilistic analysis," Ph.D. thesis, Univ. Fed. Rio Gde Sul, Porto Alegre, RS, 2018. (in Portuguese).
- [75] S. Helland, "Design for service life: implementation of fib Model Code 2010 rules in the operational code ISO 16204," *Struct. Concr.*, vol. 14, pp. 10–18, Mar. 2013, <http://dx.doi.org/10.1002/suco.201200021>.
- [76] DuraCrete, *General Guidelines for Durability Design and Redesign, The European Union – Brite EuRam III, Research Project BE95–1347, Document R 15*, USA: DuraCrete, 2000.
- [77] L. Tang and J. Gulikers, "On the mathematics of time-dependent apparent chloride diffusion coefficient in concrete," *Cement Concr. Res.*, vol. 37, pp. 589–595, Apr. 2007, <http://dx.doi.org/10.1016/j.cemconres.2007.01.006>.
- [78] International Federation for Structural Concrete, *fib Model Code for Concrete Structures 2010*, Lausanne: Int. Fed. Struct. Concr., 2013.
- [79] A. T. C. Guimarães, "Service life of reinforced concrete structures in marine environments," Ph.D. thesis, Univ. São Paulo, São Paulo, SP, 2000. (in Portuguese).
- [80] Associação Brasileira de Normas Técnicas, *Portland Cement Concrete – Preparation, Control, Receipt and Acceptance – Procedure*, NBR 12655, 2015. (in Portuguese).
- [81] C. B. Käthler et al., "Investigations of accelerated methods for determination of chloride threshold values for reinforcement corrosion in concrete," *Sustainab. Resilient Infrastruct.*, Apr., 2021, pp. 1–13. <https://dx.doi.org/10.1080/23789689.2021.1905221>.

Author contributions: GBW: conceptualization, methodology, data curation, formal analysis, writing; FCM: conceptualization, methodology, data curation, funding acquisition, formal analysis, writing; MVR: conceptualization, formal analysis, writing, supervision; LCPSF: writing, supervision.

Editors: Edna Possan, Mark Alexander



ORIGINAL ARTICLE

Optimum design of precast and prestressed beams with focus on CO₂ emission reduction

Projeto ótimo de vigas pré-fabricadas e protendidas com foco na redução da emissão de CO₂

Matheus Henrique Morato de Moraes^a

Wanderlei Malaquias Pereira Junior^b

Sylvia Regina Mesquita de Almeida^c

Geraldo Magela Gonçalves Filho^b

Rebeca Freitas Vasconcelos^d



^aUniversidade Federal de São Carlos – UFSCar, Civil Engineering Graduate Program, São Carlos, SP, Brasil

^bUniversidade Federal de Catalão – UFCAT, Civil Engineering Department, Catalao, GO, Brasil

^cUniversidade Federal de Goiás – UFG, School of Civil and Environmental Engineering, Goiânia, GO, Brasil

^dInstituto Federal do Tocantins – IFTO, Civil Engineering Department, Palmas, TO, Brasil

Received 24 March 2022

Accepted 05 October 2022

Abstract: Among the main contributors to CO₂ emissions on the ozone layer, the construction industry contributes with a significant portion. This emission is generated largely by applying concrete construction systems and their variations. Therefore, it is important to use tools that allow the development of projects which mitigate the effects of harmful gas emissions into the atmosphere. Thus, this study applied an optimization algorithm called Firefly Algorithm (FA) to design precast and prestressed rectangular beams focusing on reducing CO₂ emissions in the structural design phase. The Objective Function (OF) was defined as the total weight of CO₂ emitted in each construction phase (production, transportation, and placement) and the structural design constraints are based on the design criteria established in ABNT NBR 6118. The problem optimization's variables are geometric properties and mechanical beam's conditions, where the beam height, beam width, the proportion of height generates prestressing eccentricity, and the proportion of prestressing load were considered as design variables. Ten beams were analyzed, with different loadings, where each of these beams was submitted to the optimization process thirty times. For the proposed conditions, the ten beams had an average CO₂ emission of 3282.59 kg, maximum and minimum carbon emission of 3630.52 kg and 2910.67 kg, respectively. The study resulted in a feasibility rate higher than 90%, showing that the optimization tool was efficient in the structural design phase focusing on sustainability. Concerning carbon emission, it is possible to verify a relationship between the increase of emission and the load since element with greater inertia tend to emit a greater amount of CO₂. It was also possible to determine a regression between carbon emission and beam load.

Keywords: sustainability, CO₂ emission, optimization, precast concrete, prestressed concrete.

Resumo: Entre os principais responsáveis pelas emissões de CO₂ na camada de ozônio, a indústria da construção civil contribui com uma parcela significativa. Esta emissão é gerada em grande parte pela aplicação de sistemas de construção em concreto e suas variações. Portanto, é importante o uso de ferramentas que permitam o desenvolvimento de projetos que mitiguem os efeitos das emissões de gases nocivos para a atmosfera. Desse modo, este estudo aplicou um algoritmo de otimização chamado *Firefly Algorithm* (FA) para projetar vigas retangulares pré-fabricadas e protendidas com foco na redução da emissão de CO₂ na fase de projeto estrutural. A Função Objetiva (FO) foi definida como o peso total de CO₂ emitido em cada fase de construção (produção, transporte e montagem) e as restrições de projeto estrutural são baseadas nos critérios de projeto estabelecidos na ABNT NBR 6118. As variáveis do problema de otimização tratam de propriedades

Corresponding author: Matheus Henrique Morato de Moraes. E-mail: matheus.h.h@hotmail.com

Financial support: This study was financed in part by the Coordenação de Aperfeiçoamento de Pessoal de Nível Superior – Brasil (CAPES) – Finance Code 001.

Conflict of interest: Nothing to declare.

Data Availability: The information required to reproduce findings of this study is reported in the paper. Other data such as computer codes will be made available by the corresponding author upon reasonable request.



This is an Open Access article distributed under the terms of the Creative Commons Attribution License, which permits unrestricted use, distribution, and reproduction in any medium, provided the original work is properly cited.

geométricas e condições mecânicas da viga, onde foram consideradas variáveis de projeto a altura da viga, espessura da viga, a proporção de altura que gera excentricidade de protensão, e a proporção da força de protensão. Foram analisadas dez vigas, com diferentes carregamentos, onde cada uma dessas vigas foi submetida ao processo de otimização trinta vezes. Para as condições propostas, as dez vigas apresentaram uma emissão de CO₂ médio de 3282.59 kg, emissão de carbono máximo e mínimo de 3630.52 kg e 2910.67 kg, respectivamente. O estudo resultou em uma taxa de factibilidade superior à 90%, mostrando que a ferramenta de otimização foi eficiente na fase de projeto estrutural com foco na sustentabilidade. Em relação a emissão de carbono, é possível verificar uma relação entre o aumento da emissão e o carregamento visto que peças com maior inércia tendem a emitir uma maior quantidade de CO₂. Ainda foi possível determinar uma regressão entre a emissão de carbono e o carregamento da viga.

Palavras-chave: sustentabilidade, emissão de CO₂, otimização, concreto pré-fabricado, concreto protendido.

How to cite: M. H. M. Moraes, W. M. Pereira Junior, S. R. M. Almeida, G. M. Gonçalves Filho, and R. F. Vasconcelos, "Optimum design of precast and prestressed beams with focus on CO₂ emission reduction," *IBRACON Struct. Mater. J.*, vol. 15, no. 6, e15606, 2022, <https://doi.org/10.1590/S1983-41952022000600006>

1 INTRODUCTION

Among the main contributors to the emission of CO₂ on the ozone layer, the construction industry contributes with a significant portion [1]. This emission is largely generated by concrete structural systems and their variations, whereas in 2020, the construction industry alone was responsible for approximately 38% of all global CO₂ emissions [2]. In addition, the cement industry produces approximately 5% of global greenhouse gas emissions [3]. Therefore, using tools that allow the development of projects which mitigate the effects of greenhouse gas emissions is essential.

As every economy's sector, civil construction has been going through several changes which involve the insertion of new technologies and a new view on the rational use of materials [4]–[6]. From this perspective, precast construction offers favorable conditions to achieve these new guidelines for the sector. This model has characteristics such as fast execution, high-quality control, optimization of shapes of elements and production planning, rational use of materials, and versatility [7], [8]. Besides the fact narrated above, the prefabrication technology is already consolidated worldwide and has solutions for producing several structural models such as slabs, beams, columns, and masonry walls.

In terms of precast elements design, the biggest challenge for the designer is determining the optimal dimensions and characteristics of the structural element. In a conventional project, these characteristics are estimated intuitively and based on experience [9]. Then, the design of this structure's type becomes an iterative process of searching for the characteristics which satisfy the design criteria established by existing standards. In a corporate structural design environment, this analysis model may be inefficient, and the success rate is based entirely on the designer's experience.

Therefore, computational intelligence based on numerical analysis tools can become an ally to improve efficiency in the structure design. Such analysis tools are usually based on an optimization problem in which one wishes to determine a given function's variables, minimizing or maximizing. In structural designs, most of the time, what is sought is to optimize the cost or the total weight of the structure [10].

In the field of structural design several optimization applications can be found, such as, the researches of Al-Gahtani et al. [11], Alberio et al. [12], Navarro-Rubio et al. [8], Castilho [13], and Castilho et al. [14] that applied optimization concepts to reduce the cost and weight of precast elements. Other applications in the field of structural engineering can be observed in Azad et al. [10] applied an optimization process for steel trusses under dynamic excitation. Juliani and Gomes [15] optimized reinforced concrete (RC) frames, with genetic algorithms, such as Pires and Silva [16] which optimized slender RC columns subject to biaxial bending. Cardoso et al. [17] evaluated the static and dynamic wind effect applying structural optimization of concrete plane frames. Christoforo et al. [18] and Moraes et al. [19] applied optimization for wood truss roof structures.

In the field of sustainability, Yücel et al. [20] applied a generation of sustainable models with multi-objective optimization to design RC structures with a focus on minimizing the cost and CO₂ emission. Yu et al. [21] optimized the embodied energy and cost of RC beams under blast load. Yu et al. [22] evaluated the Life cycle embodied energy analysis of RC structures considering chloride-induced corrosion in seismic regions.

Given the possibility to apply structural optimization, this work aims to develop optimization models based on computational intelligence for application in the design of precast and prestressed concrete beams that focus on reducing CO₂ emissions. In this work, the design recommendations are based on the Brazilian standards ABNT NBR 14861 [23], ABNT NBR 9062 [24], and ABNT NBR 6118 [25].

This paper is developed in 6 sections. Sections 2 and 3 refer to the assembly of the optimization problem for precast and prestressed concrete. Section 4 presents the procedure for designing and analyzing the results. Sections 5 and 6 present the results, discussions, and conclusions regarding this research.

2 DESIGN CRITERIA FOR PRECAST AND PRESTRESSED BEAMS

This section presents the design criteria for constructing an optimal design problem for precast and prestressed concrete elements are presented.

2.1 Transient phases and mechanical properties of concrete

The first observation regarding the design of precast and prestressed elements is the consideration of transient phases in the design process. The transient phase is inherent to precast concrete and is considered an intermediate stage to the use of the structure and can become critical, leading the element to a limit [26]. According to Lewick [27] and Krahl et al. [28], the different phases must be considered, such as manufacturing in the course, storage, transport, and placement of the elements.

A concern of these transitory phases is the determination of the efforts acting on the structure that are usually different from those that occur in service situations. An example would be lifting a precast concrete beam where the lifting and transportation situation could modify the diagram of efforts of the element according to Figure 1.

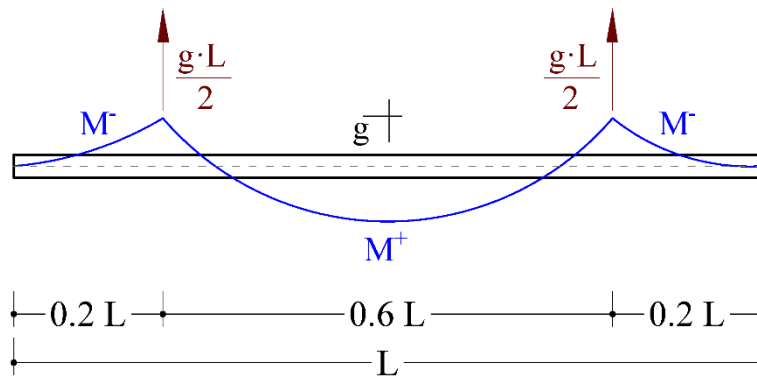


Figure 1. Example of beam and panel lifting [29].

Another important factor in the transient phase is the determination of the mechanical properties of concrete at an age j less than 28 days. Therefore, in these stages, the concrete properties, such as the characteristic compressive strength at age j ($f_{ck,j}$), can be evaluated according to Equations 1 and 2.

$$f_{ck,j} = \beta_1 \cdot f_{ck} \tag{1}$$

$$\beta_1 = e^{s \cdot \left(1 - \sqrt{\frac{28}{t}}\right)} \tag{2}$$

Where f_{ck} is the characteristic strength of concrete at 28 days, $f_{ck,j}$ is the characteristic strength of concrete at j days, t is the effective age of concrete, in days, s is a coefficient that varies according to the type of concrete, being adopted $s = 0.38$ for cement concrete CP III and IV, $s = 0.25$ for cement concrete CP I and II, and $s = 0.20$ for cement concrete CP V-ARI.

The properties derived from f_{ck} , such as tensile strength and modulus of elasticity, can be evaluated as described in sections 8.2.5 and 8.2.8 of ABNT NBR 6118 [25].

2.2 Initial prestressing stress

For prestressed concrete elements, it is necessary to determine the initial stress (σ_{pi}) in the prestressing strands. For pre-tensioned elements, normal relaxation (NR) and low relaxation (LR) steels are given in Equations 3 and 4, respectively.

$$\sigma_{pi} \leq \begin{cases} 0.74 \cdot f_{ptk} \\ 0.87 \cdot f_{pyk} \end{cases} \quad (3)$$

$$\sigma_{pi} \leq \begin{cases} 0.74 \cdot f_{ptk} \\ 0.82 \cdot f_{pyk} \end{cases} \quad (4)$$

Where f_{ptk} is the characteristic rupture stress of the steel, f_{pyk} is the characteristic yield stress of the steel, and σ_{pi} is the stress in the strand in the prestressing operation.

2.3 Prestressing losses

Another relevant observation in the design and verification of precast and prestressed concrete elements is the losses of prestressing load. These losses can be classified as time (immediate or progressive losses, see Table 1) and the cause (anchorage, steel relaxation, concrete creep, shrinkage, concrete shortening).

Table 1. Prestressing losses.

Type of loss	Classification by time
Anchorage	Immediate
Steel relaxation	Immediate
Strain immediate	Immediate
Shrinkage of concrete	Progressive
Concrete creep	Progressive
Steel relaxation with time	Progressive

Prestressing losses can be estimated or calculated. The details of prestressing losses are described in item 9.6.3 of ABNT NBR 6118 [25]. The immediate prestressing losses for precast and prestressed systems can be subdivided into: (a) attrition; (b) anchorage slippage; (c) immediate strain; (d) initial steel relaxation; and (e) initial concrete shrinkage, and the latter can be disregarded in the case of factory production since the time between the transfer of the prestressing load to the system and the concreting is small. The progressive losses can be divided into three groups: (a) concrete shrinkage; (b) concrete creep; and (c) steel relaxation.

As presented in Table 1, prestressing losses can be immediate (ΔP_{ime}) and progressive (ΔP_{pro}), so the prestressing load as a function of time ($P(t)$) is calculated based on Equation 5, where the prestressing losses reduced the initial load (P_i).

$$P(t) = P_i - \sum \Delta P_{ime} - \sum \Delta P_{pro} \quad (5)$$

The simplified process for iteration of the prestressing losses was considered. Thus, according to item 9.6.3.4.2 of ABNT NBR 6118 [25], the calculation of the simultaneous loss of concrete creep and shrinkage and steel relaxation is given by Equation 6.

$$\Delta \sigma(t, t_0) = \frac{\varepsilon_{cs}(t, t_0) \cdot E_p - \alpha_p \cdot \sigma_{c, p0g} \cdot \phi(t, t_0) - \sigma_{p0} \cdot \chi(t, t_0)}{\chi_p + \chi_c \cdot \alpha_p \cdot \eta \cdot \rho_p} \quad (6)$$

Where $\varepsilon_{cs}(t, t_0)$ is shrinkage at instant t , discounted the shrinkage that occurred up to instant t_0 , E_p is the modulus of elasticity of the prestressing steel, α_p is the ratio between the modulus of elasticity of steel (E_s) and concrete (E_c) (see Equation 10), $\sigma_{c, p0g}$ is stress in the concrete adjacent to the resulting strand, $\phi(t, t_0)$ is creep coefficient of concrete at instant t prestressing and dead load applied at instant t_0 (see Equation 9), σ_{p0} is the stress in the active reinforcement due to prestressing and dead load, ρ_p is the prestressed tendon reinforcement ratio (see Equation 12), $\chi(t, t_0)$ is the steel creep coefficient (see Equation 7 and Equation 8), and η is a geometric coefficient that depends on the eccentricity of the resultant cable relative to the barycenter of the concrete section (e_p), cross-sectional area of the concrete (A_c), and I_c is the central moment of inertia of the concrete section (see Equation 11).

$$\chi(t, t_0) = -\ln [1 - \psi(t, t_0)] \tag{7}$$

$$\chi_p = 1 + \chi(t, t_0) \tag{8}$$

$$\chi_c = 1 + 0.5 \cdot \phi(t, t_0) \tag{9}$$

$$\alpha_p = \frac{E_p}{E_{ci}} \tag{10}$$

$$\eta = 1 + e_p^2 \cdot \frac{A_c}{I_c} \tag{11}$$

$$\rho_p = \frac{A_p}{A_c} \tag{12}$$

Where $\psi(t, t_0)$ is the relaxation coefficient of steel at instant t for prestressing and dead load mobilized at instant t_0 , ρ_p is the geometric ratio of prestressing tendon reinforcement, and A_p is the cross-sectional area of the resultant active reinforcement cable.

3 OPTIMAL DESIGN CONSTRAINTS

From the point of view of optimization theory, the engineering sizing process is characterized as a constrained optimization procedure. It is necessary to evaluate constraints that delimit the search space during the method. These constraints or limitations are related to the physical feasibility of the structural element, Ultimate Limit State (ULS) constraints, and Serviceability Limit State (SLS) constraints. This section presents the design constraints for a prestressed precast concrete beam.

3.1 Verification of normal stresses

In some stages of the prestressed precast concrete beam design the structural element must satisfy the normal stresses established in Table 2.

Table 2. Conditions, combinations, and limits for verification of normal stresses [25].

Conditions to be verified		Limits	
		σ_c	σ_t
In construction			
In service	Prestressed concrete level 2 (limited prestressing)	SLS-CF	$0.70 \cdot f_{ckj}$
		FC ¹	$1.20 \cdot f_{ct,m}$
		SLS-D	0
		QPC ¹	

¹QPC – Quasi-Permanent load Combination, FC - Frequent load Combination. σ_c - Stress at the compressed region, σ_t - Stress at the tensioned region, SLS-CF - Limit state for crack formation, and SLS-D- limit state for decompression

Equations 13 and 14 are employed to calculate the stresses, representing the normal stresses in the section's bottom (σ_b) and top (σ_t) fibers, respectively.

$$\sigma_b = \frac{P(t)}{A_c} - \frac{P(t) \cdot e_p}{W_i} - \delta_{gi} \cdot \sum_{i=1}^{n_g} \frac{M_{gi}}{W_s} - \delta_{q1} \cdot \frac{\Psi_{q1} \cdot M_{q1}}{W_i} - \delta_{q2} \cdot \frac{M_{q2}}{W_i} \tag{13}$$

$$\sigma_t = \frac{P(t)}{A_c} - \frac{P(t) \cdot e_p}{W_s} + \delta_{gi} \cdot \sum_{i=1}^{n_g} \frac{M_{gi}}{W_s} + \delta_{q1} \cdot \frac{\Psi_{q1} \cdot M_{q1}}{W_s} + \delta_{q2} \cdot \frac{M_{q2}}{W_s} \tag{14}$$

Where $P(t)$ is the prestressing load for each analyzed stage, corresponding to an age t of the concrete, M_{gi} is the i -th dead load bending moment; M_{q1} and M_{q2} represent the live load moments arising from the in-service use and assembly process of the system. A_c and W represent the geometric properties of the cross-section.

In addition, the verification of normal stresses in transient phases may or may not account for the loading on the structure. Table 3 presents this summary of the coefficients used for each type of loading for each structural design stage.

Table 3. Coefficients δ_{g1} , δ_{q1} , and Ψ_{q1} in each analysis stage [9].

Stage		δ_{g1}	δ_{g2}	δ_{g3}	δ_{q1}	δ_{q2}	Ψ_{q1}
Construction	Cutting of the strands	1	0	0	0	0	0
	Lifting and transport in the industry	β_a	0	0	0	0	0
	Lifting and transport on the construction site	β_a	0	0	0	0	0
	Assembly	1	1	0	0	1	0
	Coating	1	1	1	0	1	0
SLS	In service	1	1	1/0	1	0	Ψ_{SLS}

Where the parameter Ψ_{SLS} corresponds to the reduction factor in combinations in service (Ψ_1 for frequent combination and Ψ_2 for quasi-permanent load combination) and β_a is the dynamic amplification coefficient for situations in which it is necessary to consider the vibration effects in the structural element. More details can be verified in ABNT NBR 9062 [30]. The parameter δ indicates the existence or not of the load at that stage, being g and q identification for dead and live loads, respectively.

The stress constraints include the ultimate limit state (ULS) when, for example, the verification is performed during prestressing, called here strand shear. In the verification in service, the checks correspond to the Service Limit State (SLS).

3.2 Deflection Verification (SLS)

These constraints ensure that the structural element works in service. In the case of this work, the verification used is deflection. Therefore, three verifications are required for the Serviceability Limit State of Excessive Deformations (SLS-DEF). The first two are related to the sensory acceptability of the structural element. These relate to visible displacements in structural elements (Equation 15) and vibrations felt on the floor (Equation 16).

$$(f_{p6} + f_{g1})(1 + \phi_{(T_1, \infty)}) + f_{g2}(1 + \phi_{(T_4, \infty)}) + f_{g3}(1 + \phi_{(T_5, \infty)}) + \psi_A \cdot f_q \leq \frac{L}{250} \tag{15}$$

$$f_q \leq \frac{L}{350} \tag{16}$$

Where ψ_A is the weighting coefficient for live load; T_1 is the time relative to cutting the strands; T_2 is the time relative to performing the cover or placing other dead loads in the system; and T_5 corresponds to the creep coefficient at each time informed.

The last verification of deflection refers to the manufacturing tolerance of precast elements, aiming at their linearity. For calculation purposes, positive and negative displacements should be considered, according to Equation 17.

$$f_p + f_{g1} \leq \pm \frac{L}{1000} \tag{17}$$

3.3 Bending strength section verification (ULS)

This section presents the requirements for evaluating the cross-section regarding the resistant section requirements. The resistant capacity relative to the compression struts and the resistant bending moment will be evaluated.

For verification of shear capacity, how to prescribed by ABNT NBR 6118 [25], it is necessary to calculate the design resistant shear load (V_{Rd2}) given according to Equation 18:

$$V_{Rd2} = 0.27 \cdot \alpha_{v2} \cdot f_{cd} \cdot b_w \cdot d \tag{18}$$

Where V_{Rd2} is the design resistant shear load, relative to the failure of the compressed concrete strut; f_{cd} is the compressive design strength of concrete; b_w and d are geometric properties of the section; α_{v2} is given by Equation 19. It is worth noting that this formulation is applicable to reinforced concrete and prestressed concrete elements.

$$\alpha_{v2} = 1 - \frac{f_{ck}}{250} \tag{19}$$

To determine the flexural strength section in the ULS of the prestressed elements, the principle of balance of loads is assumed in the cross-section, as shown in Figure 2.

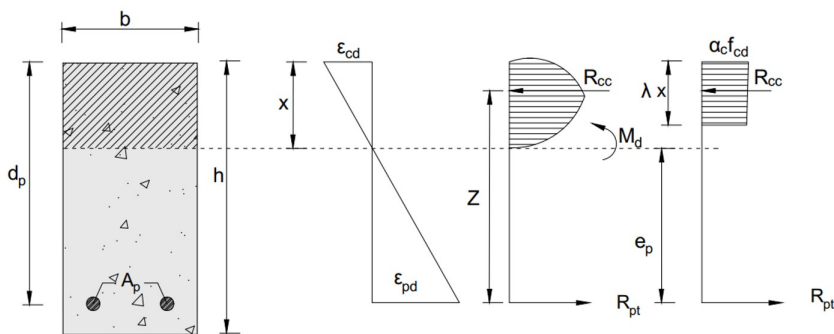


Figure 2. Stress-strain diagram of the rectangular section.

Based on the stress-strain diagram shown in Figure 2: b , d_p , and h are the width, effective depth, and height of the beam; ϵ_{cd} and ϵ_{pd} are the specific strains of the concrete and tendon; λ is the height value of the simplified rectangular diagram of the compressed concrete distribution; x is the neutral axis of the rectangular section; α_c is the multiplier value of the maximum compressive stress (Rüsch effect) for the concrete; e_p is the eccentricity of the resultant cable in relation to the barycenter of the concrete section; A_p is the area of the prestressed tendon reinforcement, M_d is the design bending moment of the section; f_{cd} is the design concrete compressive strength, Z is the lever arm of the compressive strength in concrete (R_{cc}) and tensile strength in prestressed tendon reinforcement (R_{pt}). The load R_{cc} is obtained by the product of the area of the compressed concrete ($A_c = \lambda \cdot x \cdot b$) and the acting stress in the concrete ($\sigma_{cd} = \alpha_c \cdot f_{cd}$) and the load R_{pt} is obtained by the product of the area of the tendon reinforcement (A_p) and the design stress of the prestressed tendon reinforcement (f_d), being presented in Equations 20 and 21, respectively.

$$R_{cc} = \alpha_c \cdot f_{cd} \cdot \lambda \cdot x \cdot b \tag{20}$$

$$R_{pt} = A_p \cdot f_d \tag{21}$$

The position of the neutral axis (x) is given by the Equation 22:

$$x = \frac{A_p \cdot f_d}{\alpha_c \cdot f_{cd} \cdot \lambda \cdot b} \tag{22}$$

The resistant bending moment (M_{Rd}) of the section is given by Equation 23:

$$M_{Rd} = A_p \cdot f_d \cdot \left(d_p - \frac{\lambda}{2} \cdot x \right) \tag{23}$$

Although determining the resistant bending moment is similar to the calculation model used in reinforced concrete, it is worth noting that in prestressed elements, the tendon suffers an initial prestressing that should be considered when

calculating the steel reinforcement stress (f_d). Therefore, the active tendon reinforcement level strain must consider the following portions presented in Equation 24.

$$\epsilon_{pd,total} = \epsilon_{pd,ini} + \epsilon_{pd,elo} + \epsilon_{pd,ult} \tag{24}$$

Where $\epsilon_{pd,total}$ is the strain of initial elongation of the tendon reinforcement; $\epsilon_{pd,inic}$ is the strain of initial elongation of the tendon reinforcement; $\epsilon_{pd,enc}$ is the strain due to shortening of the concrete; and $\epsilon_{pd,ult}$ is the strain corresponding to the portion of elongation of the tendon reinforcement in the ULS. To determine the strains $\epsilon_{pd,ini}$, $\epsilon_{pd,elo}$, and $\epsilon_{pd,ult}$ are presented in Equations 25, 26, and 27, respectively.

$$\epsilon_{pd,ini} = \frac{\sigma_{pd}}{E_p} = \frac{P_d}{E_p \cdot A_p} \tag{25}$$

$$\epsilon_{pd,elo} = \frac{\sigma_{cpd}}{E_c} = \frac{1}{E_c} \cdot \left(\frac{P_d}{A_c} + \frac{P_d \cdot e_p^2}{I_c} \right) \tag{26}$$

$$\epsilon_{pd,ult} = \epsilon_{cd} \cdot \frac{(d_p - x)}{x} \tag{27}$$

Where σ_{pd} is the stress in the prestressing tendon reinforcement; P_d is the prestressing load; σ_{cpd} is the concrete stress at the level of the center of gravity of the prestressing tendon reinforcement due to the P_d load; E_c is the modulus of elasticity of the concrete; E_p is the modulus of elasticity of the prestressing tendon reinforcement; and I_c is the moment of inertia of the concrete section.

4 METHODS

This section describes the procedures for building the algorithm for the optimization problem focused on minimizing the carbon footprint of a concrete beam, precast, prestressed, and straight cables. All the implementation of the optimization method and the verification processes of the concrete element were done using the Python language and the free Google Colaboratory environment.

4.1 Characteristics to build the objective function

Equation 31 is the Objective Function (OF) of the optimization problem. In this function, the dimensions of beam height (h), beam width (b), the proportion of height that generates prestressing eccentricity (e_p), and the proportion of prestressing load (P_i) are considered design variables. The design variables (\mathbf{x}) and the cross-section model of the full span beam (L) and active tendon reinforcement area (A_p), are presented in Figure 3.

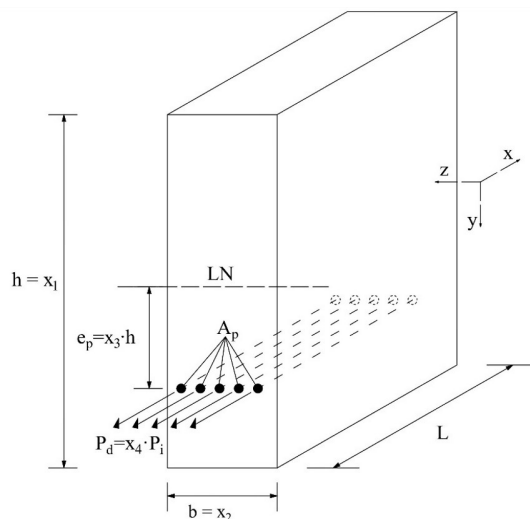


Figure 3. Cross-section of the analyzed beam

To evaluate the carbon footprint of the beam production it was taken into consideration the form work area ($A_{form\ work}$), active steel volume (V_s), concrete volume (V_c), active steel weight (P_s), concrete weight (P_c), total weight (P_{tot}) and the objective function (OF), are presented in Equations 28, 29, 30, 31, 32, 33 and 34, respectively.

$$A_{form\ work} = (2 \cdot h + b_w) \cdot L \tag{28}$$

$$V_s = A_p \cdot (L - cov) \tag{29}$$

$$V_c = b_w \cdot h \cdot L - V_s \tag{30}$$

$$P_s = V_s \cdot \gamma_s \tag{31}$$

$$P_c = V_c \cdot \gamma_c \tag{32}$$

$$P_{tot} = P_s + P_c \tag{33}$$

$$FO(\mathbf{x}) = C_{CO2} = C_p(A_{form\ work}, P_s, V_c) + C_T(L, P_{tot}) + C_s(L) \tag{34}$$

Therefore the Objective Function presented in Equation 34 is composed of the total carbon emissions (C_{CO2}) which is given by the sum of carbon emissions generated during the production (C_p), transportation (C_T), and placement (C_s) stages of the beam, cov is the cover of the concrete beam; γ_s and γ_c are the specific weights of the active reinforcement and concrete, respectively. Further details of the carbon emission calculation function are given in section 4.5.

Table 4 presents the fixed input variables of the optimization problem, i.e., independent of the algorithm iteration, these values do not change. This procedure is common in structural engineering problems since the design engineer wants to determine the best possible geometry given fixed parameters like the temperature of the project execution site, external loads, and section model requested by the contractor (in this case, the rectangular section was adopted because it is widely used in the precast industry) and the selected concrete characteristics.

Table 4. Fixed parameters of the concrete beam design.

Parameter	Value
Slump	12 cm
Cover (cov)	3.5 cm
Coefficient of unfavorable dynamic amplification (β)	1.30
Length of the prestressing course (L_{course})	150 m
Anchorage slippage (δ_{anc})	6 mm
Frequent combination reduction factor (ψ_1)	0.4
Quasi-Permanent load Combination reduction factor (ψ_2)	0.3
Modulus of elasticity of steel (E_p)	200 GPa
Specific weight of the active reinforcement (γ_s)	78.5 kN/m ³
Specific weight of simple concrete (γ_s)	24 kN/m ³
Tensile strength of steel (f_{ptk})	1900 MPa
Design temperature	30 °C
Concrete creep and shrinkage times for each stage	1/3/15/45/100/∞ days
Steel relaxation times for each	2/4/16/46/101/∞ days
Steel yield strength (f_{ptk})	1710 MPa
Steel type	NR
Type of cement	CPV-ARI
Type of prestressing	Limited prestressing (level 2)
Relative humidity (U)	70%
Length of the beam (L)	20 m
Beam compressive strength (f_{ck})	55 MPa
Type of Deferred Losses	Calculated
Distance between the production plant and the construction site (D)	50 km

The ranges of the design variables used in the beam simulation are described in Table 5.

Table 5. Range of design variables of the optimization problem.

Variable name	Variable	Range
Web height (h)	x_1	[70; 200]*
Web width (b)	x_2	[15; 60]*
Eccentricity Proportion (e_p)	x_3	[1/6; 9/20]**
Prestressing load proportion (α_{pi})	x_4	[0.85; 1.00]**

*unit in centimeters (cm) ** dimensionless unit

Table 6 presents the model of the beams studied. The relationship between live load (q) e a and the dead construction load (g_2) followed the usual prescriptions described in Santos et al. [31]. It is worth noting that load g_2 does not account for the self-weight of the element. Such consideration is made throughout the optimization process.

Table 6. Loading conditions for the simulations.

Case	g_2 (kN/m)	q (kN/m)	$\chi = q + g_2$
SIM-01	3.00	1.50	4.50
SIM-02	6.00	3.00	9.00
SIM-03	3.50	2.50	6.00
SIM-04	3.00	2.00	5.00
SIM-05	3.50	1.50	5.00
SIM-06	5.00	2.00	7.00
SIM-07	4.50	2.50	7.00
SIM-08	5.50	3.00	8.50
SIM-09	6.50	3.00	9.50
SIM-10	5.50	2.50	8.00

4.2 Bioinspired optimization algorithm

The algorithm used in this paper consists of the Firefly Algorithm (FA), which was proposed by Yang [32] and can be classified as a bioinspired probabilistic optimization. This is a population-based method. More than one particle walks through the sample space in search of the optimal feasible solution. In these methods, the concepts of the random variable are used to generate the initial population, which is a random event within limits established by the problem [32].

The theoretical source for the conception of this algorithm was inspired by the bioluminescence phenomenon and the influence of iterations between fireflies in the act of crossing. Therefore, the FA optimization method is based on the ability of fireflies to emit light and the ability of other individuals in the population to perceive this light.

When conceiving the algorithm, Yang [32] defined some precepts to help in the development, which are: all fireflies have a single gender, they are attracted to each other; the attraction capacity of each firefly is proportional to its brightness, and this decreases according to the increasing distances between individuals of the population.

With the generation of the initial populations, the firefly (or design variable) starts a random walk so that x "moves" according to an update function of the design variables (ω), as described in Equation 35, where x is the vector of design variables, ω is the update vector function of the design variable x and t is the number of iterations.

$$x^{t+1} = x^t + \omega^t \tag{35}$$

From this new direction are the new positions and possible candidate solutions for generating the optimal design point [33]. Therefore, the movement among the population of fireflies at each step of the iterative process is given by Equation 36.

$$\omega^t = \beta \cdot (x_j^t - x_i^t) + \alpha \cdot (\eta - 0.5 \cdot \epsilon) \tag{36}$$

From Equation 36, β is the attractiveness term between fireflies i and j , \mathbf{x}_i is firefly i , \mathbf{x}_j is firefly j , $\boldsymbol{\eta}$ is the vector of random numbers between 0 and 1, α is the randomness factor, and $\boldsymbol{\epsilon}$ is a unit vector.

The randomness factor α follows an exponential decay behavior according to the number of iterations t , following the formulation proposed by Equation 37, where θ is the decay constant and value equal to 0.98.

$$\alpha = \alpha_{min} + (\alpha_{max} - \alpha_{min}) \cdot \theta^t \tag{37}$$

The term β represents the attractiveness of the fireflies in the swarm. Such attractiveness is described according to Equation 38, where β_0 is the attractiveness for a distance $r = 0$, r_{ij} is a Euclidean distance between fireflies i and j (Equation 39), and γ is the light absorption parameter (Equation 40).

$$\beta = \beta_0 e^{-\gamma r_{ij}^2} \cong \frac{\beta_0}{1 + \gamma r_{ij}^2} \tag{38}$$

$$r_{ij} = \|\mathbf{x}_i - \mathbf{x}_j\| = \sqrt{\sum_{k=1}^d (\mathbf{x}_{i,k} - \mathbf{x}_{j,k})^2} \tag{39}$$

$$\gamma = \frac{1}{r^2} \tag{40}$$

$$\mathbf{r} = \mathbf{x}_{max} - \mathbf{x}_{min} \tag{41}$$

From Equations 39, 40, and 41, k is the k -th component of the vector of design variables \mathbf{x} , d is the number of design variables, \mathbf{x}_{max} is the upper bound of the design variables, \mathbf{x}_{min} is the lower bound of the design variables, and \mathbf{r} is the distance between the upper bound (\mathbf{x}_{max}) and the lower bound (\mathbf{x}_{min}).

The application of FA or any other probabilistic optimization method with population characteristics requires attention in defining the parameters of the algorithm (attractiveness: β and γ ; randomness: α).

Table 7 presents the input parameters of the FA that were based on the study by Pereira et al. [34]. In the present research, a total population of 10 individuals, randomly generated, will be considered. A total of 500 generations will be employed.

Table 7. FA input parameters.

Parameter	Meaning	Adopted value
β_0	Firefly attractiveness	0.98
N_{gen}	Number of generations	500
N_{pop}	Population size	10
α_{min}	Minimum randomness factor	0.20
α_{max}	Maximum randomness factor	0.95
R_p	Penalty factor	10^6

For this study, all simulations were evaluated 30 times to check the distribution of the optimization results.

4.3 Constraints applied to beam design and their treatment

Since this is an engineering problem, the optimization studied in this research follows the constrained optimization model. In problems of this nature, the functions that determine the constraint design conditions are relative to the limit state Equations as prescribed by ABNT NBR 6118 [25], ABNT NBR 9062 [30], and ABNT NBR 14861 [23].

The constraint Equations that determine the normative Limit States are described in Equations 42 to 45. (a) Equation 42 represents the Limit State Equations that verify the normal stresses in the design transient phases (lifting, storage, transportation, and placement) in service. σ_b and σ_t refer to the normal stress acting on the bottom and top surface, described in Equations 13 and 14 respectively. σ_{max} refers to the maximum stress allowed on the edges according to Table 2; (b) Equation 43 represents the verification of Ultimate Limit State (ULS) in bending moment,

see in section 3.3; (c) Equation 44 represents the verification of possible rupture of the compressed strut in the ULS, see in Equation 18; and (d) Finally, Equation 45 represents the verification of the deflection, considering the effects of creep, for prestressed elements. In this equation f refers to the deflection acting on the beam and f_{lim} refers to the limit deflection prescribed by the norm. The deflection calculation procedure can be seen in Equations 15 to 17.

$$\frac{\sigma_{b,t}}{\sigma_{max}} - 1 \leq 0 \quad \mathbf{g}_j, j = 1 \text{ a } 4, 10 \text{ a } 21 \tag{42}$$

$$\frac{M_{sd}}{M_{Rd}} - 1 \leq 0 \quad \mathbf{g}_j, j = 5 \tag{43}$$

$$\frac{V_{sd}}{V_{Rd2}} - 1 \leq 0 \quad \mathbf{g}_j, j = 6 \tag{44}$$

$$\frac{f}{f_{lim}} - 1 \leq 0 \quad \mathbf{g}_j, j = 7 \text{ a } 9 \tag{45}$$

As can be seen, the constraints have been normalized to avoid scaling problems within the Equations studied. This is a traditional procedure in problems of this nature, as seen in Equations 42, 43, 44, and 45.

It is worth mentioning that for this work the resistant moment (Equation 22) was limited to a ductility of 0.35 ($x/d < 0.35$) characterizing a part without compression reinforcement. Such a prescription follows the recommendation of section 14.6.4.3 of ABNT NBR 6118 [25].

For the constraint treatment procedure, the outer penalty technique was used [35], [36]. The OF is modified to obtain a pseudo-objective function, where \mathbf{g}_j represents the inequality constraints and \mathbf{h}_k the equality constraints. Equation 46 shows the adopted penalization method, and the penalized Objective Function C_{CO_2} is presented in Equation 47.

$$P(\mathbf{x}) = \sum_{j=1}^m \max[0, \mathbf{g}_j(\mathbf{x})]^2 + \sum_{k=1}^n [\mathbf{h}_k(\mathbf{x})]^2 \tag{46}$$

$$C_{CO_2}(\mathbf{x}) = FO(\mathbf{x}) + R_p \cdot P(\mathbf{x}) \tag{47}$$

From Equation 47, it is worth noting that $P(\mathbf{x})$ is the static exterior penalty function, j, k is j -th inequality constraint and k -th equality constraint, respectively, m, n are the total number of inequality and equality constraints, respectively, \mathbf{x} is the solution vector (random population), \mathbf{g}, \mathbf{h} are the set of inequality and equality constraints, and $C_{CO_2}(\mathbf{x})$ is the penalized objective function.

4.4 Characterization of the optimization problem

Figure 4 presents the complete operation of the Objective Function for each particle in the swarm, i.e., each individual in the population will have a single solution set ($\mathbf{x}^T = []_{1 \times 4}$) over a single iteration and this changes with each movement of the population.

In stage 1 (Flowchart see Figure 4) of the Objective Function the geometric and material properties are determined for all project stages. These are (a) Cable Cutting, (b) Storage, (c) Transportation, (d) Assembly, and (e) Service.

After determining all geometric and mechanical properties, the definition of a longitudinal prestressing tendon reinforcement (A_p) was performed in stage 2. Therefore, the variable A_p is a state variable that changes for each particle and each population movement of the algorithm. This procedure consisted in establishing which steel area was necessary to satisfy the axial edge tensioning condition in service. The choice of a longitudinal reinforcement via a Serviceability Limit State (SLS) is a resource widely used by design professionals since this limit state is usually predominate over other limit states. This recommendation can be seen in Cholfe and Bonilha [37], Carvalho [38], and Rodrigues [39]. Once the longitudinal tendon reinforcement is determined, it is possible to determine the prestressing losses still in stage 2. This research calculates prestressing losses as established in ABNT NBR 6118 [25] and its annexes.

After determining the tendon reinforcement, the subsequent stages 3 to 5 verify the design constraints as explained in Equations 42 to 45. In stage 6 of the algorithm, the penalty method considers the engineering problem with constraints.

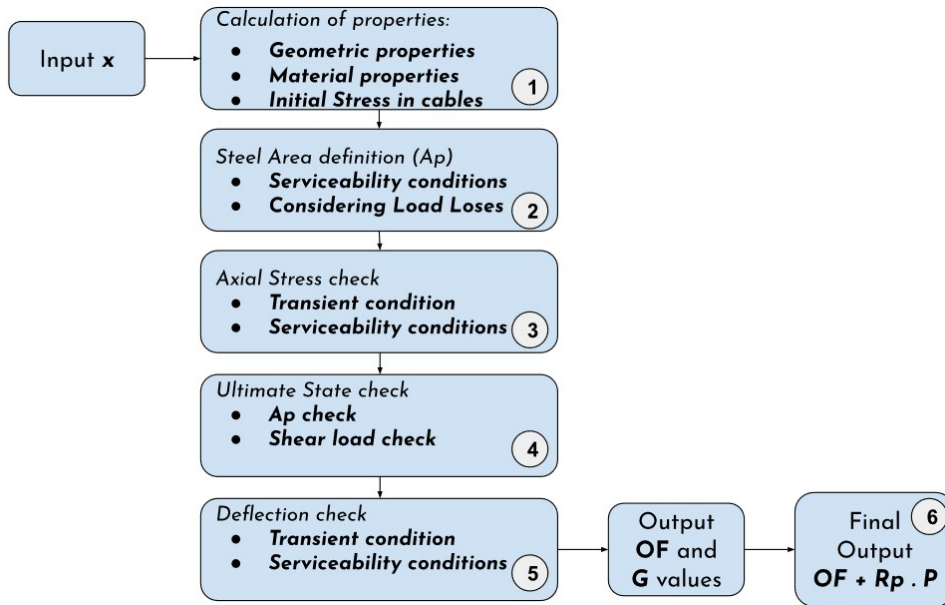


Figure 4. Flowchart of the objective function.

4.5 Carbon Emission Model

The total carbon emissions in the construction process of precast components are the sum of the emissions during the production, transportation, and placement stages. The calculation model follows the proposition of Yepes et al. [1], as shown in Equation 48:

$$C_{CO2} = C_P + C_T + C_S \tag{48}$$

Where C_{CO2} represents the total carbon emissions generated in the precast component construction process, C_P , C_T , and C_S represent the carbon emissions generated during production, transportation, and placement stages, respectively.

4.5.1 Production Stage

The carbon emissions generated during the precast elements production stage come from raw materials, fuel oil, and electrical energy consumed during production. The calculation model is shown in Equation 49:

$$C_P = \sum_{i=1}^n (A_{form\ work} \cdot F_{fw} + P_s \cdot F_s + V_c \cdot F_c) \tag{49}$$

Where C_P represents the total carbon emissions generated during the production phase of the precast element; n indicates the type of precast component. F_{fw} , F_s , e F_c represent the carbon emission coefficients for the work form, prestressing tendon reinforcement, and concrete during the production stage, respectively.

To determine the carbon emission coefficients, they were defined according to the procedures proposed by Yepes et al. [1]. It was assumed steel with production via electric arc furnace (EAF), approximately 40% recycled steel scrap. The coefficients F_{fw} , F_s , and F_c can be obtained in Table 8.

Table 8. Unit CO₂ emission of the beam in the production stage [1].

Description	CO ₂ emission (kg CO ₂ /unit)	unit
Active steel	5.64	kg
Beam formwork	2.24	m ²
Beam concrete C-35	263.96	m ³
Beam concrete C-40	298.57	m ³
Beam concrete C-45	330.25	m ³
Beam concrete C-50	358.97	m ³
Beam concrete C-55	384.76	m ³
Beam concrete C-60	407.59	m ³
Beam concrete C-70	444.43	m ³
Beam concrete C-80	469.49	m ³
Beam concrete C-90	482.77	m ³
Beam concrete C-100	484.27	m ³

4.5.2 Transportation stage

The carbon emissions generated during the transportation stage of the precast elements are mainly from the exhaust emissions of the transport vehicles. The calculation model is shown in Equation 50:

$$C_T = \sum_{i=1}^n \left(F_T \cdot P_{tot} \cdot \frac{D}{50} \right) \tag{50}$$

Where C_T represents the total carbon emissions generated during the transportation stage of the precast components, n represents the number of vehicles required to transport the precast components, F_T represents the carbon emission coefficient of transportation (kg CO₂/t) on the truck when transporting a beam of length L , and D represents the distance between the production plant and the construction site in km. It should be noted that the transportation of the beams was considered separately, and the carbon emission coefficients in transportation can be obtained in Table 9 since this depends on the length of the beam.

Table 9. CO₂ emissions from beam transportation stage (distance up to 50 km, one way) [1].

Maximum beam length (m)	Transport emission (kg CO ₂ /t)
20	76.38
25	80.12
30	98.25
35	95.38
40	93.00

4.5.3 Placement stage

The carbon emissions generated during the placement stage of the precast components come mainly from the following three aspects: raw materials, fuel oil, and electrical energy consumed during installation. The calculation model is shown in Equation 51:

$$C_S = \sum_{i=1}^n (L \cdot F_S) \tag{51}$$

Where C_S represents the total carbon emissions generated during the installation phase of precast components; n indicates the type of precast components. F_S represents the carbon emission coefficient at the placement stage (kg CO₂/m) for a beam of length L . It should be noted that the placement of the beams was considered separately, and the carbon emission coefficients at the assembly stage can be obtained from Table 10 since this depends on the length of the beam.

Table 10. CO₂ emissions from beam placement stage(distance up to 50 km, one way) [1].

Maximum beam length (m)	Placement emission (kg CO ₂ /m)
20	39.43
25	50.24
30	61.05
35	65.18
40	69.31

5 RESULTS AND DISCUSSION

In this section, the results of the optimization tests focused on the study of prestressed precast concrete beams are presented. As presented in section 4, the beams employed for this paper have a rectangular cross-section with a straight cable.

Table 11 presents the statistical values of the 30 executions of the optimization algorithm for the different types of beams considered. Figure 5 presents graphically the answers to the optimization process for the simulations, in this case, the minimum carbon emission value.

It is possible to verify through Table 11 that the optimization process presented a feasibility rate (FR) of 100% for all simulations. The answers of the 30 executions of each simulation found beams that respected all the design constraints informed for this problem.

In terms of CO₂ emission, the beams studied in this work presented an average carbon emission of 3282.59 kg, with the emission increasing according to the load imposed on the structural element. Therefore, the highest carbon emission was equivalent to the highest load given in the SIM-09 simulation. For this simulation, the total loading of 9.50 kN/m resulted in carbon emission of 3630.52 kg. The lowest carbon emission was for simulation SIM-01 with 2910.67 kg for a loading of 4.50 kN/m.

The carbon emission increased on average by about 723.01 kg between the minimum and maximum loading values. In order to mathematically represent this data set, a linear regression from the Scikit-Learn library was employed. The Equation representing this set is given by $2286.40 + 143.34 \cdot \chi$ with an $R^2 = 0.998$.

Table 11. Range of design variables for the optimization problem.

Case	$C_{CO2_{max}}$ (kg)	$C_{CO2_{min}}$ (kg)	μ (kg)	σ (kg)	FR (%)
SIM-01	2932.16	2910.67	2919.91	5.17	100
SIM-02	3604.59	3573.47	3584.36	8.80	100
SIM-03	3170.93	3150.88	3159.89	14.11	100
SIM-04	3023.86	3005.18	3013.41	5.38	100
SIM-05	3020.04	3002.77	3010.93	4.70	100
SIM-06	3325.60	3302.23	3316.57	5.68	100
SIM-07	3329.89	3307.11	3317.96	6.28	100
SIM-08	3538.36	3506.75	3517.15	7.71	100
SIM-09	3657.11	3630.52	3642.92	7.20	100
SIM-10	3470.89	3436.35	3451.99	8.33	100

C_{CO2} – CO₂ emission; μ – Mean of results; σ – Standard deviation of results; FR – feasibility rate of the optimization

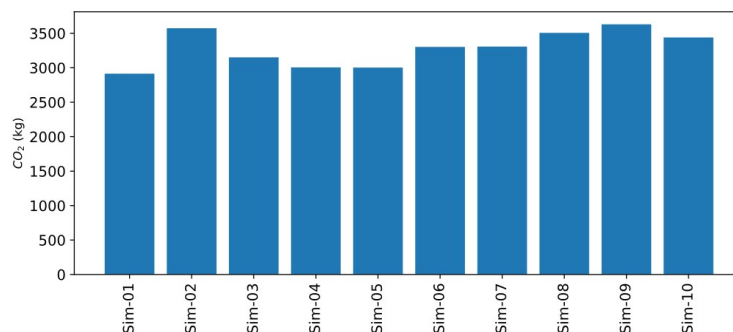


Figure 5. Carbon emission of the beams as a function of simulation.

The convergence results of the best response among the 30 repetitions are illustrated in Figure 6. It can be seen that the results show a convergence pattern from 10^3 number of evaluations of the Objective Function (NEOF).

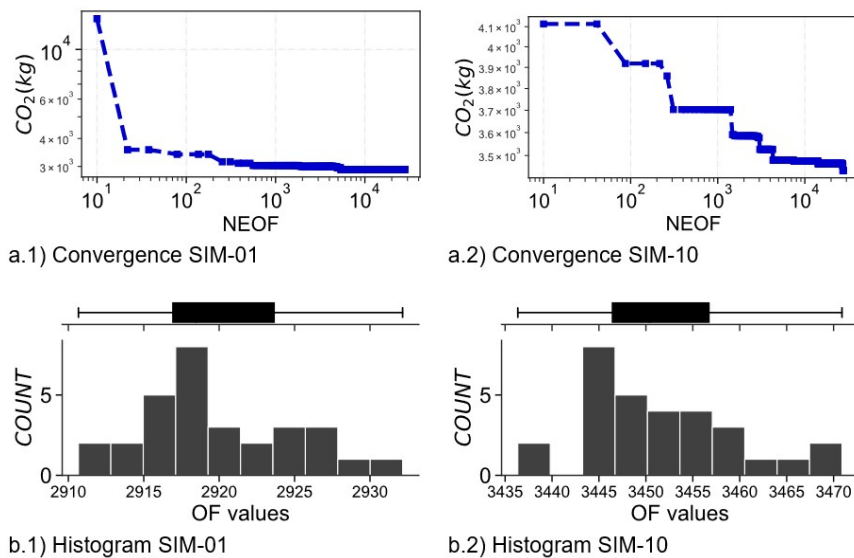


Figure 6. Result of the optimization process a) Convergence kg vs. Number of Evaluations of the Objective Function (NEOF); b) Histogram of the 30 repetition runs.

Figure 7 presents the set of constraints for the optimal response for all simulations presented in this study. It is possible to see that the limiting design constraints are the ultimate limit state (ULS) for the resistant moment (g_5) and the normal stress constraints for a serviceability limit state (SLS) in transient situations (g_{11}). In the case of these two constraints, they reached the limit $g_j = 0$ in some of the simulations.

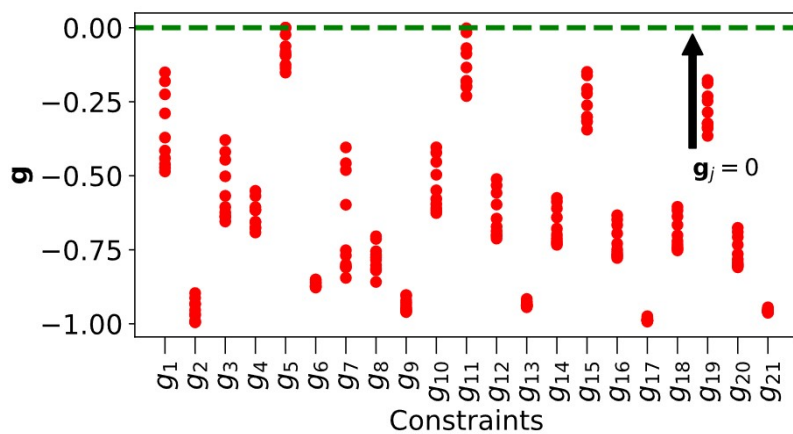


Figure 7. Evaluation of the constraints for the optimal response in simulations 01 to 10.

6 CONCLUSIONS

Firstly, it is possible to state that the optimization algorithm employed was able to be used as a tool to optimize a structural design (feasibility rate higher than 90%) of precast and prestressed beams. This fact corroborates the statement that optimization techniques can be good alternatives for structural design. Remember that the algorithm will never replace the design engineer, but it will contribute as a tool in developing a design's structure process.

Regarding carbon emission it is possible to verify a relationship between the increase of emission and the load, since elements with greater inertia tend to emit a greater amount of CO₂. It is possible to verify by the convergence diagrams in Figure 6 that the optimization process effectively reduced the carbon emission of the beams considering the design constraints imposed by ABNT NBR 6118 [25]. Besides that, the optimization process was effective in relation to the range of dimensions proposed in Table 5.

Beyond presenting a tool that enables the optimal sizing of concrete elements, the work also looks at the issue of CO₂ emission evaluation during the execution of a structural project. In this sense, the authors present some suggestions for the development of future works focused on this analysis of carbon emission in structural design:

- Development of cost functions that address not only the structural weight but also the carbon credit;
- Consideration of other structural elements as for example hollow core slabs;
- Construction of carbon emission charts as a function of load and material properties.

ACKNOWLEDGEMENTS

We would like to acknowledge the Coordenação de Aperfeiçoamento de Pessoal de Nível Superior – Brasil (CAPES) – Finance Code 001

REFERENCES

- [1] V. Yepes, J. V. Martí, and T. García-Segura, "Cost and CO₂ emission optimization of precast–prestressed concrete U-beam road bridges by a hybrid glowworm swarm algorithm," *Autom. Construct.*, vol. 49, pp. 123–134, Jan. 2015., <http://dx.doi.org/10.1016/j.autcon.2014.10.013>.
- [2] United Nations Environment Programme, "Global status report for buildings and construction: towards a zero-emission, efficient and resilient buildings and construction sector," Nairobi, Kenya: United Nations Environment Programme, Dec. 2020. https://globalabc.org/sites/default/files/inline-files/2020%20Buildings%20GSR_FULL%20REPORT.pdf (accessed Mar. 29, 2022).
- [3] E. Worrell, L. Price, N. Martin, C. Hendriks and L. O. Meida, "Carbon dioxide emissions from the global cement industry," *Annu. Rev. Energy Environ.*, vol. 26, pp. 303–329, Nov. 2001, <http://dx.doi.org/10.1146/annurev.energy.26.1.303>.
- [4] H. Su, Q. Su, C. Xu, X. Zhang, and D. Lei, "Shear performance and dimension rationalization study on the rubber sleeved stud connector in continuous composite girder," *Eng. Struct.*, vol. 240, pp. 112371, Aug. 2021, <http://dx.doi.org/10.1016/j.engstruct.2021.112371>.
- [5] G. L. Vatulia, O. V. Lobiak, S. V. Deryzemlia, M. A. Verevicheva and Y. F. Orel, "Rationalization of cross-sections of the composite reinforced concrete span structure of bridges with a monolithic reinforced concrete roadway slab," in *IOP Conf. Ser.: Mater. Sci. Eng.*, vol. 664, no. 1, p. 012014, Oct. 2019, doi: 10.1088/1757-899X/664/1/012014.
- [6] O. Petrova, O. Lugchenko, M. Hammud, and A. Nazhem "To the rationalization of the constructive solutions of the bridge supports," in *MATEC Web Conf.*, vol. 116, p. 02025, 2017, doi: 10.1051/mateconf/201711602025.
- [7] L. L. Wagner, A. L. S. Corrêa, and D. B. de Freitas, "Review on the use of prefabricated elements," *B.J.D.*, vol. 6, no. 10, pp. 75455–75465, 2020, <http://dx.doi.org/10.34117/bjdv6n10-103>.
- [8] J. Navarro-Rubio, P. Pineda, and A. García-Martínez, "Sustainability, prefabrication and building optimization under different durability and re-using scenarios: potential of dry precast structural connections," *Sustain. Cities Soc.*, vol. 44, pp. 614–628, Jan. 2019, <http://dx.doi.org/10.1016/j.scs.2018.10.045>.
- [9] R. F. Vasconcelos, "Otimização de elementos pré- moldados de concreto: lajes alveolares e vigas com cabo reto," M.S. thesis, Fed. Univ. Goiás, Goiânia, GO, 2014. [Online]. Available: <http://repositorio.bc.ufg.br/tede/handle/tede/5678>
- [10] S. K. Azad, M. Bybordiani, S. K. Azad, and F. K. J. Jawad, "Simultaneous size and geometry optimization of steel trusses under dynamic excitations," *Struct. Multidiscipl. Optim.*, vol. 58, no. 6, pp. 2545–2563, Dec 2018., <http://dx.doi.org/10.1007/s00158-018-2039-7>.
- [11] A. S. Al-Gahtani, S. S. Al-Saadoun, and E. A. Abul-Feilat, "Design optimization of continuous partially prestressed concrete beams," *Comput. Struc.*, vol. 55, no. 2, pp. 365–370, Apr. 1995, [http://dx.doi.org/10.1016/0045-7949\(94\)00481-H](http://dx.doi.org/10.1016/0045-7949(94)00481-H).
- [12] V. Albero, H. Saura, A. Hospitaler, J. M. Montalvã, and M. L. Romero, "Optimal design of prestressed concrete hollow core slabs taking into account its fire resistance," *Adv. Eng. Softw.*, vol. 122, pp. 81–92, Aug. 2018, <http://dx.doi.org/10.1016/j.advengsoft.2018.05.001>.
- [13] V. C. Castilho, "Optimization of precast prestressed elements using genetic algorithms," Ph.D. Thesis, Univ. São Paulo, São Carlos, SP, 2003. <http://dx.doi.org/10.11606/T.18.2003.tde-14102003-113629>.
- [14] V. C. Castilho, M. C. Nicoletti, and M. K. El Debs, "An investigation of the use of three selection-based genetic algorithm families when minimizing the production cost of hollow core slabs," *Comput. Methods Appl. Mech. Eng.*, vol. 194, no. 45–47, pp. 4651–4667, Nov. 2005, <http://dx.doi.org/10.1016/j.cma.2004.12.008>.

- [15] M. A. Juliani and W. J. S. Gomes, "Optimal configuration of RC frames considering ultimate and serviceability limit state constraints," *Rev. IBRACON Estrut. Mater.*, vol. 14, no. 2, pp. e14204, 2021, <http://dx.doi.org/10.1590/s1983-41952021000200004>.
- [16] S. L. Pires and M. C. A. T. da Silva, "Optimization of slender reinforced concrete columns subjected to biaxial bending using genetic algorithms," *Rev. IBRACON Estrut. Mater.*, vol. 14, no. 6, pp. e14610, 2021., <http://dx.doi.org/10.1590/s1983-41952021000600010>.
- [17] E. U. Cardoso, R. Q. Rodríguez, L. Q. Machado, F. F. Kunz, P. S. Santos and A. P. C. Quispe, "Structural optimization of concrete plane frames considering the static and dynamic wind effect," *Rev. IBRACON Estrut. Mater.*, vol. 15, no. 1, pp. e15109, 2021, <http://dx.doi.org/10.1590/s1983-41952022000100009>.
- [18] A. L. Christoforo, M. H. M. de Moraes, I. F. Fraga, W. M. Pereira Junior, and F. A. R. Lahr, "Computational intelligence applied in optimal design of wooden plane trusses," *Eng. Agric.*, vol. 42, no. spe, pp. e20210123, 2022, <http://dx.doi.org/10.1590/1809-4430-eng.agric.v42nepe20210123/2022>.
- [19] M. H. M. Moraes, I. F. Fraga, W. M. Pereira Junior, and A. L. Christoforo, "Comparative analysis of the mechanical performance of timber trusses structural typologies applying computational intelligence," *Rev. Arvore*, vol. 46, pp. e4604, 2022, <http://dx.doi.org/10.1590/1806-908820220000004>.
- [20] M. Yücel, S. M. Nigdeli, and G. Bekdaş, "Generation of sustainable models with multi-objective optimum design of reinforced concrete (RC) structures," *Structures*, vol. 40, pp. 223–236, Jun. 2022, <http://dx.doi.org/10.1016/j.istruc.2022.04.020>.
- [21] R. Yu, D. Zhang, and H. Yan, "Embodied energy and cost optimization of RC beam under blast load," *Math. Probl. Eng.*, vol. 2017, pp. 1–8, 2017, <http://dx.doi.org/10.1155/2017/1907972>.
- [22] R. Yu, L. Chen, D. Zhang, and Z. Wang, "Life cycle embodied energy analysis of RC structures considering chloride-induced corrosion in seismic regions," *Structures*, vol. 25, pp. 839–848, Jun. 2020, <http://dx.doi.org/10.1016/j.istruc.2020.03.049>.
- [23] Associação Brasileira de Normas Técnicas, *Lajes Alveolares Pré-moldadas de Concreto Protendido — Requisitos e Procedimentos*: NBR 14861, 2011.
- [24] Associação Brasileira de Normas Técnicas, *Projeto e Execução de Estruturas de Concreto Pré-moldado*: NBR 9062, 2017.
- [25] Associação Brasileira de Normas Técnicas, *Projeto de Estruturas de Concreto — Procedimento*, NBR: 6118, 2014.
- [26] G. B. Borghi, G. D. P. Lisboa, and D. D. L. Araújo, "Analysis of lateral stability of precast concrete beams for bridges in transitory phases," *REEC*, vol. 15, no. 1, Oct. 2018, <http://dx.doi.org/10.5216/reec.v15i1.49640>.
- [27] B. Lewicki, *Edifícios de Viviendas Prefabricadas con Elementos de Grandes Dimensiones*. Madrid: Insituto Eduardo Torroja de la Construcción y del Cemento, 1968.
- [28] P. A. Krah, M. C. V. Lima, and M. K. El Debs, "Recommendations for verifying lateral stability of precast beams in transitory phases," *Rev. IBRACON Estrut. Mater.*, vol. 8, no. 6, pp. 763–774, Dec. 2015, <http://dx.doi.org/10.1590/S1983-41952015000600003>.
- [29] D. A. Sheppard and W. R. Phillips, *Plant-Cast Precast and Prestressed Concrete: A Design Guide*. New York: McGraw-Hill, 1989.
- [30] Associação Brasileira de Normas Técnicas, *Projeto e Execução de Estruturas de Concreto Pré-moldado*, NBR 9062, 2017.
- [31] D. M. Santos, F. R. Stucchi, and A. T. Beck, "Reliability of beams designed in accordance with Brazilian codes," *Rev. IBRACON Estrut. Mater.*, vol. 7, pp. 723–746, Oct. 2014, <http://dx.doi.org/10.1590/S1983-41952014000500002>.
- [32] X.-S. Yang, *Nature-Inspired Metaheuristic Algorithms*. Frome: Luniver Press, 2008.
- [33] H. Wang et al., "Firefly algorithm with neighborhood attraction," *Inf. Sci.*, vol. 382–383, pp. 374–387, Mar. 2017, <http://dx.doi.org/10.1016/j.ins.2016.12.024>.
- [34] L. L. M. Pereira et al., "Estudo de sensibilidade do algoritmo de colônia de vagalumes para um problema de engenharia envolvendo dimensionamento de treliças," *Tend. Mater. Apl. Comput.*, vol. 21, no. 3, pp. 583, Nov. 2020, <http://dx.doi.org/10.5540/tema.2020.021.03.583>.
- [35] A. F. Kuri-Morales and J. Gutiérrez-García, "Penalty function methods for constrained optimization with genetic algorithms: a statistical analysis," in *MICAI 2002: Advances in Artificial Intelligence*, Berlin, Heidelberg, 2002, pp. 108–117. http://dx.doi.org/10.1007/3-540-46016-0_12.
- [36] Ö. Yeniay, "Penalty function methods for constrained optimization with genetic algorithms," *Math. Comput. Appl.*, vol. 10, no. 1, pp. 45–56, 2005, <http://dx.doi.org/10.3390/mca10010045>.
- [37] L. Cholfé and L. Bonilha, *Concreto Protendido: Teoria e Prática*. 2a ed. São Paulo: Editora Oficina de Textos, 2018.
- [38] R. C. Carvalho, *Estruturas em Concreto Protendido*. 2a ed. São Paulo: Pini, 2017.
- [39] C. Rodrigues, "Sistematização do cálculo e verificação de sistemas estruturais de galpões pré-fabricados de concreto," M.S. thesis, Univ. Fed. São Carlos, São Carlos, SP, 2012.

Author contributions: MHMM: Writing, Development, Analyses; WMPJr: Supervision, Development, Analysis; SRMA: Supervision, Development, Analysis; GMGF: Writing, Development, Analysis; RFV: Writing, Development.

Editors: Edna Possan, Mark Alexander



ORIGINAL ARTICLE

Feasibility analysis for implementing CO₂ curing in a concrete block industry in the São Paulo Region

Análise de viabilidade para implantação de cura com CO₂ em uma indústria de blocos de concreto na região de São Paulo

Lívia Regueira Fortunato^a

Guilherme Aris Parsekian^a

Alex Neves Junior^b



^aUniversidade Federal de São Carlos, Departamento de Engenharia Civil – DECiv, São Carlos, SP, Brasil

^bUniversidade Federal de Mato Grosso, Departamento de Engenharia Civil, Cuiabá, MT, Brasil

Received: 25 February 2022

Accepted: 17 October 2022

Abstract: The project feasibility analysis determines whether the project should be carried out from different spheres: strategic, technical, operational, legal, economic-financial, environmental, marketing, political, fiscal, location, among others. These are not excluding analyzes, all aspects must be assessed before implementing a new project or new process. This work will focus on the analysis of the technical feasibility of the innovative project to implement carbonation curing in a concrete block factory in the region of São Paulo. An overview of the CO₂ curing process and changing needs is presented, including identifying local CO₂ sources and delivering cost, gas consumption for chamber saturation, estimation of CO₂ uptake by masonry units during curing, estimation of consumption and monthly cost of CO₂, curing chamber changes needs, new equipment acquisition, estimation of cost for retrofit and new installations, potential best definitions on optimal temperature, humidity, and CO₂ concentration. International succeeded cases are presented. The study concludes that the technology can be easily implemented in the region, with few changes on a plant production process and on the curing chamber. There would be an increase of 4% to 14% on the block cost depending on the distance to the CO₂ supplier. Considering the Brazilian production of concrete blocks, up to 168,780 tons of CO₂ per year can be sequestered, this value is equivalent to the CO₂ sequestered by 21,100 trees.

Keywords: analysis, feasibility, technical, curing, CO₂.

Resumo: A análise de viabilidade de projetos determina se o projeto deve ou não ser colocado em prática e pode ser realizada a partir de diferentes esferas: estratégica, técnica, operacional, legal, econômico-financeira, ambiental, mercadológica, política, fiscal, localização, entre outras. As referidas análises não são excludentes, por conseguinte, é possível que para um único projeto sejam realizadas todas elas. No entanto, este trabalho terá enfoque na análise da viabilidade técnica do projeto inovador de implementação da cura química com CO₂ em fábrica de blocos de concreto na região de São Paulo. Para tanto, será apresentada uma visão geral do processo de cura com CO₂ e possíveis modificações para realizá-la na indústria, além da identificação de fontes locais de CO₂ e custo de entrega, necessidades de mudanças na câmara de cura, aquisição de novos equipamentos, possíveis melhores definições sobre temperatura ideal, umidade e concentração de CO₂. Casos de sucesso internacionais são apresentados. O estudo conclui que a tecnologia pode ser facilmente implantada na região, com poucas mudanças no processo produtivo da planta e na câmara de cura. Dependendo da distância da fábrica ao fornecedor de CO₂, poderá haver um aumento de 4% a 14% no custo do bloco. Considerando a produção brasileira de blocos de concreto, até 168.780 toneladas de CO₂ por ano podem ser sequestradas, este valor equivale ao sequestro de CO₂ realizado por 21.100 árvores.

Palavras-chave: Análise, viabilidade, técnica, cura, CO₂.

How to cite: L. R. Fortunato, G. A. Parsekian, and A. Neves Junior, "Feasibility analysis for implementing CO₂ curing in a concrete block industry in the São Paulo Region," *Rev. IBRACON Estrut. Mater.*, vol. 15, no. 6, e15607, 2022, <https://doi.org/10.1590/S1983-41952022000600007>.

Corresponding author: Lívia Regueira Fortunato. E-mail: liviarfortunato@hotmail.com

Financial support: National Council for Scientific and Technological Development (CNPq) Grant (443831/2018-1).

Conflict of interest: Nothing to declare.

Data Availability: The data that support the findings of this study are available from the corresponding author, [FORTUNATO, L. R.], upon reasonable request.



This is an Open Access article distributed under the terms of the Creative Commons Attribution License, which permits unrestricted use, distribution, and reproduction in any medium, provided the original work is properly cited.

1. INTRODUCTION

Accelerated carbonation curing or CO₂ chemical curing of concrete blocks is an innovation. According to the Oslo Manual [1], innovating means implementing a new or significantly improved product (good or service). However, chemical curing with CO₂ should not be considered just an innovation, but a sustainable innovation. According to Barbieri et al. [2] innovation and the sustainable development of organizations are one most important social movement today, since there is a global need to replace old means and practices with others that translate the principles, objectives, and guidelines new movement. When committing to sustainable development, the company must, at the very least, change the way it operates, to create strategies to reduce social and environmental impacts.

By implementing the sustainable innovation of accelerated carbonation curing, the Brazilian concrete block industries will contribute on a world scale to the reduction of global warming, reduction of water and electric energy consumption. Furthermore, they will have the benefit of reduced curing time and blocks will acquire final strength much more quickly, reducing waiting time in the industrial yard and providing faster production.

To carry out the chemical curing with CO₂, the newly manufactured unreinforced cementitious products are introduced into a carbonation chamber with adequate concentrations of CO₂, humidity, temperature, and pressure, and at the end, in a few hours, the advantages of said curing are verified that are the permanent absorption of CO₂ from the medium and premature gain in mechanical strength [3]–[6]. During curing, the CO₂ reacts with the main cement hydration product (Ca(OH)₂), C-S-H, and others) and is transformed into calcium carbonate (CaCO₃) and water. The formation of calcium carbonate promotes the permanent sequestration of CO₂ and the gain on mechanical strength, since calcium carbonate precipitates in the concrete pores, in the mineralogical form of calcite, vaterite and aragonite [7].

The idea is to capture the CO₂ emitted from the industries chimneys, use it during carbonation curing and store it permanently in unreinforced cement prefabrications. This cure type is already successfully done in countries such as the United States, Canada, and the United Kingdom, in industries like Carboclave, Solidia Technologies, CarbonBuilt and CarbiCrete [8]. Through this study we intend to analyze the technical and locational feasibility of introducing it in Brazil, more precisely in industries close to the Greater São Paulo area.

2. TECHNICAL FEASIBILITY ANALYSIS

In a technical feasibility study, also called engineering or technology study, it is necessary to understand the production processes to manufacture the product, as well as whether it is possible to produce the product or service to be commercialized in scale. As differentiated as the innovations may be, it is necessary to have coherence between the invention and its usability [9]. This technical feasibility and innovation study will comprise a) Characteristics of the innovation - description of the products, services, and technology to be used; b) Analysis of innovation process components; c) Research of similar processes and products – Success Cases.

2.1 Innovation characteristics

The concrete block industry is one of the links in the construction sector production chain, which includes cement companies, construction companies, equipment manufacturers, real estate companies linked to works and maintenance. The eco-friendly concrete block industry sector, in an unconventional way, embeds CO₂ suppliers.

Producing concrete blocks that store CO₂ is innovative. Through accelerated carbonation curing technology, carbon dioxide is chemically converted into a mineral, calcium carbonate, which definitively precipitates in the concrete pores [10]. It is sustainable, as it meets the need to reduce greenhouse gases in the atmosphere, minimizing the consequences of global warming. To the authors knowledge, technology is non-existent in the Brazilian market.

Some factors make concrete blocks ideal candidates for storing an CO₂. The block hollow geometry and thin walls facilitate the diffusivity of CO₂ inside the unit. Also, this is a large-scale product with increasing use in medium and large urban centers.

Concrete blocks that capture CO₂ also have the advantage of becoming “mature” early, that is, gaining the required compressive strength at an early age. This fact reduces the “dead time” in the industry yard and enables greater productivity. These factors benefit the possibility of practical implementing of chemical curing with CO₂, through which the blocks are placed inside the carbonation chamber with ideal conditions of temperature, pressure, humidity, and CO₂ concentration. At the end of the curing procedure, the block will permanently storage the CO₂ and with improved of mechanical resistance [6], [11].

It is a fact that non-reinforced cementitious precast can absorb CO₂ and gain strength prematurely when subjected to CO₂ curing. Fortunato [6] found that concrete paving pieces, when subjected to curing with carbon dioxide, stored 5.10% of the CO₂ present in the chamber atmosphere. Considering the consumption of cement by the Brazilian unreinforced precast industry in 2019 of 5.66 Mton [12], it would have been possible to capture approximately

290,000.00 ton of CO₂ if all production had been cured with CO₂. This value corresponds to the CO₂ sequestration of 36,250,000.00 trees in a year, since, according to the Totum Institute, a tree sequesters approximately eight kilograms of CO₂ in a year [13]. In addition, the carbonated concrete paving pieces showed superior axial compressive strength at 2-days age than the reference pieces (non-carbonated), although the 28-days were equivalent [6].

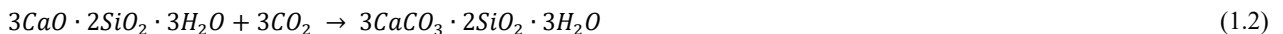
2.2 Analysis the innovation process components

2.2.1 Production of concrete blocks that sequester CO₂

The manufacturing process of concrete blocks involves the stages of mix design, in which the materials are proportioned; mixing, generally carried out in an orbital mixer; production (molding) of dry concrete in molds (forms), compaction and vibration through vibrating-pressing machines; curing and storage before delivery [14]. Concrete blocks that store CO₂ are produced in the same way as conventional concrete blocks, regardless of the industry that will produce them. It is not necessary to change the mix proportion, equipment and cycle time. The differentiation takes place in the curing procedure, which, unlike traditional industries, is not through steam or humidity, but with CO₂.

2.2.2 Innovative CO₂ chemical cure technology

The technology in question is a chemical cure that promotes the mineralization of CO₂, that is, the carbon dioxide through the cure is chemically transformed into a mineral, calcium carbonate. The permanent absorption of CO₂ in the pores of the concrete is possible due to the accelerated carbonation reaction. The main carbonation reaction occurs between Ca(OH)₂ and CO₂ in the presence of water, as shown in Equation 1.1; and in a second moment, when most of the calcium hydroxide has already been acquired, the occurrence of carbonation of hydrated calcium silicate is reported, as shown in Equation 1.2. These reactions are show below.



2.2.3 Studies on the chemical curing process with CO₂ in precast concrete materials without steel reinforcement

According to Fortunato et al. [15] several studies involving the use of accelerated carbonation curing in non-reinforced precast cementitious products have been carried out to develop a curing process to use. Table 1 summaries the related research and the carbonation parameters used.

Table 1. Research involving accelerated carbonation curing in unreinforced cementitious precast.

Authors	Samples	Time and type of initial cure (h)	Carbonation curing time (h)	Carbonation Chamber				CO ₂ absorption (%)	Compressive strength
				CO ₂ concentration (%)	Pressure (MPa)	T (°C)	RH (%)		
[3]	Cubes (100×100mm) dry concrete	no initial cure	2	100	0.5	environment	-----	7.0 – 8.0	> 40 MPa after 2hs of carbonation
[16]	Concrete masonry units and concrete units for pavement (w/c=0,25)	no initial cure	2	100	0.5	45-95	-----	9.8	10.3 MPa after 2 hours of carbonation ~ 50% increase compared to the reference at 28 days)
[16]	Cement bead board comprised cement paste and expanded polyethylene beads (w/c=0,36)	no initial cure	2	100	0.5	45-95	-----	12.2	7.8 MPa after 2 hours of carbonation, same value was obtained for reference boards at 28 days
[4]	Concrete masonry units	no initial cure	2	100	0.15	environment	-----	8.2 – 10.6	Increase of compressive strength of 78% in relation to the reference
[5]	Concrete units for pavement (10x20x64mm) (w/c=0,4)	2 – 19 wet curing	4 - 5	99,5	0.15	56	65	3.4 -7.4	Tests done after 24 hours of production: 31MPa (after 4hs of carbonation) and 46 MPa (after 5hs of carbonation)
[5]	Zero slump concrete samples (127×76×20 mm)	no initial cure	2	99,5	0.15	40 - 56	65	11.7	9.6 MPa (after 2hs of carbonation) ~ 60% increase compared to the reference at 28 days)

Table 1. Continued...

Authors	Samples	Time and type of initial cure (h)	Carbonation curing time (h)	Carbonation Chamber				CO ₂ absorption (%)	Compressive strength
				CO ₂ concentration (%)	Pressure (MPa)	T (°C)	RH (%)		
[17]	Cement paste, (14×14×6mm) (w/c = 0.36)	18 wet curing	2	99,5	0.15	environment	-----	8.9	76.8 MPa without water spray and 123,7 MPa with water spray after carbonation
[18]	Zero slump concrete samples w/c = 0,36	18 air curing	2	100	0.15	25	-----	6.9 – 7.3	28.8 MPa without water spray and 38.9 MPa with water spray after carbonation
[19]	Concrete masonry unit w/c=0,40	0, 4, 6, 8, 18 air curing	2, 4, 96	100	0.01	25	50	9.0 – 35.0	Compressive strength with water spray after carbonation comparable to non-carbonated ones with thermal curing
[20]	Concrete masonry units with recycled aggregates	no initial cure	6, 12, 24	100	0.01	-----	-----	22.49- 43.96	Compressive strength gains ranging from 108% to 151% within 24 hours of carbonation
[21]	Concrete masonry unit with blast furnace slag produced in manual factory (127×76×38 mm)	0, 4, 6, 8, 18 thermal curing	2, 4, 96	100	0.1	25	50	8.3 – 35.1	Compressive strength with water spray after carbonation comparable to non-carbonated ones with thermal curing
[22]	Concrete Masonry Units	not executed	2	100	1.39	30	50	8.62	After 2 hours, net compressive strength of 35.72MPa carbonated Concrete masonry units and 10.14MPa steam cured concrete Masonry Units
[15]	Concrete unit for pavement (100×200×60 mm)	12 hours outdoor cure and 12 hours initial steam cure	4 and 16	20	0,1	23	65	1.5% - 5.1%	At 02 days, the compressive strength of the carbonated pieces was superior to the reference and at 28 days too

In Table 1, the non-reinforced cement precast elements that underwent a compaction process for their production were shaded in gray. It was found that only Shao and Lin [5] and Fortunato et al. [15] produced the sample in the industry using a vibro-pressing process, El-Hassan et al. [19] produced blocks in the laboratory using a manual machine. The other studies used samples produced in laboratory obtained by other compaction process rather than using a manual, pneumatic or hydraulic machines, not appropriate for concrete blocks or pavers production [23]. It was observed that in the studies of Shao et al. [4], El-Hassan et al. [19] and Zhan et al. [20] the concrete blocks did not have the dimensions specified by ABNT NBR 6136:2016 and are probably not hollow. It is known that the production/compaction process and the dimensions/formats of prefabricated cementitious products directly affect the speed of the carbonation reaction and the advance of the carbonation front, promoting important variability in the percentage of CO₂ absorbed.

In most studies the concentration of CO₂ inside the carbonation chamber was 100%. The maximum concentration of CO₂ inside the chamber allows the curing of the carbonation to be accelerated by maintaining its objective, which is the maximum production of CaCO₃ in the cement matrix.

In the studies of Shao and Lin [5], Fortunato et al. [15], Rostami et al. [17], Boyd et al. [18], El-Hassan et al. [19], El-Hassan and Shao [21] it was possible to verify that the initial curing (open air curing or wet curing) carried out before the carbonation curing, directly interfered in the hydration of the non-reinforced cementitious product, and contributed to strength gain. Non-reinforced cementitious precast not subjected to initial cure absorbed more CO₂ than those submitted to initial wet curing. The hypothesis is that the non-performance of initial wet curing generated less hydration products, reducing the alkaline barrier, providing a greater advance of the carbonation front, allowing more CO₂ to be incorporated into the cement matrix. In all reported studies, the prefabricated cementitious non-reinforced carbonated yielded greater mechanical resistance when compared to the non-carbonated (reference) specimen at the earliest ages. This result is attributed to the fact that carbonation makes the sample premature, that is, its maturation is accelerated, and it gains the expected mechanical properties much faster. Among the unreinforced prefabricated samples reported tests, the concrete blocks absorbed the most CO₂. This is probably due to the smaller thickness of the block walls, allowing greater CO₂ diffusivity.

Further analyses on the literature review are reported in Fortunato et al. [[15]], that concludes the best conditions for carbon cure of concrete blocks are using a chamber at 100% of CO₂ concentration, to perform an initial air cure for at least two hours before carbon cure, the humidity shall be between 50 to 80%, temperature should be up to 60 °C to maximize carbonation.

2.2.4 Based material – CO₂ captured

The carbon dioxide to be used in curing is captured by specialized companies as AirLiquide and WhiteMartins from emitting sources with high concentrations (> 90% CO₂) and high purity (absence of contaminants such as moisture and/or other gases).

After capture, the CO₂ is purified and liquefied and can be transported by pipeline within the industry itself, as in the case of cogeneration of utility systems in which the CO₂ customer itself uses the CO₂ produced, or else, the captured CO₂ is transported in tank trucks that will supply customers in bulk or go to a filling center, where the CO₂ will be discharged into a tank and later fill the cylinders [24], [25]. Figure 1 demonstrates in a simplified way the CO₂ path from capture to the final customer.

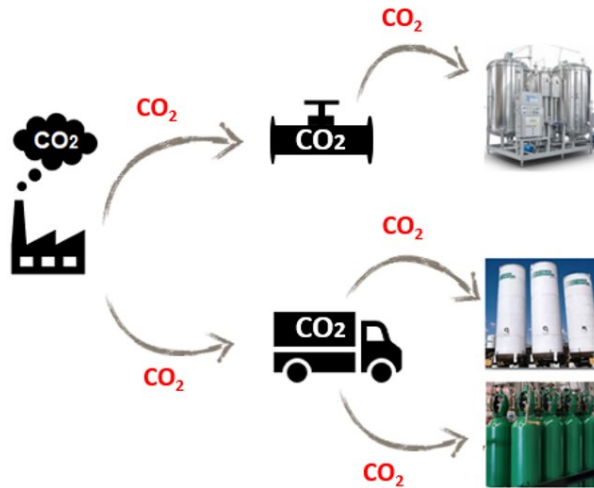


Figure 1. Transporting CO₂ to serve the industry that captured it and other customers (adapted from [[26]]).

To store CO₂ on the premises of Brazilian industries, there is no need for a government-issued environmental license. The supplying companies must only provide a safety data sheet. Since the CO₂ is an inert gas and heavier than air, it can occupy the air space. Every care must be taken to avoid cases of asphyxia. It is important that the tanks are in an open and ventilated place and that the chamber where the curing will be carried out has an efficient exhaust system [24], [25].

2.2.5 Curing chamber facilities and parameter control equipment

In the case of an existing plant, there is the possibility of retrofitting the existing chambers, if they are perfectly sealed with the installation of appropriate doors, thus avoiding the risk of accidents due to CO₂ leakage. There is also the possibility of installing new designed CO₂ curing chamber, that can be made of masonry or appropriate containers can be used [24], [25]. The control of temperature, humidity, pressure, and CO₂ concentration parameters use equipment such as a manometer to check the internal pressure of the chamber a CO₂ sensor, a temperature sensor, a humidity sensor, among others [27], [28].

2.3 Research of technological processes and similar products – Success Cases

According to Castro [29], in a technical feasibility study, it is necessary to verify if the technology to be used is applied in practice and if the technical knowledge is available. Most companies choose to invest in already used mature technologies in which the problems and adjustment that certainly arise in the development process are already known and solved. Few companies choose to use the technology present only in the state of the art. Some successful cases of industries that apply CO₂ curing in non-reinforced cement prefabricated units are presented below.

2.3.1 Solidia Technologies

▪ **Company:**

The American start-up Solidia was founded in 2008, with an investment of around US\$ 80 million, through investors such as LafargeHolcim, Total, Air Liquide, Oil & Gas Climate Initiative, BASF Venture Capital, BP Ventures, Kleiner Perkins Caufield & Byers, Bright Capital, among others [30].

▪ **Products sold:**

The company commercializes concrete masonry units and concrete paving pieces that store CO₂, as well as the CO₂ curing technology [31].

- **Manufacture and molding of prefabricated parts that store CO₂:**
The same equipment, trace, cycle time used in the production of traditional prefabricated products are used [32].
- **Accelerated carbonation cure:**
- **Based-material:** according to Meyer et al. [30] the CO₂ used by the company is supplied by AirLiquide and is usually stored in tanks like in Figure 2.



Figure 2. Tank for storing captured CO₂. Source: [33].

- **Installations:** according to Meyer et al. [30] as for the structure of the chamber, the company initially developed a prototype applied in several places of the world with more than 50 tests in companies interested in the technology. Figure 3 shows the test-chamber used by the company to carry out the cure with CO₂ on a small scale.



Figure 3. Solidia test chamber. Source: [33].

By proving the CO₂ absorption and mechanical strength improvements, the technology matured, and permanent carbonation chamber structures were developed across the world. Figure 4 shows carbonation chambers located in the United States, Canada, and the United Kingdom [30].



Figure 4. Carbonation chambers developed in Container structures, located: a) USA, b) Canada, c) d) UK. Source: [33].

- **Equipment and accessories:** according to Hall [34] the gas flow in the chamber occurs to ensure uniform evaporation on the surface of all products. This allows batch processing time to be minimized as the slowest curing-time product in the chamber defines the duration of the entire process.

Solidia has designed and built chambers 3.00 m wide x 6.00 m high x 23.00 m long [34]. The devices used for control and ventilation are shown in Figure 5.

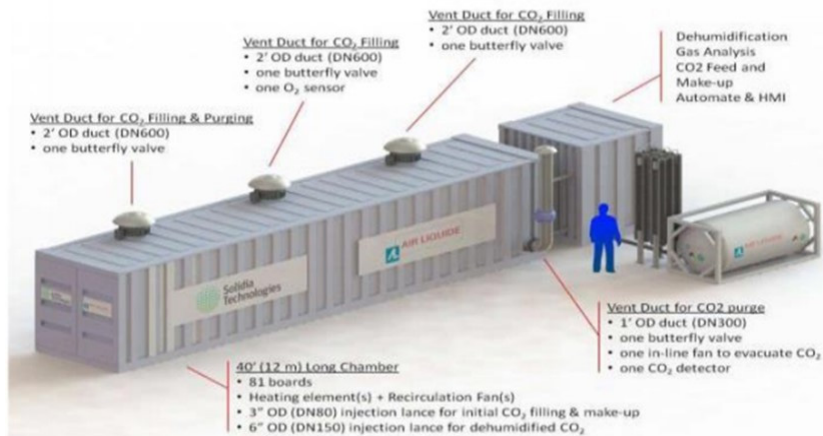


Figure 5. Solidia Carbonation Chamber. Source: [33].

- **Advantages of CO₂ curing:** Jang et al. [31], DeCristofaro et al. [32] and Meyer et al. [30] indicate the following advantages:
 - It does not consume water, but CO₂;
 - It takes advantage of existing factory facilities, production process, equipment, and raw materials;
 - It is adaptable to existing production lines;
 - Smart and fast curing, as the compressive strength results of non-reinforced precast cured with CO₂ obtained in 24 hours are equivalent to the compressive strength results of conventional unreinforced precast at 28 days;
 - Reduced inventory, due to faster curing time, enabling just-in-time production and delivery;
 - Better performance and greater durability than conventional concrete;
 - No occurrence of primary efflorescence.

2.3.2 Carboclave

- **Company:**

The company is a Canadian start-up founded in 2016 after demonstrating a series of successes in the development, validation and expansion of the CO₂ curing processing, not only with autoclaving but with all other conventional concrete curing methods.

- **Products sold:**

The company commercializes concrete masonry units that store CO₂, as well as CO₂ curing technology that can be applied to masonry units and pavers [35].

- **Manufacture and molding of prefabricated parts that store CO₂:**

According to Hargest and Al-Ghoulah [35] the process for producing precast products in an airtight enclosure, which comprises the steps of a carbonation of pre-dried concrete precast units by feeding CO₂, gas into a closed airtight enclosure under near ambient atmospheric pressure (psig between 0 and 2) and/or low pressure (between 2 and 15 psig) conditions, wherein said pre - dried concrete units have lost between 25 to 60% of their initial mix water content. The manufacturing and curing process is shown in Figure 6 below.

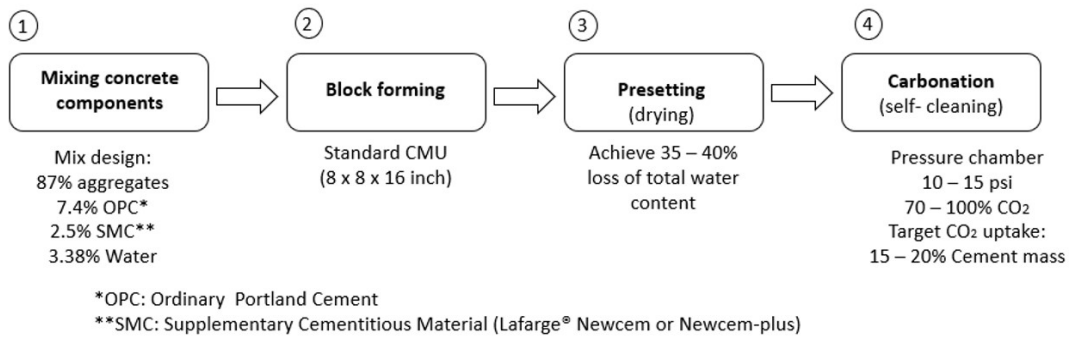


Figure 6. Manufacturing and curing process. Source: [35].

- **Accelerated carbonation cure:**
- **Based-material:** the CO₂ used by the company Carboclave is supplied by the partner Praxair.
- **Installations:** for the chamber structure, the company makes the technology available in two possibilities, retrofit and new installations. When the curing chamber already exist, it is used with adaptations, working with atmospheric pressure. The new chamber is specially designed and built for curing with CO₂ in an autoclave at high pressures. Figure 7 demonstrates a type of curing chamber used by Carboclave.



Figure 7. Carbonation chamber developed by Carboclave. Source: [[35]].

- **Equipment and accessories:** according to Hargest and Al-Ghouleh [35] before curing with CO₂, vacuum step is used to exhaust 50 to 90% of the volume of air initially present in the enclosure, then, after the CO₂ injection, applying a pressure greater than atmospheric, which is controlled by a manometer.
- **Advantages of CO₂ curing:** Hargest and Al-Ghouleh [35] verified:
 - CarboClave concrete masonry units are 25% more ecological than concrete masonry units, as they absorb up to 250g of CO₂ per 19x19x39cm concrete masonry units;
 - Non-reinforced CO₂-cured precast have greater resistance to axial compression than regular ones, greater resistance to freezing/thawing; greater resistance to sulfate attack; greater resistance to drying and atmospheric shrinkage; reduced sensitivity and permeability; and reduced efflorescence effect.

2.3.3 CarbonBuilt

- **Company:**
 CarbonBuilt was created in 2014 at the Institute for Carbon Management at the University of California, Los Angeles (UCLA). In 2020, with support from the US Department of Energy and NRG COSIA Carbon XPRIZE, they took the prototype off paper and developed CO₂ curing in practice [36].

- **Products sold:**

The company sells reverse technologies for industries which seek to make a beneficial use of the CO₂. Accelerated carbonation curing is one of them. They are producing concrete masonry units that absorb CO₂ and soon they intend to expand the range of ecological non-reinforced prefabricated elements. They develop projects in the United States, Europe and India [37].

- **Manufacture and molding of prefabricated parts that store CO₂:**

The same equipment, mix proportion, cycle time used in the production of traditional prefabricated products are used [36].

- **Accelerated carbonation cure:**

- **Based-material:** the CO₂ used comes from the plant that emits it [37]. Figure 8 shows the CO₂ piping coming from a thermoelectric plant, the gas will be sent to the carbonation chamber installed on the thermoelectric plant infrastructure.



Figure 8. Pipe containing the CO₂ that will be injected into the carbonation chamber. Source: [[38]].

- **Installations:** for the structure of the chamber, an adapted container was used for the loading of concrete masonry units through forklifts. Figure 9 shows the container-chamber [38].



Figure 9. Container-chamber. Source: [38].

- **Equipment and accessories:** the chamber is controlled by CO₂, humidity, and temperature sensors [39]. Figure 10 demonstrates their inspection.



Figure 10. Chamber control: a) CO₂ injection configuration, b) temperature measurement. Source: [[38]].

- **Advantages of CO₂ curing verified by the company:**

The main advantage emphasized by the company is the definitive incorporation of CO₂ in the concrete and the removal of this environmental liability from the atmosphere [39].

2.3.4 Carbicrete

- **Company:**

CarbiCrete is a Canadian company that commercializes CO₂ absorption technology in concrete masonry units and pieces for paving through accelerated carbonation curing. The company's patented technology was developed at McGill University and includes the production of concrete by replacing cement with steel slag [40].

- **Products sold:**

The company licenses the technology to concrete masonry units (CMUs) and precast panels; and oversees the retrofit for implementation of the process in the industry [40].

- **Manufacture and molding of prefabricated parts that store CO₂:**

According to Hahn [40] the same equipment and cycle time used in the production of traditional prefabricated products are used. The composition has replacement of cement by steel slag.

- **Accelerated carbonation cure:**

- **Raw-material:** the CO₂ used by the company Carbicrete is supplied by the partner Praxair and is stored in tanks [41].
- **Installations:** the possibility of retrofitting existing chambers and new installations using an adapted container was reported. Figure 11 demonstrates the container-chamber [41].



Figure 11. Container-chamber. Source: [41].

- **Equipment and accessories:** the chamber is controlled by CO₂, pressure, humidity, and temperature sensors. It was reported that the curing procedure with CO₂ lasts from 5 hours to 6 hours [41].
- **Advantages of CO₂ curing:** according to [41]:
 - High strength gain before 24 hours after curing with CO₂;
 - Compressive strength of CO₂ cured concrete masonry units is 30% than conventionally cured concrete masonry units;
 - According to the company, to produce a conventional concrete masonry unit, 2kg of CO₂ is generated, while the concrete masonry units cured with CO₂ is negative (-1kg), since the CO₂ is absorbed.

4. FEASIBILITY TO LOCATION

4.1 Location

According to Corrêa and Corrêa [42] decisions related to the location of the implementation of an enterprise are expensive and difficult to reverse, given that the location of an operation affects both its ability to compete and other internal and external aspects. The location directly affects the transport costs of inputs and final product, labor costs (since different regions may have different salary levels) and cost and availability of energy, in addition the choice of location influences directly on expenses, investments and even revenues. The location study has as main objective to determine the best place for the enterprise. This location, also known as the optimal location, can be understood as the one that gives the project the best cost/benefit ratio in an adequate period.

4.2 Location Variables

Location variables are factors that must be considered when choosing the ideal location for the enterprise. In general, the availability of raw materials, proximity to the consumer market and/or factors related to the production process must be considered. The analyzes must weigh between the main expenses and gains with these choices, and will be better described below [43]:

- As for the availability of raw materials: when this requires large volumes and transport is difficult or distant, it is recommended that the location of the enterprise is close to the sources of inputs;
- Regarding the consumer market: If the focus of the enterprise is the relationship with customers, the location must be close to the consumer market;
- Regarding the production process: some production processes may require certain conditions to take place, for example, they may need a source of water nearby for cooling or being close to a power substation for their perfect functioning, among others. However, it is desirable that the location of the unit is aligned with the needs of the production process.

5. TECHNICAL AND LOCATION FEASIBILITY FOR THE SÃO PAULO REGION

5.1 Methodology

In order to verify the technical feasibility and location for the implementation of CO₂ curing in concrete block factories located in the São Paulo region, several rounds of brainstorming were carried out with concrete block manufacturers, which were recruited by Associação Bloco Brasil, as well as meetings with Brazilian CO₂ suppliers. From the discussion, the equipment, material and other needs were assessed and listed, both for the case of a new or retrofit chamber. The CO₂ suppliers and block producers plant location were identified with the state. The materials, equipment, CO₂ and other supplies costs were assessed, as well as the estimated initial cost for a new or retrofit chamber. From the literature review the efficiency of the carbon cure was estimated. From this data it was possible to assess the technical and location feasibility for concrete block carbon cure implementation in the São Paulo region.

5.2 Based-material – captured CO₂

The supply of captured CO₂ is possible and viable to be carried out in the state of São Paulo, with more than one company supplying this gas. The carbon dioxide must be transported from the captured CO₂ producer to the concrete block plant using tank trucks. Then, it will be stored in tanks located in the concrete block plant premises and will later be transported through pipes provided and installed by the CO₂ supplier to the accelerated carbonation curing chambers.

For the installation and operation of the CO₂ tank, there is no need for a government environmental license. The gas is inert, does not explode and is not inflammable, but it must be stored in a well-ventilated place, as it can cause suffocation.

5.3 Installations

The CO₂ chamber can be new or can be adapted from the existing infrastructure. In both cases, airtightness must be guaranteed. Figure 12a shows a model of a new installation, like a cold chamber with temperature, humidity, and airtightness control, made in Brazil and which can be used, with the necessary adjustments, in the concrete masonry units manufacturing industry with the purpose of carrying out curing with CO₂.



Figure 12. Proposal for carbonation chambers: a) new installation; b) retrofit. Source: Author (2021).

Figure 12b shows a steam curing chamber used in an large concrete block plant located in the Great São Paulo region. To use this chamber there is the need of installing doors, control equipments, a exhaust system and the CO₂ supplier pipeline.

The analysis will be carried out considering a curing chamber with concrete masonry walls and reinforced concrete structure slab. For the installation of the CO₂ curing chamber, it must be ensured:

- **Airtight**

The airtightness of the chamber must be guaranteed by installing a guillotine door or sliding door in which carbon dioxide leakage is guaranteed no occurrence and the walls and ceiling must also be waterproofed to ensure that CO₂ does not escape through cracks or crevices. The indicated wall treatment is to apply a semi-flexible two-component waterproofing coating that shall also provide airtightness.

- **Thermal insulation**

Thermal insulation is important to standardize the curing procedure and prevent temperature changes from interfering with the process. Therefore, it is recommended that the walls and ceiling of the chamber be coated with insulating material such as isopanel composed of profiled steel sheets interspersed with polyisocyanurate.

- **CO₂ input**

The entry of CO₂ should occur in the lower region of the chamber. The pipeline from the tank to the chamber is designed by the CO₂ supplier. It is made of stainless steel and must have a pressure regulator before entering the chamber, since the pipeline will work at atmospheric pressure and the gas is pressurized to approximately 15 bar in the tank. The CO₂ supplier will design the chamber filling time according to the possible flow rate according to the pipeline diameter.

- **CO₂ and air output (exhaust)**

An exhaust system must be provided so that air is removed from the chamber when filling it with CO₂, as well as the CO₂ being expelled at the end of the curing procedure. It is recommended to use axial exhaust fans equipped with butterfly valves activated by hydraulic or pneumatic mechanisms, designer according to the dimensions of the chamber. A duct located in the lower region of the chamber must also be provided for the exhaustion of CO₂ after curing.

- **Ventilation**

Ventilation inside the chamber is essential so that the CO₂ is distributed evenly. The fans (blowers) must be positioned in the sides of the walls, in the upper region at one side and in the lower region on the other side, creating an air flow to promote greater contact between the CO₂ and the blocks.

- **Air conditioning**

The air in chamber must be conditioned to specific temperature and humidity. The system must contain an automation panel to make it possible to set the desired parameters. The air flow must be carried out through a buster interconnected in flexible and shielded pipe made with high performance material to prevent CO₂ from escaping. The humidification system must be coupled to the refrigeration equipment.

- **Safety**

An automated security panel equipped with red and green lights must be installed outside of the chamber, which will secure the opening of the chamber door. The red light will be directly related to the high concentration of CO₂ inside the chamber and the green light will indicate the low concentration of CO₂ in the chamber, communicating to the operator the prohibition or permission to open the door of the carbonation chamber.

5.4 Equipment and sensors for parameter control

The temperature, humidity, pressure, and CO₂ concentration parameters must be controlled using the equipment described below.

• **CO₂ sensor**

The sensor for evaluating carbon dioxide concentration must have an evaluation range between 0% and 100%. The sensor must be installed in the upper region of the chamber to verify that it is filled with CO₂. Since it is heavier than the air it tends to stay below reaching 100% at the top ensures the chamber is fully filled. Another CO₂ sensor must be installed in the lower region, close exhaust duct. This will indicate when the CO₂ concentration inside the chamber is low, communicating the security system that will automatically turn on the green indicator light, allowing the door to be safely open.

• **Relative humidity sensor**

The Relative Humidity Sensor monitors the relative humidity in the range of 0 to 95% (± 5%). This sensor should be positioned in the center region of the chamber, as this location represents the average humidity of the chamber.

• **Temperature sensor**

The temperature sensor, in general must range between -40°C to 135°C. This sensor should also be positioned in the center region of the chamber.

• **Manometer**

The Bourdon type manometer, stainless steel case and brass alloy internals can be used, which controls the pressure from 0 to 20kgf/cm² and has an accuracy of 1.6%.

Figure 13 demonstrates the installations of the chamber and the supply of CO₂, as well as the equipment and sensors necessary to carry out the curing with CO₂ in the industry, both for chambers made for this purpose and for retrofit chambers.

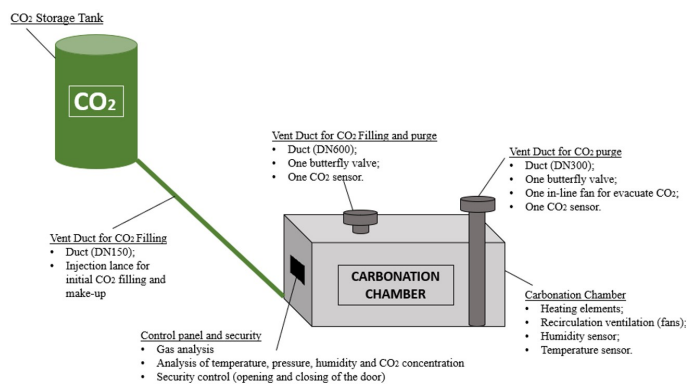


Figure 13. Chamber and CO₂ supply facilities, equipment, and sensors for carrying out CO₂ curing in the industry. Source: Author (2022).

5.5 Location

This study assesses industries consolidated in the market, within the state of São Paulo. The locational variable is related to the availability of raw material, CO₂. The industries that are closer located to the sources that generate CO₂ will have lower transport costs, not to mention the environmental issue related to lower gas emission due to transport. Figure 14 demonstrates the CO₂ gas sources sources and the concrete block plants in the state of São Paulo.

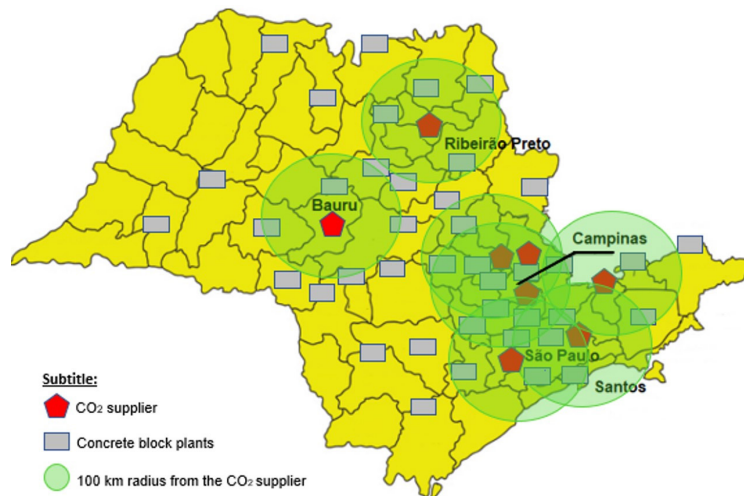


Figure 14. Radius of 100 km for CO₂ distribution. Source: Author (2022).

In Figure 14 it is possible to see that most of the main cities in the state of São Paulo have concrete block plants. CO₂ suppliers are more concentrated close to São Paulo city, with some suppliers in the inland part of the state. In this figure a radius of 100 km of the CO₂ suppliers was delimited. It is possible to observe that several concrete block plants that are within these perimeters.

5.6 Estimated CO₂ consumption for curing chamber saturation

To calculate the consumption of CO₂ for saturation of the curing chamber, the dimensions and storage capacity of concrete masonry units of an existing steam curing chamber in a concrete block plant, as shown by the Figure 15.



Figure 15. Steam curing chamber in a concrete block industry in the state of São Paulo. Source: Author (2022).

The following information was collected:

- Dimension of the curing chamber: 4.00 × 4.00 × 4.00 m (length × height × depth);
- Tray dimension: 0.66 × 0.54 × 0.03 m;
- Shelf dimension: 1.60 × 1.80 × 1.10 m;

The chamber accommodates 12 stacked shelves, 06 on the bottom and 06 on the top. Each shelf supports 20 trays and 80 concrete blocks with dimensions of 14×19×39 cm. Therefore, it is possible to cure 960 concrete masonry units per cycle, as calculated below:

- Curing chamber volume: 64.00 m³;
- Net volume of one concrete block (14×19×39 cm): 0.0078 m³;

- Net volume occupied by the concrete blocks in the chamber: 7.49 m³;
- Volume occupied by the trays in the chamber: 2.57 m³
- Volume occupied by the shelves in the chamber: 1.00 m³

The calculation of the volume of CO₂ to be injected into the chamber for its saturation is demonstrated through Equations 2.1 and 2.2:

$$CO_2 \text{ volume injected} = Vol_{\text{chamber}} - Vol_{\text{net concrete masonry units}} - Vol_{\text{trays}} - Vol_{\text{shelves}} \tag{2.1}$$

$$CO_2 \text{ volume injected} = 52,94 \text{ m}^3 \tag{2.2}$$

One kilogram of CO₂ occupies 0.534m³, then considering a 10%-waste, 109 kg of CO₂ will be needed to saturate the curing chamber.

Considering a production of three cycles per minute of the concrete block machine and eight hours worked per day, 5,760 concrete block units are produced per day. This production will fill six curing chambers/day, each cycle consuming 654 kg CO₂/day. Considering 22 workdays per month at total of and 14,388 kg CO₂/month for saturation of the curing chamber. A total of 126,720 blocks are produced per month.

5.7 Estimation of CO₂ absorption during curing by concrete masonry units

To calculate the monthly estimate of CO₂ absorption by the concrete masonry units, the mix proportion is considered as in Table 2.

Table 2. Mix proportion of the concrete blocks

Mix	Cement (kg)	Fine gravel (l)	Crushed sand (l)	Dust of stone (l)	Water (l)	Admixture (l)	Water/cement factor
Concrete masonry units	40	160	160	240	50	0,1	1,25

With this mix proportion, 64 concrete masonry units are produced, so block consumes 0.625 kg of cement. Considering the monthly production of 126,720 concrete masonry units, 79,200 kg of cement/month is consumed.

Considering the literature review, it was found that the lowest CO₂ absorption rate in concrete masonry units produced with natural aggregates, cured with 100% CO₂ concentration, is 8.62% for 2 hours of cure with CO₂ as (MacMaster and Tavares [22]). The highest reported absorption is 36.03% but with 24 hours of curing with CO₂ (Zhan et al. [20]). Considering the 2-hours cure and the smallest reported absorption, it is possible to sequester from 6,827 kg CO₂/month. Since six 2-hours cycles are necessary per day, two chambers will be necessary for the 8-hour workday.

5.8 Estimate of initial cost

For the new installation of the curing chamber, budgets were made considering a cold chamber with dimensions of 4.00 × 4.00 × 4.00 m (length × height × depth), equipped with a temperature, humidity, thermal insulation and tightness. The average value found was R\$ 37,500.00. The devices for inlet and outlet of the pressure and CO₂ system, equipped with a pressure regulator and axial exhausters, cost around R\$5,525.00. The CO₂, humidity, temperature, pressure gauge and interface sensors averaged R\$ 8,760.00. Totaling R\$ 51,786.00.

For retrofitting of an existing curing chamber with the same dimensions of 4.00 × 4.00 × 4.00 m (length × height × depth), it was verified through the SINAPI Price Bulletin (base date August/2022) that the waterproofing service walls and ceiling costs R\$ 3,594.00. For thermal insulation, after budgeting with companies in the sector, the average value was R\$18,697.00. The air conditioning system, including humidity and temperature control, has an average value of R\$ 20,500.00. The devices required for the inlet and outlet of air and CO₂, equipped with a pressure regulator and axial exhaust fans with shutters to maintain the system's sealing, amounted to R\$ 5,525.00. The CO₂, humidity, temperature, pressure gauge and interface sensors averaged R\$ 8,760.00. Totaling R\$57,076.00.

Considering that the chamber is a durable good, diluting the investment value for a minimum period of ten years. Considering that the production of concrete blocks for the same period is 15,206,400; the increase in cost per block will be R\$0.0034 for a new installation and R\$0.0037 for a retrofit, without impacting the final cost of the product.

5.8 Estimate of monthly CO₂ consumption and cost

To analyze the CO₂ cost to produce 126,720.00 concrete masonry units two situations were considered. The first scenario considers that concrete block plant is located 30 km from the CO₂ supplier. In the second case the plant is 100 km away from the CO₂ supplier. In the first situation, the cost of CO₂ will be R\$ 14,000/month or R\$ 0.11/ block. In the second case, the CO₂ cost will be R\$ 46,673/month or R\$ 0.37/block. According to a survey with the industries in May 2022, the conventionally cured 14×19×39 cm concrete masonry unit cost R\$2.65 (not considering the delivering freight cost) each. Therefore, the concrete masonry units cured with CO₂ will present an extra cost that can vary from 4% to 14%, depending on the distance from the factory to the CO₂ supplier and the CO₂ absorption rate applied. The closer the industry is to the CO₂ supplier; the more viable the CO₂-cured concrete masonry units will be.

In any case, considering the environmental benefits this cost does not seem to be a barrier to the technology implementation. Also, it has already been discussed to monetarily compensate the CO₂ sequestration. Although no practical regulation is in practice, this good environmental-friendly process may soon turn into a monetary profit.

The CO₂ emission related to cement production in 2020 in Brazil was approximately 34,907,896 tons [[44]]. In that year, 61,052,000 tons of cement were produced, of which 3,952,000 were representative of the non-reinforced prefabricated industry and 1,958,000 were for the manufacture of concrete masonry units [[45]]. This industry mainly uses CP-V cement which emits about 858 kg of CO₂ per cement tonne [[46]]. With the CO₂ absorption rate considered in this study, of 8.62%, it would have been possible to sequester approximately 168,780 ton of CO₂ per year if the entire production of concrete masonry units had been subjected to carbonation cure. This would correspond to ~ 0.5% of the total CO₂ emitted by the Brazilian cement production in 2020, or ~ 10% of the concrete masonry units industry, and equivalent to the sequestration of 21,100 trees in one year.

6 CONCLUSION

Carbonic curing is a sustainable innovation that helps to reduce global warming. According to the International Energy Agency [47], CO₂ capture and storage technology, by the year 2050, will be responsible for a reduction of up to 56% of CO₂ emissions in the cement sector. Therefore, accelerated carbonation curing technology becomes indispensable to achieve this objective.

This innovation is already successfully applied in countries such as Canada, the United States, and the United Kingdom. Cases of success are detailed in this paper.

According to the technical feasibility here reported, is possible to implement the technology in the state of São Paulo, with all of the innovative process need available in the region. A map showing CO₂ suppliers and concrete block plants located in the state is presented; the greater the distance between the supplier and the plant, the higher will be the cost.

An increase of R\$ 0.11 and R\$ 0.37 was estimated after implementing the carbonation cure if the plant is located 30km and 100 km from the CO₂ supplier, respectively. Those costs represent 4 to 14% of the concrete block production cost (not considering the delivering freight cost).

If all of the Brazilian concrete blocks industry implements the carbonation cure, considering the smallest absorption rate, it would have been possible to sequester approximately 168,780 ton of CO₂/year. This would correspond to ~ 0.5% of the annual total CO₂ emitted by the Brazilian cement production, or ~ 10% concrete block industry, and the sequestration equivalent to 21,100 trees in one year.

7 ACKNOWLEDGMENTS

The authors thank CNPq Project 443831/2018-1 - Academic Doctorate for Innovation at the Universidade Federal de São Carlos; CNPq - Process: 407060/2021-9 and to Associação Bloco Brasil for their encouragement and support.

8 REFERENCES

- [1] Organisation for Economic Co-operation and Development, *The Oslo Manual: The Measurement of Scientific and Technical Activities*, Paris: OECD; Eurostat, 1997.
- [2] J. C. Barbieri, I. F. G. Vasconcelos, T. Andreassi, and F.C. Vasconcelos, "Inovação e sustentabilidade: novos modelos e proposições", *RAE*, v. 50, n. 2, pp. 146-154, 2010.
- [3] G. Ye, "*Carbon dioxide uptake by concrete through early-age curing*", MSc dissertation, Dept. Civil Eng. Applied Mech., McGill Univ., Montreal, Canada, 2003.
- [4] Shao, Y., Zhou, X. and Monkman, S., 'A new CO₂ sequestration process via concrete products production', in *IEEE EIC Climate Change Technology*, Ottawa, ON, Canada, 10-12 May, 2006.

- [5] Y. Shao, and X. Lin, "Early-age carbonation curing of concrete using recovered CO₂", *Concr. Int.*, v. 33, pp. 50-56, 2011.
- [6] L. R. Fortunato, "Captura de CO₂ em peças de concreto para pavimentação através da cura por carbonatação acelerada", M.S. thesis, Univ. Fed. São Carlos, São Carlos, SP, Brasil, 2019.
- [7] H. G. Smoczyk, "Physical and chemical phenomena of carbonation," in *Proc. RILEM Colloquium on Carbonation of Concr.*, Paper 1.1, 1976, 10 p.
- [8] J. G. Jang, G. M. Kim, H. J. Kim, and H. K. Lee, "Review on recent advances in CO₂ utilization and sequestration technologies in cement-based materials," *Constr. Build. Mater.*, vol. 127, pp. 762-773, 2016, <http://dx.doi.org/10.1016/j.conbuildmat.2016.10.017>.
- [9] J. Schneider, "A viabilidade da inovação." Notisul, 2019. <https://notisul.com.br/colonistas/agencia-de-inovacao-e-empreendedorismo-da-unisul-agetec/a-viabilidade-da-inovacao/> (accessed: June 1, 2021).
- [10] A. Neves Jr., "Captura de CO₂ em materiais cimentícios através de carbonatação acelerada". Ph.D. dissertation. Univ. Fed. Rio de Janeiro, Rio de Janeiro, RJ, Brasil, 2014.
- [11] Y. Shao, S. Monkman, and E.S. Yuan, "Market analysis of CO₂ sequestration in concrete building products", *Proc. 2nd Int. Conf. Sustain. Constr. Mater. Tech.*, Italy, Ancona, 28-30 June, 2010.
- [12] Sindicato Nacional da Indústria do Cimento, *Relatório Anual*, Rio de Janeiro: SNIC, 2019.
- [13] Instituto Totum, "Cada árvore da Mata Atlântica chega a retirar 163 kg de CO₂ da atmosfera". <https://www.institutototum.com.br/index.php/noticias/20-verificacao-de-inventarios-de-gases-de-efeito-estufa/135-cada-arvore-da-mata-atlantica-chega-a-retirar-163-kg-de-co2-da-atmosfera> (accessed: June 8, 2021).
- [14] A. J. Salvador Fo., Bloco de concreto para alvenaria em construções industrializadas [Ph.D. dissertation]. Esc. Eng. São Carlos, Univ. São Paulo, 2007.
- [15] L. R. Fortunato, G. A. Parsekian, and A. Neves Jr., "CO₂ capture of concrete units for pavement through accelerated carbonation cure", *Int. J. Mason. Res. Innov.*, vol. 7, no. 3, pp. 233-265, 2022.
- [16] Y. Shao, S. Monkman, and E. S. Yuan, "Market analysis of CO₂ sequestration in concrete building products", in *Proc. 2nd Int. Conf. Sustain. Constr. Mater. Tech.*, Italy, Ancona, 28-30 June, 2010.
- [17] V. Rostami, Y. Shao, and A.J. Boyd, "Microstructure of cement paste subject to early carbonation curing," *Cem. Concr. Res.*, vol. 42, no. 1, pp. 186-193, 2012.
- [18] Boyd, A. J., Rostami, V. and Shao, Y., "Carbonation curing versus steam curing for precast concrete production", *J. Mater. Civ. Eng.*, vol. 24, no. 9, pp. 1221-1229, 2012.
- [19] H. El-Hassan, Y. Shao, and Z. Ghoulch, "Effect of initial curing on carbonation of lightweight concrete masonry units", *ACI Mater. J.*, vol. 110, no. 4, pp. 441-450, 2013.
- [20] B. Zhan, C. Poon, and C. Shi, "CO₂ curing for improving the properties of concrete blocks containing recycled aggregates," *Cement Concr. Compos.*, vol. 42, pp. 1-8, 2013.
- [21] El-Hassan, H. and Shao, Y., "Early carbonation curing of concrete masonry units with Portland limestone cement", *Cem & Concr. Compos.*, vol. 62, pp. 168-177, 2015. <https://doi.org/10.1016/j.cemconcomp.2015.07.004>.
- [22] D. MacMaster, and O. Tavares, "Carbon sequestration of concrete masonry units," *ACI Mater. J.*, vol. 112, no. 6, pp. 775-780, 2015.
- [23] I. D. Fernandes, *Blocos & pavers – produção e controle de qualidade*, 2. ed. Jaraguá do Sul, SC, Brasil: Treino Assessoria e Treinamentos Empresariais Ltda, 2011. 182 p.
- [24] L. Rodrigues, *Entrevista concedida a Livia Regueira Fortunato Benitez*. São Carlos, SP, 15 out. 2021.
- [25] H. Prado, *Entrevista concedida a Livia Regueira Fortunato Benitez*. São Carlos, SP, 27 out. 2021.
- [26] White Martins, "Opções de abastecimento." (accessed Apr. 11, 2021). <https://www.praxair.com.br/gases/buy-liquid-or-compressed-carbon-dioxide-gas/?tab=op%C3%A7%C3%B5es-de-abastecimento>
- [27] F. J. M. Saldanha, "Development of an accelerated carbonation test device with relative humidity control", M.S. thesis. Univ. Beira Interior, Covilhã – Portugal, 2013.
- [28] C.M. Lucena, "Avaliação da eficiência de uma câmara de carbonatação acelerada projetada e montada em laboratório", M.S. thesis, Univ. Fed. Rio Gde. Norte, Natal – RN, 2016.
- [29] J. Castro, *O estudo de viabilidade*. Recife: UFPE, 2011. Apostila.
- [30] J. B. Meyer, and S. Sahu, "Solidia technologies: an example of carbon capture and utilization", in *Int. VDZ Congress 2018*. Düsseldorf, Germany, Sep. 26-28, 2018.
- [31] J. Jain, O. Deo, S. Sahu, and N. DeCristofaro, *Solidia Concrete™*. Solidia Technologies, 2014. White Paper. <http://solidiatech.com> (accessed 2022 Apr. 10).
- [32] N. DeCristofaro, V. Meyer, S. Sahu, J. Bryant, and F. Moro, "Environmental impact of carbonated calcium silicate cement-based concrete", in *Proc. 1st Int. Conf. Constr. Mater. Sustain. Future*, April 19-21, 2017, Zadar, Croatia.
- [33] Solidia, (accessed Apr. 16, 2021). <https://www.solidiatech.com/solutions.html>

- [34] K. Hall, "The role of CFD in process development and optimization". Aldenlab, 2019 <https://www.verdantas.com/alden/blog/the-role-of-cfd-in-process-development-and-optimization> (accessed 2022 Apr 10).
- [35] P. W. Hargest, and Z. Al-Ghouleh, CO₂ - laden concrete precast products and the method of making the same. U.S. 2019/0047175 A1. Feb. 14, 2019.
- [36] C. W. Lee, "Team led by UCLA professor wins \$7.5 million NRG COSIA Carbon XPRIZE". UCLA, 2021. [accessed Apr. 10, 2022]. <https://newsroom.ucla.edu/releases/ucla-nrg-cosia-carbon-xprize-concrete>
- [37] J. Williams, "CO₂ concrete rebrands as carbonbuilt." CarbonBuilt, 2021. <https://www.carbonbuilt.com/post/co-2-concrete-changes-name-to-carbonbuilt> (accessed Apr. 11, 2022).
- [38] CarbonBuilt, "Solutions." (accessed June 16, 2021). <https://www.carbonbuilt.com/technology>
- [39] B. Wang, L. G. Pilon, N. Neithalath, and G. Sant, "Upcycled CO₂-negative concrete product for use in construction", U.S. WO/2018/081308. May 3, 2018.
- [40] J. Hahn, "We're taking CO₂ out of the system" says carbon-capturing concrete maker Carbicrete." Dezeen. (accessed Apr. 10, 2022). <https://www.dezeen.com/2021/06/15/carbon-capturing-concrete-carbicrete/>
- [41] Carbicrete, Technology (accessed June 16, 2021). <https://carbicrete.com/technology/>
- [42] H. L. Corrêa, and C.A. Corrêa, *Administração de produção e de operações: manufatura e serviços: uma abordagem estratégica*. São Paulo: Editora Atlas, 2011.
- [43] Lima, F. M. S., and Silva, A. C., *Estudo de viabilidade econômica de implantação de uma fábrica de cimento*. Rio de Janeiro: UFRJ/Escola Politécnica, 2012.
- [44] Sistema de Estimativa de Emissões de Gases de Efeito Estufa. *Emissões por atividade econômica*, Brasil: SEEG. <https://plataforma.seeg.eco.br/sankey> (accessed Apr. 1, 2022).
- [45] Sindicato Nacional da Indústria do Cimento, *Relatório sobre produção anual de cimento Portland*. 2012. (accessed May 10, 2022). http://snic.org.br/assets/pdf/relatorio_anual/rel_anual_2020.pdf
- [46] Conselho Brasileiro de Construção Sustentável. *Projeto avaliação de ciclo de vida modular de blocos e pisos de concreto*, São Paulo: CBCS, 2014, 93 p.
- [47] International Energy Agency, *CO₂ capture in the cement industry*. 2009. <http://www.iea.org/publications/freepublications/publication/name,3862,en.html> (accessed Apr. 11, 2022).

Author contributions: LRF: formal analysis, methodology, writing; GAP, ANJ: conceptualization, methodology, supervision.

Editors: Edna Possan, Mark Alexander.



ORIGINAL ARTICLE

Mechanical performance and chloride penetration resistance of concretes with low cement contents

Desempenho mecânico e resistência à penetração de cloretos de concretos com baixo teor de cimento

Taíssa Guedes Cândido^a Gibson Rocha Meira^{a,b} Marco Quattrone^c Vanderley Moacyr John^c ^aUniversidade Federal da Paraíba – UFPB, Programa de Pós-Graduação em Engenharia Civil e Ambiental, João Pessoa, PB, Brasil^bInstituto Federal de Educação, Ciência e Tecnologia da Paraíba – IFPB, Departamento de Construção Civil, João Pessoa, PB, Brasil^cUniversidade de São Paulo – USP, INCT Tecnologias Ecoeficientes Avançadas em Produtos Cimentícios, São Paulo, SP, Brasil

Received 24 March 2022

Accepted 17 October 2022

Abstract: The concern about the environment has been leading the construction industry to adopt more sustainable practices. The main environmental impact of concrete is related to CO₂ emissions coming from cement, particularly from the cement content in concrete. For this reason, this research evaluates the performance of concretes with partial replacement of Portland cement by limestone filler and silica fume. These concretes were proportioned to improve particles' packing and paste volume optimization. The compressive strength was determined to assess their mechanical performance. Their durability was investigated by capillary absorption and chloride penetration resistance. Results indicate that concretes showed a better efficiency in terms of binder intensity, with values close to the minimum found in literature (5 kg.m⁻³.MPa⁻¹). It was also observed that even concretes with cement content lower than the minimum recommended by standards showed better performance than regular concretes regarding the chloride's penetration.

Keywords: ecoefficient concrete, low binder concrete, limestone filler, durability, chloride resistance.

Resumo: A preocupação com o meio ambiente vem impulsionando a indústria da construção civil a adotar práticas mais sustentáveis. Seu maior impacto ambiental está relacionado com a emissão de CO₂ do cimento, particularmente do teor de cimento no concreto. Por isto, essa pesquisa avalia o desempenho de concretos com substituição parcial do cimento Portland por filer calcário e sílica ativa. A dosagem desses concretos foi realizada utilizando conceitos de empacotamento e otimização da pasta. Foi realizado ensaio de resistência à compressão para verificar o desempenho mecânico desses materiais. A durabilidade foi analisada por ensaios de absorção por capilaridade e pela resistência à penetração dos cloretos. Os resultados indicam que os concretos otimizados, apresentaram melhor eficiência segundo o indicador Intensidade Ligante (IL), com valores próximos aos mínimos encontrado na literatura (5 kg.m⁻³.MPa⁻¹). Foi verificado também que mesmo concretos com consumo de cimento inferior ao recomendado por normas, apresentaram desempenho superior aos concretos convencionais, quanto à penetração de cloretos.

Palavras-chave: concreto sustentável, concretos com baixo teor de cimento, filer calcário, durabilidade, resistência à cloretos.

How to cite: T. G. Cândido, G. R. Meira, M. Quattrone, and V. M. John, "Mechanical performance and chloride penetration resistance of concretes with low cement contents" *Rev. IBRACON Estrut. Mater.*, vol. 15, no. 6, e15608, 2022, <https://doi.org/10.1590/S1983-41952022000600008>

Corresponding author: Taíssa Guedes Cândido. E-mail: taissaguedes1@hotmail.com

Financial support: This research is part of the CEMtec project, National Institute on Advanced Eco-Efficient Cement-Based Technologies, supported by the National Council for Scientific and Technological Development - CNPq (Process 485340/2013-5) and by São Paulo Research Foundation - FAPESP (Process 14/50948-3 INCT/2014).

Conflict of interest: Nothing to declare.

Data Availability: The data that support the findings of this study are available from the corresponding author, [TGC], upon reasonable request.



This is an Open Access article distributed under the terms of the Creative Commons Attribution License, which permits unrestricted use, distribution, and reproduction in any medium, provided the original work is properly cited.

1 INTRODUCTION

The population growth has led to an increase of the demand for dwellings and infrastructures and, as a consequence, for construction materials, especially concrete [1]. Over the past 10 years, the global Portland cement manufacturing grew by approximately 25% [2]. Cement production is expected to increase even more, between 12% and 24% [3]. Undoubtedly, this increase will impact in terms of energy consumption and CO₂ emissions [4].

Due to the increasing of CO₂ emissions from large-scale cement production, the Cement Industry focused on different CO₂ mitigation strategies, including the use of alternative materials in the cement composition [1]. The most common strategy for reducing the environmental impacts of cement is the replacement of clinker by mineral additions, reactive or non, such as fly ash, blast furnace slag, and limestone filler [5], [6]. However, the limited availability of fly ash and blast furnace slag, which will represent less than 20% of global cement demand by 2050, is a significant factor to consider [1], [7]. Therefore, due to the lower availability of these reactive materials, there should be a preference for inert materials such as limestone filler, with greater availability [8]. This strategy together with the reduction of cement content in concretes would facilitate the production of more sustainable construction materials [5], [8], [9]. Nevertheless, improving the durability of low binder concretes is essential to reduce the maintenance cost and increase the service-life of the concrete structures [9].

Improving the durability of low binder concretes requires an adequate mix design to allow balancing the reduction of binder and its effect against environmental aggressive agents which can induce corrosion of reinforcement.

1.1 Mix proportioning of low binder concretes

Supplementary cementitious materials (SCMs) used as clinker replacement influence the particle packing and the water demand of the mixture. The water demand is influenced by the specific surface area of these SCMs, usually higher than that of cement [10], [11]. They also contribute to the formation of nucleation points that lead to a faster hydration rate [12].

Superplasticizers are used to reduce water demand and promote the dispersion of solid particles [13]. The use of mineral additions and dispersants compensates for the cement reduction maintaining the desired workability of the mixture.

Optimizing the aggregates packing, by theoretical models [14] and/or experimental tests [15], is also needed. This process allows working with a lower volume of interparticle voids to be filled by a volume of cement paste necessary to guarantee the workability. Therefore, reducing the interparticle porosity enables reducing the paste volume [16]–[19] and also, reduce the porosity, increase the mechanical performances [20] and improve the durability.

1.2 Durability of low binder concretes and reinforcement corrosion

Corrosion of steel in concrete initially involves the transport of aggressive agents into its interior. When these agents reach the reinforcement, they can change the equilibrium conditions of the steel, and the corrosion process starts, followed by the corrosion propagation phase [21].

The corrosion initiation period is considered the period from the time when the aggressive agents penetrate the concrete until the reinforcement depassivation occurs. The duration of this initiation period defines the service-life of structures in the marine environment, as corrosion rates are usually very high [22]. Reducing the material porosity can hinder the entry of aggressive agents and increase the initiation period.

Standards establish minimum or maximum parameters for concrete according to the exposure environment of the structure, aiming to improve the durability of concrete structures. Table 1 presents some of these specifications considering national and international standards for reinforced concrete structures located in the marine atmosphere, where chlorides ions are mainly responsible for the reinforcement corrosion.

Table 1. Requirements for concrete in marine atmosphere zones - data from national and international standards

Standard	Exposure condition	Minimum cement content (kg/m ³)	Maximum w/c	Minimum compressive strength (MPa)
NBR 12655 [23]	Marine atmosphere zone (III)	320	0.55	30
ACI 318 [24]	Exposed to moisture and an external source of chlorides (C2)	-	0.4	34.5
IS 456 [25]	Marine aerosol (IV)	340	0.45	-
NP EN 206 [26]	Exposed to airborne salt but not in direct contact with sea water (XS1)	300	0.5	30
BS 8500 -1 [27]	Exposed to airborne salt but not in direct contact with sea water (XS1)	340	0.5	35
AS 3600 [28]	Within 1 km from coastline (B2)	-	-	40

Although the normative recommendations indicate a cement consumptions above 300 kg/m³ (Table 1), some studies suggest that concretes with cement content lower than this amount meet the durability requirements recommending a revision of these criteria [5], [15], [29], [30].

Table 2 presents results of a few studies related to concretes with low binder content that evaluated properties linked to the corrosion of reinforcement. It is easier to see the positive impact on the performance of concrete when a reactive addition is used. However, it is also possible to improve the concrete performance replacing binders by inert fillers. In this regard, there is still no agreement in the literature on the levels of binder replacement. In addition, analysed studies show that there is also no standardization on the best way to assess the transport of chlorides into these materials.

For these reasons, more studies about the assessment of performances of low binder concrete in protecting steel from corrosion are needed. Therefore, the objective of this work is to assess the transport of chlorides in low binder concrete, in which binder was replaced by limestone filler.

Table 2. Literature data on concrete with low cement consumption - mechanical strength and chloride transport

Reference	Year	Cement type	Uses particle size optimization concepts	water/fines	Water/binder	Cement content (kg/m ³)	Fly Ash content (kg/m ³)	Slag content (kg/m ³)	Limestone powder content (kg/m ³)	Quartz powder content (kg/m ³)	Compressive strength (MPa)		Rapid chloride migration (C)		Non-steady-state migration coefficient (x 10 ⁻¹² m ² /s)	
											28 days	91 days	91 days	28 days	35 days	98 days
Naik et al. [31]	1996	Type I-ASTM C 150 (correspond to CP I-NBR 5732)	N/A	0.31-0.36	0.31-0.36	375-398					53.2-60.7		1729-2488			
				0.33-0.37	0.33-0.37	220-328	71-182			41.7-56.7		1576-1907				
				0.33-0.37	0.33-0.37	107-179	216-316			29.2-39.8		1620-2750				
Isaia and Gastaldini [29]	2009	CP V-ARI NBR 5733	N/A	0.35-0.55	0.35-0.55	309-540						46.1-72.4	2380-3134			
				0.35-0.55	0.35-0.55	155-270	155-270			25.4-59.1	754-1190					
				0.35-0.55	0.35-0.55	93-162	216-378			32.6-49.1	840-1140					
				0.35-0.55	0.35-0.55	31-54	61-108	216-378		20-46.1	448-651					
Lollini et al. [32]	2014	CEM I 52.5R EN 197 (correspond to CP V-ARI)	Yes	0.42-0.61	0.42-0.61	300-350					60-85	65-105		5-12		
				0.42-0.61	0.49-0.72	212.5-340		37.5-60		45-85	55-95		11-19			
				0.42-0.61	0.6-0.87	210-245		90-105		40-70	45-75		13-38			
Müller et al. [9]	2014	CEM I 52.5R EN 197 (correspond to CP V-ARI)	Yes	0.26-0.39	0.43-0.69	112.8-268.2				114.3-216.4	48.5-88		11-20			
Palm et al. [33]	2016	CEM II/A-LL 32.5R (Correspond to CP II-F NBR 11578)	Yes	0.5	0.5	320						54		17	13	
				0.5	0.5	320						52		25	15	
				0.35	0.54-1.0	133-247		133-247		40-80		19-30	15-18.5			
				0.45	0.9	167.5		167.5		28-40		35-50	21-39			
				0.5	1	160		160		30-38		48-60	30-50			

2 MATERIALS AND METHODS

2.1 Production and characterization of concrete

Two groups of concretes, proportioned and tested in two laboratories, were analyzed. The first group (C1, C2, and C3) was characterized by a powder content of about 350 kg/m³ in which limestone filler represented between 5 and 13% of the total powder mass; for the second one (C4, C5, and C6) the limestone content was between 40% and 70% by mass of powder (Table 3). The cement was a CP V – ARI (Portland cement with about 5%wt. of limestone), supplied

by two manufacturers. A small amount of silica fume was used as cement replacement in concretes C2 and C3. Density and BET N₂ specific surface area of cements, fillers and silica fume are presented in Table 4.

The reference concrete (C1) was proportioned according to recommendations of NBR 12655 [23] for aggressiveness class III - marine atmosphere environment (Table 1). This concrete was proportioned to have a 28-days compressive strength ≥ 30MPa, a water-to-cement ratio of 0.55 and a cement content of 350 kg/m³. In the other concretes, mineral additions were used partially replacing the Portland cement. The packing of the mixture was improved by blending fine and coarse aggregates with different grain size distributions. The concrete workability was adjusted by using water-reducer admixtures. It is noteworthy that for the C4, C5, and C6 concrete, the grain size distribution of aggregates, the volume of paste (cement + filler + water) were kept constant (Figure 1).

Table 3. Mix design of the cement reduced concretes.

Materials	C1	C2	C3	C4	C5	C6
Water (kg/m ³)	192.6	148.3	139.1	160	160	160
Filler 1 (kg/m ³)		12.1	24.5			
Filler 2 (kg/m ³)		12.1	24.5			
Filler 3 (kg/m ³)				139.84	139.84	139.84
Filler 4 (kg/m ³)				54.5	100.22	189.22
Silica fume (kg/m ³)		10	17.7			
Portland cement (kg/m ³)	350.1	319.5	284.7	300	250	150
Binder (clinker + gipsite + pozolana) (kg/m ³)	332.6	313.5	288.2	286	237.5	143
Polycarboxylate-based superplasticizer content (mass % of cement)	0.5	2.55	2.8	3.63	2.21	1.85
Lignosulfonate-based plasticizer content (mass % of cement)		1	1			
Fine sand (kg/m ³)		544.6	544.6	684.36	684.36	684.36
Coarse sand (kg/m ³)	903.6	445.6	445.6	634.78	634.78	634.78
Gravel 12.5 - 4.75 mm (kg/m ³)		449.2	449.2	535.13	535.13	535.13
Gravel 19 - 4.75 mm (kg/m ³)	983.8	548.2	548.2			
Total fines (kg/m ³)	350.1	353.7	351.4	480.38	477.56	472.07
Water/binder (kg/kg)	0.55	0.46	0.49	0.53	0.64	1.07
Water/fine (kg/kg)	0.55	0.42	0.4	0.33	0.34	0.34
Slump (cm)	12	15.5	7	SCC*	SCC*	SCC*

*Self-consolidating concrete.

Table 4. Physical characterization of fines.

Material	F1	F2	F3	F4	SF	Cem 1	Cem 2
Density (g/cm ³)	2.77	2.7	2.76	2.74	2.12	3.13	3.06
BET N ₂ SSA (m ² /g)	2.23	4.07	3.73	1.16	1.5	1.16	0.97

The optimization of the paste was achieved by reducing the cement and water content, increasing the proportion of filler and silica fume in some cases. The mixture C3 presents a reduction in cement content of 19% compared to C1. This reduction is 57% in C6, i.e., 30% Portland cement and 70% limestone filler (Figure 2).

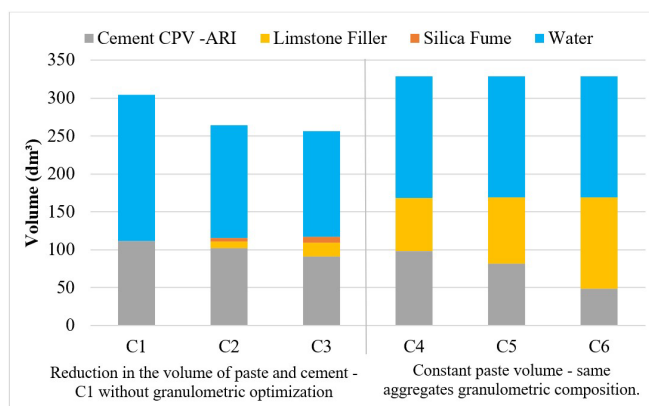


Figure 1. Volume of phases in cement paste.

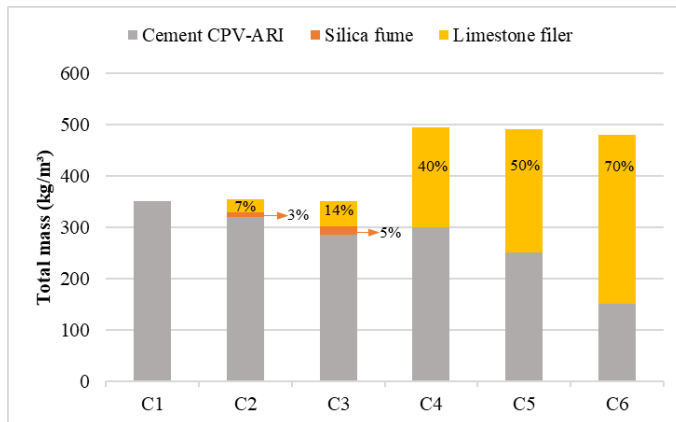


Figure 2. Amount of powder by mass per cubic meter in studied concretes. Percentages represent the filler and silica fume content by mass of powder.

After mixing, cylindrical specimens ($\varnothing 10 \times 20$ cm) were casted according to the recommendations of NBR 5738 [34]. Specimens were demolded after 24 hours and wet-cured for seven days. This period represents conditions closer to construction site reality. Then, specimens were stored in the laboratory environment until the age of the tests. Compressive strength at 28 days was carried out according to NBR 5739 [35] and sorptivity according to NBR 9779 [36].

2.2 Rapid Chloride Migration (RCM) test

The resistance to chloride penetration was analyzed using the rapid chloride migration test according to NT BUILD 492 [37]. The test specimens ($\varnothing 10 \times 5$ cm) cut from cylinders ($\varnothing 10 \times 20$ cm) were saturated in a calcium hydroxide solution before the exposure to the test.

During the test, the specimen was interspersed between a 10% sodium chloride solution by mass (used at the cathode) and a 0.3N sodium hydroxide solution (used at the anode). A voltage of 30 V was applied, which generated an initial current. According to its value, the applied voltage was adjusted to 50 V, and the duration of the test was determined (24h). The applied voltage makes the chlorides present in the cathode solution to migrate, through the specimen, towards the anode solution.

At the end of the test, the specimen was split by diametral compression and a 0.1M silver nitrate solution sprayed on the fractured surface. When the white silver chloride precipitation on the split surface is clearly visible, the chloride penetration depth can be measured (Figure 3).

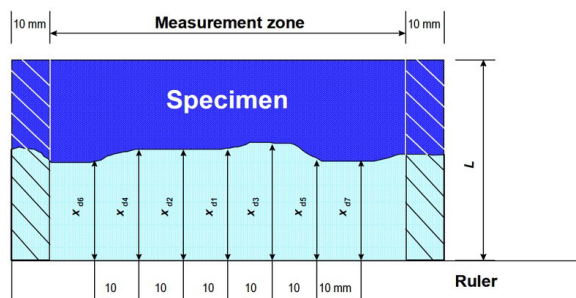


Figure 3. Illustration of the chloride penetration depth measurements [37].

The average chloride penetration depth x_d (mm) was measured and the non-steady-state migration coefficient was calculated by Equation 1.

$$D_{nssm} = \frac{0.0239 (273+T)L}{(U-2)t} \left(x_d - 0.0238 \sqrt{\frac{(273+T)Lx_d}{U-2}} \right) \tag{1}$$

Where: D_{nssm} = non-steady-state migration coefficient, $\times 10^{-12}$ m²/s; U = absolute value of the applied voltage, V; T = average value of the initial and final temperatures in the anolyte solution, °C; L= thickness of the specimen, mm; x_d = average value of the penetration depths, mm; t= test duration, hours.

According to the value of this coefficient, the concrete can be classified corresponding to its resistance to chloride penetration, based on the values (Table 5) proposed by Nilsson et al. [38].

Table 5. Classification according to resistance to chloride penetration

Diffusion coefficient ($D_{28} \times 10^{-12}$ m ² /s)	Resistance to chloride penetration
>15	Low
10-15	Moderate
5-10	High
2.5-5	Very high
<2.5	Extremely high

2.3 Rapid chloride permeability (RCP) test

Rapid chloride permeability (RCP) test according to ASTM 1202 [39] was performed at 28 days. For each mixture, three specimens (ø 10 x 5 cm) cut from cylinders (ø 10 x 20 cm) were tested.

Each specimen was placed between a 3% sodium chloride solution by mass and a 0.3 N sodium hydroxide solution. In each solution, a conductive plate was introduced and connected to a source of 60 ± 0.1 V. The test lasted 6 hours and electric current readings were taken every 30 min. The electric current multiplied by time, expressed in coulombs (C), represents the passing charge on the concrete, which indirectly indicates the resistance of concrete to chloride ions penetration, according to the classification presented in Table 6.

Table 6. Chloride Ion Penetrability Based on Charge Passed [39].

Charge passed (C)	Chloride ion penetrability
>4.000	High
2.000 – 4.000	Moderate
1.000 – 2.000	Low
100 – 1.000	Very Low
<100	Negligible

2.4 Unidirectional diffusion test

The unidirectional diffusion test, by the ponding method, was carried out in accordance with the EN 12390-11 [40]. Cylindrical specimens (ø 10 x 10 cm thick), extracted from prismatic ones, were tested.

Before starting the test, a slice 1mm-thick was used to determine the initial content of free and total chlorides. The following slices were used to determine these parameters over the specimen thickness.

Specimens, after being sealed by epoxy resin on the lateral surface, were saturated with deionized water and placed in a calcium hydroxide saturated solution for 18 hours. Then, a pond was placed to the cross surface of the specimen, sealed and filled with a 3% NaCl deionized water solution. Afterwards, the specimens were stored in a chamber (relative humidity $\geq 95\%$ vol.) to avoid loss of surface moisture. After 90 days of exposure, eight successive and parallel layers were dryly ground from the specimen, starting at the exposure surface. Then, these samples were sifted and used to determine the chloride content by potentiometric titration by using an automatic titrator from Metrohm.

The chloride concentration in each layer enables the determination of the chloride profiles, from which the diffusion coefficient (D), and the surface concentration (Cs) for each analyzed concrete were determined by fitting the solution of the Fick’s second law (Equation 2) to the experimental data.

$$C(x, t) = C_s + (C_0 - C_s) \cdot \left[\operatorname{erf} \left(\frac{x}{2\sqrt{D_{nss}t}} \right) \right] \tag{2}$$

Where: $C_{(x,t)}$ is the chloride content measured at average depth x and exposure time t , % by mass of concrete; C_s is the calculated chloride content at the exposed surface, % by mass of concrete; C_0 is the initial chloride content, % by mass of concrete; x is the depth below the exposed surface to the mid-point of the ground layer, m; D_{nss} is the non-steady-state chloride diffusion coefficient, m^2s^{-1} ; t is the exposure time, seconds.

3 RESULTS

3.1 Compressive strength

Table 7 shows the average values of compressive strength at 28 days. Concretes C2, C3, and C4 had higher compressive strength than the reference concrete (C1). Despite a binder content 30% lower than C1, C5 achieved a comparable compressive strength. On the other hand, C6 concrete, with a cement content of 150 kg/m^3 , had the lowest compressive strength.

The binder intensity (BI), the total amount of binder necessary to deliver one MPa of compressive strength [41], of the analyzed concretes were also calculated. Table 7 summarizes the BI of concretes.

Table 7. Compressive strength and binder intensity of the concretes.

Concrete	C1	C2	C3	C4	C5	C6
Binder content (kg/m^3)	332.6	313.5	288.2	286	237.5	143
Compressive strength at 28 days (MPa)	42.94	60.43	61.39	52.8	41.8	28.4
BI ($\text{kg}\cdot\text{m}^{-3}\cdot\text{MPa}^{-1}$)	7.75	5.18	4.69	5.42	5.68	5.04

This indicator was around $5\text{ kg}\cdot\text{m}^{-3}\cdot\text{MPa}^{-1}$ for concretes with low binder content and close to $8\text{ kg}\cdot\text{m}^{-3}\cdot\text{MPa}^{-1}$ for reference concrete. C3 obtained a reduction in BI of approximately 9.5% compared to C2 and 39.5% compared to C1. The C4, C5, and C6 concretes presented reductions in the binder intensity between 27% and 35% when compared to the reference C1.

Figure 4 presents the calculated binder intensity *versus* compressive strength of Brazilian concretes [41] and of those studied in this work. The greater the strength for the same binder content, the lower the BI, thus the efficiency, in terms of the use of binder is greater. Daminieli [5] claims that the lower BI values of Brazilian concretes are linked to improved aggregate packing or the combination of a low water/cement ratio and superplasticizer. The results in this study corroborate this statement.

Concretes with low binder content were characterized by BI close to the minimum values found in literature, which are slightly lower than $5\text{ kg}\cdot\text{m}^{-3}\cdot\text{MPa}^{-1}$ for concretes strength classes higher than 40 MPa. However, C1 presents value within a typical range for usual concretes. C6 has a much lower BI than other concretes of the same strength class, demonstrating its efficiency.

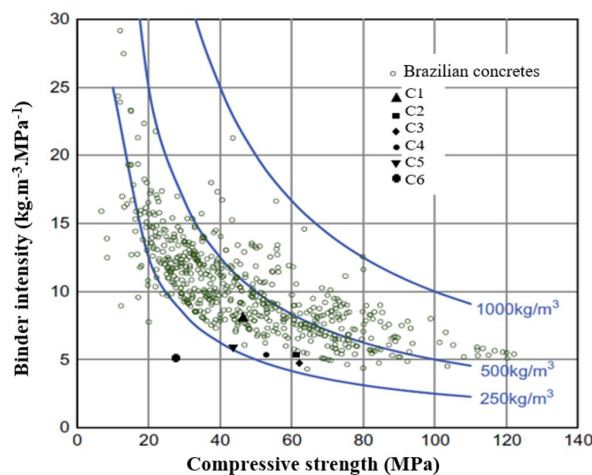


Figure 4. Binder intensity versus Compressive strength. Adapted from Daminieli et al. [41].

3.2 Sorptivity

Sorptivity or capillary water absorption, expressed in g/cm^2 , is a linear function of the square root of time (Figure 5). The capillary absorption coefficient (c) is represented by the slope of regression lines. Table 8 presents the values of ' c ' and the maximum water penetration height.

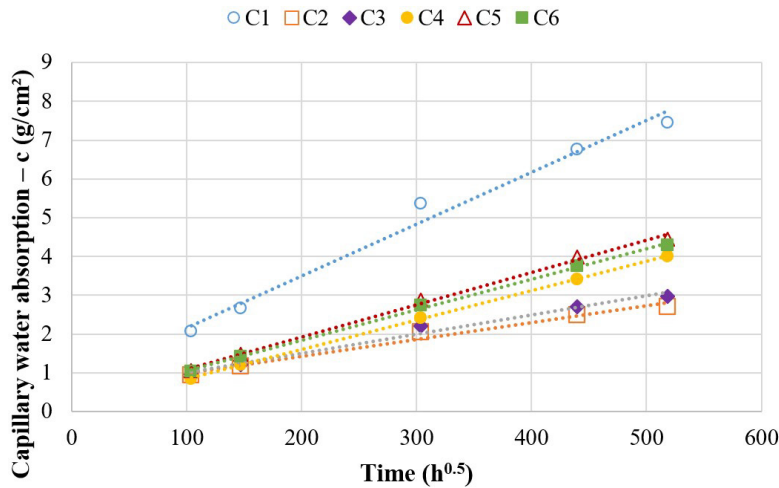


Figure 5. Capillary water absorption versus square root of time.

Table 8. Capillary absorption coefficient and maximum water penetration height.

	C1	C2	C3	C4	C5	C6
c ($\text{g}/\text{cm}^2\text{h}^{0.5}$)	0.0829	0.027	0.0308	0.0474	0.0519	0.0492
I (mm)	7.46	2.70	2.97	4.01	4.46	4.29

The higher capillary absorption coefficient of C3 compared to C2 can be explained by its porous structure, which possibly has smaller pores, favoring faster capillary absorption. This same relationship may explain the higher coefficient of C5 compared to C4 and C6. The C1 absorption coefficient was much higher than that of optimized concretes, even though they probably have smaller pores. This is due to its void volume, which is much higher, and yet, it certainly has greater pores interconnectivity. It is also noteworthy that C6, even with lower mechanical strength than the reference concrete, had a lower absorption coefficient than C1 concrete.

3.3 Rapid Chloride Migration (RCM) test

Table 9 presents the values non-steady-state migration coefficient of concretes and the classification of resistance to chloride penetration according to Nilsson et al. [38].

C1 had a penetration depth of 30.2 mm, while C2 had a penetration depth of 15.3 mm and C3 of 7.3 mm (Table 9), which indicates a significantly higher resistance to chloride penetration of optimized concretes.

Table 9. Concretes non-steady-state migration coefficient

Concrete	Average penetration depth (mm)	D_{nssm} ($\times 10^{-12}$ m^2/s)	Resistance to chloride penetration
C1	30.2	21.76	Low
C2	15.3	5.19	High
C3	7.3	1.81	Extremely high

C1 obtained low resistance to chloride penetration, even meeting the parameters from compressive strength, cement consumption, and water/binder established by standards. C2 and C3 showed a better performance. This is an indicator of the concrete porosity reduction probably due to the particle packing optimization, the paste volume reduction, the correct

dispersion of powders, and the contribution of silica fume. Furthermore, silica fume is efficient in reducing the interfacial transition zone (ITZ) thickness [42], which contributes to reduce chloride transport into concrete [43]. The amount of cement at C3 was 11% lower than C2. For this level of reduction, the small paste volume reduction, the porosity reduction due to the action of silica fume and the filler seems to compensate the possible decrease in binding capacity due to the decrease at Al_2O_3 content in concrete. The compressive strength results corroborate the above statement.

Lollini et al. [32], Müller et al. [9], and Palm et al. [33] assessed the transport of chlorides by the same migration test analyzing Portland cement concretes where binder was partially replaced by limestone filler. Figure 6 illustrates the migration coefficient as a function of the Portland cement content for the above-mentioned studies and the results of this research. From this Figure, it is possible to observe that the migration coefficient, in general, tends to decrease with Portland cement content. However, there are some points that do not follow this relationship and present an opposite behaviour. In general, the increase of cement content leads to more aluminates available to bind chlorides. In the specific case of Müller results, the opposite behaviour is related to the decrease of the water to binder ratio as cement content decreased. In this case, there seems to be a prevalence of this last effect.

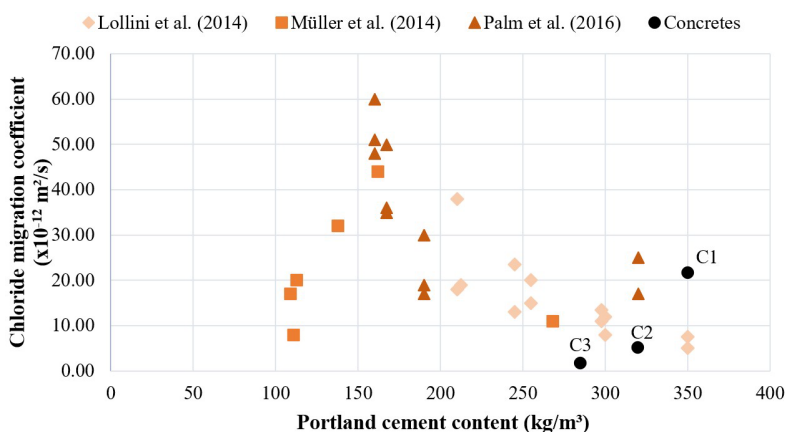


Figure 6. Chloride migration coefficient versus Portland cement content

The direct relationship between the chloride migration coefficient and the water/binder ratio (Figure 7) shows the effect of material porosity on the migration coefficient. In other words, porosity, and tortuosity of pores, obtained by particle packing optimization, seem to be more important than the amount of Portland cement. According to Ribeiro et al. [44] higher cement levels for concretes without additions and with the same characteristics (w/c, type of cement and mortar content) should favor an increase in durability (less diffusivity), as a result of the increase in the aluminate content in the mixture, originated from the Portland cement. However, this effect is less significant than the change of more representative parameters, mainly the water/binder ratio.

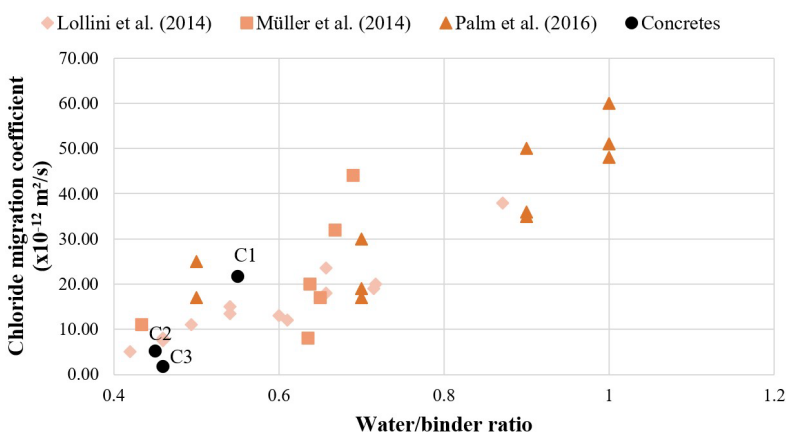


Figure 7. Chloride migration coefficient versus water/binder ratio.

3.4 Rapid chloride permeability (RCP) test

The values of passed charge and the classification for chloride penetration according to ASTM 1202 [39] are presented in Table 10. C4, C5, and C6, which were those submitted to this test, presented an increase in the charge passed as the replacement ratio increases. However, all of them met the moderate condition of resistance to chloride penetration.

Table 10. Results of charge passed and chloride ion penetrability

Concrete	Charge passed (C)	Chloride ion penetrability
C4	2235.00	Moderate
C5	2906.76	Moderate
C6	3534.27	Moderate

Figure 8 illustrates the values of the charge passed as a function of the concrete binder content. The dotted lines represent the limit for the charge passed values to classified chloride penetration resistance according to ASTM 1202 [39]. The values found in the literature refer to concretes without mineral addition subjected to the same test conditions as the concretes studied in this research. The Portland cement content in these concretes ranged from 260 kg/m³ to 550 kg/m³. The concretes that showed low penetration to chlorides had a water/cement ratio ranging from 0.28 to 0.38 [45]–[47]. Despite having parameters close to these, concretes with a water/cement ratio of 0.35 to 0.40 and cement content of 450 kg/m³ [48] to 500 kg/m³ [49] presented moderate chloride penetration resistance. Concretes studied by Das et al. [50], with cement contents from 300 kg/m³ to 360 kg/m³ and water/cement ratio from 0.4 to 0.55 were within this same class.

In this research, concretes with low cement contents had a similar or better performance than concretes with higher cement contents. For instance, the concrete C6, which had 70% of the fines constituted by limestone filler, presented a charge passed value comparable to that of concrete with a cement content of 300 kg/m³. Based on this test, although the reduction of cement content led to an increase in the total passed charge, this increase was not enough to change the level of chloride ion penetrability according to ASTM 1202 [39] classification. From a practical point of view and considering only this test, the mixture optimization including cement replacements up to 70% by lime filler was not enough to significantly compromise the performance of concretes, remaining them at the same level of chloride ion penetrability.

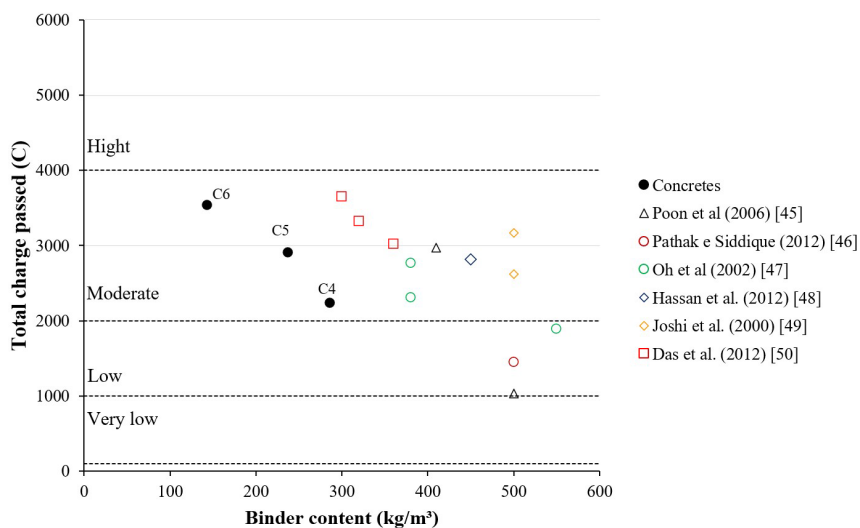


Figure 8. Charge passed versus binder content

3.5 Unidirectional chloride diffusion test

The chloride diffusion test was performed on concretes C4, C5, and C6. The chloride concentration profiles were used (Figure 9) to determine the diffusion coefficients (D) and the surface concentrations (C_s) applying the solution of the 2nd Law of Fick (Table 11). Variations in chloride concentration are expected and are related to the difference in the amount of aggregates present in each sample layer.

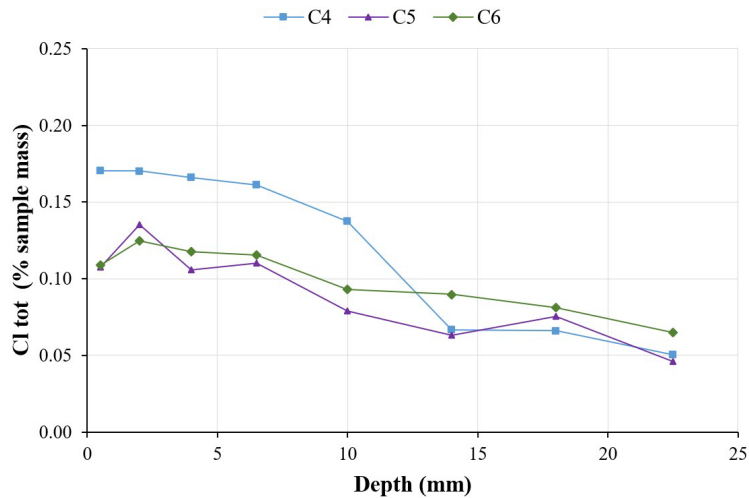


Figure 9. Chloride content as function of the depth from the exposed surface.

Table 11. Concrete transport parameters

Concrete	Non-steady-state chloride diffusion coefficient ($\times 10^{-8} \text{ cm}^2/\text{s}$)	Cl Surface concentration (%sample mass)	Cl Total concentration (%sample mass)
C4	10.44	0.1891	0.1125
C5	10.77	0.1272	0.0844
C6	35.51	0.1248	0.0959

The concrete C4 had the lowest apparent diffusion coefficient. In other words, the chlorides transport into its interior is slower than in the others. However, the surface concentration, which represents the availability of ions to penetrate the concrete and the average total concentration of chlorides, was higher in this concrete. This is probably a result of the better chloride binding due to its higher cement content. The apparent diffusion coefficient of C5 was slightly higher than that of C4. C5 has 17% less cement content than C4, which seems to be compensated by a performance filler that changes the pores network structure. Whereas the C6, which has 50% lower cement content than C4, had a much higher coefficient. This result indicates that, in this case, the contributions of performance filler is not enough to compensate the reduction on aluminate content in the mixture, due to the lower Portland cement volume in the mixture.

Figure 10 shows results of the diffusion coefficient as a function of the cement content; experimental data were plotted together with literature data [51]–[53] related to concretes tested under the same conditions.

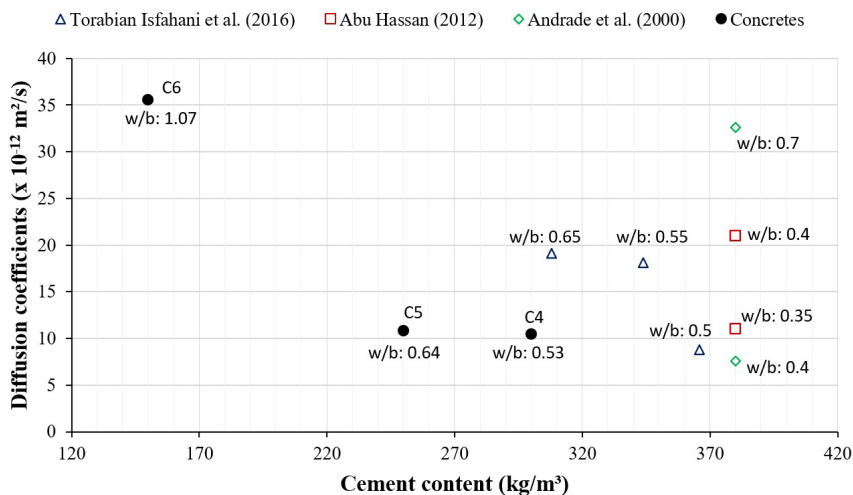


Figure 10. Diffusion coefficients – experimental and literature results; labels represent the water/cement ratio.

The results showed that the C4 and C5 presented a chloride diffusion coefficient close to the minimum obtained by Abu Hassan [52] which was $11 \times 10^{-12} \text{ m}^2/\text{s}$, and slightly higher than the minimum obtained by Torabian Isfahani et al. [51], $8.8 \times 10^{-12} \text{ m}^2/\text{s}$, and Andrade et al. [53], $7.6 \times 10^{-12} \text{ m}^2/\text{s}$. The C6 had the highest coefficient value. It is noteworthy that this was close to that obtained by Andrade *et al.* [53], with was $32.6 \times 10^{-12} \text{ m}^2/\text{s}$, for concrete with a cement content of 380 kg/m^3 and factor $w/c = 0.7$.

It's known that the aluminate content in the mixture and the porosity of concrete are fundamental parameters in the control of chloride diffusion [44], [54]. Comparing the results of the optimized concretes with those from literature, the results show that the lower chloride binding capacity can be compensated using particle packing optimization to change the concrete pores network structure in concrete with low cement content until certain levels. Thus, it is possible to point out that the optimized concretes were able to meet the usually required durability properties with lower cement content.

Comparing RCP and Dns results, although it is possible to see increasing tendencies of passed charge and Dns with reducing cement content, there are differences respect to each test that impact in each data set behaviour. RCP is a fast test and conceals the Joule effect, which makes more difficult to bind more chlorides in cement paste phase. On the other hand, natural diffusion test, that is a longer test, contributes to make more evident the binding differences among C4, C5 and C6.

4 CONCLUSIONS

The Binder Intensity showed that low cement content concretes, which were proportioned to improve particles' packing and paste volume optimization, perform better than the conventionally proportioned concrete from a mechanical point of view, reaching values close to the minimum found in literature ($5 \text{ kg.m}^{-3}.\text{MPa}^{-1}$).

The sorptivity test proves the modification of the microstructure, i.e., pores network, due to the particle packing optimization. The reference concrete, C1, showed higher water absorption by capillary action, indicating its higher porosity and probably less durability when exposed to aggressive agents.

The rapid chloride migration test verified that on one side the reference concrete obtained low resistance to chloride penetration, still meeting the standard requirements. On the other hand, C2 and C3 concretes showed higher resistance to chloride migration.

The rapid chloride permeability test and the unidirectional chloride diffusion test showed that C4, C5, and C6 had a performance that can be classified at a similar level of most conventional concretes found in literature.

As it can be seen from the results, the particle packing optimization and the reduction of water volume in the concrete mixture using a superplasticizer allows reducing the Portland cement content without compromising the chloride resistance. These optimized concretes may possess acceptable durability when they are subjected to aggressive exposure conditions, however research and experimental data on this field are still needed.

ACKNOWLEDGMENT

This research is part of the CEMtec project, National Institute on Advanced Eco-Efficient Cement-Based Technologies, supported by the National Council for Scientific and Technological Development - CNPq (Process 485340/2013-5) and by São Paulo Research Foundation - FAPESP (Process 14/50948- 3 INCT/2014). Authors also thank the Laboratory of Microstructure and Eco-efficiency (LME) of Construction Materials at USP, the Construction Materials and Waste Research Group (GMAT) at the IFPB, and the Materials and Structures Testing Laboratory (LABEME) for the technical support provided.

REFERENCES

- [1] S. A. Miller, V. M. John, S. A. Pacca, and A. Horvath, "Carbon dioxide reduction potential in the global cement industry by 2050," *Cement Concr. Res.*, vol. 114, pp. 115–124, Dec 2018, <http://dx.doi.org/10.1016/j.cemconres.2017.08.026>.
- [2] International Energy Agency. "Cement", IEA. <https://www.iea.org/reports/cement> (accessed Mar. 24, 2020).
- [3] International Energy Agency. "Technology roadmap low-carbon transition in the cement industry", IEA. <https://www.iea.org/reports/technology-roadmap-low-carbon-transition-in-the-cement-industry> (accessed Mar. 24, 2018).
- [4] A. Hasanbeigi, L. Price, and E. Lin, "Emerging energy-efficiency and CO2 emission-reduction technologies for cement and concrete production: A technical review," *Renew. Sustain. Energy Rev.*, vol. 16, no. 8, pp. 6220–6238, Oct 2012, <http://dx.doi.org/10.1016/j.rser.2012.07.019>.
- [5] B. L. Daminieli, "Conceitos para formulação de concretos com baixo consumo de ligantes: controle reológico, empacotamento e dispersão de partículas", Ph.D. dissertation, Poli Univ. São Paulo, São Paulo, Brasil, 2013.

- [6] V. Oliveira, B. Damineli, V. Agopyan, and V. John, "Estratégias para a minimização da emissão de CO₂ de concretos," *Ambient. Constr.*, vol. 14, no. 4, pp. 167–181, Oct 2014.
- [7] V. M. John, B. L. Damineli, M. Quattrone, and R. G. Pileggi, "Fillers in cementitious materials — Experience, recent advances and future potential," *Cement Concr. Res.*, vol. 114, pp. 65–78, Dec 2018, <http://dx.doi.org/10.1016/j.cemconres.2017.09.013>.
- [8] T. Proske, S. Hainer, M. Rezvani, and C.-A. Graubner, "Eco-friendly concretes with reduced water and cement content – Mix design principles and application in practice," *Constr. Build. Mater.*, vol. 67, pp. 413–421, Sep 2014, <http://dx.doi.org/10.1016/j.conbuildmat.2013.12.066>.
- [9] H. S. Müller, R. Breiner, J. S. Moffatt, and M. Haist, "Design and properties of sustainable concrete," *Procedia Eng.*, vol. 95, pp. 290–304, 2014, <http://dx.doi.org/10.1016/j.proeng.2014.12.189>.
- [10] B. L. Damineli, V. M. John, B. Lagerblad, and R. G. Pileggi, "Viscosity prediction of cement-filler suspensions using interference model: A route for binder efficiency enhancement," *Cement Concr. Res.*, vol. 84, pp. 8–19, Jun 2016, <http://dx.doi.org/10.1016/j.cemconres.2016.02.012>.
- [11] A. L. de Castro and V. C. Pandolfelli, "Revisão: conceitos de dispersão e empacotamento de partículas para a produção de concretos especiais aplicados na construção civil," *Cerâmica*, vol. 55, no. 333, pp. 18–32, Mar 2009, <http://dx.doi.org/10.1590/S0366-69132009000100003>.
- [12] Y. Knop and A. Peled, "Setting behavior of blended cement with limestone: influence of particle size and content," *Mater. Struct.*, vol. 49, no. 1–2, pp. 439–452, Jan 2016, <http://dx.doi.org/10.1617/s11527-014-0509-y>.
- [13] L. G. Li and A. K. H. Kwan, "Effects of superplasticizer type on packing density, water film thickness and flowability of cementitious paste," *Constr. Build. Mater.*, vol. 86, pp. 113–119, Jul 2015, <http://dx.doi.org/10.1016/j.conbuildmat.2015.03.104>.
- [14] M. T. de Grazia, L. F. M. Sanchez, R. C. O. Romano, and R. G. Pileggi, "Investigation of the use of continuous particle packing models (PPMs) on the fresh and hardened properties of low-cement concrete (LCC) systems," *Constr. Build. Mater.*, vol. 195, pp. 524–536, Jan 2019, <http://dx.doi.org/10.1016/j.conbuildmat.2018.11.051>.
- [15] M. S. Rebmann, "Durabilidade de concretos estruturais com baixo consumo de cimento Portland e alta resistência", M.S. thesis, EESC Univ. São Paulo, São Carlos, Brasil, 2011.
- [16] F. de Larrard, "A method for proportioning high-strength concrete mixtures," *Cem. Concr. Aggreg.*, vol. 12, no. 1, pp. 47, 1990, <http://dx.doi.org/10.1520/CCA10388J>.
- [17] B. Esmaeilhanian, K. H. Khayat, and O. H. Wallevik, "Mix design approach for low-powder self-consolidating concrete: Eco-SCC—content optimization and performance," *Mater. Struct.*, vol. 50, no. 2, Apr 2017, <http://dx.doi.org/10.1617/s11527-017-0993-y>.
- [18] P. C. C. Gomes and A. R. Barros, *Métodos de dosagem de concreto autoadensável*. São Paulo, Brasil: Pini, 2009.
- [19] V. O'Reilly Díaz, *Método de dosagem de concreto de elevado desempenho*. São Paulo, Brasil: Pini, 1998.
- [20] K. Sobolev and A. Amirjanov, "The development of a simulation model of the dense packing of large particulate assemblies," *Powder Technol.*, vol. 141, no. 1–2, pp. 155–160, Mar 2004, <http://dx.doi.org/10.1016/j.powtec.2004.02.013>.
- [21] G. R. Meira, "Agressividade por cloretos em zona de atmosfera marinha frente ao problema da corrosão em estruturas de concreto armado", Ph.D. dissertation, UFSC, Florianópolis, Brasil, 2004.
- [22] A. Costa and J. Appleton, "Análise da penetração de cloretos em estruturas de betão armado expostas ao ambiente marítimo," *Rev. Port. Eng. Estrut.*, vol. 46, pp. 12–19, 1999.
- [23] Associação Brasileira de Normas Técnicas, *Concreto de cimento Portland - preparo, controle e recebimento - Procedimento*, ABNT NBR 12655, 2015.
- [24] America Concrete Institute Committee, *Building Code Requirements for Structural Concrete and Commentary*, ACI 318-11, Detroit, USA, 2002.
- [25] Indian Standard, *Plain and Reinforced concrete - Code of Practice*, IS-456, 2000.
- [26] Norma Portuguesa, *Betão: Especificação, desempenho, produção e conformidade*, NP EN 206-1, 2007.
- [27] British Standards Institution, *Concrete - Complementary British standard to BS EN 206-1 - Part 1: Method of specifying and guidance for the specifier*, BS 8500-1, 2006.
- [28] Australian Standard, *Concrete Structures*, AS 3600, 2001.
- [29] G. C. Isaia and A. L. G. Gastaldini, "Concrete sustainability with very high amount of fly ash and slag," *Rev. IBRACON Estrut. Mater.*, vol. 2, pp. 244–253, 2009.
- [30] R. Wassermann, A. Katz, and A. Bentur, "Minimum cement content requirements: a must or a myth," *Mater. Struct.*, vol. 42, no. 7, pp. 973–982, Aug 2009, <http://dx.doi.org/10.1617/s11527-008-9436-0>.
- [31] T. R. Naik, D. N. Singh, and M. M. Hossain, "Permeability of high-strength concrete containing low cement factor," *J. Energy Eng.*, vol. 122, no. 1, pp. 21–39, 1996.
- [32] F. Lollini, E. Redaelli, and L. Bertolini, "Effects of portland cement replacement with limestone on the properties of hardened concrete," *Cement Concr. Compos.*, vol. 46, pp. 32–40, Feb 2014, <http://dx.doi.org/10.1016/j.cemconcomp.2013.10.016>.

- [33] S. Palm, T. Proske, M. Rezvani, S. Hainer, C. Müller, and C.-A. Graubner, "Cements with a high limestone content – Mechanical properties, durability and ecological characteristics of the concrete," *Constr. Build. Mater.*, vol. 119, pp. 308–318, Aug 2016, <http://dx.doi.org/10.1016/j.conbuildmat.2016.05.009>.
- [34] Associação Brasileira de Normas Técnicas, *Concreto – Procedimento para moldagem e cura de corpos de prova*, ABNT NBR 5738, 2015..
- [35] Associação Brasileira de Normas Técnicas, *Concreto – Ensaio de compressão de corpos de prova cilíndricos*, NBR 5739, 2018.
- [36] Associação Brasileira de Normas Técnicas, *Argamassa e concreto endurecidos – determinação da absorção de água por capilaridade*, ABNT NBR 9779, 2012.
- [37] Nordtest Method, *Concrete, mortar and cement-based repair materials: Chloride migration coefficient from non-steady-state migration experiments*, NT BUILD 492, 1999.
- [38] L. Nilsson, M. H. Ngo, and O. E. Gjorv, "High-performance repair materials for concrete structure in the port of Gothenburg", in *Concrete under severe conditions 2: Environment and loading: Proceedings of the Second International Conference on Concrete Under Severe Conditions*, vol. 2, 1998, p. 1193–1198.
- [39] ASTM Committee, *Standard test method for electrical indication of concrete's ability to resist chloride ion penetration*, ASTM 1202, 2012.
- [40] European Committee for Standardization, *Determination of the chloride resistance of concrete, unidirectional diffusion*, EN 12390-11, 2015.
- [41] B. L. Daminieli, F. M. Kemeid, P. S. Aguiar, and V. M. John, "Measuring the eco-efficiency of cement use," *Cement Concr. Compos.*, vol. 32, no. 8, pp. 555–562, Sep 2010, <http://dx.doi.org/10.1016/j.cemconcomp.2010.07.009>.
- [42] V. Nežerka, P. Bílý, V. Hrbek, and J. Fládr, "Impact of silica fume, fly ash, and metakaolin on the thickness and strength of the ITZ in concrete," *Cement Concr. Compos.*, vol. 103, pp. 252–262, Oct 2019, <http://dx.doi.org/10.1016/j.cemconcomp.2019.05.012>.
- [43] S. Gao, J. Guo, Y. Gong, S. Ban, and A. Liu, "Study on the penetration and diffusion of chloride ions in interface transition zone of recycled concrete prepared by modified recycled coarse aggregates," *Case Stud. Constr. Mater.*, vol. 16, pp. e01034, Jun 2022, <http://dx.doi.org/10.1016/j.cscm.2022.e01034>.
- [44] D. V. Ribeiro et al., "Effects of binders characteristics and concrete dosing parameters on the chloride diffusion coefficient," *Cement Concr. Compos.*, vol. 122, pp. 104114, Sep 2021, <http://dx.doi.org/10.1016/j.cemconcomp.2021.104114>.
- [45] B. H. Oh, S. W. Cha, B. S. Jang, and S. Y. Jang, "Development of high-performance concrete having high resistance to chloride penetration," *Nucl. Eng. Des.*, vol. 212, no. 1–3, pp. 221–231, Mar 2002, [http://dx.doi.org/10.1016/S0029-5493\(01\)00484-8](http://dx.doi.org/10.1016/S0029-5493(01)00484-8).
- [46] N. Pathak and R. Siddique, "Properties of self-compacting-concrete containing fly ash subjected to elevated temperatures," *Constr. Build. Mater.*, vol. 30, pp. 274–280, May 2012, <http://dx.doi.org/10.1016/j.conbuildmat.2011.11.010>.
- [47] C. S. Poon, S. C. Kou, and L. Lam, "Compressive strength, chloride diffusivity and pore structure of high performance metakaolin and silica fume concrete," *Constr. Build. Mater.*, vol. 20, no. 10, pp. 858–865, Dec 2006, <http://dx.doi.org/10.1016/j.conbuildmat.2005.07.001>.
- [48] A. A. A. Hassan, M. Lachemi, and K. M. A. Hossain, "Effect of metakaolin and silica fume on the durability of self-consolidating concrete," *Cement Concr. Compos.*, vol. 34, no. 6, pp. 801–807, Jul 2012, <http://dx.doi.org/10.1016/j.cemconcomp.2012.02.013>.
- [49] R. Joshi, S. Chatterji, G. Achari, and P. Mackie, "Reexamination of ASTM C 1202—Standard test method for electrical indication of concrete's ability to resist chloride ion penetration," *J. Test. Eval.*, vol. 28, no. 1, pp. 59, 2000, <http://dx.doi.org/10.1520/JTE12075J>.
- [50] B. B. Das, D. N. Singh, and S. P. Pandey, "Rapid chloride ion permeability of OPC- and PPC-based carbonated concrete," *J. Mater. Civ. Eng.*, vol. 24, no. 5, pp. 606–611, May 2012, [http://dx.doi.org/10.1061/\(ASCE\)MT.1943-5533.0000415](http://dx.doi.org/10.1061/(ASCE)MT.1943-5533.0000415).
- [51] F. Torabian Isfahani, E. Redaelli, F. Lollini, W. Li, and L. Bertolini, "Effects of nanosilica on compressive strength and durability properties of concrete with different water to binder ratios," *Adv. Mater. Sci. Eng.*, vol. 2016, pp. 1–16, 2016., <http://dx.doi.org/10.1155/2016/8453567>.
- [52] Z. F. Abu Hassan, "Rapid assessment of the potential chloride resistance of structural concrete", Ph.D. dissertation, Univ. Dundee, Dundee, United Kingdom, 2012. [Online]. Available: <https://discovery.dundee.ac.uk/en/studentTheses/rapid-assessment-of-the-potential-chloride-resistance-of-structur>
- [53] C. Andrade, M. Castellote, C. Alonso, and C. González, "Non-steady-state chloride diffusion coefficients obtained from migration and natural diffusion tests. Part I: Comparison between several methods of calculation," *Mater. Struct.*, vol. 33, no. 1, pp. 21–28, Jan 2000, <http://dx.doi.org/10.1007/BF02481692>.
- [54] R. Malheiro, G. Meira, M. Lima, and N. Perazzo, "Influence of mortar rendering on chloride penetration into concrete structures," *Cement Concr. Compos.*, vol. 33, no. 2, pp. 233–239, Feb 2011, <http://dx.doi.org/10.1016/j.cemconcomp.2010.11.003>.

Author contributions: TGC: conceptualization, data curation, formal analysis, writing; GRM: conceptualization, supervision, methodology, formal analysis; MQ: formal analysis, writing; VMJ: funding acquisition, supervision.

Editors: Edna Possan, Mark Alexander



ORIGINAL ARTICLE

Transportation impact on CO₂ emissions of concrete: a case study in Rio Branco/Brazil

Impacto do transporte nas emissões de CO₂ do concreto: um estudo de caso em Rio Branco/Brasil

Antonia Alana Lima Pacheco^a Lidiane Santana Oliveira^a Vanderley Moacyr John^a Sérgio Cirelli Angulo^a ^aUniversidade de São Paulo – USP, Escola Politécnica, Departamento de Engenharia de Construção Civil, São Paulo, SP, Brasil

Received 23 March 2022

Accepted 17 October 2022

Abstract: Due to the scarcity of crystalline massifs in the north of Brazil, concrete producers have been using crushed stone and cement from suppliers located hundreds of kilometers away. In this case, CO₂ emissions related to material transportation for concrete production may become significant. Thus, this study aims to analyze the influence of the transportation of the materials in CO₂ emissions of ready-mix concrete production in Rio Branco (Acre). Concrete compositions were obtained from a local concrete producer. Brazilian methods of dosage were not applicable due to the high fineness of the regional sand available; the mix designs were adjusted empirically. Two types of cement (CP V-ARI and CP IV) were considered to create the studied scenarios. Transportation distances of the raw materials (cement and aggregates) ranged from 20 km (local sand supplier) to 3,592 km (cement supplier from Sete Lagoas, MG). CO₂ emissions to produce concrete (f_{ck} of 25 MPa, cement consumption of 426 kg/m³) ranged from 208 kgCO₂/m³ to 573 kgCO₂/m³. Transportation was responsible for up to 20% of total emissions. The emissions in this study are considerably higher than the national data of concrete production available in the Construction Environmental Performance Information System (Sidac) due to the higher cement consumption and higher transportation distances. Although cement consumption in Acre represents less than 1% of Brazilian consumption, the results reveal the impact of transportation distances in CO₂ emissions of concrete in cities that deal with local scarcity.

Keywords: concrete, CO₂ emission, transportation, construction materials.

Resumo: Devido à escassez de maciços cristalinos no norte do Brasil, produtores de concreto têm usado pedra britada e cimento de fornecedores localizados a centenas de quilômetros. Nesse caso, as emissões de CO₂ relacionadas ao transporte de materiais na produção de concreto podem ser significativas. Assim, este estudo tem como objetivo analisar a influência do transporte dos materiais nas emissões de CO₂ da produção de concreto usinado em Rio Branco (Acre). As composições de concreto foram obtidas de um produtor de concreto local. Os métodos brasileiros de dosagem não foram aplicáveis devido à alta finura da areia regional disponível; os traços foram ajustados empiricamente. Dois tipos de cimento (CP V-ARI e CP IV) foram considerados para criar os cenários estudados. As distâncias de transporte das matérias-primas (cimento e agregados) variaram de 20 km (fornecedor local de areia) a 3.592 km (fornecedor de cimento de Sete Lagoas, MG). As emissões de CO₂ para a produção de concreto (f_{ck} de 25 MPa, consumo de cimento de 426 kg/m³) variaram de 208 kgCO₂/m³ a 573 kgCO₂/m³. O transporte foi responsável por até 20% do total de emissões. As emissões neste estudo são consideravelmente maiores do que os dados nacional de produção de concreto disponíveis no Sistema de Informação do Desempenho Ambiental da Construção (Sidac) devido ao maior consumo de cimento e maiores distâncias de transporte. Embora o consumo de cimento no Acre represente menos de 1% do consumo

Corresponding author: Antonia Alana Lima Pacheco. E-mail: alanapacheco@usp.br

Financial support: CNPq grant number 140054/2020-0 and CAPES grant number 88887.463874/2019-00.

Conflict of interest: Nothing to declare.

Data Availability: The data that support the findings of this study are available from the corresponding author, A. A. L. Pacheco, upon reasonable request.



This is an Open Access article distributed under the terms of the Creative Commons Attribution License, which permits unrestricted use, distribution, and reproduction in any medium, provided the original work is properly cited.

brasileiro, os resultados revelam o impacto das distâncias de transporte nas emissões de CO₂ do concreto em cidades que lidam com a escassez local.

Palavras-chave: concreto, emissão de CO₂, transporte, materiais de construção.

How to cite: A. A. L. Pacheco, L. S. Oliveira, V. M. John, and S. C. Angulo, “Transportation impact on CO₂ emissions of concrete: a case study in Rio Branco/Brazil”, *Rev. IBRACON Estrut. Mater.*, vol. 15, no. 6, e15609, 2022, <https://doi.org/10.1590/S1983-41952022000600009>

1 INTRODUCTION

The growing need of concrete for habitation and urban infrastructure leads to increasing consumption of minerals for construction [1]. This happens in great part because concrete, the most consumed construction material in the world, has approximately 75% of its volume composed of aggregates [2], [3]. In the last decades, BRIC countries (Brazil, Russia, India and China) were responsible for the extraction of one third of global resources, which includes Brazil [4]. In Brazil, more than 600 million of tons of minerals have been consumed in 2016 [5], and around 50% of it was used for concrete [6], [7].

The fabrication of Portland cement also depends on the extraction of minerals as limestone (in which part of it is converted in CO₂ during production [8]) and clay, its main raw materials. Although the cement consumption decreased in the country from 2015 to 2018, consequence of the economic crisis, since 2019 it has been observed the increasing in its consumption [9] as in many other BRIC countries. The same is happening in the northern region of Brazil, which has population growth above the national average and a growing need for infrastructure in transportation, sanitation and housing for the population [9], [10].

Although the minerals used in civil construction are considered abundant in nature [11], [12], in many regions of Brazil or abroad [13], [14] these resources are far away. Areas located in sedimentary basins generally do not have hard rocks for crushing. In the northern region of Brazil, states such as Amapá, Roraima and Amazonas have rare crystalline massifs, depending on alternative materials and long-distance transportation [15], [16]. As an example, in the city of Manaus (state of Amazonas, AM) gravel is frequently used as a substitute material for crushed stone [17]. Also, in the Southern and Southeast regions, many cities located in the Paraná sedimentary basin require the transportation of coarse aggregates over distances greater than 100 km [15]. Globally, the scarcity of aggregates due to geological restrictions was also observed in the Netherlands [18], and in the central region of United States [19].

The state of Acre stands out in this scenario due to the absence of mineral deposits (Figure 1). The construction industry in this state depends mainly on coarse aggregates from the state of Rondônia. This makes the price of crushed stone the highest in Brazil, up to R\$ 286.54/m³ in April of 2022 [20]. In addition, due to the lack of limestone reserves in the region, Acre does not have cement production [21] and this material needs to be transported from neighboring states over distances that can reach up to 3,500 km.

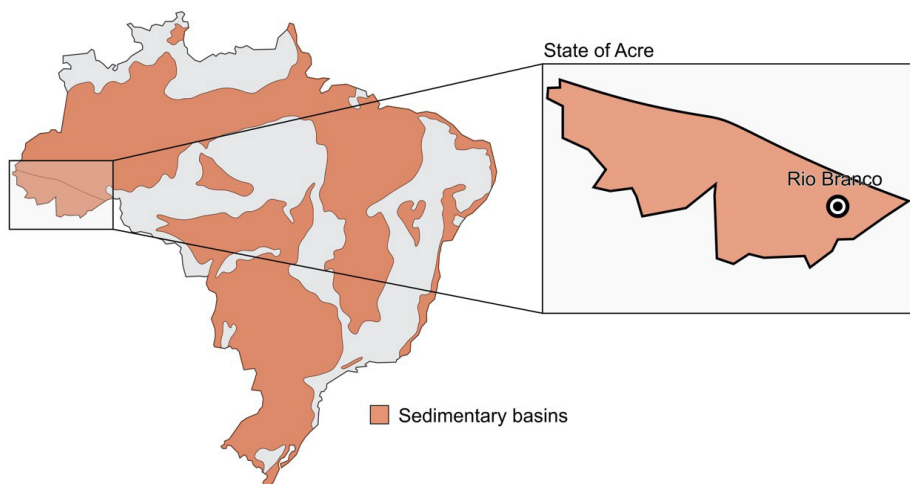


Figure 1. Map of Brazil identifying the sedimentary basins and the State of Acre.

Cement production is the main responsible for environmental impacts of concrete, especially in CO₂ emissions from limestone decarbonation and energy consumption [22]. According to the Global Cement and Concrete Association [23], [24], the average cement emission in 2019 was 564 kg CO₂/t in Brazil and 635 kg CO₂/t in the world. The emission due to the transportation of concrete materials differs depending on the region and the means of transportation [8], being generally adopted as less than 5% of the total emissions. However, most studies consider distances of aggregates transportation between 20 and 400 km and cement transportation between 100 and 900 km [25], [26], values much lower than those found in the northern region of Brazil.

Based on this context, the objective of this work is to quantitatively analyze the impact of the material transportation stage on the CO₂ emission of the ready-mix concrete produced in the city of Rio Branco, state of Acre, in Brazil. The results were compared to the national data of concrete production available in the Construction Environmental Performance Information System (Sidac), a platform for the assessment and calculation of environmental performance indexes of Brazilian construction products.

2 METHODOLOGY

The methodology used in this work is based on the Life Cycle Assessment (LCA) framework, using a simplified approach that focus more on the inventory (quantity of natural resource extraction, and CO₂ footprint), similar to the methodology adopted by the Environmental Performance in Construction Assessment (ADAC is its acronym in Portuguese¹) [27]. It consists of an inventory analysis with the objective of quantifying the CO₂ emission of the production of concrete in the city of Rio Branco, with emphasis on the materials transportation impact.

The methodology for calculating the CO₂ emissions of concrete considered the material's production and transportation to Rio Branco, as shown in Figure 2. All emission factors were adopted from Sidac database, as the data is up to date. The details for the method are described in item 2.1. Thus, first, it was assessed the CO₂ emissions for cement and aggregates production and transportation to Rio Branco. Then, the CO₂ emissions of a local mix design of concrete grade C25 ($f_{ck} = 25$ MPa) was calculated from the present methodology and the results were compared to the same mix design of C25 calculated using Sidac product calculator (details in item 2.2). Finally, it was calculated the maximum and minimum CO₂ emissions of concretes C15 to C35 and the results were compared to generic ready-mix concrete (C20 to C35) products available in Sidac database.

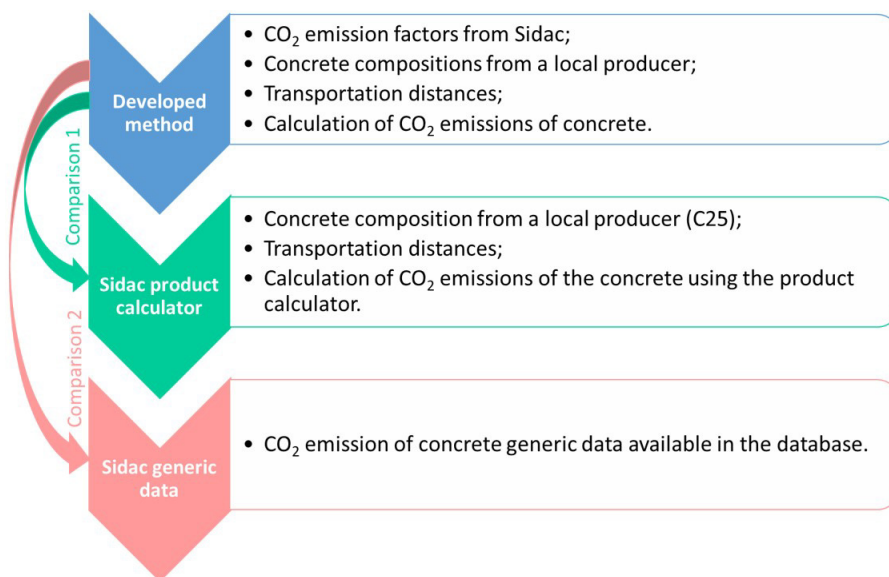


Figure 2. Flowchart of the methodology adopted in this study.

¹ Avaliação do Desempenho Ambiental da Construção.

2.1 Method to calculate CO₂ emissions of concrete

CO₂ emissions of concrete comprise the emission of the materials' production ($E_{CO_2,M}$) and their transportation to the place where concrete will be produced ($E_{CO_2,T}$), a "cradle-to-gate" framework, like it is presented by the Equation 1.

$$E_{CO_2,conc} = E_{CO_2,M} + E_{CO_2,T} \tag{1}$$

In the assessment, Rio Branco was considered the only destination of the materials, whereas their origins were defined consulting local concrete plants. The materials analyzed in transportation over long distances were cement and crushed stone, as they are constituents of concrete which are not produced in the city. The transportation distance of the sand was considered fixed (one single value) because its extraction takes place within Rio Branco, not being transported over long distances. The road modal was adopted as the only means of transportation.

2.1.1 CO₂ emission factors

CO₂ emissions from raw materials used to produce concrete are the sum of the emissions from energy consumed in the production of the materials, electricity and fuels, and the emissions originated in the process due to chemical reactions [28], when they occur.

The unitary emission of cement ($E_{CO_2,cem}$), given in kgCO₂/t_{cement}, was calculated from Equation 2.

$$E_{CO_2,cem} = \%_{clinker} \cdot EF_{clinker} + \%_{SCMs} \cdot EF_{SCMs} + E_{energy,cem} \tag{2}$$

Where: $\%_{clinker}$ is the clinker content and $EF_{clinker}$ is the emission factor from clinker production, which includes the emission from limestone decarbonation and the energy to produce clinker (fossil fuels and electricity); $\%_{SCMs}$ is the content of supplementary cementitious materials (SCMs) and EF_{SCMs} is the emission factor of SCMs, which includes the energy to produce SCMs (fossil fuels and electricity); and $E_{energy,cem}$ is the emission from electricity used in cement production during milling of clinker with SCMs.

This study limited the analysis to two types of cement with different clinker content according to the Brazilian standard, shown in Table 1. Emission factors of clinker, calcined clay and limestone fillers, such as the CO₂ emissions from energy used in cement production were adopted from Sidac data [30] and are presented in Table 2. When blast furnace slags and fly ash are used as SCMs, the emission of SCMs is considered zero.

Table 1. Cement types and their proportions according to the Brazilian standard NBR 16697 [29].

Cement ID	Cement type	Clinker content	Addition	Addition content
C1	CP V – ARI	90 – 100%	Limestone filler	0 – 10%
C2	CP IV	45 – 85%	Calcined clay	15 – 50%

Table 2. Emission factors of raw materials and energy consumed. Range (min-max) values from Sidac database [30].

CO ₂ emission source	Emission factor (kgCO ₂ /t _{material})
Clinker	845.1 – 1049
Calcined clay	144.4 – 435.6
Limestone filler	0.6 – 7.2
Sand	0 – 12.51
Crushed stone	0 – 4.67
Energy - cement	2.5 – 4.6 ²

Besides cement, the other materials composing concrete are fine and coarse aggregates, and water. The emission of the aggregates production was also collected from Sidac database [30]. CO₂ emissions from aggregates include the energy

² Calculated considering the electricity consumption of 51 kWh/t of cement ± 2 times the standard deviation of 7.3, and 0.07 kgCO₂/kWh [31].

consumed during the extraction and production process, once there is no chemical reaction like in the cement production. CO₂ emissions related to water extraction and its availability to consumption are not considered in this study.

The fuel emission factor adopted in this study was 2.29 kgCO₂/L_{diesel} from Sidac database [30], which considered the emission by direct diesel combustion and the percentage of biodiesel present in Brazilian diesel (defined as 13%). For the electricity use it was considered 0.07 kgCO₂/kWh, published by Sidac [30], which considers the Brazilian electric matrix composition.

2.1.2 Material’s consumption of concrete

According to the local ready-mix concrete producers, some of the Brazilian methods of mix design for determining the materials consumption, as ABCP method, are not applicable for the concrete of the region, which uses sand from Acre River (Rio Acre). The granulometry of sand is fine (fineness of 0.9), implying in a greater demand of water and, consequently, a greater consumption of cement in experimental dosage concrete mixes. Thus, this study considered the mix designs of a local concrete plant for different concrete grades, varying from C15 to C35. The materials were cement, sand and crushed stone (0 – 6.3 mm) as fine aggregates, crushed stone (9.5 – 19 mm) as coarse aggregate and superplasticizer admixture. The granulometries of aggregates are similar to the work of Santos [32].

Table 3 presents the material consumptions for each mix design based on the estimated f_{ck} (characteristic of compressive strength) at 28 curing days. In this work, the same materials consumption of concrete was adopted for the two different types of cement considered. It seems reasonable since the effect of granulometry of the aggregates will be the mandatory and it is constant for both cements used.

Table 3. Materials consumption for one cubic meter of concrete

Concrete grade	Estimated f_{ck} (MPa)	$C_{i,conc}$ (t/m ³)			
		Cement	Fine Sand	Crushed stone (0-6.3 mm)	Crushed stone (9.5 – 19 mm)
C15	15	0.350	0.484	0.322	1.023
C20	20	0.400	0.456	0.304	1.029
C25	25	0.426	0.438	0.294	1.026
C30	30	0.450	0.423	0.279	1.017
C35	35	0.464	0.409	0.265	1.017

2.1.3 Fuel consumption in transportation

The CO₂ emission during the materials transportation by road was determined by the fuel consumption multiplied by its emission factor. Many factors can influence the fuel consumption, such as the travel distance, vehicle efficiency, load capacity, fuel type, road conditions, driving preferences, weather, and others [33]. In this study, the fuel consumption was simplified as the traveled distance divided by the efficiency of the vehicle. Diesel was considered the only fuel type. The distances included the round trip with loaded truck in the way out and empty truck on the way back.

Minimum and maximum emission conditions were considered for vehicle efficiency, from two types of road train trucks (*bitrem*) with different diesel consumptions based on the work of Campos [34], as shown in Table 4. The information about considered load weights were obtained from concrete plant producers, adopting the maximum load weight for the minimum emission condition and the minimum load weight for the maximum emission condition. Furthermore, according to concrete producers in the region, there is no supply of bulk cement to Rio Branco.

Table 4. Load weight and efficiency of vehicles.

Emission condition	Vehicle type	Load weight, P_v (t)	Truck weight (t)	Diesel consumption factor (L _{diesel} /t.km)	Vehicle efficiency (km/L _{diesel})	
					Empty, $e_{f,e}$	Loaded, $e_{f,l}$
Minimum	Volvo FH 440 6x2	48.0	9.2	0.004	27.17	4.37
Maximum	Volvo FH 520 6x4	38.0	9.2	0.015	7.25	1.41

Table 5 presents the main cities of origin of the materials. This study considered the two types of cement presented in the previous section (C1 and C2)), each one from a different city of origin, and two cities of origin of crushed stone (B1 and B2). Road distances were collected using GoogleMaps [35], considering the shortest route simulated by the website. It was established a fixed distance for sand because its transportation takes place within Rio Branco. The cement C2 is constituted by clinker from Nobres (MT), which is transported to Porto Velho (RO) where it is mixed with calcined clay from the region, packed and distributed. Thus, the considered distance was from Nobres to Rio Branco. Figure 3 shows a map including the states of origin and destination of the materials and the transportation roads.

Table 5. Cities of origin of the materials and their distances to Rio Branco

Material	City of origin	Distance to destination (km)
Sand A	Rio Branco (AC)	20
Crushed stone B1	Porto Velho (RO)	510
Crushed stone B2	Vista Alegre do Abunã (RO)	250
Cement C1	Sete Lagoas (MG)	3,592
Cement C2	Nobres (MT) (clinker)	1,844
	Porto Velho (RO) (calcined clay)	510



Figure 3. Map of Brazil showing the states of origin and destination of the materials and the transportation roads collected using GoogleMaps (2022).

2.1.4 CO₂ emissions from transportation

Based on the methodology presented above, Equation 3 is proposed to determine the CO₂ emissions from the transportation of concrete materials ($E_{CO2,T}$), given in kgCO₂/m³ of concrete. The development of the equation is detailed in Appendix A.

$$E_{CO2,T} = EF_F \cdot \frac{e_{f,l} + e_{f,e}}{e_{f,l} e_{f,e} P_v} \sum_{i=1}^{n=3} (C_{i,conc} \cdot d_i) \tag{3}$$

Where, EF_F is the fuel emission factor (kg CO₂/L), $e_{f,e}$ is the efficiency of the empty vehicle (km/L), $e_{f,l}$ is the efficiency of the loaded vehicle (km/L), P_v is the maximum load capacity of the vehicle (t), i is the type of material (cement, sand or gravel), $C_{i,conc}$ is the consumption of material i necessary to produce 1 m³ of concrete (t/m³) and d_i is the transportation distance of the material i (km).

2.2 CO₂ emissions of concrete C25 using Sidac product calculator

The CO₂ emissions of concrete C25 were calculated using the Sidac product calculator from the data adopted in this study, i.e., type of materials, mix proportions of the local concrete C25 and transportation distances. The objective was to assess the variation in CO₂ emissions resulting from different methodologies between this study and Sidac product calculator. The main differences relied on the materials emission factors, in which Sidac uses a medium value, and the transportation method of calculation, in which it is used a single vehicle efficiency and consider the same efficiency for empty and loaded trucks.

3 RESULTS AND DISCUSSION

3.1 CO₂ emission of cement and aggregates

The results of CO₂ emission from each cement are shown in Figure 4. Cement C1 presented minimum and maximum emissions of 809 and 1,237 kgCO₂/t of cement respectively, whereas cement C2 had a lower emission range, from 478 to 1,056 kgCO₂/t. The difference between cements relies on both production and transportation stages. In the production stage, cement C1 had a greater emission range due to the higher clinker content of the CP V-ARI cement type, compared to cement C2 (CP IV), which had higher substitution of clinker for calcined clay. In Brazil, 63% of the CO₂ emissions of the cement production process, without accounting the transport, it occurs in consequence of the chemical reactions [28]. Regarding the transportation stage, the distance from the factory to Rio Branco is greater for cement C1 as well, reaching 3,592 km, thus the transportation can contribute with up to 15% of the emissions from this cement.

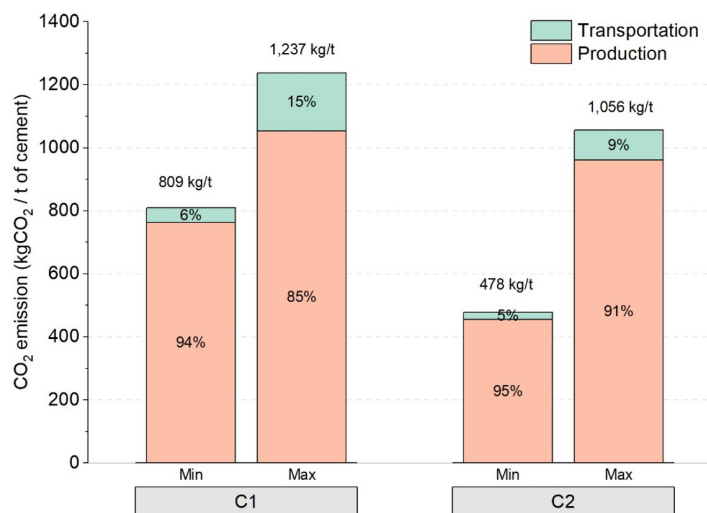


Figure 4. Minimum and maximum CO₂ emissions of cements considered in this study.

The values found in this study differ significantly from the emissions reported in the literature. In the Brazilian scenario, Lima [25] indicated a total cement emission in the range of 603 to 714 kgCO₂/t of cement. Souza [31] calculated 590 and 840 kgCO₂/t of cement for low and high emission cement, respectively, where the materials' transportation in São Paulo did not reach 1% of the total CO₂ emissions. In an international scenario the values found also differ significantly. In China, for example, a blended Portland cement emits around 543 kgCO₂/t of cement, and transportation is responsible for 2.5% of the total emission.

For the aggregates, the calculated emission ranges are displayed in Figure 5. The minimum CO₂ emission from sand was 0.25 kgCO₂/t because it was considered zero emission from production. For the maximum CO₂ emission from sand (13.5 kgCO₂/t), production was responsible for 92% of the total emission. The difference between minimum and maximum CO₂ emissions of the crushed stones (3.17 to 30.7 kgCO₂/t) consisted mostly of the transportation stage, which was responsible for 85% of the maximum value, in which the aggregate was transported for 512 km. Similar to cement, the aggregate emissions in this work were higher than other values founded in Brazilian studies, such as 2.75 kgCO₂/t obtained by Souza [31] and 23.0 kgCO₂/t calculated by Lima [25] and Marcos [36]. This is mainly due to transportation distances considered in this study, which are far above to the ones of the Southern region of Brazil.

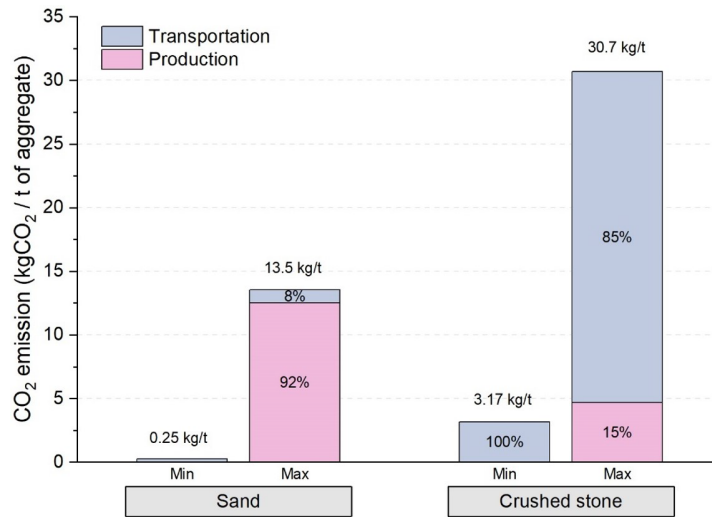


Figure 5. Minimum and maximum CO₂ emissions of aggregates.

3.2 Analysis of CO₂ emission from concrete C25

Figure 6 presents the CO₂ emissions per cubic meter of concrete for C25 concrete produced with C1 and C2 cements. Cement production was the factor that most contributed to concrete emissions, regardless the type of cement. However, in the case of concrete produced with C1, the transportation of cement and aggregates were together responsible for up to 20% of the total concrete emissions, which added up 113 kgCO₂/m³ of concrete to a maximum of 573 kgCO₂/m³. This value is far above the emission ranges of Brazilian references [37], which point to a maximum emission of approximately 350 kgCO₂/m³ of concrete for this concrete grade. The concrete produced with C2 cement showed lower emissions, in the range of 208 to 496 kg CO₂/m³ of concrete. Thus, in this study case, the value of 5% generally adopted to concrete emissions from raw materials transportation does not apply.

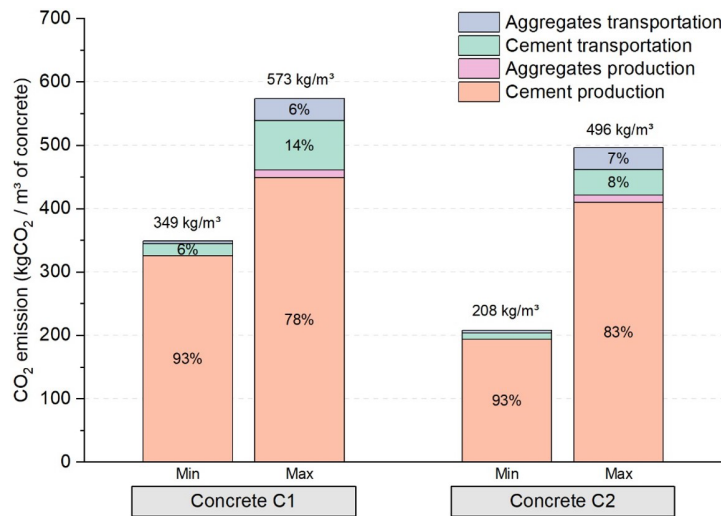


Figure 6. Minimum and maximum CO₂ emissions from C25 concrete with C1 and C2 cements.

The large variation between the minimum and maximum emissions found in Figure 6 is mainly due to the range of emissions from cement production. However, in the maximum emission conditions, the transportation stage was considerable. The parameter with the larger influence in the transport emission is the fuel consumption factor, a value that depends on the transportation distances, type of vehicle, vehicle efficiency, transported load and others [33]. For long distances, the difference in fuel consumption accentuates emissions.

Figure 7 presents the values of CO₂ emissions from the same C25 concrete but estimated from Sidac calculator tool and its database, available in its website³ [30]. It is observed that the maximum emission values of both concrete produced with cement C1 and C2 were similar to the ones calculated in this study. However, the minimum values estimated by Sidac calculator were considerably higher than from this study calculation, for both production and transportation stages. In the production stage, this happened because Sidac database considers a medium value of clinker in the composition of the cements, while in this study was consider the minimum and maximum clinker content indicated by the Brazilian standard for Portland cement, ABNT NBR 16697 [29]. In the transportation stage, Sidac database considers only one type of vehicle, differently what was considered in this study, and simplifies the calculation by adopting the same vehicle efficiency for empty or loaded trucks.

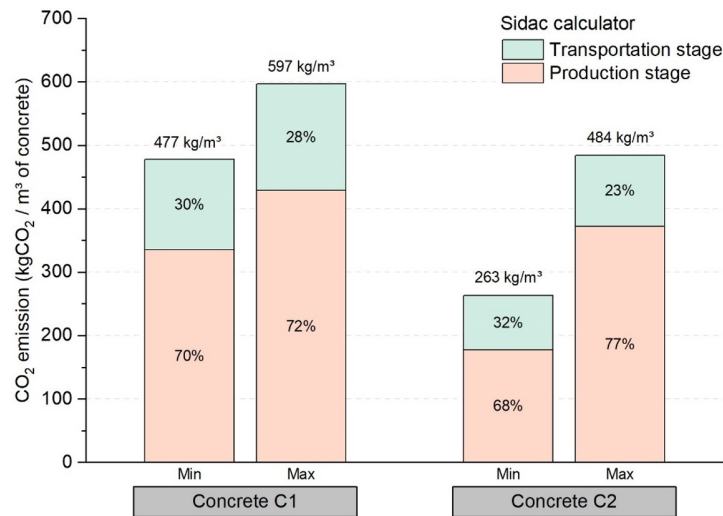


Figure 7. Minimum and maximum CO₂ emissions from C25 concrete estimated using the Sidac calculator and its database.

3.3 CO₂ emissions of different concrete strength: comparison with Sidac database

The emissions for concretes of different strength with C1 cement are calculated. There is an increase in the emissions with increasing strength (Figure 8). C15 concrete has a maximum emission of 481 kgCO₂/m³, while C35 concrete has a maximum emission of 619 kgCO₂/m³. The increase in emissions was due to increasing cement consumption. For all strength values, the transportation stage obtained similar proportions in relation to the total emission of concrete, approximately 7% for the minimum emissions and 20% for the maximum emissions of each mix.

Figure 8 also presents the CO₂ emissions of different concrete grades obtained in Sidac products, as being an average of Brazilian data. Even the concrete with the lowest strength (and the lowest consumption of cement) presented a maximum emission higher than the Brazilian Sidac estimates [37]. This difference is attributed to two main factors. First, the high cement consumption in the mix design for concretes produced in Rio Branco, since Brazilian methods of dosage were not applicable, being adjusted empirically because of the characteristics of the regional sand (fineness of 0.9) [32]. The cement consumptions of concretes C20 to C35 of Sidac products varied from 0.260 to 0.385 ton of cement per cubic meter of concrete; values much lower than those generally adopted in Rio Branco. Secondly, for the emission in the transportation of materials, a medium value of transportation distances of 564 km for cement and 80 km for crushed stone were considered by Sidac, far below than those found in this study case. Thus, it is possible to conclude that the range of CO₂ emissions from concrete calculated by Sidac Brazilian averages does not include the reality of the city of Rio Branco.

Most of the data considered to calculate the indicators of Sidac's concrete processes refer to the Southeast region of Brazil, which represents 47% of ready-mix concrete production in the country [38]. Thus, although the Sidac database has a representative sample, it does not include extreme conditions observed in specific regions of Brazil, where there is a shortage of some minerals, such as in Acre. Because the cement consumption in this state represents only 1% of the national cement consumption, the impact on national data may be insignificant. Nevertheless, the adoption of the data available in Sidac must be done with caution and analysis of data consistency must be done for specific regions and cases.

³ <https://sidac.org.br/>

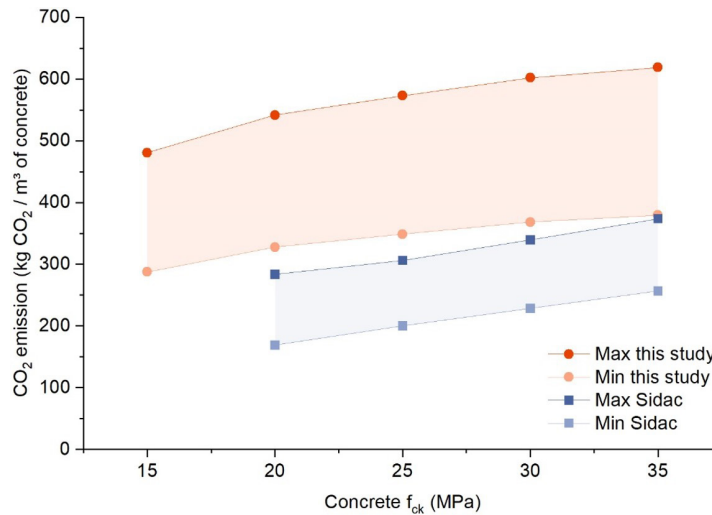


Figure 8. CO₂ emissions for concretes of different grades produced in Acre calculated using the methodology developed in the study in comparison with CO₂ emissions for similar concretes available in the Sidac database.

Thus, because of both higher cement consumption and longer transportation distances, CO₂ emissions of concrete produced in Acre are substantially higher than usual from Brazil. Comparing the results of CO₂ emissions of concrete calculated in this study with some which can be found in Brazilian literature, none are representative to Acre. Oliveira presents the maximum emission for concrete with 20 MPa as 270 kgCO₂/m³ and with 40 MPa as 392 kgCO₂/m³ [39]. Santoro and Kripka present 123 kgCO₂/m³ to concrete with 20 MPa and 168 kgCO₂/m³ to concrete with 40 MPa [40]. The use of generic data must be avoided if possible. Sidac offers cradle-to-gate emission data for different cement types and aggregates, emission factors for various transportation modals as well as a convenient calculator to make the estimative. This certainly allows a more accurate estimative considering actual formulation, transportation distances.

4 CONCLUSIONS

Considering the compositions analyzed in this study, ready-mixed concrete produced in Rio Branco has higher CO₂ emissions than concrete produced in other regions of Brazil. Cement content and transportation of materials contribute significantly to CO₂ emissions in all concrete strength. We estimate emissions of up to 573 kgCO₂/m³ of C25 concrete, where transportation was responsible for 20% of the total emissions. The CO₂ emissions will increase with concrete strength increases.

The transportation fuel consumption is the most influencing factor on the transportation emissions. This value depends on the transportation distances, type of vehicle, vehicle efficiency, transported load and others.

Therefore, Sidac's generic Brazilian data is not representative for the case of the city of Rio Branco and possible other regions with long transportation distances for aggregate or higher cement consumption associated to aggregate characteristics.

We recommend care on use generic data and always consider use other Sidac information to make accurate estimative considering actual transportation distances and cement consumption.

ACKNOWLEDGEMENTS

A. A. L. Pacheco acknowledges CNPq grant number 140054/2020-0 and L. S. Oliveira acknowledges CAPES grant number 88887.463874/2019-00. The authors would like to thank the local specialist who helped with information about the region.

REFERENCES

- [1] F. Krausmann, S. Gingrich, N. Eisenmenger, K. Erb, H. Haberl, and M. Fischer-Kowalski, "Growth in global materials use, GDP and population during the 20th century," *Ecol. Econ.*, vol. 68, pp. 2696–2705, 2009, <http://dx.doi.org/10.1016/j.ecolecon.2009.05.007>.
- [2] A. M. Neville, *Properties of Concrete*, 5th ed. Harlow, England: Pearson, 2016.

- [3] A. Miatto, H. Schandl, T. Fishman, and H. Tanikawa, "Global patterns and trends for non-metallic minerals used for construction: Global non-metallic minerals account," *J. Ind. Ecol.*, vol. 21, pp. 924–937, 2017, <http://dx.doi.org/10.1111/jiec.12471>.
- [4] R. Wu, Y. Geng, and W. Liu, "Trends of natural resource footprints in the BRIC (Brazil, Russia, India and China) countries," *J. Clean. Prod.*, vol. 142, pp. 775–782, 2017, <http://dx.doi.org/10.1016/j.jclepro.2016.03.130>.
- [5] Agência Nacional de Mineração, *Sumário Mineral 2017*. Brasília, Brasil: ANM, 2019.
- [6] D. Costa Reis, Y. Mack-Vergara, and V. M. John, "Material flow analysis and material use efficiency of Brazil's mortar and concrete supply chain," *J. Ind. Ecol.*, vol. 23, pp. 1396–1409, 2019, <http://dx.doi.org/10.1111/jiec.12929>.
- [7] D. C. Reis, "Fluxo de materiais e eficiência no uso de recursos na indústria da construção," Ph.D. dissertation, Dep. Eng. Constr. Civ., Univ. São Paulo, São Paulo, Brasil, 2020. [Online]. Available: <https://doi.org/10.11606/T.3.2020.tde-26052021-100321>
- [8] IEA CSI, "Technology roadmap: Low-carbon transition in the cement industry". <https://iea.org/reports/technology-roadmap-low-carbon-transition-in-the-cement-industry> (accessed Mar. 23, 2018).
- [9] Sindicato Nacional das Indústrias de Cimento, "Relatório Anual 2020". http://snic.org.br/assets/pdf/relatorio_anual/rel_anual_2020.pdf (accessed Mar. 23, 2021).
- [10] R. R. Silva and C. J. C. Bacha, "Acessibilidade e aglomerações na Região Norte do Brasil sob o enfoque da Nova Geografia Econômica," *Nova Econ.*, vol. 24, pp. 169–190, 2014.
- [11] B. L. Weaver and J. Tarney, "Empirical approach to estimating the composition of the continental crust," *Nature*, vol. 310, pp. 575–577, 1984, <http://dx.doi.org/10.1038/310575a0>.
- [12] K. L. Scrivener, "Options for the future of cement," *Indian Concr. J.*, vol. 88, pp. 11–21, 2008.
- [13] G. Habert, Y. Bouzidi, C. Chen, and A. Jullien, "Development of a depletion indicator for natural resources used in concrete," *Resour. Conserv. Recycling*, vol. 54, pp. 364–376, 2010, <http://dx.doi.org/10.1016/j.resconrec.2009.09.002>.
- [14] D. Ioannidou, G. Meylan, G. Sonnemann, and G. Habert, "Is gravel becoming scarce? Evaluating the local criticality of construction aggregates," *Resour. Conserv. Recycling*, vol. 126, pp. 25–33, 2017, <http://dx.doi.org/10.1016/j.resconrec.2017.07.016>.
- [15] H. de La Serna and M. M. Rezende, "Agregados para a construção civil", in *Economia Mineral do Brasil*, Departamento Nacional de Produção Mineral, Ed. Brasília, Brasil: DNPM, 2009, p. 764. [Online]. Available: <http://www.dnpm.gov.br/dnpm/publicacoes/serie-estatisticas-e-economia-mineral/outras-publicacoes-1/>
- [16] A. Luz, S. Almeida, *Manual de Agregados para a Construção Civil*, 2. ed. Rio de Janeiro, Brasil: CETEM/MCTI, 2012.
- [17] E. M. Cabral, "Fabricação de concreto com agregado de argila calcinada produzida com solo do pólo oleiro do Amazonas", M.S. thesis, Univ. Fed. Amazonas, Manaus, Brasil, 2008. [Online]. Available: <https://tede.ufam.edu.br/bitstream/tede/3482/1/Dissertacao%20Final%20Edisley.pdf>
- [18] E. F. J. Mulder, "A geological approach to traditional and alternative aggregates in the Netherlands," *Bull. Int. Assoc. Eng. Geol.*, vol. 29, pp. 49–57, 1984, <http://dx.doi.org/10.1007/BF02594374>.
- [19] W. H. Langer, *Aggregate Resource Availability in the Conterminous United States, Including Suggestions for Addressing Shortages, Quality, and Environmental Concerns*. Reston, VA, USA: U.S. Geological Survey, 2011. Accessed: May 24, 2022. [Online]. Available: https://pubs.usgs.gov/of/2011/1119/pdf/OF11-1119_report_508.pdf.
- [20] Caixa Econômica Federal, *SINAPI: Referências de Preços de Insumos AC Desonerado (Abril/2022)*. Brasília, Brazil: Caixa Econômica Federal, 2022.
- [21] Sindicato Nacional da Indústria do Cimento, "Produção nacional de cimento por regiões e estados 2017" <http://snic.org.br/assets/pdf/numeros/1537281236.pdf> (accessed May 24, 2018).
- [22] K. L. Scrivener, V. M. John, and E. M. Gartner, "Eco-efficient cements: Potential economically viable solutions for a low-CO₂ cement-based materials industry," *Cement Concr. Res.*, vol. 114, pp. 2–26, 2018.
- [23] Global Cement and Concrete Association, *GNR - Indicator Gross CO₂ Emissions - World, GNR Project Reporting CO₂*. London, United Kingdom: GNR Project Management Committee, 2022.
- [24] Global Cement and Concrete Association, *GNR - Indicator Gross CO₂ Emissions - Brazil, GNR Project Reporting CO₂*. London, United Kingdom: GNR Project Management Committee, 2022.
- [25] J. A. R. Lima, "Avaliação das conseqüências da produção de concreto no Brasil para as mudanças climáticas", Ph.D. dissertation, Universidade de São Paulo, São Paulo, Brasil, 2010.
- [26] D. Costa Reis and V. John, *Relatório de Coleta de Dados para o Sistema de Informação do Desempenho Ambiental da Construção: Concreto*. São Paulo, Brasil: Sidac, 2022.
- [27] V. M. John et al., "Proposta de método prático para avaliar o desempenho ambiental no ciclo de vida da construção", *Concreto & Construções*, 48-56, 2020. <http://dx.doi.org/10.4322/1809-7197.2020.100.0002>.
- [28] Sindicato Nacional das Indústrias de Cimento, "Roadmap Tecnológico do Cimento - Potencial de redução das emissões de carbono da indústria do cimento brasileira até 2050" (accessed May 24, 2019). https://www.dropbox.com/s/9cbtj1c9quif8/Roadmap%20Tecnol%C3%B3gico%20do%20Cimento_Brasil.pdf?dl=0.
- [29] Associação Brasileira de Normas Técnicas, *Cimento Portland – Requisitos*, ABNT NBR 16697:2018, 2018.

- [30] SIDAC: Sistema de Informação do Desempenho Ambiental da Construção. <https://sidac.org.br> (accessed May 1, 2019).
- [31] M. P. R. Souza, "Avaliação das emissões de CO₂ antrópico associadas ao processo de produção e concreto, durante a construção de um edifício comercial, na região metropolitana de São Paulo," M.S. thesis, IPT, São Paulo, Brasil, 2012.
- [32] D. P. Santos, "Estudo sobre a utilização de cinza da casca da castanha do Brasil como adições em traços de concreto," M.S. thesis, Univ. Fed. Acre, Rio Branco, Brasil, 2015.
- [33] A. L. A. Novo, "Perspectivas para o consumo de combustível no transporte de carga no Brasil: Uma comparação entre os efeitos estrutura e intensidade no uso final de energia do setor", M.S. thesis, COPPE/UFRJ, Rio de Janeiro, Brasil, 2016.
- [34] É. F. Campos, "Emissão de CO₂ da madeira serrada da Amazônia: O caso da exploração convencional", M.S. thesis, POLI, Univ. São Paulo, São Paulo, Brasil, 2012.
- [35] Google, "Google Maps". <http://maps.google.com> (accessed May 1, 2022).
- [36] M. H. C. Marcos, "Análise da emissão de CO₂ em edificações através do uso de uma ferramenta CAD-BIM", in *SIGraDi 2009*, E. Nardelli and C. Vincent, Eds. São Paulo, Brazil, Nov. 2009, pp. 54-58.
- [37] V. C. H. C. Oliveira, B. L. Damineli, V. Agopyan, and V. M. John, "Estratégias para a minimização da emissão de CO₂ de concretos," *Ambient. Constr.*, vol. 14, pp. 167–181, 2014, <http://dx.doi.org/10.1590/S1678-86212014000400012>.
- [38] D. C. Reis and V. John, "Concreto dosado em central fck 25Mpa – Sidac." <https://sidac.org.br/produtos/119> (accessed June 6, 2022).
- [39] V. C. H. C. Oliveira, "Estratégias para minimização da emissão de CO₂ de concretos estruturais", M.S. thesis, POLI, Univ. São Paulo, São Paulo, Brasil, 2015.
- [40] J. F. Santoro and M. Kripka, "Determinação das emissões de dióxido de carbono das matérias primas do concreto produzido na região norte do Rio Grande do Sul," *Ambient. Constr.*, vol. 16, pp. 35–49, 2016, <http://dx.doi.org/10.1590/s1678-86212016000200078>.

Author contributions: AALP: conceptualization, formal analysis, investigation, methodology, visualization, writing – original draft; LSO: conceptualization, formal analysis, investigation, methodology, visualization, writing – review and editing; VMJ, SCA: conceptualization, investigation, supervision, writing – review and editing.

Editors: Edna Possan, Mark Alexander

APPENDIX A – Development of the equation of CO₂ emissions from materials transportation

This Appendix presents the development of the equations for calculating CO₂ emissions from materials transportation.

First, it is understood that the CO₂ emission from transportation of a material i ($E_{CO_2,Ti}$), in kgCO₂, occurs from burning the fuel and it is obtained by the fuel consumption multiplied by its emission factor, as shown in Equation A1.

$$E_{CO_2,Ti} = EF_F \cdot C_F \quad (A1)$$

where, EF_F is the fuel emission factor (kgCO₂/L) and C_F is the fuel consumption (L).

The fuel consumption (C_F), in liter (L), modeled for the round trip of the vehicle, can be written as shown in Equation A2.

$$C_F = \frac{d}{e_{f,l}} + \frac{d}{e_{f,e}} \quad (A2)$$

where, d is the traveled distance (km) and $e_{f,l}$ and $e_{f,e}$ are the efficiencies of the loaded and empty vehicle, respectively (km/L_{diesel}).

To determine the fuel consumption of transporting each material to produce one cubic meter of concrete ($C_{F,i}$), in L/m³, the fuel consumption should be multiplied by the number of trucks needed for transporting this material. The estimate of the number of trucks is made by the consumption of the material i necessary to produce one cubic meter of concrete as function of the vehicle's load capacity, as shown in Equation A3.

$$C_{F,i} = \frac{C_{i,conc}}{P_v} \left(\frac{d_i}{e_{f,l}} + \frac{d_i}{e_{f,e}} \right) \quad (A3)$$

where, i is the type of material (cement, sand or gravel), $C_{i,conc}$ is the consumption of a material i necessary to produce 1 m³ of concrete (t/m³), P_v is the maximum load capacity of the vehicle (t) and d_i is the transportation distance of the material i (km).

Finally, as the CO₂ emission from the transportation of concrete materials ($E_{CO_2,T}$), given in kgCO₂/m³ of concrete, is the sum of the emission of transporting each material, we arrive at Equation A4 and its simplification, Equation A5, the last one presented in the body of the work.

$$E_{CO_2,T} = EF_F \cdot \sum_{i=1}^{n=3} \left(\frac{C_{i,conc} \cdot d_i}{P_v \cdot e_{f,l}} + \frac{C_{i,conc} \cdot d_i}{P_v \cdot e_{f,e}} \right) \quad (A4)$$

$$E_{CO_2,T} = EF_F \cdot \frac{e_{f,l} + e_{f,e}}{e_{f,l} \cdot e_{f,e} \cdot P_v} \sum_{i=1}^{n=3} (C_{i,conc} \cdot d_i) \quad (A5)$$



ORIGINAL ARTICLE

Reduction of the environmental impacts of reinforced concrete columns by increasing the compressive strength: a life cycle approach

Redução dos impactos ambientais de pilares de concreto armado ao aumentar a resistência à compressão: uma abordagem de ciclo de vida

Bruno Athaíde Bacelar^a Thalita Cardoso Dias^{a,b} Péter Ludvig^a ^aCentro Federal de Educação Tecnológica de Minas Gerais – CEFET-MG, Programa de Pós-graduação em Engenharia Civil, Belo Horizonte, MG, Brasil^bUniversidade do Estado de Minas Gerais – UEMG, Departamento de Engenharia Civil, Divinópolis, MG, Brasil

Received 24 March 2022
 Accepted 17 October 2022

Abstract: The building industry is one of the greatest environmental impact causers in the planet. Cement is the second most used material in the world and the consumption of concrete ranges between 20 to 30 Gt yearly. This demand for the materials tends to increase for the next 100 years. The increase of concrete strength to reduce the material consumption is one of the options proposed in literature to reduce the environmental impacts in building industry. However, few studies have been carried about the actual advantages of this strategy in building production. In this paper, a 15-storey reinforced concrete building was designed with three different concrete grades for its columns: 30 MPa, 40 MPa and 50 MPa. The results for the volume of concrete and the amount of reinforcing steel to produce the columns were used to perform a cradle-to-gate life cycle assessment (LCA) to determine the alternative with less environmental impacts in the production stage. Results indicate an advantage to adopt higher strength concretes in columns to reduce environmental impacts and the consumption of materials. Direct effects of higher strength in concretes made possible to reduce the consumption of concrete by 15%. There was also a significant reduction caused by indirect effects of higher strengths in concrete, with the reducing of steel consumption up to 22%. With the combination of the direct and indirect effects of higher compressive strengths, it was possible to reduce the environmental impacts of reinforced concrete in all categories studied in the LCA.

Keywords: reinforced concrete, life cycle assessment, sustainability, concrete columns.

Resumo: A indústria da construção é uma das maiores causadoras de impactos ambientais do planeta. O cimento é o segundo material mais utilizado no mundo e o consumo de concreto varia entre 20 a 30 Gt por ano. Isto faz com que a demanda pelos materiais apresente uma tendência de aumento durante os próximos 100 anos. O aumento da resistência do concreto para reduzir o consumo de materiais é uma das opções propostas na literatura para reduzir os impactos ambientais na indústria da construção. No entanto, poucos estudos têm sido realizados sobre as vantagens reais desta estratégia na construção de edifícios. Neste artigo, um edifício de concreto armado de 15 andares foi dimensionado com três tipos diferentes de concreto para os pilares: 30 MPa, 40 MPa e 50 MPa. Os resultados para o volume de concreto e a quantidade de aço de armadura para produzir os pilares foram utilizados para realizar uma avaliação do ciclo de vida (ACV) do berço ao portão da fábrica para determinar a alternativa com menos impactos ambientais na fase de produção. Os resultados indicam uma vantagem em adotar concretos de maior resistência em pilares de concreto armado para reduzir os impactos ambientais e o consumo de materiais. Os efeitos diretos da maior resistência dos concretos tornaram possível reduzir o consumo de concreto em 15%. Houve também uma redução

Corresponding author: Bruno Athaíde Bacelar. E-mail: brunoathaide@gmail.com

Financial support: Centro Federal de Educação Tecnológica de Minas Gerais (CEFET-MG), Fundação do Amparo à Pesquisa de Minas Gerais (FAPEMIG), Coordenação de Aperfeiçoamento de Pessoal de Nível Superior (CAPES) and Conselho Nacional de Desenvolvimento Científico e Tecnológico (CNPQ).

Conflict of interest: Nothing to declare.

Data Availability: The data that support the findings of this study are openly available in Scielo Data in <https://doi.org/10.48331/scielodata.BXKHHP>.



This is an Open Access article distributed under the terms of the Creative Commons Attribution License, which permits unrestricted use, distribution, and reproduction in any medium, provided the original work is properly cited.

significativa causada pelos efeitos indiretos da maior resistência dos concretos, com a redução do consumo de aço até 22%. Com a combinação dos efeitos diretos e indiretos da maior resistência à compressão, foi possível reduzir os impactos ambientais do concreto armado em todas as categorias estudadas na ACV.

Palavras-chave: concreto armado, avaliação do ciclo de vida, sustentabilidade, pilares de concreto armado.

How to cite: B. A. Bacelar, T. C. Dias, and P. Ludvig, "Reduction of the environmental impacts of reinforced concrete columns by increasing the compressive strength: a life cycle approach," *Rev. IBRACON Estrut. Mater.*, vol. 15, no. 6, e15610, 2022, <https://doi.org/10.1590/S1983-41952022000600010>.

1 INTRODUCTION

Concrete is one of the most consumed materials in the world. It is estimated a consumption of concrete between 20 to 30 Gt yearly [1], [2]. Cement, the main material of concrete, is most used manufactured material in the world and responsible for large CO₂ emissions. In Brazil, the cement industry was responsible for 23.144 kt of CO₂ emissions in the industrial processes and product use (IPPU) sector in 2020, which represents 22.7% of the emissions from this sector [3].

The production of cement in Brazil is greener than the average worldwide. The estimated CO₂ emissions from cement in Brazil are 564 kg/ton, against the world average of 635 kg/ton [4]. However, efforts aiming to reduce environmental impacts in the construction and cement industry still should be taken.

For the last decades, the demand for cement and concrete was increased and the projected urbanization for the next 100 years is an indicative that this demand will continue to increase for that period. Thus, it is necessary to study strategies to limit the environmental impacts of concrete constructions [5], [6].

Steel, necessary for reinforcement bars in concrete, has a total production of 1.5 Mt yearly. Global steel production is estimated to be around 2.6 GtCO₂ per year [7]. Steel production is dependent on non-renewable fuels, making it a material with use of fossil energy and high emissions of CO₂ in the atmosphere [8].

Many alternatives have been proposed to make the concrete and cement industries more sustainable, such as the use of supplementary cementitious materials (SCM) [9]–[11], recycled concrete [9] and the optimization of the mixing design process [12]. Mehta [6] presents three tools to achieve sustainability in concrete and cement industries: (1) to consume less concrete in new structures, (2) to consume less cement in concrete mixtures and (3) to consume less clinker for making cements, as seen in Figure 1. Reducing the concrete volume by enhancing the concrete performance may be one option to reduce the environmental impacts in the building industry. By increasing the concrete strength, less concrete and reinforcing bars will be necessary in building production [13], which may lead to the reduction of environmental impacts.

The production of higher strength concretes has been increasing in the last years to improve the performance of the structures [14]–[16]; however, the increased strength is achieved by higher amount of cements, which increase the environmental impacts of the concrete mixture.

Different studies found in literature use the strategy of increasing the concrete strength to reduce the environmental impacts by assessing the impacts of individual columns [17], bridge girders [18] or variations of both design strategies and the adoption of different compressive strengths along the length of the columns [19].

Increasing the concrete strength will certainly reduce the cross section of the structural members and the volume of concrete and consumption of steel in reinforced concrete buildings. The consumption of concrete and reinforcing steel can be reduce by 5.4% and 38.6%, respectively, changing the compressive strength of RC columns from grade C30 to grade C60 [13].

However, as cement is the main contributor for CO₂ emissions of concrete, it is important to quantify and verify if the reductions of material consumption are enough to compensate the higher environmental impacts from the higher amount of cement in the concrete mixture.

Life cycle assessment (LCA) is a powerful sustainability assessment tool to quantify the environmental impacts of a product or a system [20]. The LCA methodology is based on ISO 14040 [21]. LCA is considered to be one promising technique more ecological design of products [22].

This study aims to evaluate the feasibility and validity of the option to increase compressive strength of concrete to lower the environmental impacts of the structure. A reinforced concrete (RC) residential building was designed with columns in three different concrete grades of strength (f_{ck} s) to obtain the quantitative results of volume of concrete and steel reinforcement weight. With the quantitative values, a LCA was performed to assess and compare the environmental impacts for the different scenarios considered and the contribution of each material present in reinforced concrete in different impact categories.

2 METHODOLOGY

2.1 Building design

The object of study of this paper was based on an architectural design of a 15-store RC residential building (Figure 1) located in Belo Horizonte, Minas Gerais, Brazil. Building design was performed using Cypecad software. The design of the structure followed the method established by Brazilian standard NBR 6118 [23].

Three different models were designed with different concrete characteristic strengths for columns (f_{cks}): 30 MPa (C30), 40 MPa (C40) and 50 MPa (C50). Slabs and girders defined with compressive strengths of 30 MPa for all the situations, as shown in Table 1.

To determine service loads of the building, this study followed de recommendations of NBR 6120 [24]. The procedures presented by NBR 7480 [25] were followed for requirements of reinforcing steel bars in structural members. For combinations of actions in the structure, the methods presented in NBR 8681 [26] were adopted. For wind load, a speed of wind of 35 m/s was considered for the city of Belo Horizonte MG, following the procedures of NBR 6123 [27].

For reinforcement of the structural members, the area of steel reinforcement (A_s) was defined as the minimum calculated area of steel reinforcement (A_{smin}). Detailed information and the calculation logs of this study are openly available in Scielo Data.

Table 1. Compressive strengths of structural members

Model	Slabs	Girders	Columns
C30	30 MPa	30 MPa	30 MPa
C40	30 MPa	30 MPa	40 MPa
C50	30 MPa	30 MPa	50 MPa

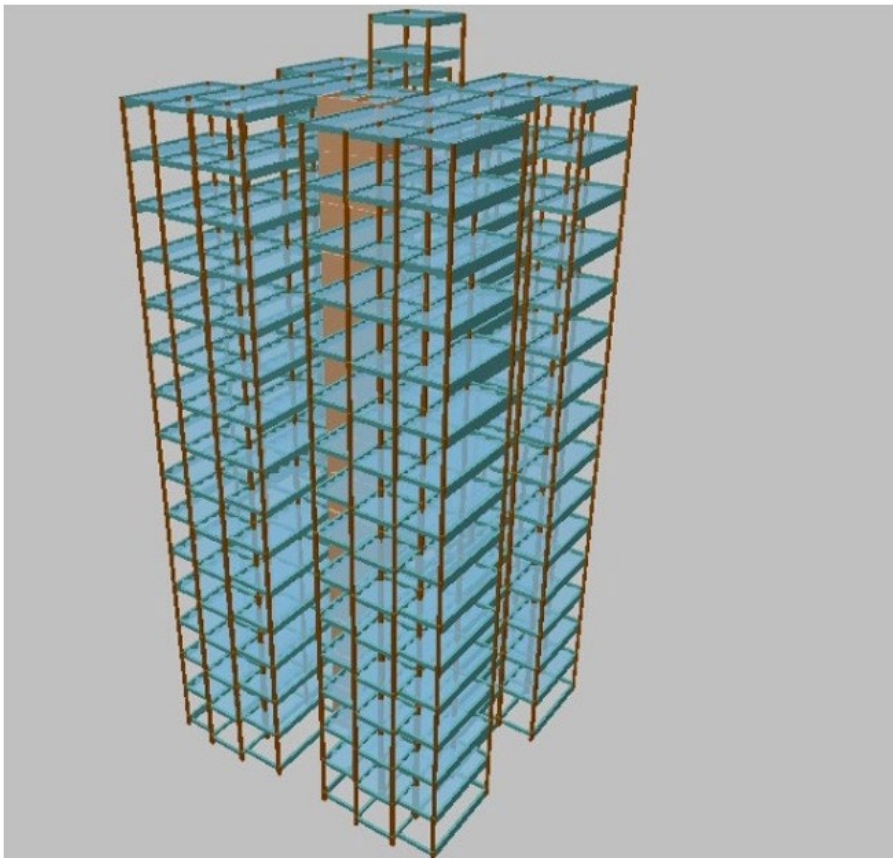


Figure 1. Structural model of the residential building

After verification and error correction of the structure, quantitative tables were generated to obtain the values of concrete consumption (m³) and the weight of reinforcement (kg) to produce the columns. From this, it was possible to compare the variations of concrete materials (cement, sand, gravel, water and superplasticizer) and steel reinforcement with the changes in the f_{ck} .

2.2 Concrete mix design

To achieve the goal of this study, the definition of concrete composition was necessary for each design model developed in 2.1. The mix design is presented in Table 2.

The mix design was produced following the method presented by Thomaz [28]. In this method, data from over 200 concrete mixes available in the literature were selected to perform correlations between water/cement ratio, water amount, aggregates, superplasticizers and compressive strength. From this, it was possible to estimate the amount of materials to achieve the desired f_{ck} s.

The compressive strength (f_c) to achieve the desired f_{ck} s was used as the input to obtain the quantitative of cement, sand, gravel, water and superplasticizer in a Microsoft Excel spreadsheet. The mix design data from the spreadsheets are available in Scielo Data.

Equation 1 gives the relation between f_c and f_{ck} :

$$f_c = f_{ck} \times 1.65 \times sd \tag{1}$$

Where,

f_c : Target mean compressive strength of the concrete mixture;

f_{ck} : Characteristic compressive strength of the concrete mixture;

sd: Standard deviation of the distribution, defined as 4 with a better technological control in the production.

Table 2. Mix design formulations for the concrete columns

Components	C30	C40	C50
Cement (kg/m ³)	345	394	432
Gravel (kg/m ³)	1042	1057	1067
Sand (kg/m ³)	751	733	721
Water (kg/m ³)	186	178	171
Superplasticizer (kg/m ³)	0	0,1	3,3

2.3 Life Cycle Assessment (LCA)

The LCA was performed in four steps, as recommended by ISO 14040 [21]: Goal and Scope, Life Cycle Inventory (LCI), Life Cycle Impact Assessment (LCIA) and Interpretation of the results.

2.3.1 Goal and scope

The LCA performed in this study aimed to quantify and compare the environmental impacts of columns of RC buildings designed and produced with different characteristic strengths (f_{ck} s): 30 MPa (C30), 40 MPa (C40) and 50 MPa (C50). The OpenLCA software was chosen to perform the LCA [29] was chosen for being free and open source and for having the collaboration of researchers from all over the world for the improvements LCA studies, which makes it a transparent tool.

Since the construction phase is the main contributor for the environmental impacts of a building [19], [30], system boundaries were set from cradle to gate, i.e., from material extraction to the finished product. The boundaries and stages considered are indicated in Figure 2.

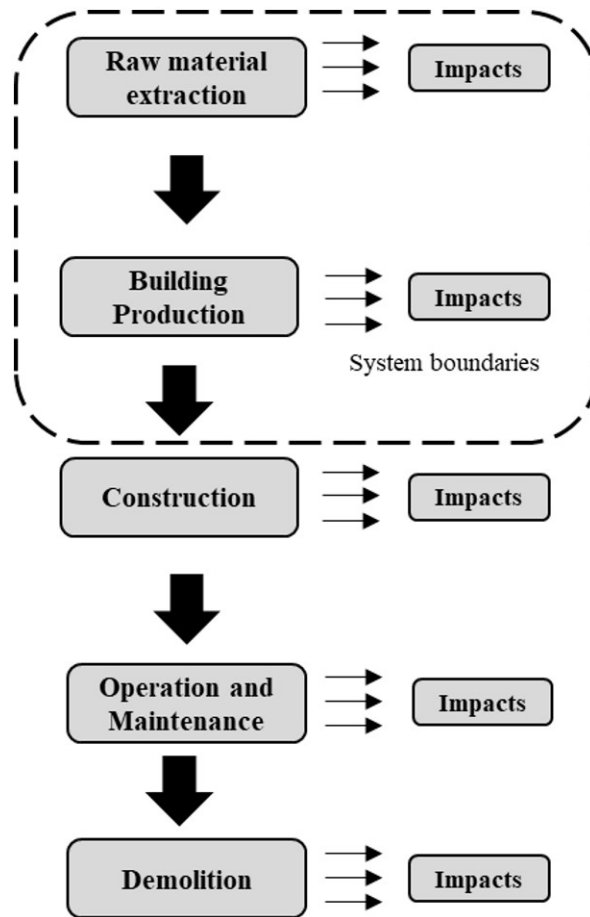


Figure 2. System boundaries of the LCA

Two sets of analysis are presented for a better understand of the impacts in concretes, with two functional unities. First considering a functional unity of 1 m³ of concrete to analyze the impacts of conventional concrete and the influence of its components in the results.

Additionally, for the second set of analysis, the impacts of the total amount of concrete and reinforcing steel to produce the columns for the building were analyzed. For this purpose, a functional unity of 1 item, equivalent to the total amount of columns combined, was adopted.

2.3.2 Life Cycle Inventory (LCI)

For the LCI, the Ecoinvent database was used to provide the inventory for the materials of this study. The processes used LCI are shown in Table 3.

Table 3. Processes in the Life Cycle Inventory

Material	Process
Cement	market for cement, Portland cement, Portland APOS,U - RoW
Gravel	market for gravel, crushed gravel, crushed APOS,U - RoW
Sand	market for silica sand silica sand APOS,U - GLO
Water	market for tap water tap water APOS,U - RoW

The superplasticizer inventory is not present in the ecoinvent database. Thus, it was necessary to insert manually the inventory available in the EFCA Environmental Declaration of superplasticizing admixtures [31]. The input of raw materials and the processes used for 1 kg of superplasticizer in the LCA are presented in Table 4.

Table 4. Raw inputs for superplasticizing admixture

Raw material	Value	Process
Coal (g)	62	market for hard coal hard coal APOS,U - RoW
Crude oil (g)	91	market for petroleum petroleum APOS,U - GLO
Crude oil (g)	74	market for heavy fuel oil heavy fuel oil APOS,U - RoW
Natural gas (dm ³)	0.13	market for natural gas, vented natural gas, vented APOS,U - GLO
Natural gas (m ³)	0.21	market for petroleum petroleum APOS,U - GLO
Water (kg)	7.4	market group for tap water tap water APOS,U - GLO

2.3.3 Life Cycle Impact Assessment (LCIA)

The Impact World+ method with an endpoint indicator was chosen for the LCIA step of this study. The method was designed as a joint update to traditional methods IMPCAT 2002+, EDIP and LUCAS and with the goal to create a regionalized method that covers the entire world [32]. The impact categories covered by the method are indicated in Table 5.

Table 5. Impact categories of the Impact World+ LCIA method

Impact Category	Unity
Climate change, long term	kg CO ₂ eq (long)
Climate change, short term	kg CO ₂ eq (short)
Fossil and nuclear energy use	MJ deprived
Freshwater acidification	kg SO ₂ eq
Freshwater ecotoxicity	CTUe
Freshwater eutrophication	kg PO ₄ P-lim eq
Human toxicity cancer	CTUh
Human toxicity non cancer	CTUh
Ionizing radiations	Bq C-14 eq
Land occupation, biodiversity	m ² arable land eq .yr
Land transformation, biodiversity	m ² arable land eq
Marine eutrophication	kg N N-lim eq
Mineral resources use	kg deprived
Ozone Layer Depletion	kg CFC-11 eq
Particulate matter formation	kg PM _{2.5} eq
Photochemical oxidant formation	kg NMVOC eq
Terrestrial acidification	kg SO ₂ eq
Water scarcity	m ³ world-eq

Calculations for all the impact categories available in the methodology were made for this study. However, for further analysis, five impact categories were selected for a deeper look in the results and to understand of the roles of each material in the environmental impacts: climate change (long term), fossil and nuclear energy use, freshwater eutrophication, mineral resources use and ozone layer depletion.

For the first set of the analysis, the m³ comparison of the three concrete grades, results were detailed for cement, sand, gravel, water and superplasticizer. For the comparison of the columns productions, results were detailed by concrete and reinforcing steel.

2.4 Cement and environmental efficiencies

Cement efficiency is a factor present in different studies to assess the relation of the characteristic strength of the concretes designed and the amount of cement to produce them [17], [33], [34]. Cement efficiency was calculated as the ratio of the cement content in 1 m³ of concrete and the concrete strength obtained in MPa, as shown in Equation 2:

$$E_c = \frac{c}{f_{ck}} \tag{2}$$

Where,

Ec = Cement efficiency;
 C = Cement content for 1 m³ of concrete;
 f_{ck} = Characteristic strength

A parameter called environmental efficiency was also calculated to analyze the results of the LCA. In this case, the results for the Climate change category, i.e., CO₂ emissions, were considered. The environmental efficiency of cement was calculated as follows:

$$Eco_c = \frac{CO_2}{f_{ck}} \tag{3}$$

Where,
 Eco_c = Eco-efficiency of cement;
 CO₂ = Environmental impacts from the climate change (long term) category.

3 RESULTS AND DISCUSSIONS

3.1 Building Design

For this study, a 15 store residential building was designed and the quantitative results for concrete and reinforcing bars were extracted. Results are shown in Table 6. The quantitative results for cement, sand, gravel, water and superplasticizer are shown in Table 7.

The adoption of higher concrete grades made the reduction of the consumption of both concrete and reinforcing bars to produce the columns in the building possible. When comparing the results for grade C30, reductions in the amount of concrete by 3.8% and 11.2% were possible for C40 and C50 grades, respectively. For reinforcing bars, reductions of 13.7% and 22.3% were achieved for C40 and C50 grades. This result is similar to what was found previously when comparing columns produced with grade C30 concrete and grade C60 [13].

To achieve higher concrete strengths, it is necessary to increase cement content and to reduce the w/c ratio. In this study, the reduction of concrete observed in grades C40 and C50 was not enough to reduce the cement content in the RC columns.

Table 6. Total of materials consumed in columns

Concrete grade	Concrete (m ³)	Δ	Reinforcing bars (kg)	Δ
C30	260	-	38773	-
C40	250	3.8%	33480	13.7%
C50	222	11.2%	30132	22.3%

Table 7. Total of materials consumed in the concrete used in the columns

Material	C30	C40	Δ	C50	Δ
Cement (ton)	89.7	98.5	10%	95.9	7%
Gravel (ton)	27.1	26.4	-2%	23.7	-13%
Sand (ton)	19.5	18.3	-6%	16.0	-18%
Water (ton)	48.4	44.5	-8%	38.0	-22%
SP (ton)	0	98.5	-	0.73	2830%

3.2 Life Cycle Impact Assessment

3.2.1 m³ comparison

Results were normalized in relation to the 30 MPa class of concrete. A preliminary comparison considering the impacts of 1 m³ of concretes was performed. As expected, the higher amount of cement in concretes C40 and C50 resulted in higher environmental impacts in all categories, as seen in Figure 3. This is explained by cement being the material with most environmental impacts in concrete. To achieve higher compressive strength, higher amounts of

cement are necessary and, as consequence, when the functional unity of 1 m³ is evaluated, the concretes with higher compressive strength present higher environmental impacts.

Further analysis was necessary understand the roles of the materials in the environmental impacts of the concrete. For that purpose, five categories were selected: Climate change (long term), Fossil and nuclear energy use, Freshwater eutrophication, Mineral resources use and Ozone layer depletion. Results are presented in Figure 4.

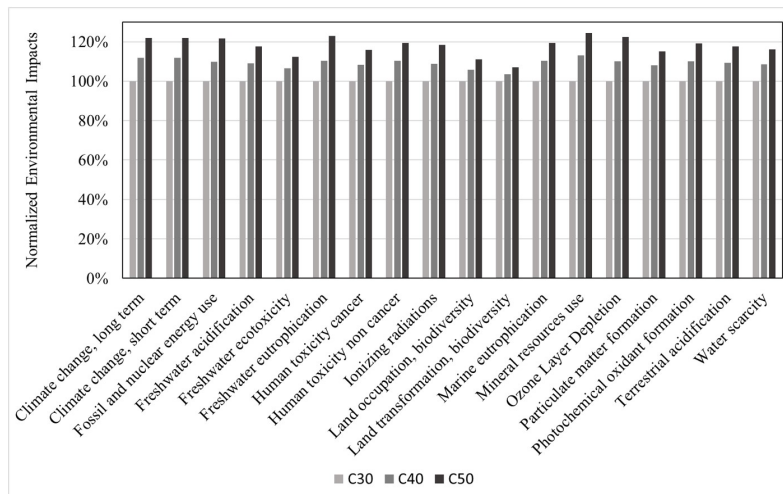


Figure 3. Normalized LCA results for 1 m³ of concrete

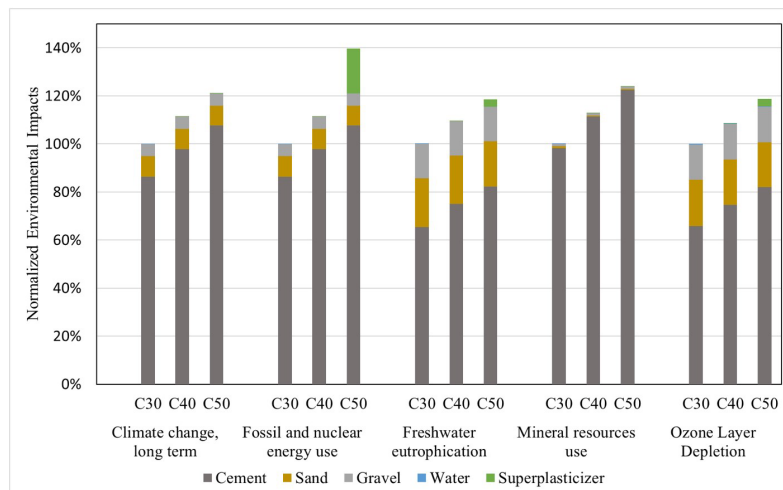


Figure 4. Impacts 1 m³ of concrete detailed by the materials

The LCA results for concrete indicate the predominance of cement in the environmental impacts when compared to the other materials (gravel, sand, water and superplasticizer, cement). In this study, cement is present in the concrete mix in average of 16.5% by weight of the materials and is responsible, in average, for 68% of the environmental impacts of concrete.

In contrast to the use of cement, sand and gravel represent 76% of the materials in concrete by weight and are responsible, in average for 32% of the environmental impacts to produce 1 m³ of concrete. Impacts of sand and gravel are caused mostly by transportation. Average distances of transportation are accounted in the market process chosen in the LCI phase of this study [35].

The high values of climate change for concrete are due to carbon dioxide emissions to air originated by clinker production and from the use of petrol and coke to power the furnaces in cement factories. This use of petrol and coke is responsible also for the higher values of environmental impacts in fossil energy.

The mineral resources use impact categories have cement as the predominantly responsible component for the environmental impacts. Cement is accounted for 98.3% for C30 concretes, 99.7% for C40 and 99.8% for C50. Those impacts are caused by mining and extraction of clay and limestone to produce clinker.

The contributions of superplasticizer in the environmental impacts of concrete are not relevant in the production of 1 m³ of concrete. This is the result of the lower content of 0 kg, 0.1 (0.01% of the total weight) kg and 3.1 kg (0.43% of total weight) in 1 m³ of concrete in C30, C40 and C50, respectively.

It is important to note that superplasticizers should be a concern in concrete production. As seen in Table 3, superplasticizers' raw materials are petroleum based, which explain the influence in the results in fossil and nuclear energy use. Analyzing the categories, values of impacts of 18.6% and 2.90% were noticed in relation to the total impacts of the C30 grade concrete if only 3 kg of superplasticizers are added in the mixture.

3.2.2 Cement efficiency and eco efficiency.

Cement efficiency and eco-efficiency of the concretes are shown in Table 8.

The increase of compressive strength in the concretes resulted in a better efficiency and a lower amount of cement necessary to reach 1 MPa. That means that, besides having a higher content of cement for higher strength concretes, this amount is used in a more efficient way to improve the mechanical the mechanical properties.

Results for the eco-efficiency followed the trend observed in cement efficiency. Although the emissions of CO₂ observed for concretes C40 and C50 are higher, less CO₂ is emitted in the atmosphere to achieve 1 MPa of compressive strength in concretes. This result is an indicator that higher compressive strengths and, thus, the reduction of the volume of concrete and the weight of reinforcing steel bars, lead to the reduction of the environmental impacts.

Similar results are found in the literature. Pacheco et al. [17]. The efficiency of concrete increased with higher compressive strengths, varying from 12.20 kg/m³/MPa in C20 concretes to 5.75 kg/m³/MPa in C80 concretes. Miranda de Souza et al. [36] found similar trends for the eco-efficiency of concretes with different concrete grades. results of 15.72 kgCO₂eq/MPa were found for C20 concretes, whereas values of 12.28 kgCO₂eq/MPa were found for C30 class concretes

Table 8. Cement efficiency

Concrete grade	f _{ck}	Cement (kg)	Efficiency (kg/m ³ /MPa)	eco-efficiency (kgCO ₂ eq/MPa)
C30	30	345	11,50	11,58
C40	40	414	10,35	9,71
C50	60	465	9,30	8,48

3.2.3 Columns

The LCA for the columns was performed using the results of the building design and the mix design chosen for the concrete. The first set of analysis aimed to compare the results of the columns produced in three different grades: C30, C40, C50. For that, the results were normalized in relation to the C30 columns. Results are presented in Figures 5 and 6.

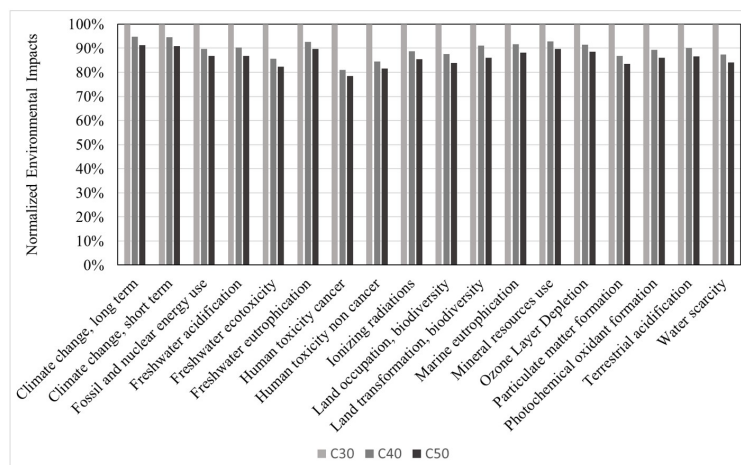


Figure 5. Normalized LCA results for RC columns

For further analysis, and to understand the roles of the materials, now including reinforcing steel, the same five impact categories selected for the m³ analysis were studied for the RC columns.

The analysis of the proportions of the materials in the results of impact categories was important to understand the influence of the impacts of reinforcing steel. It is important to acknowledge the effect the indirect advantages of the increased concrete strength to produce the RC columns.

It is possible to note in the five highlighted impact categories that the environmental impacts accounted for the concrete portion of RC present some reduction for the different concrete grades, even with the reduction of volume of concrete in C40 and C50 columns.

CO₂ emissions (Climate change impact category) from grade C50 columns were 10% lower than the grade C30 RC columns. Habert and Roussel [37] estimates that this reduction can be up to 30% if the strategy to increase strength is combined with cement replacement. As observed in Table 6, the cement consumption increases for C40 and C50 grade mixes of concrete in relation to the C30 grade. To reduce the environmental impacts of the concrete portion of the RC columns, it would be necessary to reduce the cement content cement in concrete mixtures.

Rohden and Garcez [19] and Peyroteo et al. [38] state that the reduction of steel is an advantage concerning the environmental impacts of the building. Reinforcing steel, as can be seen in Figure 6 is the greater responsible for the environmental impacts of RC columns. Thus, the reduced need for reinforcing bars in the column results in the lower environmental impacts of RC columns produced is C40 and C50 concretes.

Figures 7, 8, 9, 10 and 11 show the tendencies of the environmental impacts of concrete and reinforcing steel in contrast to the total environmental impacts for categories. It can be seen in the figures that even with the reduction in the volume of concrete in the structure, not much variation is observed in the portion of the environmental impacts of concrete in the RC columns. The lower environmental impacts caused by the reduction of reinforcing bars in the columns was essential to the reductions found in this study.

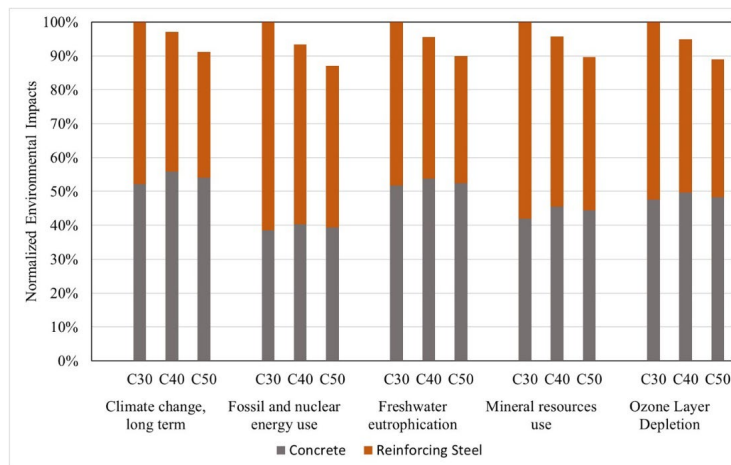


Figure 6. Impacts of RC columns detailed by concrete and reinforcing steel

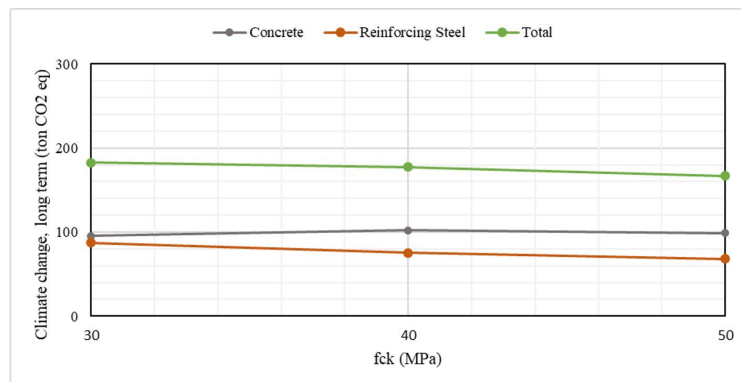


Figure 7. Climate change, long-term impacts for RC columns

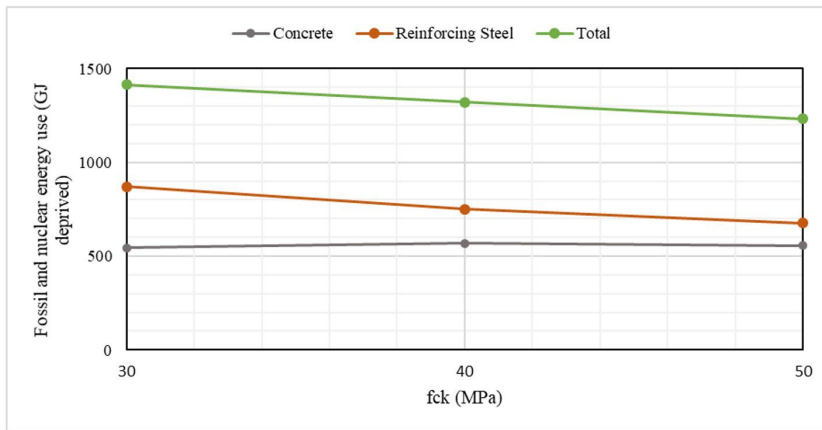


Figure 8. Fossil and nuclear energy use for RC columns

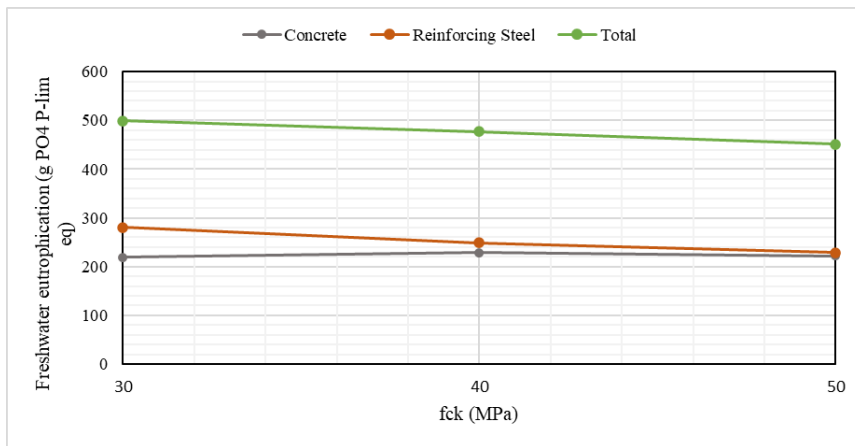


Figure 9. Freshwater eutrophication impacts for RC columns

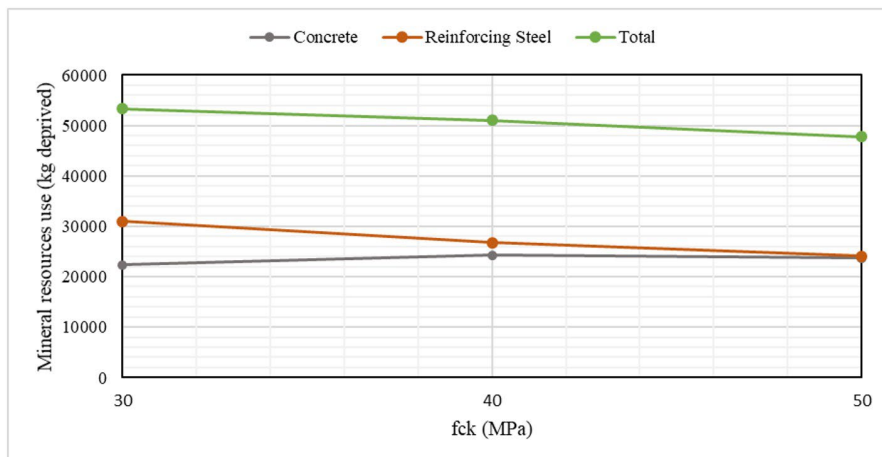


Figure 10. Mineral resources use for RC columns

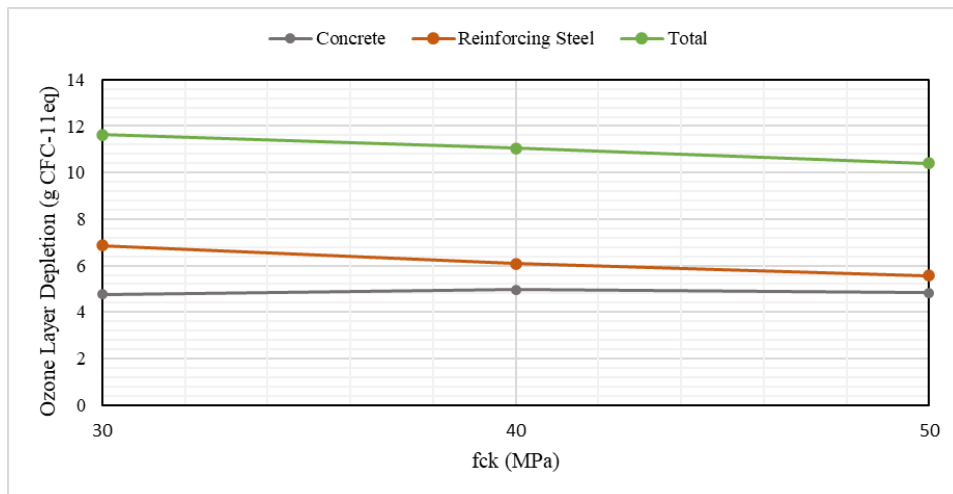


Figure 11. Ozone layer depletion for RC columns

4 CONCLUSIONS

In this study, a cradle to gate LCA was performed to assess the possibility of increasing the concrete strength of RC columns to reduce the environmental impacts.

First, three concrete mixes of different grades were selected as basis for input in the LCA: 30 MPa, 40 MPa and 50 MPa. Then, the LCA was performed for two sets of analysis: the production of 1 m³ of concrete and the production of the RC columns.

Results show great influence of cement in the environmental impacts of concrete. The process of production with mining and extraction of materials and the use of non-renewable energy in cement plants.

Even though there is a greater utilization of sand and gravel by weight, the impacts to extract the materials were not as significant as cement, which is present in lower amounts per m³ of concrete.

Superplasticizers are produced with petroleum-based raw material that can be relevant in environmental impacts such as fossil and nuclear energy use and for increase of freshwater ecotoxicity, with higher biological and chemical oxygen demands. However, the impacts in RC columns are overshadowed by the impacts of cement and steel when the results RC columns are analyzed.

The increase of concrete strength to produce the RC columns showed as a good alternative to reduce the total environmental impacts in to produce the building. However, the reduction of impacts is not caused by the reduction of the volume of concrete in the columns, but by the reduction of reinforcing bars, as steel production are responsible for a great portion of the environmental impacts of RC.

The increase of the concrete strength is also positive when cement efficiency and eco-efficiency were assessed. Concrete grades C40 and C50 increased the cement efficiency in 10% and 19.1%, respectively to produce 1 m³ of concrete.

As of eco-efficiency, higher compressive strengths increased the eco-efficiency, the ratio between the CO₂ emissions for 1 m³ of concrete and the compressive strength. In relation to C30 concretes, results were 16.1% and 26.8% for C40 and C50 concretes, respectively.

As seen in the three tools proposed to achieve sustainability in building construction, the reduction of concrete in structures can be a viable option, but the high amount in cement in concrete mixture is still an obstacle, since the environmental impacts of the concrete portion of RC slightly increased.

ACKNOWLEDGEMENTS

We gratefully acknowledge the universities Federal Center for Technological Education of Minas Gerais (CEFET-MG) and State University of Minas Gerais (UEMG) for the support. We are also grateful for the agencies CNPq, CAPES, FAPEMIG and CEFET-MG for providing financial support.

REFERENCES

- [1] N. Randl, T. Steiner, S. Ofner, E. Baumgartner, and T. Mészöly, "Development of UHPC mixtures from an ecological point of view," *Constr. Build. Mater.*, vol. 67, pp. 373–378, 2014, <http://dx.doi.org/10.1016/j.conbuildmat.2013.12.102>.
- [2] P. J. M. Monteiro, S. A. Miller, and A. Horvath, "Towards sustainable concrete," *Nat. Mater.*, vol. 16, no. 7, pp. 698–699, 2017, <http://dx.doi.org/10.1038/nmat4930>.
- [3] Brasil, Ministério da Ciência, Tecnologia e Inovações, *Estimativas anuais de emissões de gases de efeito estufa no Brasil*, Brasília, DF, Brasil: Ministério da Ciência, Tecnologia e Inovações, 2022.
- [4] Sindicato Nacional da Indústria do Cimento, *Relatório Anual*, São Paulo, SP, Brasil: Sindicato Nacional da Indústria do Cimento, 2020.
- [5] G. Habert et al., "Environmental impacts and decarbonization strategies in the cement and concrete industries," *Nat. Rev. Earth Environ.*, vol. 1, 559–573, 2020, <http://dx.doi.org/10.1038/s43017-020-0093-3>.
- [6] P. K. Mehta, "Global concrete industry sustainability," *ACI Mater. J.*, no. 31, vol. 2, pp. 45–48, 2009.
- [7] M. Fischedick et al., "Industry," in *Climate Change 2014: Mitigation of Climate Change. Contribution of Working Group III to the Fifth Assessment Report of the Intergovernmental Panel on Climate Change*, 2014.
- [8] M. A. Quader, S. Ahmed, R. A. R. Ghazilla, S. Ahmed, and M. Dahari, "A comprehensive review on energy efficient CO₂ breakthrough technologies for sustainable green iron and steel manufacturing," *Renewable Sustainable Energy Rev.*, vol. 50, pp. 594–614, Oct. 2015. <https://doi.org/10.1016/j.rser.2015.05.026>.
- [9] C. L. Gomes, F. S. J. Poggiali, and R. C. de Azevedo, "Concretes with recycled aggregates of construction and demolition waste and mineral additions: a bibliographic analysis," *Rev. Materia*, vol. 24, no. 2, 2019, <http://dx.doi.org/10.1590/s1517-707620190002.0673>.
- [10] M. A. Mosaberpanah and S. A. Umar, "Utilizing rice husk ash as supplement to cementitious materials on performance of ultra high performance concrete: a review," *Mater. Today Sustain.*, vol. 7–8, pp. 100030, 2019., <http://dx.doi.org/10.1016/j.mtsust.2019.100030>.
- [11] B. S. Thomas et al., "Sugarcane bagasse ash as supplementary cementitious material in concrete – a review," *Mater. Today Sustain.*, vol. 15, pp. 100086, Nov. 2021. <http://dx.doi.org/10.1016/j.mtsust.2021.100086>.
- [12] C. Londero, N. S. Klein, and W. Mazer, "Study of low-cement concrete mix-design through particle packing techniques," *J. Build. Eng.*, vol. 42, Oct. 2021, <http://dx.doi.org/10.1016/j.jobe.2021.103071>.
- [13] B. A. Bacelar, L. S. Wolbert, and Mello, G. N. A., "Estudo comparativo do cálculo e dimensionamento de uma edificação em concreto armado utilizando fck's diferentes segundo a NBR 6118:2014," in *58º Congr. Bras. Concr.*, Belo Horizonte, MG, Brasil, 2016.
- [14] T. M. Viana, B. A. Bacelar, I. D. Coelho, P. Ludvig, and W. J. Santos, "Behaviour of ultra-high performance concretes incorporating carbon nanotubes under thermal load," *Constr. Build. Mater.*, vol. 263, Dec 2020., <http://dx.doi.org/10.1016/j.conbuildmat.2020.120556>.
- [15] H. Dong, J. Zhu, W. Cao, Y. Rao, and Y. Liu, "Structural behavior of mega steel-reinforced high-strength concrete rectangular columns under axial compression," *J. Build. Eng.*, no. 61, pp. 105272, 2022, <http://dx.doi.org/10.1016/j.jobe.2022.105272>.
- [16] A. Christian and G. O. K. Chye, "Performance of fiber reinforced high-strength concrete with steel sandwich composite system as blast mitigation panel," *Procedia Eng.*, vol. 95, pp. 150–157, 2014, <http://dx.doi.org/10.1016/j.proeng.2014.12.174>.
- [17] J. Pacheco, L. Doniak, and M. Carvalho, "The paradox of high performance concrete used for reducing environmental impact and sustainability increase," in *Proc. 2nd Int. Conf. Concrete Sustain.*, pp. 442–453, 2016.
- [18] G. Habert, D. Arribe, T. Dehove, L. Espinasse, and R. le Roy, "Reducing environmental impact by increasing the strength of concrete: Quantification of the improvement to concrete bridges," *J. Clean. Prod.*, vol. 35, pp. 250–262, 2012., <http://dx.doi.org/10.1016/j.jclepro.2012.05.028>.
- [19] A. B. Rohden and M. R. Garcez, "Increasing the sustainability potential of a reinforced concrete building through design strategies: case study," *Case Stud. Constr. Mater.*, vol. 9, e00174, Dec. 2018, <http://dx.doi.org/10.1016/j.cscm.2018.e00174>.
- [20] M. Z. Hauschild, R. K. Rosenbaum, and S. I. Olsen, *Life Cycle Assessment: Theory and Practice*. USA: Springer International Publishing, 2018. <http://dx.doi.org/10.1007/978-3-319-56475-3>.
- [21] International Organization for Standardization, *Environmental Management - Life Cycle Assessment - Principles and Framework*, ISO 14040, 2006.
- [22] C. Dossche, V. Boel, and W. de Corte, "Use of life cycle assessments in the construction sector: critical review," *Procedia Eng.*, vol. 171, pp. 302–311, 2017, <http://dx.doi.org/10.1016/j.proeng.2017.01.338>.
- [23] Associação Brasileira de Normas Técnicas, *Projeto de estruturas de concreto — Procedimento*, NBR 6118, 2014.
- [24] Associação Brasileira de Normas Técnicas, *Cargas para o Cálculo de Estruturas de Edificações*, NBR 6120, 2019.
- [25] Associação Brasileira de Normas Técnicas, *Aço Destinado a Armaduras para Estruturas de Concreto Armado – Especificação*, NBR 7480, 2008.
- [26] Associação Brasileira de Normas Técnicas, *Ações e Segurança nas Estruturas – Procedimento*, NBR 8681, 2004.

- [27] Associação Brasileira de Normas Técnicas, *Forças Devidas ao Vento em Edificações*, NBR 6123, 1988.
- [28] E. C. S. Thomaz, *Concretos de Alta Resistência: Traços - Tendências*, 2008, pp. 1–18. Notas de aula. http://aquarius.ime.eb.br/~webde2/prof/ethomaz/cimentos_concretos/traco.pdf (accessed Jun. 2, 2022).
- [29] A. Ciroth, "ICT for environment in life cycle applications openLCA – A new open source software for Life Cycle Assessment," *Int. J. Life Cycle Assess.*, vol. 12, no. 4, pp. 209–210, 2007, <https://doi.org/10.1065/lca2007.06.337>.
- [30] S. Tae, C. Baek, and S. Shin, "Life cycle CO2 evaluation on reinforced concrete structures with high-strength concrete," *Environ. Impact Assess. Rev.*, vol. 31, no. 3, pp. 253–260, Apr 2011., <http://dx.doi.org/10.1016/j.eiar.2010.07.002>.
- [31] European Federation of Concrete Admixture Associations, "EFCA Environmental Declaration: Superplasticizing admixtures – June 2002." EFCA, 2022 <https://swe.sika.com/dms/getdocument.get/60b7f6a6-92fc-36b7-ae01-45e0c48e395d/SuperplasticizerED.pdf> (accessed Mar. 1, 2022).
- [32] C. Bulle et al., "IMPACT World+: a globally regionalized life cycle impact assessment method," *Int. J. Life Cycle Assess.*, vol. 24, no. 9, pp. 1653–1674, 2019, <http://dx.doi.org/10.1007/s11367-019-01583-0>.
- [33] M. Franco, D. Carvalho, W. Carvalho, C. Felipe, and Azevedo, D., "Enhancing the eco-efficiency of concrete using engineered recycled mineral admixtures and recycled aggregates," vol. 257, p. 120530, 2020, <http://dx.doi.org/10.1016/j.jclepro.2020.120530>.
- [34] D. Fan et al., "Precise design and characteristics prediction of Ultra-High Performance Concrete (UHPC) based on artificial intelligence techniques," *Cem. Concr. Compos.*, vol. 122, pp. 104171, Sep 2021, <http://dx.doi.org/10.1016/j.cemconcomp.2021.104171>.
- [35] A. Tama, "Application of life-cycle assessment for the study of carbon and water footprints of the 16.5 MWe wind farm in Villonaco, Loja, Ecuador," *Smart Grid Renew. Energy*, vol. 12, no. 12, pp. 203–230, 2021, <http://dx.doi.org/10.4236/sgre.2021.1212012>.
- [36] A. Miranda de Souza et al., "Application of the desirability function for the development of new composite eco-efficiency indicators for concrete," *J. Build. Eng.*, vol. 40, pp. 102374, Aug. 2021, <http://dx.doi.org/10.1016/j.jobe.2021.102374>.
- [37] G. Habert and N. Roussel, "Study of two concrete mix-design strategies to reach carbon mitigation objectives," *Cement Concr. Compos.*, vol. 31, no. 6, pp. 397–402, Jul 2009, <http://dx.doi.org/10.1016/j.cemconcomp.2009.04.001>.
- [38] A. Peyroteo, M. Silva, and S. Jalali, *Life Cycle Assessment of Steel and Reinforced Concrete Structures: A New Analysis Tool*, Amsterdam, The Netherlands: IOS Press, 2007. accessed Mar. 1, 2022. [Online]. Available: <https://hdl.handle.net/1822/7578>

Author contributions: BAB: Conceptualization, Methodology, Writing – original draft preparation; TCD: Methodology; PL: Methodology, Writing – review and editing, Supervision.

Editors: Edna Possan, Mark Alexander



ORIGINAL ARTICLE

Analysis of CO₂ emissions and waste elimination capacity of different recycling strategies applied in ready-mixed concrete plants

Análise das emissões de CO₂ e capacidade de eliminação de resíduos de diferentes estratégias de reciclagem aplicadas em centrais dosadoras de concreto

Luiz de Brito Prado Vieira^{a,b}

Antônio Domingues de Figueiredo^a

Fabio Cirilo^b

Vicente Bueno Verdiani^c

Leonardo Moreira de Lima^c



^aUniversidade de São Paulo – USP, Escola Politécnica, São Paulo, SP, Brasil

^bVotorantim Cimentos, São Paulo, SP, Brasil

^cUniversidade Federal de São Carlos – UFSCar, Centro de Ciências e Tecnologias para Sustentabilidade, Sorocaba, SP, Brasil

Received 11 March 2022

Accepted 25 October 2022

Abstract: The volume of waste generated by ready-mix concrete (RMC) plants in Brazil is significant. According to Oliveira et al. [1] waste from construction and demolition in Brazil was approximately 45-79 million tons and most of those waste is sent to landfills (79%). This study presents an assessment of the RMC plant waste reduction capacity using 3 different methods: (a) reuse of concrete in the fresh state by using hydration-stabilizing admixtures (HSA); (b) recycling of concrete aggregates by separating the aggregates from the cement paste before the concrete hardens; (c) recycling of hardened concrete as aggregates through the crushing process. Results indicated that concretes with compressive strengths up to 25.0 MPa are more effective in reducing CO₂ emission and consequently CO₂ footprint when using method (b); if evaluating higher resistance classes, method (a) was the most effective.

Keywords: ready mix concrete waste, CO₂ footprint, field test, recycled aggregate, hydration stabilizing admixtures.

Resumo: O volume de resíduos gerados pelas centrais dosadoras de concreto (CDC) no Brasil é expressivo, de acordo com Oliveira et al [1] o resíduo de construção e demolição no Brasil foi de aproximadamente 45-79 milhões de tons e grande parte desse resíduo é enviada para aterros sanitários (79%). Este estudo avalia a capacidade de redução de resíduos da CDC usando 3 diferentes métodos: (a) reaproveitamento do concreto no estado fresco por meio de aditivos estabilizadores de hidratação (AEH); (b) reciclagem dos agregados de concreto separando os agregados da pasta de cimento antes que endureça; (c) reciclagem de concreto endurecido como agregados através do processo de britagem. Resultados apontam que concretos de resistências até 25,0 MPa, são mais efetivos na redução de CO₂ e pegada de carbono quando utilizado o método (b), se avaliada classes de resistências maiores, o método (a) foi o mais efetivo.

Palavras-chave: resíduos de concreto usinado, pegada de carbono, teste de campo, agregado reciclado, aditivos estabilizadores de hidratação.

How to cite: L. B. P. Vieira, A. D. Figueiredo, F. Cirilo, V. B. Verdiani, and L. M. Lima, "Analysis of CO₂ emissions and waste elimination capacity of different recycling strategies applied in ready-mixed concrete plants," *Rev. IBRACON Estrut. Mater.*, vol. 15, no. 6, e15611, 2022, <https://doi.org/10.1590/S1983-41952022000600011>

Corresponding author: Luiz de Brito Prado Vieira. E-mail: luiz.vieira@vcimentos.com

Financial support: None.

Conflict of interest: Nothing to declare.

Data Availability: All the data used is available and can find at the references used.



This is an Open Access article distributed under the terms of the Creative Commons Attribution License, which permits unrestricted use, distribution, and reproduction in any medium, provided the original work is properly cited.

1 INTRODUCTION

Cement-based materials represent about 1/3 of the global material consumption [1] and ready-mix concrete (RMC) is a major product on cement markets in most countries. In Brazil, RMC constitutes ~21% of all cement produced in the country [2]. According to ERMCO [3], the average fraction of the cement market taken by RMC is 50% for the European Union, in the USA and Japan this fraction is above 70%. Considering the consumption of cement, water, and aggregates, RMCs have a sizable environmental impact and, consequently, a high mitigation potential.

The average values of raw material consumption in the production of RMCs reported in the survey by Lima [4] indicate that the annual volume of concrete produced by RMC plants in Brazil is around 50 million cubic meters. Consequently, 14 million tons of cements, 98 million tons of aggregates, 9 million tons of water, and 70 thousand tons of admixture, are used annually. Much attention has been given recently to the dosage optimization for reducing the carbon footprint [5] because most of the CO₂ emissions associated with concrete are due to the cement production process and is related to the clinkerization process. To produce 1 ton of clinker around the same quantity of CO₂ is also produced [6]. However, relatively little attention was paid to the aspects related to the resource use efficiency, such as the generation and reuse of concrete waste by RMC plants.

Evaluating the impact of the concrete industry, Vieira et al. [7] estimated that approximately 3% of all concrete produced in RMC plants returns as waste. If we consider the 50 million m³ as a Brazilian production, this represents 1.5 million m³ of waste.

In many countries, the cost of disposing such waste in landfills is growing, which requires developing strategies for minimizing the generation of waste in their operation. According to John [8], although construction companies use large amounts of waste from other industries, recycling rates are low and the mere fact that a product contains waste does not guarantee that its environmental impact is lower than a product consisting of virgin materials.

Based on Xuan et al. [9], there are three main methods for diverting waste from landfills: (a) reuse of concrete in the fresh state by using hydration-stabilizing admixtures (HSA); (b) recycling concrete aggregates by separating the aggregates from the cement paste before concrete hardening; (c) recycling of concrete in the hardened state by crushing, transforming it into recycled aggregates. Selecting the best strategy for waste minimization and management depends on technical conditions, costs, and even on cultural factors.

For reusing waste concrete when it is still fresh, hydration reactions of the cement present in the waste that returns to the RMC plant are delayed for a few hours or even for a few days by adding special chemical products, called hydration-stabilizing admixtures (HSA). Gebremichael et al. [10] demonstrated the possibility of adding the HSA to stop the hydration of the concrete and allow its reuse. They also indicated that in some cases using HSA-stabilized concrete as a raw material for new concrete may increase the compressive strength of the final product. Haddad et al. [11] concluded that the reuse of HSA-treated concrete could be viable from both economic and technical points of view.

Removal of aggregates from returned concrete in the fresh state can be achieved by rotational sieving and washing by water. This process allows the reuse of recovered aggregates [12] but yields a slurry as a secondary waste. Scale tests using two different types of recyclers, carried out by Vieira and Figueiredo [13], concluded that the physical characteristics of the obtained washed aggregates are similar to those of the original aggregates, and the influence of the equipment type is negligible. The reuse of the slurry has an intrinsic difficulty associated with the need to adjust the rheology of new concrete that incorporates this waste [14]. The produced slurry can be treated using decantation systems, recovering most of the water and reducing the amount of disposable waste [15]. The other route consists of submitting the slurry to a filter-press system [16]. Therefore, this approach in general incurs an extra work to eliminate the entire waste volume produced in the RMC production.

The third approach is to use hardened concrete as crushed recycled aggregates. The resulting aggregates have higher porosity than ordinary aggregates. They are normally processed to have the same particle size distribution as the original coarse aggregates, to enable the reintroduction of this waste into new formulations [17]. Fines generated during the crushing process are usually transformed into new waste, reducing the recovering rate to ~30–50% [18]. Because higher-porosity recycled aggregates yield lower-strength concretes than regular aggregates, higher cement content may be required to compensate for this loss [19], [20]. Therefore, partial substitution of natural aggregates for recycled aggregates could be an interesting venue. The substitution percentage likely depends on the properties of crushed recycled aggregates and strength requirements for the new concrete [21].

The reuse of waste by RMC companies using different recycling techniques is a relatively well-established practice in many markets, such as in North America [22], China [23], and Turkey [24]. However, there are no studies of industrial-scale comparison of the environmental efficiency of these recycling methods, at least to the knowledge of the authors.

As stated by Damineli *et al.* [25], comparative assessment of the environmental efficiency of concretes can be performed in terms of the ratio of the cement consumption per cubic meter of concrete per unit of compressive strength obtained for the material. This consideration is convenient for measuring the overall environmental impact of any level

of strength of structural concrete. Therefore, this study aimed to evaluate the environmental indicators of the three main methods of concrete waste reuse, in terms of CO₂ emission and the waste reduction capacity during the concrete production by RMC plants. In that sense, this work compares the production of conventional concretes and concretes that use reused materials obtained using different strategies.

2 MATERIALS AND EXPERIMENTAL PROGRAM

This study consists of two parts. In the first one, the different strategies are evaluated in terms of their capacity of waste reuse in the concrete production together with the potential sub-product generation. In the second, these strategies are evaluated in terms of their generated CO₂ emission. The first part of the study was performed using previously published data for individual strategies: 1) reuse of fresh concrete waste with stabilizer admixtures [26], 2) recycling of hardened concrete by crushing [27] and 3) recycling of fresh concrete by mechanical processing through washing and sieving [13]. In this study, two different types of equipment used in fresh concrete recycling by mechanical processing were evaluated: 3.1) drum-type (D) and 3.2) rotary sieve-type (R). It is important to mention that, owing to the lack of reliable data, this study did not account for the capacity of these processes to reduce the amount of water used to wash concrete trucks, moisten aggregates, and clean the plant floor.

The notation used to represent the recycled concrete was as follows:

- Reuse - HSA: Concrete produced by reusing fresh concrete waste with a stabilizing admixture
- Recovery - D: Concrete produced from aggregates recovered by recycling fresh concrete by mechanical processing and drum-type equipment
- Recovery - R: Concrete produced from aggregates recovered using the mechanical concrete recycling method and rotary-type equipment
- Recycle - C: Crushed concrete aggregates obtained using the crushing hardened concrete recycling method

To estimate the waste reduction capacity in the production of RMC, it was limited to ordinary concrete only that means to those cases where ordinary raw materials are used, which corresponds to approximately 90% of concrete produced by RMC plants [13]–[27]. This is because normal concretes are more easily reusable than special concretes, such as those containing fibers, pigments, or any other addition. It also separately analyzed the impact of each one of the concrete reuse procedures according to the type of waste generated.

The differences that involve the reuse of adhered concrete and concrete leftovers have also been considered. According to Sealey et al. [28], adhered concrete is a fraction of ready mixed concrete that returns because it remains adhered to the inner surface of a mixer drum and is removed only by washing. Leftover concrete covers fresh concrete that for various reasons is returned to the plant [29]. Vieira et al. [7] showed that, in Brazil, the volume of adhered concrete ranges between 90 and 200 liters per truck trip, and the volume of concrete leftovers is mainly associated with two factors: excessive concrete order and excessive application time. The average volume of leftovers is under 1.5 m³ and only occurs in 5% of deliveries. The efficiency analysis considered the potential capacity of each strategy to reuse each of these waste volumes: adhered concrete and leftovers. The volume of the total waste generated corresponds to ~3.0% of the volume of concrete produced, which corresponds to 53% of the waste (1.6% of the volume produced) owing to adhered concrete and 47% of the waste (1.4% of the volume produced) owing to leftovers [7]. Taking to account the volume of concrete produced by the RMC plants in Brazil described by Lima [4], it is estimated that nearly 420 thousand tons of cement, 2,940 thousand tons of aggregates, and 270 thousand tons of water are returned to the Brazilian RMC plants each year.

The CO₂ emission of concretes produced exclusively using raw materials and those produced using inputs from waste reuse/recycling techniques was compared for concretes in different compressive strength categories (C20, C30, C30, C35, and C40). To enable this comparison, all concretes were mix-designed according to the method traditionally used by RMC producers [30]. The dosage curves for the concrete produced using conventional raw materials and using reused raw materials were reported previously by some of the authors of this article [13], [26], [27].

In a comparative evaluation of the CO₂ emission, the impact of raw materials and their transportation from the place of production to the RMC plant and the impacts to transport during the preparation and delivery of the concrete were analyzed. The impact of reuse/recycled inputs on the mechanical strength of concrete and the CO₂ emission of the respective production process, as well as the impact of the emission owing to the waste freight from the concrete plant to landfill were analyzed. The compositions studied refer to the concrete in the S100 category (slump class of 100 mm) and strength classes C20, C25, C30, C35, and C40.

The CO₂ emission of concrete was calculated by multiplying the CO₂ emission factor of each input by the CO₂ emitted in the concrete production process at the plant. This calculation accounts for loading raw materials into the plant and their mixture. Therefore, the final CO₂ emission factor represents all the CO₂ emission generated in the entire production process of concrete.

The cement considered was CP II E 40, which was produced by Votorantim Cimentos at the Santa Helena factory. The cement production process includes the phases of extraction of raw materials, processing, homogenization, flour production, clinker production, cooling, milling, storage and dispatch of the cement, internal transportation at the plant was also factored in.

The processes of production of conventional aggregates include multiple stages: extraction of resources, processing, sieving, storage and dispatch of materials for the RMC plant, and internal transportation. Usually in the Brazilian market “natural sands” refers to the aggregates derived from sandbanks, while fine aggregates from rock crushing are known as “artificial sands”. Natural sands account for ~20% of all aggregates used by the analyzed RMC producer.

The water used by RMC producers was a mixture of water from semi artesian wells, reused rainwater, and water for cleaning the mixing trucks. Concretes formulated with water-reducing plasticizer additive and HSA were analyzed, respectively classified as Type A and Type D additives according to ASTM C494.

The boundaries of the concrete production and waste reuse system (Figure 1) considered the inputs used to produce concrete in mass quantity and in volume the returned concrete. The recycled waste was considered free of the CO₂ emission, except for the emission attributed to the reuse process itself. The concrete specific weight used was 2.461 ton/m³ (the reference concrete was C30, slump class S100), but it can change according to the compressive strength adopted.

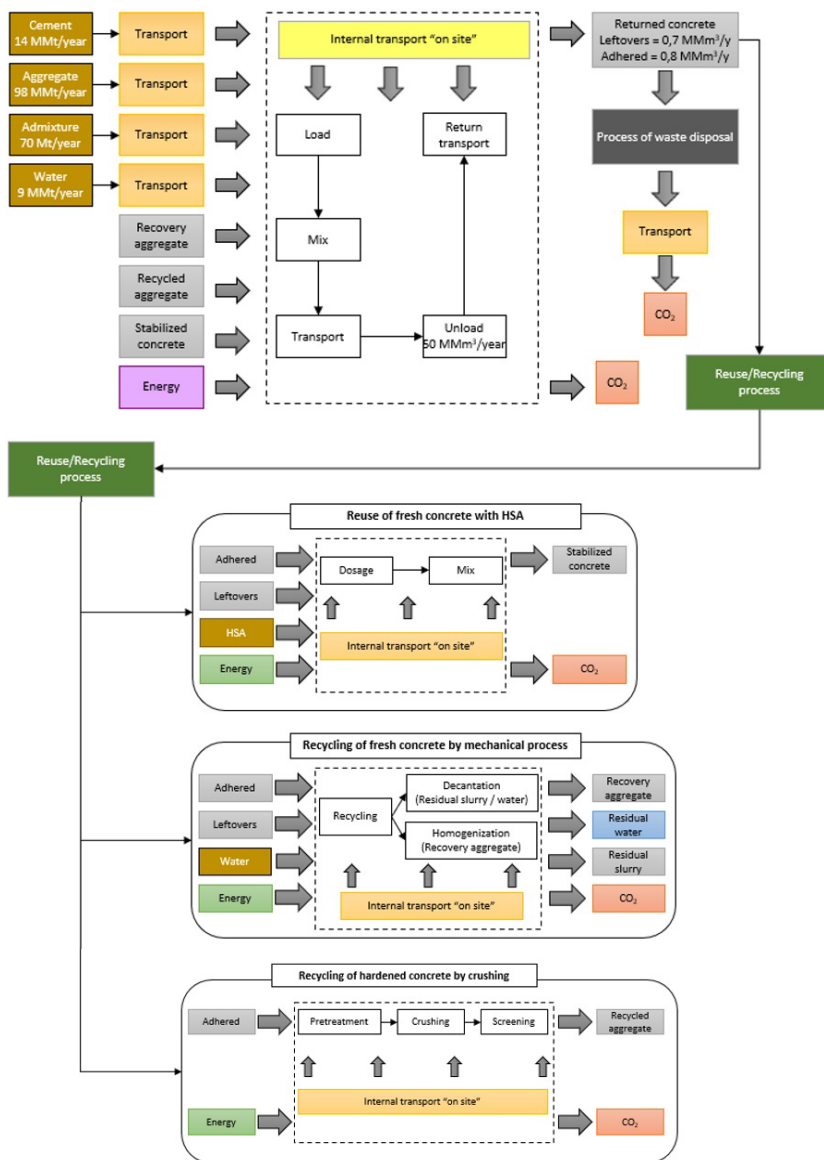


Figure 1. Boundaries of the RMC production system.

The CO₂ emission of concrete can be calculated by incorporating the CO₂ emission factors of all raw materials, based on the amount of raw materials. To the obtained value, one should add CO₂ emission owing to the concrete production and transport operations, as explained by Hong et al. [31]. Table 1 lists the CO₂ emission factors associated with the production of different raw materials used in this study.

Table 1. CO₂ emission factors for virgin raw materials.

Material	CO ₂ emission factor (t CO ₂ /t)	Source
Cement	0.789*	[32]
Fine aggregate - Natural sands	0.0069	[33]
Fine aggregate - Artificial sands	0.0046	[34]
Coarse aggregate	0.0013	[35]
Admixture	-0.000855**	[36]
Water	0.0002***	[37]

* Considering that all CO₂ emitted comes from the calcination of limestone and there isn't other source of CO₂ in the process. ** Admixture contribution is negligible and won't be considered. The quantity of admixture in 1 m³ is related of the quantity of cement and a ordinary C30 class concrete uses around 2,5 liters of admixture. Then the contribution in a 1m³ of concrete is approximately -0.000855 t CO₂. *** Water contribution is also negligible and won't be considered.

The production process of concrete involves weighing all raw materials, their homogenization, transporting the concrete to the job site, unloading the concrete, and returning the truck to the RMC plant. This process also assumes that all the movement and transportation of the materials is performed at the plant, which indicates that the CO₂ emission factor of the concrete production, measured at RMC plant, is 0.0065 t CO₂ / t. The data used for the inventory analysis of the concrete production process were obtained by direct measurements, which were performed for the elaboration of the environmental product declaration, registered in the International EPD System: SP-00896 [38]. The numbers showed at LCA describe all the environment impacts related to the process and was showed in CO₂ eq.

The nominal capacity of operation, power and energy consumption considered for the calculation of the CO₂ emission factor related to the production of reused and recycled aggregates were obtained directly from the technical specifications of each equipment [39]–[41]. The CO₂ emission factor owing to the generation of electric energy was obtained from official data published by the Ministry of Science and Technology (MCT) [42].

Calculation of the transportation-related emission accounted for the average distances obtained from truck drivers and also accounted for loading and unloading of the materials. The CO₂ emission factor was calculated according to the inventory proposed by the Brazilian Program GHG Protocol [43] and Carvalho [44] accounted for the characteristics of national fuels and vehicles. The values adopted in this study for the CO₂ emission analysis were 0.00242 kg CO₂/t.km for silo and tipper trucks and 0.00584 kg CO₂/t.km for tanker and drum trucks.

3 RESULTS AND DISCUSSIONS

3.1 Efficiency Analysis

The method that reuses fresh concrete with HSA can be utilized for reusing adhered concrete and leftover concrete that is returned to a plant within 4 hours of starting the cement hydration [45]. Studies by Vieira and Figueiredo [26] showed that, in Brazil, ~99% of concrete waste that returned to plants satisfy this requirement. Thus, this method has the potential to reuse 89% by mass of raw materials that are returned to a typical RMC plant, which corresponds to the volume related to all ordinary concretes less special concretes [13]–[26].

The method that recycles fresh concrete by washing and sieving can also be utilized for reusing adhered concrete and leftover concrete. Full-scale tests performed by Vieira and Figueiredo [13] concluded that reused recovered aggregates are often used in concretes with compressive strength up to 25 MPa. However, the same tests showed that using slurries in new concrete mixtures is not economically viable, because the negatives effects in compressive strength and workability [13]. Therefore, in practice, this technique allows to reuse only the water and the aggregates that are contained in the leftover concrete that are returned to RMC plants; this method can account for ~88% of the mass amount of leftover concrete (considering the 99% less the 11%, in average, of cement [7]). Considering only ordinary concretes, this method can reuse only 36% (leftover waste represent 45% by mass [7]) of the materials that are returned to a typical RMC plant.

The method that recycles concrete in the hardened state by crushing and producing crushed aggregates that are used within 48 hours from the beginning of the cement hydration as natural aggregate substitutes, increases the mechanical strength owing to a high w/c ratio, because a portion of this aggregate consists of the cement that is not fully hydrated [46].

A study by Vieira et al. [27] showed that this technique can be successfully used with concrete leftovers returned to RMC plants. However, reusing adhered concrete is not operationally feasible as the amount of water necessary to remove the adhered concrete from the inside of the concrete mixer drum prevents this waste from being crushed within 48 hours. Considering that, in paper [27], the concrete reuse technique through the production of recycled aggregates was not used to eliminate adhered concrete waste, which correspond to approximately 55% of the total volume of concrete returned to Brazilian RMC plants, it is possible to deduce that this method allows the reuse about 41% (leftover waste represent 45% by mass [7]) of the total concrete waste that is currently generated by RMC producers [13].

The methods of recycling fresh concrete by washing and sieving, or the methods of recycling hardened concrete by crushing and producing recycled aggregates, are operationally suitable for reusing concrete leftovers [13]–[27]. However, they are not suitable for reusing concrete that is adhered to the concrete truck drum. The reuse method of fresh concrete with HSA allows both the reuse of adhered and leftover concrete [26]. However, there is one important limitation, in this case - it is only possible to reuse concrete with cement for which hydration had been started at most 4 hours before. On the other hand, this method does not generate slurries, which is a significant advantage for RMC plants, implying the plants do not have to deal with this secondary waste.

Individually, none of the analyzed methods can eliminate the waste generated during the RMC plant operation (Table 2). One main limitation is the fact that there are operational difficulties associated with reusing certain concretes that are considered as "specials" (e.g., concretes with fibers, concretes with pigments). Therefore, the analysis of the waste reduction capacity was performed considering only the regular concrete volume. In addition, the calculation of the waste reduction ability assumed that 45% of the waste is leftover concrete and 55% is adhered concrete.

Table 2. Waste reduction capacity of each evaluated method in terms of regular concretes produced at an RMC plant.

Method	Ability to waste reduction					Source
	Nominal		Real			
	Leftover	Adhered	Leftover	Adhered	Total	
Reuse of fresh concrete with HAS	99%	99%	89%	89%	89%	[13]–[26]
Recycling of fresh concrete by mechanical process	88%	0%	79%	0%	36%	[7]–[13]
Recycling of hardened concrete by crushing	100%	0%	90%	0%	41%	[13]–[27]

From the operational point of view (process implementation) it is important to keep in mind that, in the case of the method that reuses fresh concrete through HSA, concrete truck drivers need to be very well trained in reuse procedures. In addition, there is always a risk of concrete hardening inside the mixing drum. The processes that recycle fresh concrete by mechanical processing and recycle hardened concrete by crushing are simpler to implement, because there is no need to train the concrete truck drivers, and there is no risk of concrete hardening in the trucks’ mixing drums because concrete recycling is not accomplished in the concrete trucks’ drums.

3.2 CO₂ Emission Analysis

Figure 2 shows the dosage curves for concretes produced using conventional components that are normally used by RMC producers, and for other concretes considered in this study, based on the previous studies by the authors: Reuse - HSA [26]; Recovery - D and Recovery - R [13]; Recycle - C [27].

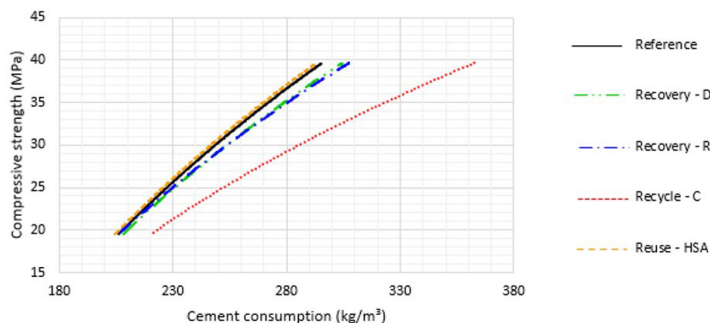


Figure 2. Concrete mixing design curves.

The method that reuses fresh concrete with HSA does not require investing into the equipment acquisition, and the electricity and water consumption of the plant are not affected. The other methods analyzed in this study require equipment-related investments; in addition, using such specialized equipment increases the power and water consumption of the plant.

The measurements performed by the RMC producer with respect to the equipment installed in the plant, were based on the equipment producer information [39]–[41] and calculated using the concrete specific weight as 2.461 ton/m³ (the reference concrete was C30, slump class S100) [7].

- The spiral recycler (Liebherr LRS 806) has the capacity of 12 m³/h, power of 11.0 kw, and energy consumption of 0.36 kwh/t.
- The rotary-type equipment (Schwing-Stetter RA 12) has the capacity of 12 m³/h, power considered of 22.5 kw, and energy consumption of 0.76 kwh/t.
- The jaw crusher (Nordberg® C80) used in the production of recycled aggregate has the capacity of 25 m³/h, power of 75 kw, and energy consumption of 1.22 kwh/t.
- The HSA is transported in a 12-ton-capacity tank truck from Sorocaba/SP to São Paulo/SP (74 km from the producer to the concrete plant).

Capacity, power, and energy consumption data allow to calculate the CO₂ emission factors for each type of raw material produced using the different reuse techniques; these factors are listed in Table 3.

Table 3. CO₂ emission factors for reused raw materials.

Material	CO ₂ emission factor (t CO ₂ /t)
Reuse – HSA concrete	3x10 ⁻⁴
Recycle aggregate (C)	4x10 ⁻⁴
Recovery aggregate (D)	5x10 ⁻⁴
Recovery aggregate (R)	5x10 ⁻⁴

CO₂ emission analysis (Figure 3) shows that the type of cement explains more than 90% of CO₂ emission. Concrete production is the second most important influencer of the CO₂ emission factor, explaining 3%, mostly owing to the impact of concrete transportation between the plant and work sites. In turn, the aggregate type and the admixture type explain only ~2% and ~1.5%, respectively. Considering the overall CO₂ emission for compressive strength C30 class concrete, the emission associated with the Reuse - HSA case is 1% lower than the emission associated with the reference concrete case and is nearly the same as the emission associated with the concrete produced using recovered aggregates (Recovery - D and Recovery - R). That is possible, because the consumption of cement, the most responsible for CO₂ emission, is almost the same in those tests (Reference, Recovery-D, Recovery-R and Reuse-HSA). The emission associated with the concrete produced from recycled aggregates obtained from crushed hardened concrete (Recycling - C) is 13% higher than the reference case.

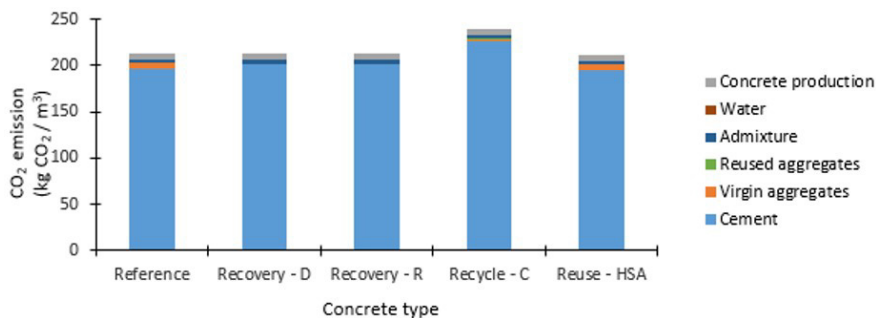


Figure 3. CO₂ emission levels for compressive strength class C30 concretes.

Within the constraints of the system and the methods used in this study, it was possible to estimate CO₂ emission factors associated with the production of one cubic meter of concrete slump 100 mm, as shown in Figure 4. The CO₂ emission factor increases with increasing the compressive strength, confirming the conclusions of Flower and Sanjayan [47] and Oliveira et al. [48].

The CO₂ emission factor for concretes prepared using recycled aggregates (Recycling - C) is higher than that of all other concretes, for all considered compressive strengths. On the other hand, the smallest emission factor was obtained for the concretes prepared using stabilized concretes (Reuse - HSA), for all considered compressive strengths. The concretes prepared using recovered aggregates (Recovery - D and Recovery-R) lower weaker CO₂ emission than the reference concrete when the concrete compressive strength was below C30; the effect was the opposite for the concrete compressive strengths above C30.

This increase in emission is attributed to the requirement that the complementary cement that is used in concrete will mitigate the loss of strength caused by the use of waste. In the case of concrete with compressive strength under 30 MPa, the lower CO₂ emission resulting from the replacement of "virgin" aggregates with recovered aggregates is sufficient to compensate the CO₂ emission owing to the increase in the cement amount. Note that the higher the concrete compressive strength, the higher is its load capacity. Therefore, higher load capacities require smaller amounts of concrete, as pointed out by Habert et al. [49].

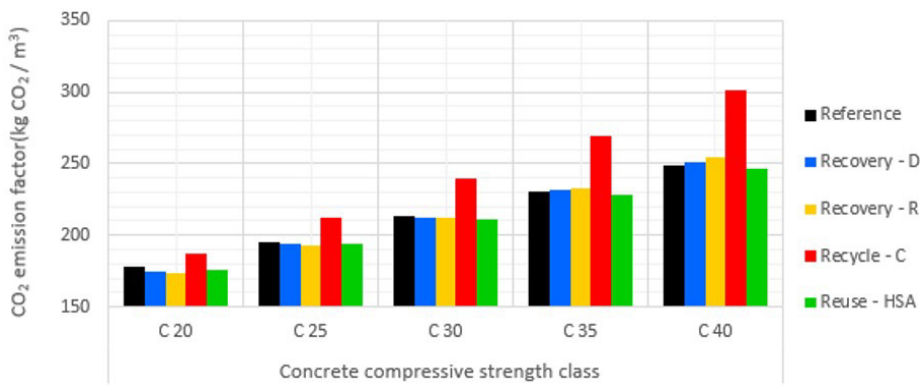


Figure 4. CO₂ emission of 1 m³ of concrete with 100 mm slump, for different concrete types.

From the observed results (Figure 5), it is possible to state that the waste reuse strategy that uses HSA (Reuse - HSA) is more efficient with respect to the CO₂ emission than the approach that uses virgin raw materials (Reference concrete), regardless of the concrete compressive strength.

In the case of concretes with compressive strength C20, the method that recycles fresh concrete by mechanical processing (Recovery - D and Recovery-R) yielded the highest overall efficiency in terms of the CO₂ emission. For C25 compressive strength concretes, recycling of fresh concrete by mechanical processing and reusing fresh concrete with HSA yielded the same CO₂ emission. For the concrete compressive strength C30, the reference concrete had the same CO₂ emission as that obtained by recycling fresh concrete using mechanical processing. This reflected the need to add an incremental amount of cement to compensate the strength loss of recycled concrete. Therefore, there is a critical compressive strength (C35), above which replacing recovered aggregates with virgin aggregates increases the CO₂ footprint.

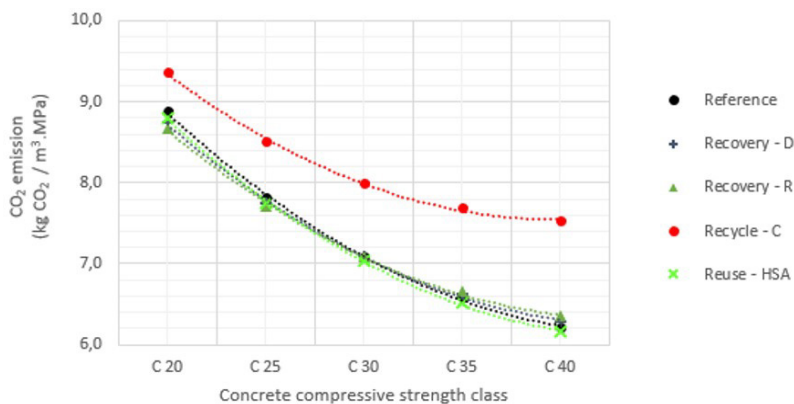


Figure 5. CO₂ emission per MPa of 1 m³ of concrete with 100 mm slump, vs. concrete compressive strength.

4 CONCLUSIONS

Despite being within the world average, the RMC industrial sector in Brazil generates a significant amount of waste, approximately 45-79 million tons and most of this waste is sent to landfills (79%) [6]. Vieira et al. [7] also mentioned that approximately 3% of all concrete produced in a RMC plant is returned as waste, representing something around 1,5 million m³ per year [4]. This creates significant problems and incurs a high cost on the transportation and proper disposal of this waste.

When the problem is evaluated globally, the RMC industry produces 14 billion m³ of concrete [50] and keeping the same percentage of 3% as a reference, the volume of waste generated would be approximated 420 million m³, which highlights the high potential for greater investments in the management of construction waste to reduce CO₂.

The method that reuses fresh concrete with HSA is capable of reusing leftover and adhered concrete. Using this method allows to eliminate 89% of the concrete that returns to RMC factories; however, its implementation requires training concrete truck drivers, and there is a risk of concrete hardening inside the mixer drum. Operationally, the other methods analyzed are simpler to implement in RMC plants; however, these other methods require investments for the specialized equipment acquisition, as well as an area for the equipment installation; this can be an impediment, especially for plants in large urban centers, where little area is available. The crushing recycling method has a 5% higher waste reuse capacity than the fresh concrete recycling method that uses mechanical processing. This is because, in practice, scale tests performed by Vieira and Figueiredo [13] show that slurry recycling is not feasible.

Approximately 90% of the CO₂ emission associated with concrete comes from cement. Consequently, the recycling methods that require the addition of incremental cement exhibited, in general, higher CO₂ emission rates and higher CO₂ footprints. The concrete produced using the method that reused fresh concrete with HSA yielded a lower CO₂ emission factor than the reference concrete. This was attributed to the fact that it was not necessary to add extra cement during the process, as well as to the small amount of HSA used.

The CO₂ specific footprint analysis clearly identified that concretes with compressive strength above 30 MPa are likely to generate higher total CO₂ emission when concrete is produced with aggregates recovered by recycling fresh concrete. Consequently, the increase in the CO₂ emissions owing to the need for additional cement to compensate the loss of strength of recycled concrete has a greater influence on the CO₂ footprint than the volume of virgin aggregates replaced by recovered aggregates.

Recycling of fresh concrete by mechanical processing is the best solution for mitigating the CO₂ emission for concretes with compressive strength below C25. For higher compressive strength, using hydration-stabilizing admixtures is the best solution for reusing the concrete waste by RMC plants. This latter method is also the best option for reducing the waste generation in general, as it allows to reuse almost all of the generated waste (adhered concrete and leftovers), with the exception of concrete returned with cement that started its reaction over a period of more than 4 hours.

The method that recycles concrete in the hardened state by crushing and producing crushed aggregates offers an intermediate waste reduction strategy, between those of the method for recycling fresh concrete using mechanical processing and the method that reuses fresh concrete with HSA. However, in terms of the CO₂ footprint reduction, this method exhibits the worst performance among the evaluated methods as well as the reference concrete.

Another line of research is the reduction of the cement clinker factor through the addition of reactive or non-reactive materials. In Brazil, several materials are added: blast furnace slag, pozzolan, carbonate material, etc. Oliveira et al. [6] studied the addition of the fine fraction of concrete waste as an addition to cement replacing part of clinker. This would reduce not only construction waste but also the cement clinker factor.

ACKNOWLEDGEMENTS

The author thanks Votorantim Cimentos for all the help provided.

REFERENCES

- [1] F. Krausmann, S. Gingrich, N. Eisenmenger, K. H. Erb, H. Haberl, and M. Fischer-Kowalski, "Growth in global materials use, GDP and population during the 20th century," *Ecol. Econ.*, vol. 68, no. 10, pp. 2696–2705, 2009. Accessed: Sept. 1, 2022. [Online]. Available: https://www.researchgate.net/profile/Marina-Fischer-Kowalski/publication/222430349_Growth_in_global_materials_use_GDP_and_population_during_the_20th_century/links/59e336b3a6fdcc7154db72b8/Growth-in-global-materials-use-GDP-and-population-during-the-20th-century.pdf
- [2] Sindicato Nacional da Indústria de Cimento – SNIC. "Relatório Anual da Indústria Brasileira de cimento – 2013." http://smic.org.br/assets/pdf/relatorio_anual/rel_anual_2013.pdf (accessed Sept. 1, 2013).
- [3] European Ready Mixed Concrete Organization – ERMCO. "Ready-mixed concrete industry statistics." <https://ermco.eu/statistics-2003-2018/> (accessed July 28, 2016).

- [4] J. A. R. Lima, "Avaliação das conseqüências da produção de concreto no Brasil para as mudanças climáticas", PhD dissertation, Esc. Politéc., Univ. São Paulo, São Paulo, Brasil, 2010. [Online]. Available: https://teses.usp.br/teses/disponiveis/3/3146/tde-23082010-105858/publico/Tese_Jose_Antonio_Ribeiro_Lima.pdf
- [5] V. M. John and F. P. Glasser, "Editorial", *Adv. Cem. Res.*, vol. 28, no. 6, pp. 355-356, 2016. Accessed: Sept. 1, 2022. [Online]. Available: <https://www.icevirtuallibrary.com/doi/full/10.1680/jadcr.2016.28.6.355>
- [6] T. C. F. Oliveira, B. G. S. Dezen, and E. Possan, "Use of concrete fine fraction waste as a replacement of Portland Cement," *J. Clean. Prod.*, vol. 273, no. 123126, 2020, <http://dx.doi.org/10.1016/j.jclepro.2020.123126>.
- [7] L. D. B. P. Vieira, A. D. Figueiredo, V. M. John, and T. Moriggi, "Waste generation resulting from the production of ready-mixed concrete," *Waste Manag.*, vol. 94, pp. 146-152, 2019, <http://dx.doi.org/10.1016/j.wasman.2019.05.043>.
- [8] V. M. John, "Materiais de construção e o meio ambiente", in *Materiais de Construção Civil e Princípios de Ciência e Engenharia de Materiais*, G. Isaia, Ed., São Paulo: IBRACON, 2010, pp. 97-121. Accessed: Sept. 1, 2022. [Online]. Available: <https://prp.usp.br/wp-content/uploads/sites/277/2017/05/VMJOHN-Materiais-e-o-meio-ambiente-2017-09-30-1.pdf>
- [9] D. Xuan, B. Zhan, C. S. Poon, and W. Zheng, "Management and sustainable utilization of processing wastes from ready-mixed concrete plants in construction: A review," *Resour. Conserv. Recycling*, vol. 136, pp. 238-247, 2018, <http://dx.doi.org/10.1016/j.resconrec.2018.04.007>.
- [10] N. N. Gebremichael, M. Karakouzian, and K. Jadidi, "Investigation of setting time and compressive strength of ready-mixed concrete blended with returned fresh concrete," *Constr. Build. Mater.*, vol. 197, pp. 428-435, 2019, <http://dx.doi.org/10.1016/j.conbuildmat.2018.11.201>.
- [11] A. N. Haddad, B. G. F. R. Cortes, and A. C. J. Evangelista, "Use of cement hydration stabilizer admixture at ready mix concrete to avoid material waste," *Adv. Mat. Res.*, vol. 818, pp. 24-29, 2013, <http://dx.doi.org/10.4028/www.scientific.net/AMR.818.24>.
- [12] V. W. Y. Tam and C. M. Tam, "Economic comparison of recycling over-ordered fresh concrete: A case study approach," *Resour. Conserv. Recycling*, vol. 52, no. 2, pp. 208-218, 2007, <http://dx.doi.org/10.1016/j.resconrec.2006.12.005>.
- [13] L. D. B. P. Vieira and A. D. Figueiredo, "Evaluation of concrete recycling system efficiency for ready-mix concrete plants," *Waste Manag.*, vol. 56, pp. 337-351, 2016, <http://dx.doi.org/10.1016/j.wasman.2016.07.015>.
- [14] D. O. F. Silva, M. Quattrone, R. C. O. Romano, and S. C. Angulo, "Reuse of fines from ready-mix concrete washing slurries," *Resour. Conserv. Recycling*, vol. 155, pp. 104653, 2020, <http://dx.doi.org/10.1016/j.resconrec.2019.104653>.
- [15] C. Lobo and G. M. Mullings, "Recycled water in ready mixed concrete operations," *Concr. InFOCUS*, vol. 2, no. 1, pp. 17-26, 2003.
- [16] M. Zervaki, C. Leptokaridis, and S. Tsimas, "Reuse of by-products from ready-mixed concrete plants for the production of cement mortars," *J. Sustain. Dev. Energy Water Environ. Syst.*, vol. 1, no. 2, pp. 152-162, 2013, <http://dx.doi.org/10.13044/j.sdewes.2013.01.0011>.
- [17] S. Manzi, C. Mazzotti, and M. C. Bignozzi, "Short and long-term behavior of structural concrete with recycled concrete aggregate," *Cement Concr. Compos.*, vol. 37, pp. 312-318, 2013, <http://dx.doi.org/10.1016/j.cemconcomp.2013.01.003>.
- [18] M. Quattrone, S. C. Angulo, and V. M. John, "Energy and CO₂ from high performance recycled aggregate production," *Resour. Conserv. Recycling*, vol. 90, pp. 21-33, 2014, <http://dx.doi.org/10.1016/j.resconrec.2014.06.003>.
- [19] R. V. Silva, J. De Brito, and R. K. Dhir, "Properties and composition of recycled aggregates from construction and demolition waste suitable for concrete production," *Constr. Build. Mater.*, vol. 65, pp. 201-217, 2014, <http://dx.doi.org/10.1016/j.conbuildmat.2014.04.117>.
- [20] S. C. Angulo, P. M. Camijo, A. D. D. Figueiredo, A. P. Chaves, and V. M. John, "On the classification of mixed construction and demolition waste aggregate by porosity and its impact on the mechanical performance of concrete," *Mater. Struct.*, vol. 43, no. 4, pp. 519-528, 2010, <http://dx.doi.org/10.1617/s11527-009-9508-9>.
- [21] M. Etxeberria, E. Vázquez, A. Mari, and M. Barra, "Influence of amount of recycled coarse aggregates and production process on properties of recycled aggregate concrete," *Cement Concr. Res.*, vol. 37, no. 5, pp. 735-742, 2007, <http://dx.doi.org/10.1016/j.cemconres.2007.02.002>.
- [22] R. Jin, Q. Chen, and A. Soboyejo, "Survey of the current status of sustainable concrete production in the US," *Resour. Conserv. Recycling*, vol. 105, pp. 148-159, 2015, <http://dx.doi.org/10.1016/j.resconrec.2015.10.011>.
- [23] J. Xiao, Z. Ma, and T. Ding, "Reclamation chain of waste concrete: A case study of Shanghai," *Waste Manag.*, vol. 48, pp. 334-343, 2016, <http://dx.doi.org/10.1016/j.wasman.2015.09.018>.
- [24] A. Kazaz and S. Ulubeyli, "Current methods for the utilization of the fresh concrete waste returned to batching plants," *Procedia Eng.*, vol. 161, pp. 42-46, 2016, <http://dx.doi.org/10.1016/j.proeng.2016.08.495>.
- [25] B. L. Damineli, F. M. Kemeid, P. S. Aguiar, and V. M. John, "Measuring the eco-efficiency of cement use," *Cement Concr. Compos.*, vol. 32, no. 8, pp. 555-562, 2010, <http://dx.doi.org/10.1016/j.cemconcomp.2010.07.009>.
- [26] L. D. B. P. Vieira and A. D. Figueiredo, "Implementation of the use of hydration stabilizer admixtures at a ready-mix concrete plant," *Case Stud. Constr. Mater.*, vol. 12, pp. e00334, 2020, <http://dx.doi.org/10.1016/j.cscm.2020.e00334>.
- [27] L. D. B. P. Vieira, A. D. Figueiredo, and V. M. John, "Evaluation of the use of crushed returned concrete as recycled aggregate in ready-mix concrete plant," *J. Build. Eng.*, vol. 101408, 2020, <http://dx.doi.org/10.1016/j.jobbe.2020.101408>.
- [28] B. J. Sealey, P. S. Phillips, and G. J. Hill, "Waste management issues for the UK ready-mixed concrete industry," *Resour. Conserv. Recycling*, vol. 32, no. 3-4, pp. 321-331, 2001, [http://dx.doi.org/10.1016/S0921-3449\(01\)00069-6](http://dx.doi.org/10.1016/S0921-3449(01)00069-6).
- [29] O. Corbu, A. Puskás, A. V. Sandu, A. M. Ioani, K. Hussin, and I. G. Sandu, "New concrete with recycled aggregates from leftover concrete," *Appl. Mech. Mater.*, vol. 754-755, pp. 389-394, 2015., <http://dx.doi.org/10.4028/www.scientific.net/AMM.754-755.389>.

- [30] P. J. M. Monteiro, P. R. L. Helene, and S. H. Kang, "Designing concrete mixtures for strength, elastic modulus and fracture energy," *Mater. Struct.*, vol. 26, pp. 443–452, 1993., <http://dx.doi.org/10.1007/BF02472804>.
- [31] T. Hong, C. Ji, and H. Park, "Integrated model for assessing the cost and CO₂ emission for sustainable structural design in ready-mix concrete," *J. Environ. Manage.*, vol. 103, pp. 1–8, 2012, <http://dx.doi.org/10.1016/j.jenvman.2012.02.034>.
- [32] The International EPD® System. "Environmental Product Declaration (EPD): Product information EPD S-P-00895." Votorantim Cimentos. <https://api.environdec.com/api/v1/EPDLibrary/Files/84e325d9-49a8-4e39-b2fd-9ace124446b8/Data> (accessed Sept. 1, 2017)
- [33] M. P. R. Souza, "Avaliação das emissões de CO₂ antrópico associadas ao processo de produção e concreto, durante a construção de um edifício comercial, na região metropolitana de São Paulo," Inst. Pesq. Tecnol. Est. São Paulo, São Paulo, Brasil, 2012. [Online]. Available: http://cassiopea.ipt.br/teses/2012_TA_Milena_Pinto.pdf
- [34] J. F. Santoro and M. Kripka, "Determinação das emissões de dióxido de carbono das matérias primas do concreto produzido na região norte do Rio Grande do Sul," *Ambient. Constr.*, vol. 16, pp. 35–49, 2016, <http://dx.doi.org/10.1590/s1678-86212016000200078>.
- [35] E. Rossi, "Avaliação do ciclo de vida da brita para a construção civil: estudo de caso," M.S. thesis, Univ. Fed. São Carlos, São Carlos, Brasil, 2013. [Online]. Available: <https://repositorio.ufscar.br/handle/ufscar/4359>
<https://repositorio.ufscar.br/bitstream/handle/ufscar/4359/5350.pdf?sequence=1&isAllowed=y>
- [36] The International EPD® System. "Environmental Product Declaration (EPD): Plasticizing admixture for concrete", <https://api.environdec.com/api/v1/EPDLibrary/Files/60107ad0-5151-4c7a-818e-08d941d5f1c9/Data> (accessed Sept. 28, 2022).
- [37] Companhia de Saneamento Básico do Estado de São Paulo – SABESP, "Sustainability Report Sabesp (english version)", http://site.sabesp.com.br/site/uploads/file/relatorios_sustentabilidade/sabesp_rs_2018_english.pdf (accessed May 9, 2018).
- [38] The International EPD® System. "Environmental Product Declaration (EPD): Product information EPD S-P-00896." Votorantim Cimentos. <https://api.environdec.com/api/v1/EPDLibrary/Files/26d3e953-3198-4fea-b97b-6633ce982b9b/Data> (accessed Sept. 1, 2017)
- [39] Liebherr. "LRS 806: Recycling plant - screw system". <https://www.liebherr.com/en/bra/products/construction-machines/concrete-technology/recycling-plants/lrs-screw-system/details/85992.html> (accessed Jan. 11, 2019)
- [40] Schwing-Stetter. "RA 12: Stetter concrete recycling plants". <https://schwing-stetter.com/products/concrete-recycling-plants/?L=1> (accessed Dec. 7, 2019).
- [41] Metso:Outotec. "Nordberg C Series: Jaw crushers technical specifications". <https://www.mogroup.com/portfolio/nordberg-c-series/?r=1> (accessed Sept. 1, 2019).
- [42] Ministério da Ciência, Tecnologia e Inovações– MCTI. "Fator médio – Inventários corporativos". <https://www.gov.br/mcti/pt-br/acompanhe-omcti/cgcl/paginas/fator-medio-inventarios-corporativos> (accessed June 13, 2018).
- [43] Programa Brasileiro GHG Protocol, *Contabilização, Quantificação e Publicação de Inventários Corporativos de Emissões de Gases de Efeito Estufa*. São Paulo, Brasil: FGV, WRI, 2016. Accessed: Sept. 1, 2022. [Online]. Available: https://s3-sa-east-1.amazonaws.com/arquivos.gvces.com.br/arquivos_ghg/152/especificacoes_pb_ghgprotocol.pdf
- [44] C. H. R. Carvalho, *Emissões Relativas de Poluentes do Transporte Motorizado de Passageiros nos Grandes Centros Urbanos Brasileiros*. Brasília, Brasil: IPEA, 2011. Accessed: Sept. 1, 2022. [Online]. Available: http://repositorio.ipea.gov.br/bitstream/11058/1578/1/td_1606.pdf
- [45] H. R. Benini, "Reaproveitamento de concreto fresco dosado em central com o uso de aditivo estabilizador de hidratação," M.S. thesis, Esc. Politéc., Univ. São Paulo, São Paulo, Brasil, 2005. Accessed: Sept. 1, 2022. [Online]. Available: <https://repositorio.usp.br/item/001488714>
- [46] M. S. Rashwan and S. AbouRizk, "The properties of recycled concrete," *Concr. Int.*, vol. 19, no. 7, pp. 56–60, 1997. Accessed: Sept. 1, 2022. [Online]. Available: <https://www.concrete.org/publications/internationalconcreteabstractsportal/m/details/id/54>
- [47] D. J. Flower and J. G. Sanjayan, "Green house gas emissions due to concrete manufacture," *Int. J. Life Cycle Assess.*, vol. 12, no. 5, pp. 282, 2007, <http://dx.doi.org/10.1065/lca2007.05.327>.
- [48] L. S. Oliveira, S. A. Pacca, and V. M. John, "Variability in the life cycle of concrete block CO₂ emissions and cumulative energy demand in the Brazilian Market," *Constr. Build. Mater.*, vol. 114, pp. 588–594, 2016., <http://dx.doi.org/10.1016/j.conbuildmat.2016.03.134>.
- [49] G. Habert, D. Arribe, T. Dehove, L. Espinasse, and R. Le Roy, "Reducing environmental impact by increasing the strength of concrete: quantification of the improvement to concrete bridges," *J. Clean. Prod.*, vol. 35, pp. 250–262, 2012, <http://dx.doi.org/10.1016/j.jclepro.2012.05.028>.
- [50] Global Cement and Concrete Association. "Global cement and concrete industry announces roadmap to achieve groundbreaking 'net zero' CO₂ emissions by 2050". <https://gccassociation.org/news/global-cement-and-concrete-industry-announces-roadmap-to-achieve-groundbreaking-net-zero-co2-emissions-by-2050> (accessed Oct. 24, 2022)

Author contributions: LBPV: conceptualization, data curation, formal analysis, investigation, methodology, project administration, resources, supervision, validation, writing – original draft; ADF: formal analysis, supervision, validation, writing – review & editing; FC: supervision, data curation; VBV and LML: review, editing.

Editors: Edna Possan, Mark Alexander.



ORIGINAL ARTICLE

Assessment of properties of ultra-high performance cementitious composites with glass powder waste

Avaliação das propriedades de compósitos cimentícios de ultra-alto desempenho com resíduos de pó de vidro

Silvete Mari Soares^a

Taís Oliveira Gonçalves Freitas^b

Adalberto Oliveira Júnior^c

Fernanda Giannotti da Silva Ferreira^d

José Américo Alves Salvador Filho^a



^aInstituto Federal de Educação, Ciência e Tecnologia de São Paulo – IFSP, Caraguatatuba, SP, Brasil

^bUniversidade de São Paulo – USP, Departamento de Ciência dos Materiais, Pirassununga, SP, Brasil

^cROG Locações & Entulhos, Parauapebas, PA, Brasil

^dUniversidade Federal de São Carlos – UFSCar, Departamento de Engenharia Civil, São Carlos, SP, Brasil

Received 14 March 2022

Accepted 25 October 2022

Abstract: Novel developments on concrete technology such as high and ultra-high-performance concrete (HPC and UHPC) are notorious by its high consumption of Portland cement. Supplementary cementitious materials have been used as partial replacement of Portland cement aiming to minimizing clinker content, optimizing the use of binders, reducing CO₂ emissions, and increasing durability. Waste glass powder could be an alternative due to its silica-rich nature and wide availability. This work aims to assess the influence Portland cement substitution by finely ground waste glass powder in contents of 10%, 20%, 30% and 50% on physical and mechanical behavior of ultra-high-performance cementitious composites (UHPC). Results indicates the use of glass powder as substitution up to 50% of Portland cement does not significantly affect the analyzed properties at 28 days.

Keywords: cementitious composite, ultra-high performance, glass powder.

Resumo: Novos desenvolvimentos na tecnologia do concreto, como concretos de alto e ultra-alto desempenho (CAD e UHPC) são notórios não apenas pela elevada resistência mecânica e durabilidade, como também pelo alto consumo de cimento Portland. Materiais cimentícios suplementares têm sido utilizados como substitutos parciais do cimento Portland visando minimizar o consumo de clínquer, otimizando o uso de aglomerantes, reduzindo as emissões de CO₂ e aumentando a durabilidade. O pó de vidro residual pode ser uma alternativa viável devido à sua natureza rica em sílica, ampla disponibilidade e baixo custo. Este trabalho tem como objetivo avaliar a influência da substituição do cimento Portland por pó de vidro residual finamente moído em teores de 10%, 20%, 30% e 50% no comportamento físico e mecânico de compósitos cimentícios de ultra alto desempenho (UHPC). Os resultados indicam que o uso de pó de vidro como substituição de até 50% do cimento Portland não afeta significativamente as propriedades analisadas aos 28 dias.

Palavras-chave: compósito cimentício, ultra-alto desempenho, pó de vidro.

How to cite: S. M. Soares, T. O. G. Freitas, A. Oliveira Júnior, F. G. S. Ferreira, and J. A. A. Salvador Filho, "Assessment of properties of ultra-high performance cementitious composites with glass powder waste". *Rev. IBRACON Estrut. Mater.*, vol. 15, no. 6, e15612, 2022, <https://doi.org/10.1590/S1983-41952022000600012>

Corresponding author: Silvete Mari Soares. E-mail: silvetemari@ifsp.edu.br

Financial support: None.

Conflict of interest: Nothing to declare.

Data Availability: The data that support the findings of this study are openly available in <https://repositorio.ufscar.br/handle/ufscar/14126?show=full>.



This is an Open Access article distributed under the terms of the Creative Commons Attribution License, which permits unrestricted use, distribution, and reproduction in any medium, provided the original work is properly cited.

1 INTRODUCTION

The use of cement as the main material in civil construction is associated with high environmental pollution and high-energy consumption. Given the limitations of fossil fuel resources and strict environmental regulations, to develop sustainable cement production is an urgent initiative to be followed up [1]. Some of the alternatives for decreasing the use of finite resources in clinker production are energy efficiency improvements, waste heat recovery, reduced clinker/cement ratio, alternative raw materials, and substitution of fossil fuels by alternative energy sources [2].

Although UHPCC production uses high cement consumption, the performance achieved by these composites is proportionally superior to traditional cementitious composites regarding the consumption of materials for its production. One of the most efficient alternatives for reducing Portland cement consumption in the UHPCC is the use of supplementary cementitious materials, consisting mainly of pozzolanic materials. Industrial tailings with pozzolanic properties contributed to the improvement of cementitious composites. minimizing clinker content, optimizing the use of binders, reducing CO₂ emissions, and increasing durability.

According to Jokar and Mokhtar [1], the ground glass powder is potentially used as a pozzolanic material [3]–[12]. About 980 thousand tons of glass are produced per year in Brazil, and 53% of this production is not recycled [13]. This glass waste also represents about 3% of all municipal waste produced in Brazil [14].

Glass is a material composed mainly of amorphous silica and present pozzolanic properties when finely ground [7]–[9]. According to Patel et al. [15], glass particles up to 75 µm can replace Portland cement in amounts from 10% to 25%, showing satisfactory results in the production of cementitious composites, and several authors attributes improvements in mechanical properties to pozzolanic reactions from glass powder [3]–[12].

Pozzolanic materials reduce the strength gain rate of cementitious composites at the early age, so that composites containing pozzolanic material, such as glass, acquire a slow strength and should be analyzed at older ages [16]. According to Li et al. [3], when the waste glass powder (WGP) particle size was 20–44 µm, the compressive strength was lower than that of the control group at 7 days of curing, whereas it was 3.5% and 9.6% higher than that of the control group at 28 d and 90 days curing, respectively, with a WGP content 20%. According to Raydan et al. [4], glass powder with particle size < 75 µm can exhibit pozzolanic characteristics inhibiting the ASR gel formation, improving the durability and strength performance. This behavior was confirmed by Higuchi et al. [8], Fanijo et al. [9] and Jiang et al. [10].

This work aims to investigate the effects of the replacement of Portland cement by glass powder at high levels, up to 50% on the mechanical behaviour and microstructure ofUHPC mixtures. The use of glass powder as Portland cement replacement in ultra-high performance cementitious composites is relatively recent. In addition, the replacement of 50% cement by glass powder and its influence on mechanical properties is not yet established in the scientific community.

2 MATERIALS AND METHODS

2.1 Materials used

In this work were used Brazilian Portland cement type CP V ARI, silica fume, glass powder, quartz sand, superplasticizer admixture, shrinkage reducing admixture and water to produce cementitious composites.

Amber glass bottles were used to minimize uncontrolled variations in chemical composition of the cementitious composites mixtures. The glass powder used is the bypass in the 200-mesh sieve, obtained from grinding in a ball mill for 14 hours and mechanically sieved. The fine natural aggregate used is quartz from a riverbed and manually sifted through a 1.2 mm aperture mesh.

The authors Wille and Boisvert-Cotulio [17] used fine aggregate up to 1.2 mm to obtain high strength composites. According to Azme and Sha [18], the use of smaller aggregates reduces their heterogeneity and promotes the densification of the mixture. In Figure 1 are presented the dry materials used.



Figure 1. From left to right: fine aggregate, glass powder, silica fume, and cement.

Were performed laser granulometry, specific gravity [19] and specific surface [20] trials to analyze the physical characteristics of the Portland cement, silica fume and glass powder. The fine aggregate specific gravity was determined according to NBR 16916 [21]. In Figure 2 are presented particle size distribution of Portland cement, silica fume, and glass powder determined by laser granulometry and the characterization of fine aggregate by NBR 17054 [22].

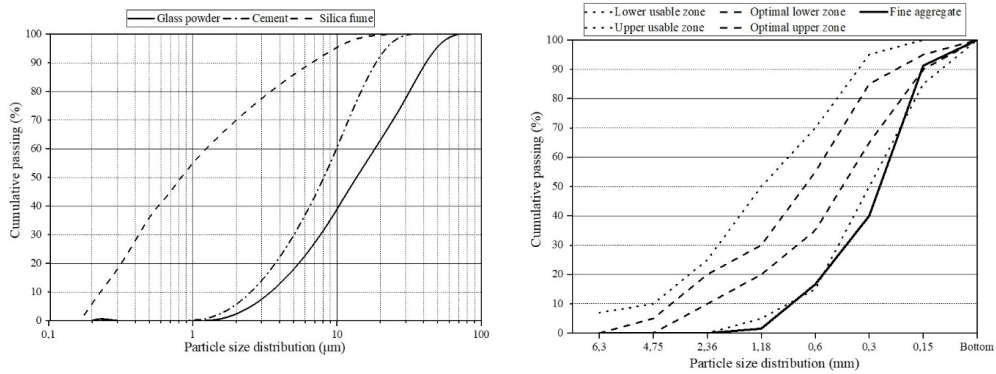


Figure 2. Particle size distribution results of the Portland cement, silica fume and glass powder (left) and fine aggregate (right).

The fine granulometry of the glass powder contributes to its pozzolanic activity. Matos and Sousa-Coutinho [23], Soliman and Tagnit-Hamou [24] and Pan et al. [25] used glass powder with particle size in d_{50} of 9 µm, 12 µm and 20 µm, respectively. Table 1 shows the physical properties values of Portland cement, silica fume, glass powder, and quartz sand.

Table 1. Physical properties of the materials.

Physical properties	Portland cement	Silica fume	Glass powder	Quartz sand
Specific gravity (g/cm ³)	3.16 ^a	2.25 ^a	2.55 ^a	2.56 ^b
Specific surface (m ² /kg)*	665	247	393	-
Water absorption (%)	-	-	-	0.64 ^b
Maximum dimension (mm)**	0.03	0.023	0.075	1.2

* NBR 16372 [20]. ** Maximum size determined by laser granulometry, except in quartz sand which was determined by NBR 17054 [22]. ^a NBR 16605 [19]; ^b NBR 16916 [21]

The chemical characterization of the fine materials was performed by X-ray fluorescence spectrometry assay, which allows the identification of the elements present in each material. Table 2 shows the percentage of chemical composition of cement, silica fume, and glass powder.

Table 2. Chemical composition of cement, silica fume, and glass powder.

Components	Portland cement (%)	Silica fume (%)	Glass powder (%)
Silica oxide (SiO ₂)	23.00	94.10	74.00
Ferric oxide (Fe ₂ O ₃)	2.49	< 0.5	0.42
Aluminum oxide (Al ₂ O ₃)	4.31	< 0.2	3.70
Calcium oxide (CaO)	61.40	< 0.2	9.10
Sulfuric anhydride (SO ₃)	2.97	-	-
Strontium Oxide (SrO)	0.27	< 0.2	0.04
Thorium Oxide (ThO ₂)	< 0.01	< 0.01	< 0.01
Potassium oxide (K ₂ O)	0.96	1.28	0.56
Sodium oxide (Na ₂ O)	-	-	11.00
Uranium Oxide (U ₃ O ₂)	< 0.01	< 0.01	< 0.01
Phosphorus oxide (P ₂ O ₅)	0.52	-	-
Chloride (Cl ⁻)	0.12	-	-
Magnesium oxide (MgO)	-	-	0.74
Loss on ignition	4.05	3.60	0.58

The presence of high levels of SiO_2 (74%) in glass powder is highly desirable for the development of the pozzolanic reaction. The chemical composition of binders is equivalent to those found by researchers such as Matos and Sousa-Coutinho [23], Soliman and Tagnit-Hamou [24], Pan et al. [25], Harbec et al. [26] and Ibrahim and Meadwad [27].

For mineralogical analysis, we used the X-ray diffraction (XRD) to characterize the mineralogical phases present in each material. Figure 3 shows the diffractograms of Portland cement, silica fume, and glass powder.

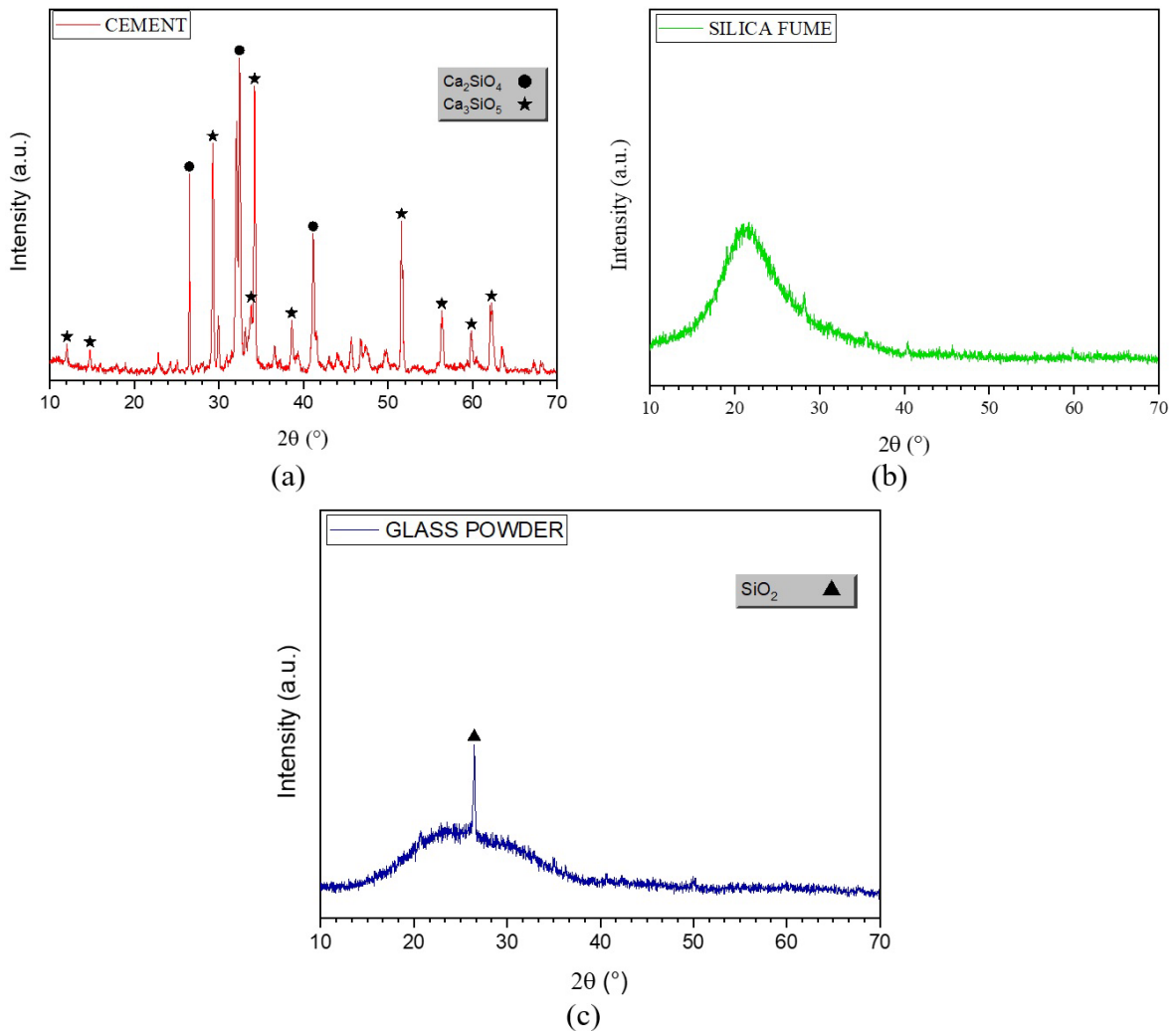


Figure 3. X-ray diffraction patterns for cement (a), silica fume (b) and glass powder (c).

In glass powder diffractometry, the material showed a large amount of amorphous silica, except for a crystalline quartz peak, probably incorporated into the material in one of the grinding steps consisted of using steel ball, concrete mixer, and flint stone ball mill (crystalline silica).

Elaqra and Rustom [28] identified contamination of glass powder by cement that was derived from material residues in the grinding equipment. For other authors such as Soliman and Tagnit-Hamou [24] and Ibrahim and Meadwad [27], the glass powder showed completely amorphous behavior in the DRX analysis.

The pozzolanic activity of the glass powder was evaluated by determining the lime performance at 7 days according to NBR 5751 [29]. It showed compressive strength of 4.97 MPa, below the limit of 6.0 MPa defined by the standard. By the modified Chapelle method, according to NBR 15895 [30] it presented calcium hydroxide fixation of 654 mg $Ca(OH)_2/g$. Raverdy et al. [31] and Hoppe Filho [32] established the limit of 330 mg $Ca(OH)_2/g$ from the modified Chapelle methodology.

By scanning electron microscopy (SEM) analysis performed on the FEI Company Inspect F50 equipment, we observed the morphology of the Portland cement, silica fume, and glass powder (Figure 4).

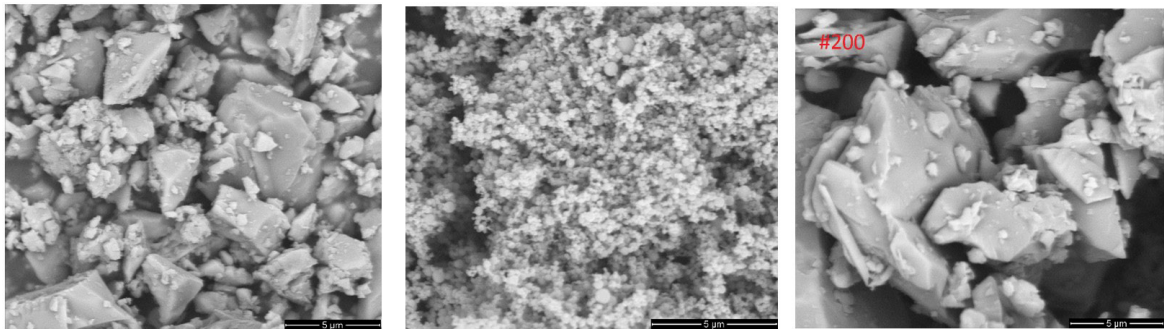


Figure 4. Photomicrographs from SEM of Portland cement (left), silica fume (center) and glass powder (right).

The morphology of Portland cement is similar to the morphology of glass powder, with angular particles of different sizes and shapes with well-defined and smooth surfaces, while the silica fume, highly thin material, presents regular and spherical particles.

A polycarboxylate based superplasticizer admixture with a content of 2.25% relative to binder volume and the shrinkage-reducing admixture was used at a content of 1%, also relative to binder volume.

The saturation point of the superplasticizer admixture is the level from which the effect of the admixture on the mixture is no longer significant and was determined by the Marsh cone test performed according NBR 7681 [33]. The 2.25% superplasticizer content was the optimal content.

The mini-slump test developed by Kantro [34] was performed to determine the compatibility between the groups with glass powder and the superplasticizer admixture used. The mini-slump test with the optimum content of 2.25% was performed to verify the compatibility of the superplasticizer admixture with the glass powder. The mini-slump test results for each analyzed paste of 0%, 10%, 20%, 30% and 50% glass powder content was calculated. The incorporation of glass powder did not interfere with the compatibility of the superplasticizer admixture with the binders.

Although the absolute values of scattering are different, the difference between the largest and smallest is not significant, only 7 mm, or approximately 2%. Thus, the superplasticizer was shown to be compatible with Portland cement and glass powder.

2.2 Cementitious composites mixtures

Five groups of cementitious composites with different glass powder contents were prepared. The water/binder ratio adopted was 0.18, with the addition of 8% silica fume concerning the Portland cement consumption of the reference group. The use of glass powder contents was carried out in the levels of 0%, 10%, 20%, 30%, and 50% in volumetric replacement to cement, represented by the nomenclature REF, VD10, VD20, VD30, and VD50, respectively. Table 3 shows the consumption of materials used in each mixture.

Table 3. Consumption of materials to produce the cementitious composite.

Group	Consumption of materials (kg/m ³)							Consistency (mm)
	Cement	Silica fume	Glass powder	Quartz sand	Water*	SP ⁽¹⁾	SR ⁽²⁾	
REF	1000	80	-	1074	181.28	24.3	10.8	379.5
VD10	900	80	81	1074	181.28	24.3	10.8	377.0
VD20	800	80	161	1074	181.28	24.3	10.8	375.5
VD30	700	80	242	1074	181.28	24.3	10.8	381.5
VD50	500	80	403	1074	181.28	24.3	10.8	382.5

*Corrected water value for 46% solids of superplasticizer. SP⁽¹⁾ = superplasticizer; SR⁽²⁾ = shrinkage reducer.

Replacing a product (cement) with a slightly thicker product (glass powder) ensures greater availability of water for fluidizing the mixture. However, water adsorption on the surface of the glass powder particles decreased the amount of water for fluidization, as commented by Pan et al. [25]. The combination of these two effects may have ensured equivalent dispersion values.

Soliman and Tagnit-Hamou [24] observed an increase in workability, with approximately 13% difference between the mixtures with 0% (reference) and 50% of glass powder substitution. The researchers attributed the higher workability to the greater availability of water for fluidization due to the low water absorption by the glass particles, dilution of the replacement cement, and the lower friction between the mix components and the smooth glass surface.

The consistency of cementitious composites was verified according to NBR 13276 [35], and the determination of specific gravity and air entrained content were evaluated according to NBR 13278 [36].

Cylindrical specimens 5 x 10 cm were molded, manually compacted, and cured in lime-saturated water. The tests to verify the compressive strength of UHPCC were performed according to NBR 5739 [37], at ages 2, 7, 28 and 91 days, and the tensile strength tests by diametral compression, performed according to NBR 7222 [38], at the age of 28 days.

The test for obtaining the static elastic modulus of the UHPCC was performed according to NBR 8522 [39], at the age of 28 days. Besides the determination of the static modulus of elasticity, the dynamic modulus of elasticity was also determined, which is a non-destructive test performed by the propagation of longitudinal waves obtained by ultrasonic pulses, according to ASTM E1876-21 [40] and ASTM C215-08 [41]. Capillary water absorption from the UHPCC was also determined following the recommendations of NBR 9779 [42].

3 RESULTS AND DISCUSSION

3.1 Specific gravity and air entrained content

Figure 5 presents the results of the UHPCC specific gravity and air entrained content test.

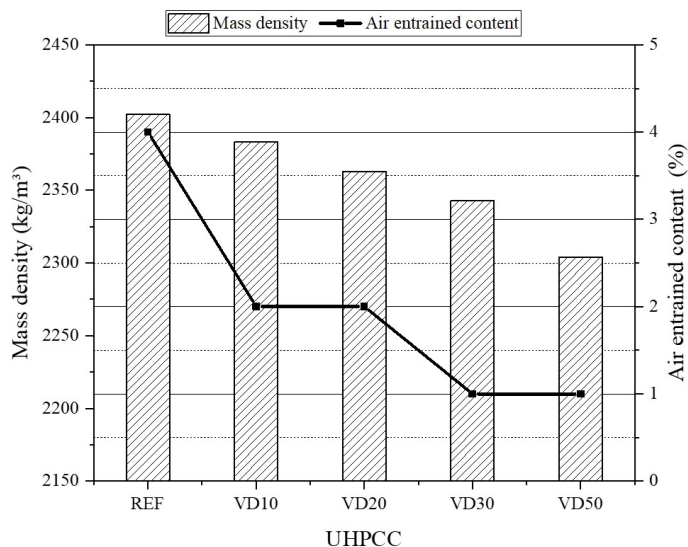


Figure 5. Specific gravity and air entrained content of UHPCC.

The density of the mixture decreased with increasing glass powder incorporation. The reference group presented higher specific gravity, 2338 kg/m³, and the 50% of glass powder group present 2273 kg/m³, approximately 4% difference, with the replacement of a denser product (cement) by a less dense product (glass powder) being the most likely hypothesis.

Although replacing denser products with less dense products reduces the density of the mixture, the lower presence of air entrained content in the 50% of glass powder group ensured that the difference to the reference group was not so pronounced.

A similar behaviour is described by Sharif et al. [43] which considers that blends with glass powder present the mixture densification by filler effect by air content reduction. Although Soliman and Tagnit-Hamou [24] observed a decrease in mass density of the mixture in minor values, with differences of approximately 3% between the reference line and the 50% glass powder line.

3.2 Mechanical and physical properties

Figure 6 shows the average results of the compressive strength test and capillary water absorption values at seven days and at 28 days of UHPCC.

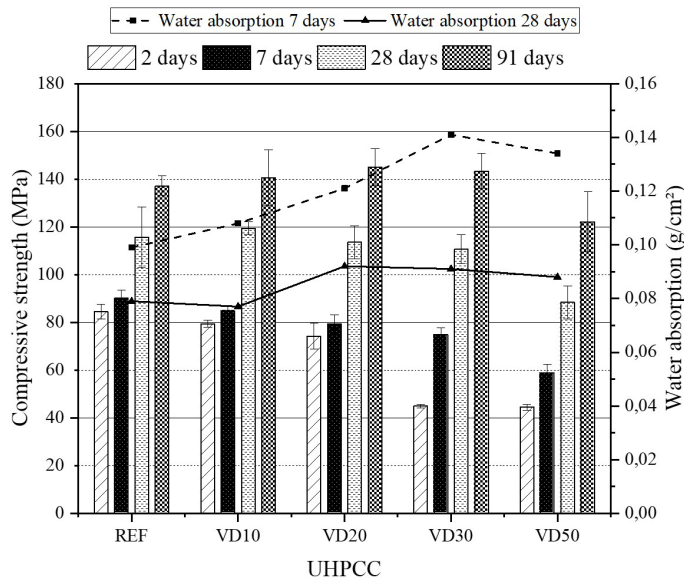


Figure 6. Compressive strength and water absorption of UHPCC.

Changes in the compressive strength development were sensitive to different glass powder incorporation amounts for different ages.

Researchers such as Matos and Sousa-Coutinho [23] analyzed contents of up to 20% of glass powder and did not observe compressive strength higher than the reference group at 28 days.

Soliman and Tagnit-Hamou [24] obtained compressive strength values at approximately 28 days for contents of 0%, 10%, 20%, and 30% of glass powder, being 170 MPa, 165 MPa, 170 MPa and 165 MPa, respectively.

Pan et al. [25], with a 5% glass powder content and 53 MPa compressive strength at 28 days obtained a higher value than the 47 MPa without glass powder group, while the 10% content presented 45 MPa compressive strength.

The better development of compressive strength at older ages can be attributed to the formation of C-S-H by the pozzolanic effect, which promotes the composite densification. The incorporation of a larger amount of glass powder as a substitute for cement directly changes the water/binder ratio, making more water available for a smaller proportion of cement, intensifying the formation of $\text{Ca}(\text{OH})_2$ which naturally reacts with the highest amount of pozzolanic material available by glass powder [24].

The differences observed at the age of 7 days could be explained by the incorporation of larger amounts of glass powder in the VD30 and VD50 groups, which in early ages could not densify the cementitious composite efficiently. At 28 days age, matrices with glass powder presents better developed hydration, with refined pores and lower water absorption through the capillary pores.

Matos and Sousa-Coutinho [23] observed that at up to 4.5 hours of capillary water absorption, samples with 0%, 10% and 20% glass powder at two months age presented no significant absorption differences. The authors attributed the small absorption difference to the Portland cement and glass powder particles size, both around 9 μm at d50, clogging the pores by physical effect.

Figure 7 shows the average results of the UHPCC splitting tensile strength test and the mean values of dynamic and static modulus of elasticity.

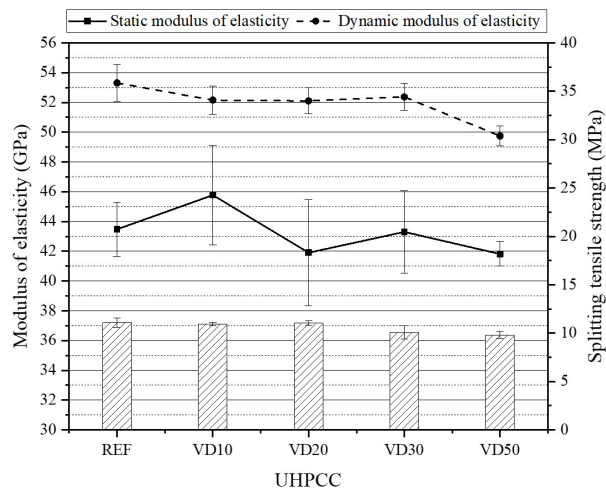


Figure 7. Splitting tensile strength and modulus of elasticity of UHPCC.

Using 0%, 10%, 20%, 30%, and 50% glass powder contents, Soliman and Tagnit-Hamou [24] observed slight differences between the modulus of elasticity values between the different groups, ranging from 50 to 55 GPa. The authors also commented that the glass powder particles naturally present high stiffness (in the order of 70 GPa) and may contribute indirectly to the stiffness of the composite.

In Figure 8 are presented three curves of empirical models by Abdelgader and Ben-Zeitun [44], Rajabi and Moaf [45], and Li et al. [46] and one new model that follows a polynomial equation curve, proposed to describe the correlation between compressive strength and tensile strength of ultra-high performance cementitious composites.

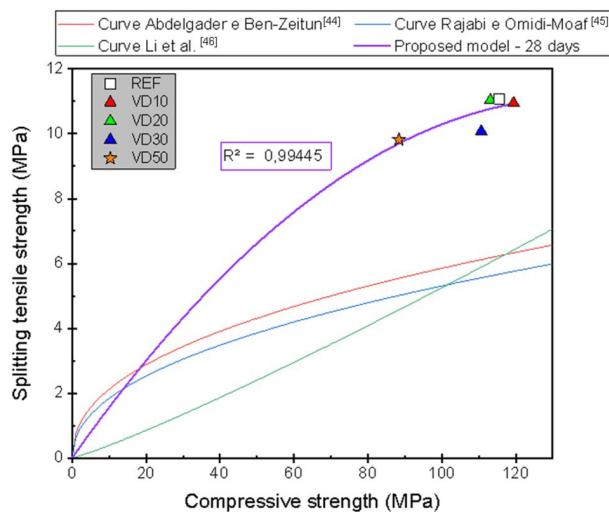


Figure 8. Splitting tensile strength versus compressive strength of UHPCC.

The prediction of polynomial curve presents an R^2 value of 0,99 that indicates the experimental results of the UHPCC are above the empirical curves. UHPCC presents a higher splitting tensile strength / compressive strength ratio compared to other composites, suggesting a greater potential for application in engineering due to the greater tensile strength.

3.3 Microstructural Analysis

In Figure 9 are presented the diffractograms of the REF and VD50 cement pastes mixtures at the ages of 28 days and 91 days. The dilution effect of cement promoted by its replacement with glass powder is mainly responsible for

reducing peaks on older ages. For the portlandite peaks between the angles of 15° to 20° and 45° to 50° at 28 days, mixtures REF and VD50 presented similar intensity since the glass powder participation in pozzolanic hydration still show minor differences. While at 91 days ages, the same portlandite peaks already show visible differences between mixtures REF and VD50, due it consumes by the glass powder pozzolanic reaction.

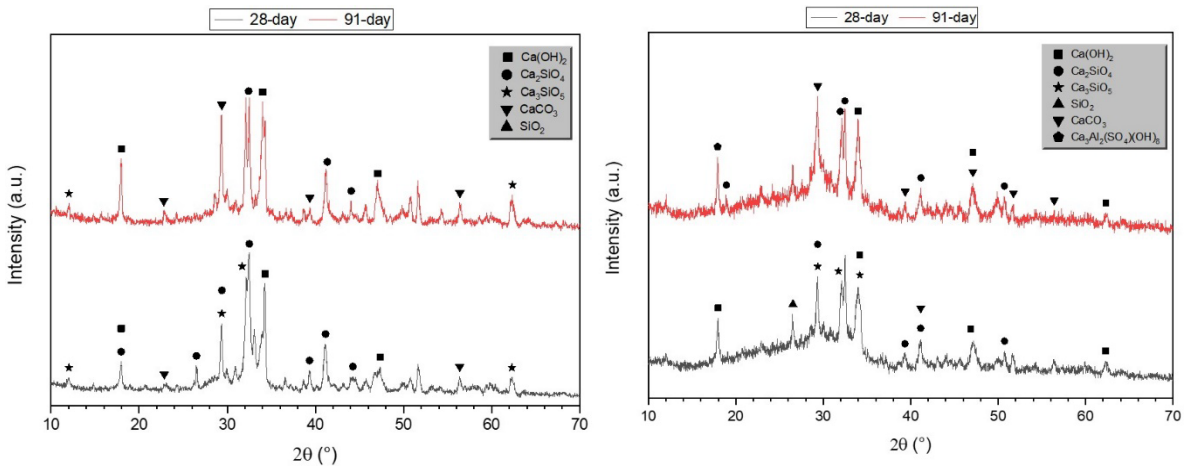


Figure 9. X-ray diffraction patterns at 28-day and 91-day of REF (left) and VD50 (right).

The presence of silica fume, a pozzolanic material, in UHPCC composition may influence the observations of the pozzolanic effect of glass powder. Silica fume presents a greater specific surface and much smaller particles which reacts more quickly and intensely than glass powder. These characteristics allow the consumption of much the previously available portlandite and which could react with glass powder.

In Figure 10 are presented the SEM microstructural analysis on REF and VD50 mixtures at 28 days and 91 days.

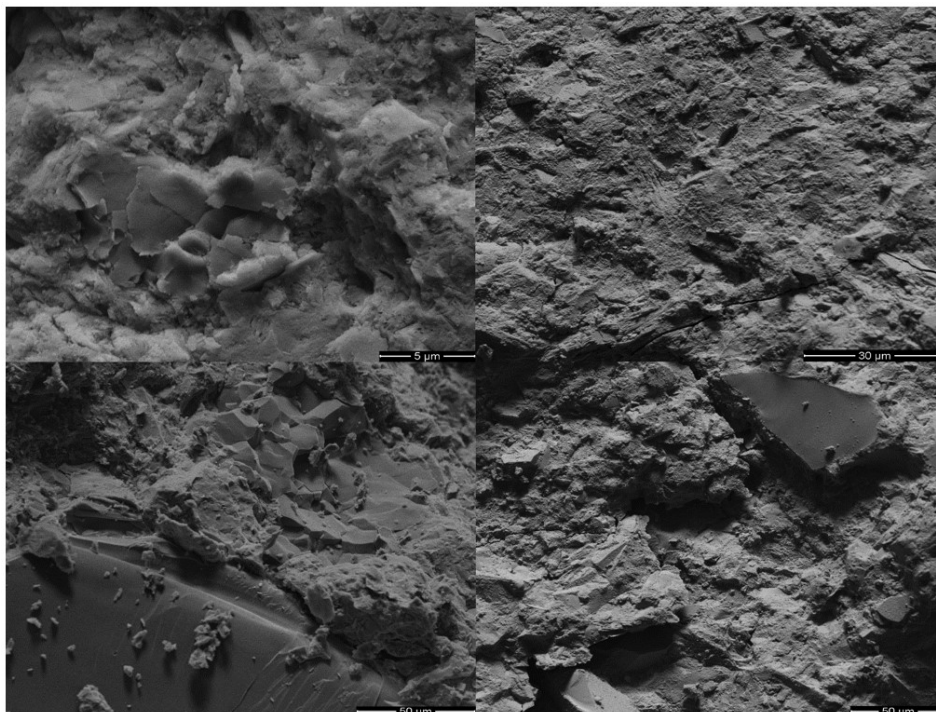


Figure 10. Photomicrographs from SEM of REF 28-day (upper left), REF 91-day (upper right), VD50 28-day (lower left) and VD50 91-day (lower right).

The presence of small cracks in cementitious matrix can be observed in the micrographs of the reference paste at 91 days. And, in addition to the presence of small cracks, the presence of glass dust particles is observed at the ages of 28 days and 91 days in VD50 paste.

3.4 UHPCC statistical analysis and summary of the properties

Table 4 shows the summary of the statistically analyzed properties of UHPCC with glass powder at the age of 28 days concerning the REF group, which is without glass powder.

Table 4. Summary of the properties and statistical analysis of UHPCC.

Properties	UHPCC				
	REF	VD10	VD20	VD30	VD50
Compressive strength (MPa)	116.0	119.0	114.0	111.0	88.0
Statistically different from REF?	-	No	No	No	Yes
Tensile strength (MPa)	11.08	10.94	11.03	10.07	9.82
Statistically different from REF?	-	No	No	No	No
Static modulus of elasticity (GPa)	43.09	45.51	41.67	42.94	41.51
Statistically different from REF?	-	No	No	No	No
Dynamic modulus of elasticity (GPa)	53.31	52.15	52.10	52.37	49.75
Statistically different from REF?	-	Yes	Yes	No	Yes
Capillary water absorption at 72h (g/cm²)	0.079	0.077	0.092	0.091	0.088
Statistically different from REF?	-	No	No	No	No

Although the UHPCC studied have high cement consumption, it is observed high-energy efficiency in its use compared to traditional cementitious composites. They showed the same order of magnitude of composites efficiency with cement consumption around 450 kg/m³, as shown in Table 5.

Table 5. Energy efficiency of UHPCC.

Groups / Researchers	Cement Consumption (kg/m ³)	SCM Consumption (kg/m ³)			Compressive strength at 28 days (MPa)	Energy efficiency of binders (kg/m ³ MPa ⁻¹)	Cement energy efficiency (kg/m ³ MPa ⁻¹)
		Silica Fume	Fly Ash	Glass Powder			
REF	1000	80	-	0	106.81	10.11	10.11
VD10	900	80	-	81	98.58	10.76	9.13
VD20	800	80	-	161	121.69	8.55	6.57
VD30	700	80	-	242	110.70	6.3	9.20
VD50	500	80	-	403	105.86	9.29	4.72
Pelisser et al. [47]	472	-	52	-	67.2	7.8	7.02
Corinaldesi and Moriconi [48]	440	-	100	-	45.0	12.0	9.78
	625.7	41.7	-	-	113.0	5.9	5.5
Li et al. [49]	426.1	28.4	-	-	116.2	3.9	3.7
	341.5	22.8	-	-	121.1	3.0	2.8

Figure 11 shows the results of a binder intensity (BI) benchmark on compressive strength and binder consumption data from concretes produced in Brazil and 28 other countries. The results obtained in this study were included in this chart.

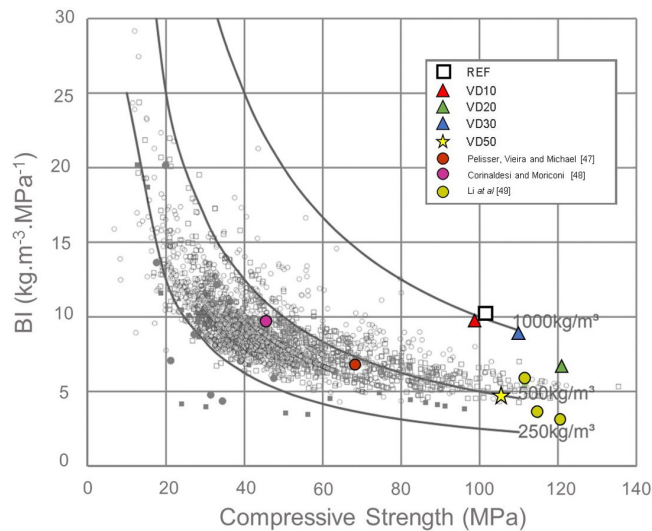


Figure 11. Benchmark of binder intensity adapted from Daminielli, Pileggi and John [50].

It is observed for most concretes that compressive strength above 50 MPa represents binder intensity is above $5 \text{ kg}\cdot\text{m}^{-3}\cdot\text{MPa}^{-1}$. In this study, the cement efficiency of ultra-high performance concretes was from 4.7 to $10.11 \text{ kg}\cdot\text{m}^{-3}\cdot\text{MPa}^{-1}$, for mixtures with the incorporation of 50% glass powder in substitution of Portland Cement and reference mixtures without glass powder, respectively. It is also noteworthy the use of a high content of glass powder, providing an appropriate destination for a waste, since the industry cannot absorb all the recycling demand of the waste glass it produces. Therefore, the incorporation of great amounts of glass waste powder in substitution of Portland cement is a possible way to produce more sustainable UHPC using lower amounts of clinker.

4 CONCLUSIONS

From the characterizations and results, we obtained the following conclusions:

- The glass powder used in the study was suitable for UHPCC Portland cement replacement as a binder. Although the granulometry is 75% larger than in the cement and the specific surface is approximately 59% smaller, the experimental results analyzed presented values equivalent to the reference UHPCC, despite the high levels of substitution.
- The incorporation of glass powder in contents of 10, 20, 30, and 50% did not affect the workability and density of the cementitious composite in the fresh state, presenting values close to the reference line, with a maximum difference of 1% and 4%, respectively.
- For early ages such as 2 and 7 days, the greater the incorporation of glass powder, the lower the development of compressive strength due to the pozzolanic effect. However, at 28 days, the incorporation of high glass powder content as 50% have decreased the strengths refer to the powder-free group, with strengths of 88,37 MPa and 115,58 MPa, respectively. At 91 days there is no significant difference in compressive strength between the evaluated mixtures.
- In mechanical and physical evaluations such as splitting tensile strength, static modulus of elasticity, and capillary water absorption, at 28 days, there were no statistically different values. Although in the dynamic modulus of elasticity there was not a statistical difference between the REF and VD30.
- The results of compressive strength and tensile strength by diametrical compression obtained at 28 days for the cementitious composite with 50% replacement of the Portland cement by glass powder allow to classify it as a high-performance concrete.
- An amount of 50% of glass powder enable the greatest reduction of cement consumption and better energy efficiency as none of the studied mixtures obtained significantly different values and, mainly, no performance reduction on the evaluated properties.

ACKNOWLEDGMENTS

This research did not receive any specific grant from funding agencies in the public, commercial, or not-for-profit sectors.

REFERENCES

- [1] Z. Jokar and A. Mokhtar, "Policy making in the cement industry for CO₂ mitigation on the pathway of sustainable development-A system dynamics approach," *J. Clean. Prod.*, vol. 201, pp. 142–155, 2018, <http://dx.doi.org/10.1016/j.jclepro.2018.07.286>.
- [2] H. Mikulčić, J. J. Klemeš, M. Vujanović, K. Urbaniec, and N. Duić, "Reducing greenhouse gasses emissions by fostering the deployment of alternative raw materials and energy sources in the cleaner cement manufacturing process," *J. Clean. Prod.*, vol. 136, pp. 119–132, 2016, <http://dx.doi.org/10.1016/j.jclepro.2016.04.145>.
- [3] Q. Li, H. Qiao, A. Li, and G. Li, "Performance of waste glass powder as a pozzolanic material in blended cement mortar," *Constr. Build. Mater.*, vol. 324, pp. 126531, 2022, <http://dx.doi.org/10.1016/j.conbuildmat.2022.126531>.
- [4] R. Raydan, J. Khatib, A. Jahami, A. K. El Hamoui, and F. Chamseddine, "Prediction of the mechanical strength of concrete containing glass powder as partial cement replacement material," *Innov. Infrastruct. Solut.*, vol. 7, pp. 311, 2022, <https://doi.org/10.1007/s41062-022-00896-8>.
- [5] A. L. Borges, S. M. Soares, T. O. G. Freitas, A. Oliveira Júnior, E. B. Ferreira, and F. G. S. Ferreira, "Evaluation of the pozzolanic activity of glass powder in three maximum grain sizes," *Mater. Res.*, vol. 24, no. 4, pp. e20200496, 2021, <http://dx.doi.org/10.1590/1980-5373-MR-2020-0496>.
- [6] A. S. Raju, K. B. Anand, and P. Rakesh, "Partial replacement of Ordinary Portland cement by LCD glass powder in concrete," *Materials Today Proceedings*, vol. 46, pp. 5131–5137, 2021, <http://dx.doi.org/10.1016/j.matpr.2020.10.661>.
- [7] B. A. Tayeh, H. M. Hamada, I. Almehsal, and B. H. Abu Bakar, "Durability and mechanical properties of cement concrete comprising pozzolanic materials with alkali-activated binder: a comprehensive review. *Case Stud. Constr. Mater.*, vol. 17, pp. e01429, 2022. <https://doi.org/10.1016/j.cscm.2022.e01429>.
- [8] A. M. D. Higuchi, M. G. S. Marques, L. F. Ribas, and R. P. Vasconcelos, "Use of glass powder residue as an eco-efficient supplementary cementitious material," *Constr. Build. Mater.*, vol. 304, pp. 124640, 2021, <http://dx.doi.org/10.1016/j.conbuildmat.2021.124640>.
- [9] E. O. Fanijo, E. Kassem, and A. Ibrahim, "ASR mitigation using binary and ternary blends with waste glass powder," *Constr. Build. Mater.*, vol. 280, pp. 122425, 2021, <http://dx.doi.org/10.1016/j.conbuildmat.2021.122425>.
- [10] X. Jiang, R. Xiao, Y. Bai, B. Huang, and Y. Ma, "Influence of waste glass powder as a supplementary cementitious material (SCM) on physical and mechanical properties of cement paste under high temperatures," *J. Clean. Prod.*, vol. 340, pp. 130778, 2022, <http://dx.doi.org/10.1016/j.jclepro.2022.130778>.
- [11] M. Mejdí, W. Wilson, M. Saillio, T. Chaussadent, L. Divet, and A. Tagnit-Hamou, "Hydration and microstructure of glass powder cement pastes—A multi-technique investigation," *Cement Concr. Res.*, vol. 151, pp. 106610, 2022, <http://dx.doi.org/10.1016/j.cemconres.2021.106610>.
- [12] O. Y. Bayraktar, "Possibilities of disposing silica fume and waste glass powder, which are environmental wastes, by using as a substitute for Portland cement," *Environ. Sci. Pollut. Res. Int.*, vol. 28, no. 13, pp. 16843–16854, 2021, <http://dx.doi.org/10.1007/s11356-020-12195-9>.
- [13] Associação Brasileira de Bebidas – ABRABE. *Glass is Good*. <https://www.abrabe.org.br/glass-is-good/> (accessed Nov. 1, 2022).
- [14] Compromisso Empresarial para Reciclagem – CEMPRE. *Vidro*. CEMPRE, 2022. <http://cempre.org.br/artigo-publicacao/ficha-tecnica/id/6/vidro> (accessed Jan. 25, 2022).
- [15] D. Patel, R. P. Tiwaric, R. Shrivastava, and R. K. Yadave, "Effective utilization of waste glass powder as the substitution of cement in making paste and mortar," *Constr. Build. Mater.*, vol. 199, pp. 406–415, 2019, <http://dx.doi.org/10.1016/j.conbuildmat.2018.12.017>.
- [16] A. Shayan and A. Xu, "Value-added utilisation of waste glass in concrete," *Cement Concr. Res.*, vol. 34, no. 1, pp. 81–89, 2004, [http://dx.doi.org/10.1016/S0008-8846\(03\)00251-5](http://dx.doi.org/10.1016/S0008-8846(03)00251-5).
- [17] K. Wille and C. Boisvert-Cotulio, "Material efficiency in the design of ultra-high performance concrete," *Constr. Build. Mater.*, vol. 86, no. 1, pp. 33–43, 2015, <http://dx.doi.org/10.1016/j.conbuildmat.2015.03.087>.
- [18] N. M. Azmee and N. Sha, "Ultra-high performance concrete: from fundamental to applications," *Case Stud. Constr. Mater.*, vol. 9, pp. e00197, Dec. 2018, <http://dx.doi.org/10.1016/j.cscm.2018.e00197>.
- [19] Associação Brasileira de Normas Técnicas, *Cimento Portland e outros Materiais em Pó – Determinação da massa específica*, ABNT NBR 16605, 2017.
- [20] Associação Brasileira de Normas Técnicas, *Cimento Portland e outros materiais em pó – Determinação da finura pelo método de permeabilidade ao ar (método de Blaine)*, ABNT NBR 16372, 2015.
- [21] Associação Brasileira de Normas Técnicas, *Agregado Miúdo - Determinação da Densidade e da Absorção de Água*, ABNT NBR 16916, 2021.
- [22] Associação Brasileira de Normas Técnicas, *Agregados - Determinação da Composição Granulométrica – Método de Ensaio*, ABNT NBR 17054, 2022.
- [23] A. M. Matos, and J. Sousa-Coutinho, "Durability of mortar using waste glass powder as cement replacement," *Constr. Build. Mater.*, vol. 36, pp. 205–215, 2012.

- [24] N. A. Soliman, and A. Tagnit-Hamou, "Development of ultra-high-performance concrete using glass powder – Towards ecofriendly concrete," *Constr. Build. Mater.*, vol. 125, pp. 600–612, 2016.
- [25] Z. Pan, Z. Tao, T. Murphy, and R. Wuhler, "High temperature performance of mortars containing fine glass powders," *J. Clean. Prod.*, vol. 162, pp. 16–26, 2017, <https://doi.org/10.1016/j.jclepro.2017.06.003>.
- [26] D. Harbec, A. Zidol, A. Tagnit-Hamou, and F. Gitzhofer, "Mechanical and durability properties of high performance glass fume concrete and mortars," *Constr. Build. Mater.*, vol. 134, no. 1, pp. 142–156, 2017., <http://dx.doi.org/10.1016/j.conbuildmat.2016.12.018>.
- [27] S. Ibrahim and D. Meawad, "Assessment of waste packaging glass bottles as supplementary cementitious materials," *Constr. Build. Mater.*, vol. 182, no. 10, pp. 451–458, 2018, <http://dx.doi.org/10.1016/j.conbuildmat.2018.06.119>.
- [28] H. Elaqra and R. Rustom, "Effect of using glass powder as cement replacement on rheological and mechanical properties of cement paste," *Constr. Build. Mater.*, vol. 179, no. 10, pp. 326–335, 2018, <http://dx.doi.org/10.1016/j.conbuildmat.2018.05.263>.
- [29] Associação Brasileira de Normas Técnicas, *Materiais Pozolânicos – Determinação da Atividade Pozolânica com Cal aos Sete Dias*, ABNT NBR 5751, 2015.
- [30] Associação Brasileira de Normas Técnicas. *Materiais Pozolânicos – Determinação do Teor de Hidróxido de Cálcio Fixado – Método Chapelle Modificado*, ABNT NBR 15895, 2010.
- [31] M. Raverdy, F. Brivot, A. M. Paillere, and R. Dron, "Appreciation of pozzolanic reactivity of minor components," *Proc. 7th Int. Congr. Chem. Cem.* Paris: Éditions Septima, 1980, pp. 36–41.
- [32] J. Hoppe Filho, *Sistemas cimento, cinza volante e cal hidratada: mecanismo de hidratação, microestrutura e carbonatação de concreto*. PhD Thesis, Esc. Politéc., Univ. São Paulo, São Paulo, SP, 2008.
- [33] Associação Brasileira de Normas Técnicas, *Calda de cimento para injeção*, ABNT NBR 7681, 2013.
- [34] D. Kanro, "Influence of water-reducing admixtures on properties of cement paste - a miniature slump test," *Cem. Concr. Aggreg.*, vol. 2, no. 2, pp. 95–102, 1980.
- [35] Associação Brasileira de Normas Técnicas, *Argamassa para Assentamento e Revestimento de Paredes e Tetos – Preparo da Mistura e Determinação do Índice de Consistência*, ABNT NBR 13276, 2016.
- [36] Associação Brasileira de Normas Técnicas, *Argamassa para Assentamento e Revestimento de Paredes e Tetos – Determinação da Densidade de Massa e do Teor de ar Incorporado*, ABNT NBR 13278, 2005.
- [37] Associação Brasileira de Normas Técnicas, *Concreto - Ensaio de Compressão de Corpos de Prova Cilíndricos*, ABNT NBR 5739, 2018.
- [38] Associação Brasileira de Normas Técnicas, *Concreto e Argamassa- Determinação da Resistência à Tração por Compressão Diametral de Corpos de Prova Cilíndricos*, ABNT NBR 7222, 2011.
- [39] Associação Brasileira de Normas Técnicas, *Concreto Endurecido - Determinação dos Módulos de Elasticidade e de Deformação*, ABNT NBR 8522, 2021.
- [40] American Society for Testing and Materials, *Standard Test Method for Dynamic Young's Modulus, Shear Modulus, and Poisson's Ratio by Impulse Excitation of Vibration*, ASTM E1876-21, 2021.
- [41] American Society for Testing and Materials, *Standard Test Method for Fundamental Transverse, Longitudinal and Torsional Resonant Frequencies of Concrete Specimens*, ASTM C215-08, 2008.
- [42] Associação Brasileira de Normas Técnicas. *Argamassa e concreto endurecidos - Determinação da absorção de água por capilaridade*, ABNT NBR 9779, 2012.
- [43] Y. Sharifi, I. Afshoon, and Z. Firoozjaie, "Fresh properties of self-compacting concrete containing ground waste glass microparticles as cementing material," *J. Adv. Concr. Technol.*, vol. 13, no. 2, pp. 50–66, 2015, <http://dx.doi.org/10.3151/jact.13.50>.
- [44] H. S. Abdelgader, A. E. Ben-Zeitun, R. K. Dhir, K. A. Paine, and A. M. C. Tang, "Tensile strength of two-stage concrete measured by double-punch tests," in *Role of Concrete in Nuclear Facilities*, R. K. Dhir, K. A. Paine and A. M. C. Tang, London, United Kingdom: Thomas Telford Publishing, pp. 43-50, 2005.
- [45] A. M. Rajabi and F. O. Moaf, "Simple empirical formula to estimate the main geomechanical parameters of preplaced aggregate concrete and conventional concrete," *Constr. Build. Mater.*, vol. 146, pp. 485–492, 2017, <http://dx.doi.org/10.1016/j.conbuildmat.2017.04.089>.
- [46] P. P. Li, Q. L. Yu, H. J. H. Brouwers, and W. Chen, "Conceptual design and performance evaluation of two-stage ultra-low binder ultra-high performance concrete," *Cement Concr. Res.*, vol. 125, pp. 105858, Nov. 2019, <http://dx.doi.org/10.1016/j.cemconres.2019.105858>.
- [47] F. Pelisser, A. Vieira, and A. M. Bernardin, "Efficient self-compacting concrete with low cement consumption," *J. Clean. Prod.*, vol. 175, pp. 324–332, 2018, <http://dx.doi.org/10.1016/j.jclepro.2017.12.084>.
- [48] V. Corinaldesi and G. Moriconi, "The role of industrial by-products in self-compacting concrete," *Constr. Build. Mater.*, vol. 25, no. 8, pp. 3181–3186, 2011, <http://dx.doi.org/10.1016/j.conbuildmat.2011.03.001>.

- [49] P. P. Li, Q. L. Yu, H. J. H. Brouwers, and W. Chen, "Conceptual design and performance evaluation of two-stage ultra-low binder ultra-high performance concrete," *Cement Concr. Res.*, vol. 125, pp. 105858, 2019, <http://dx.doi.org/10.1016/j.cemconres.2019.105858>.
- [50] B. L. Damineli, R. G. Pileggi, and V. M. John, "Lower binder intensity eco-efficient concretes," in *Eco-Efficient Concrete*, F. Pacheco-Torgal, S. Jalali, J. Labrincha and V. M. John, eds., Sawston, Reino Unido: Woodhead Publishing, 2013, pp. 26–44. <https://doi.org/10.1533/9780857098993.1.26>.

Author contributions: S M Soares contributed with the activities of conceptualization, development, results and discussion, writing and preparation of the original text; T. O. G. Freitas contributed to the activities of development, results and discussion of results and writing; A. Oliveira Júnior development, results and discussion of results and writing; F. G. S. Ferreira contributed with conceptualization, supervision, discussion of results and review and J. A. A. Salvador Filho contributed with conceptualization, supervision, discussion of results and review.

Editors: Edna Possan, Mark Alexander